M.Sc. Corrado Nai

Rock-inhabiting fungi studied with the aid of the model black fungus *Knufia petricola* A95 and other related strains

BAM-Dissertationsreihe • Band 119
Berlin 2014

Die vorliegende Arbeit entstand an der BAM Bundesanstalt für Materialforschung und -prüfung.

Impressum

**Rock-inhabiting fungi studied
with the aid of the model black fungus
Knufia petricola A95 and other related strains**

2014

Herausgeber:
BAM Bundesanstalt für Materialforschung und -prüfung
Unter den Eichen 87
12205 Berlin
Telefon: +49 30 8104-0
Telefax: +49 30 8112029
E-Mail: info@bam.de
Internet: www.bam.de

Layout: BAM-Referat Z.8

ISSN 1613-4249
ISBN 978-3-9816380-8-0

Rock-inhabiting fungi studied with the aid of the model black fungus *Knufia petricola* A95 and other related strains

Inaugural dissertation
to obtain the academic degree
Doctor rerum naturalium (Dr. rer. nat.)

Submitted to the
Department of Biology, Chemistry and Pharmacy
of the Freie Universität Berlin

by

CORRADO NAI

from Wallisellen (Switzerland)

April 2014

First reviewer Prof. Dr. Rupert Mutzel
Second reviewer Prof. Dr. Anna A. Gorbushina

Day of disputation 11 July 2014

To Pia & Marco and Emilia & Oscar,
without whom I would not be writing this.

To Sissi,
– always.

Considerate la vostra semenza:
Fatti non foste a viver come bruti,
Ma per seguir virtute e canoscenza.
Dante, *Inferno XXVI*, 118-120

ACKNOWLEDGMENTS

This work was primarily conducted at the Federal Institute for Materials Research & Testing (BAM) in Berlin, Germany, in the framework of its Ph.D. Programme, between August 2010 and February 2014. While I hope to have made an interesting contribution to the Black Yeast Community, this would not have been possible without many persons.

Thank you to Prof. Dr. Anna Gorbushina for giving me the chance to write the Ph.D. Thesis in an exciting research subject at the Department "Materials & Environment" of the BAM, Research Group "Model Biofilm in the Material Sciences," as well as for her supervision and the scientific discussions.

Thank you to Prof. Dr. Rupert Mutzel at the Freie Universität Berlin for being the *Erstgutachter* and allowing me to graduate at the Department of Biology, Chemistry and Pharmacy, and for the excellent chili con carne at the *Lange Nacht der Wissenschaften*.

Dr. Francesc X. Prenafeta-Boldú hosted me as research student in autumn 2012 in his group at the Institute of Agrifood Research & Technology (IRTA) in Torre Marimon (Catalonia, yet Spain). Parts of this thesis could only be developed due to his skilled supervision and sharp observations. I was amazed by the friendliness and open-heartedness of the Catalan people. *Gràcies, Francesc.*

Science is a community effort, and I am indebted to Nicole Knabe, Pedro Martin-Sanchez, Annette Naumann, Steffi Noack-Schönmann, Franz Seiffert and Jörg Toepel at the BAM for their collaboration, their constructive criticism and the collegial working atmosphere.

Thank you to Dr. Barry Bochner from Biolog Inc. (United States) for his professional and friendly support with the Biolog System and for being a kind host at the 2013 Biolog Conference in San Francisco.

A valuable part of the experimental results was produced by several undergraduate students whom I was fortunate enough to supervise, in particular Leoni Lang, Annette Pannenbecker, Michael Riddermann, Marco Tosi and Helen Y. Wong. I hope they learned from me as much as I learned from them thanks to their curiosity and enthusiasm.

Thank you to Prof. Dr. Regine Hengge for the participation at her *Science&Theatre* seminar at the Freie Universität Berlin and her insights on science and its social and cultural implications, for which I am truly grateful.

Thank you to my brother Alessandro for being a conspicuous role model. I suspect that if I wouldn't have chosen to study another discipline this thesis became a faded blueprint of yours.

A sincere thanks to Sissi and all my family and friends scattered throughout many locations for their continuous support, friendship, patience – and love. If I don't mention you by name here, be sure than exclusively word savings – not oblivion – gained the upper hand.

Halfway through this work I stopped cutting my hair, and besides the fact that it appealed my girlfriend it had two further advantages. Firstly, it was a tangible morning reminder of the efforts spent so far; and, secondly, it was a growing incentive for a swift graduation – if anything just for the sake of savings in shampoo. A Berliner barber will hopefully be pleased soon.

Without you he must have waited way longer.

Thank you. Danke. Grazie. спасибо. Gràcies. Gracias. 谢谢 Merci.

ABSTRACT

Black fungi are recently described microorganisms and amongst the most stress-tolerant eukaryotes currently known. They are a taxonomically diverse, but morphologically similar group of filamentous fungi that share two distinct signature characteristics, i.e. melanisation of the cell wall and compact colony morphology, which confer them passive, constituent extremotolerance. Albeit morphologically undifferentiated, black fungi show extensive phylogenetic and ecological diversity. Due to their persistence in unfavourable niches, they are ubiquitous on deserts and in glaciers and are permanent settlers of rock and other atmosphere-exposed material surfaces as well as man-made environments like salterns, humidifiers and dishwashers, and thus widespread in temperate regions worldwide. Some members are devastating opportunistic pathogens of invertebrates or vertebrates, including humans; others show symbiotic potentials with co-occurring microorganisms in extreme ecosystems. Beside their interest for fundamental biology, black fungi are important for several applied applications, e.g. in biotechnology, astrobiology, bioremediation and material preservation. Despite recent advances in the study of these fungi, many biological questions remain to be clarified regarding the molecular mechanisms underlying persistence, their physiology and nutritional modes, and their specific interactions with putative symbiotic partners. Models for pathogenic and halotolerant black fungi are established; however, no model was yet available for rock- and material-inhabiting ones. This thesis introduces the strain *Knufia petricola* A95 as a suitable model to study rock-inhabiting lifestyle. For this purpose, the strain was characterised at the physiological and molecular levels by phenotype microarrays, growth experiments and genome analyses as well as further methods. Cell-wall mutants of *K. petricola* A95 isolated during the course of this study were described and included in the comparative analysis to investigate effect of melanisation on physiology and stress tolerance. Direct comparisons were also performed between the model strain and the phylogenetically distant but ecologically, biogeographically and morphologically highly similar rock inhabitant *Coniosporium apollinis*. Preliminary observations of a model biofilm of *K. petricola* A95 and the photosynthetic cyanobacterium *Nostoc punctiforme* ATCC 29133 are introduced to study symbiotic interactions of rock-inhabiting microorganisms. Data presented here are a contribution to the understanding of ecophysiology and extremotolerance of rock-inhabiting black fungi.

ZUSAMMENFASSUNG

Schwarze Hefen sind jüngst beschriebene Mikroorganismen und zählen zu den widerstandsfähigsten derzeitig bekannten Eukaryonten. Diese taxonomisch sehr unterschiedlichen, jedoch morphologisch undifferenzierten filamentösen Pilze teilen zwei Hauptcharakteristika, nämlich die Melanisierung der Zellwand und die kompakte, blumenkohlartige Koloniebildung, was den Organismen passive und konstitutive Extremotoleranz verleiht. Obwohl morphologisch meist ununterscheidbar, weisen Schwarze Hefen eine ausgeprägte phylogenetische und ökologische Diversität auf. Aufgrund ihrer Beständigkeit in widrigen ökologischen Nischen, sind solche Mikroorganismen sowohl ubiquitär in Wüsten und auf Gletschern als auch dauerhafte Ansiedler von Stein- und weiteren umgebungsexponierten Oberflächen sowie anthropogenen Umgebungen wie Salzwerken, Luftbefeuchtungsanlagen und Geschirrspülern, und sind daher in der gemäßigten Klimazone weltweit verbreitet. Einige Mitglieder dieser Gruppe sind verheerende opportunistische Pathogene von Wirbellosen oder Wirbeltieren, einschließlich Menschen; für weitere Mitglieder, weisen einige Beobachtungen auf eine symbiotische Lebensweise mit gleichzeitig auftretenden Mikroorganismen an extremen Standorten hin. Neben ihrem Interesse in der Grundlagenforschung, sind Schwarze Hefen wichtig für zahlreiche angewandte Bereiche wie z.B. in der Biotechnologie, Astrobiologie, Bioremediation und im Materialschutz. Trotz neuerlicher Fortschritte in der Untersuchung solche Pilze, sind viele biologische Fragestellungen zurzeit noch abzuklären, wie z.B. hinsichtlich der molekularen Mechanismen ihrer Stresstoleranz, ihrer Physiologie und Ernährungsweise, und ihrer spezifischen Wechselwirkungen mit vermeintlichen symbiontischen Partnern. Modellorganismen für pathogene und salztolerante Schwarze Hefen sind bereits beschrieben; allerdings war noch kein passendes Modell für stein- und materialbesiedelnde Pilze vorhanden. Diese Doktorarbeit führt den Stamm *Knufia petricola* A95 als geeigneten Modellorganismus zur Untersuchung gesteinsbesiedelnder Lebensweise ein. Unter dieser Zielsetzung, wurde der Stamm auf physiologischer und molekularbiologischer Ebene anhand phänotypischer Microarrays, Genomanalysen, Wachstumsexperimenten und weiterer Methoden beschrieben. Zellwand-Mutanten von *K. petricola* A95 wurden während dieser Studie isoliert und beschrieben und in die komparative Analyse des Einflusses von Melanisierung auf Physiologie und Stresstoleranz eingeschlossen. Ein direkter Vergleich mit der phylogenetisch sehr unterschiedlichen, jedoch ökologisch, biogeographisch und morphologisch höchst ähnlichen gesteinsbesiedelnden Spezies *Coniosporium apollinis* wurde durchgeführt. Anfängliche Betrachtungen der Interaktionen zwischen *K. petricola* A95 und dem photosynthetisch aktiven Cyanobakterium *Nostoc punctiforme* ATCC 29133 wurden vorgestellt, um einen geeigneten Modellbiofilm aus gesteinsbesiedelnden Mikroorganismen zu etablieren. Die hier vorgestellten Ergebnisse sind ein Beitrag, um die Ökophysiologie und Extremotoleranz von Schwarzen Hefen zu verstehen.

TABLE OF CONTENTS

For a complete table of contents, see *A.1 Detailed table of contents* in the appendix.

1 INTRODUCTION

1.1 Life on the rocks – Some like it hot, cold, dry and frugal

A conspicuous part of the terrestrial surface is dominated by ecosystems seemingly inhospitable to life – subtropical arid deserts, glaciers and polar area, alpine mountains – characterised by extreme environmental conditions as intense solar irradiations, wide temperature fluctuations, lack of water and nutrient paucity [47,52,95,118]. Humanity strivings toward urbanisation expand these habitats with such interventions as the construction of concrete buildings and paved roads which offer, for dwelling life forms, little nourishment and protection from environmental exposure [132]. As harsh as this might seem, these surfaces are, however, far from sterile and harbour a wealth of specialised microorganisms from at least three different life kingdoms as permanent settlers, in particular fungi, bacteria and archaea [52,54].

Seemingly diverse ecosystems as hot and cold deserts, alpine regions or surfaces of buildings share in fact similar conditions, i.e. the direct exposure to environmental extremes and the strong fluctuation in external conditions. This entails direct solar irradiation, which includes mutagenic ultraviolet light and causes sudden and dramatic rises in temperature; deserts, including polar ones, are distinctively dry due to evaporation or to unavailability of free water; dryness results in local increases in ion concentrations; and, except for minerals, substances required for growth (primary nutrient sources, growth factors) are mostly scant. Rock surfaces are primordial terrestrial niches in which life has evolved early during Earth history, and paradigmatic for conditions encountered in such diverse habitats, insofar exposed to the atmosphere, oligotrophic and mostly detrimental to microbial development and persistence [52].

Microorganisms that dwell on rocks are not only able to withstand unfavourable conditions but, due to their specialised lifestyle, possess active metabolism, albeit extremely reduced. They have adapted to thrive in niches at the edge of life and gained a competitive advantage toward possibly co-occurring microorganisms; for the same reason, antibiosis is uncommon and neutral or mutually beneficial interactions are mostly observed [54,118]. Although rock dwellers are capable of growing alone, they are mainly organised in so-called subaerial biofilms (SABs) [52]. This consortium of loosely associated co-inhabiting species differs substantially from lichens, where the organisms are strictly symbiotic and have lost the ability to live on their own [1]. Although microbial composition of SABs varies, core settlers are known and include phototrophs (algae and cyanobacteria) and heterotrophs (actinobacteria and, in arid climates, predominantly black fungi) [52]. Such communities of microorganisms are mostly self-sufficient. The phototrophic partner is capable of atmospheric carbon and nitrogen fixation into organic compounds, providing a source of energy and nutrient to the heterotrophic counterpart(s) [86]; this latter, by contrast, is able to mobilise trace elements like minerals and offers protection from environmental stresses

like solar irradiation and desiccation [52]. Microorganisms in SABs are enmeshed in an extracellular matrix providing further shelter against dryness and mechanical stress [52].

Mechanisms of life development, persistence and propagation on rock surfaces are, as of today, not fully understood. This is partly dictated by the complex interactions of microorganisms and their slow growth in SABs or lichens, as well as the unavailability of suitable working models. Recently, interplays between phototrophic and heterotrophic rock-inhabitants has been reproduced in the laboratory [15,53] and a simplified model composed of the black fungus *Knufia petricola* A95 and the cyanobacterium *Nostoc punctiforme* ATCC 29133 has been proposed to study SABs [54]. While the phototrophic partner of this model biofilm is well studied at the molecular level [20,23,85,157], biology of black fungi is less understood and gained attention only in the last few decades.

1.2 Black fungi – Survival of the toughest

Rock-inhabiting black fungi were first isolated in the early '80s from three different locations – the Arizona (United States) and Negev (Israel) deserts and the Antarctica – and described as rock varnishes or compact microcolonial structures [47,76,123]. Black stains on rocks, previously mistaken as abiotic, were thus recognised of fungal origin and gained increasingly attention [67,96,97]. Soon, a link with already described black yeasts of medical relevance was established [27,29,30,33,35,83,84,145] and isolates from temperate climate regions were gained and described [14,37,57,121,125,128,156]. Despite their different ecology, today the term "black fungi" is used as an umbrella term to encompass filamentous ascomycetes with different ecology that share the following signature characteristics:

(i) incrustation of the cell wall with melanins, causing its distinctive brown to black colouration;
(ii) slow, isodiametric (meristematic) growth, resulting in the formation of compact, cauliflower-like microcolonies; and
(iii) occasional ability of the cells to reproduce by budding and absence of sexual stages.

Thus, the terms "black yeasts" or "black yeast-like fungi", as well as "meristematic fungi", "microcolonial fungi" (MCF) or the obsolete "dematiaceous fungi" are interchangeable with "black fungi" [27,35,126]. Microorganisms that share these features are morphologically very similar or even indistinguishable; this, along with their slow growth, is responsible for the scarce attention that they gained in microbiology until few decades ago [129]. However, the relevance of black fungi in microbial ecology, geomicrobiology, medicine and fungal phylogenetics as well as other applied researches is increasingly acknowledged [31].

Black fungi are amongst the most stress-resistant eukaryotes known to date and are described as polyextremotolerant or poikilotolerant [51,60,62,94,119]. Constitutive melanin synthesis from 1,8-dihydroxynaphtalene (1,8-DHN) monomers confers passive resistance toward environmental exposure to solar irradiation, dryness, temperature and pH extremes, hyperosmolarity and even ionising radiations [8,18,26,56,65,69,74,75,109,124]. Compact meristematic growth is a further adaptive trait that counteracts crumbling and dispersal of cells as well as water evaporation by minimising surface-to-volume ratio [97,130]. Additionally, many black fungi possess secondary metabolites, i.e. cell membrane associated carotenoids and intracellular mycosporines and mycosporine-like amino acids [56,73,148-150]. These confer, together with external melanins and compact colony morphology, a three-layered protection. Sexual reproduction and active dispersal have not been described [33,120], except for the genus *Capronia*, which is described as the teleomorph of the black-fungal genera *Cladophialophora* and *Exophiala* [4]. Instead black fungi acquire genetic variability by accumulating mutations in the genome [118,120] and rely on passive transport mechanisms to travel long distances [55]. The term “vegetative spore” has been introduced to describe undifferentiated, asexual and stress-tolerant black-fungal cells [59]. These adaptations enabled them to survive in ecological niches not colonised by most microorganisms, yet the specialisation resulted in constitutive slow metabolism, and black fungi lost the ability to compete with other species upon favourable environments; despite this, growth optima are mostly observed at mesophilic conditions and black fungi are extremotolerant rather than extromophilic [60]. Most probably, these reasons – adaptation to adverse conditions yet active metabolism at mesophilic conditions, as well as presence of a passive transport mechanism – contribute to in their worldwide distribution.

Besides their interest for basic research – e.g. in the investigation of extremotolerance at the biochemical and molecular level [61,71,99,135,144,159] or of phylogenetic relationships between rock-inhabiting, symbiotic and pathogenic fungi [62,64,89] – due to their persistence these microorganisms have attracted attention for several applications, e.g. in astrobiology [58,94] and bioremediation [103,104,163] as well as biodeterioration and preservation of materials and cultural heritage [40,57,127,131,153].

1.2.1 Variety undercover

Diversity of black fungi is not apparent at first glance and their multifarious ecology is not mirrored by considerable morphological differences. Yet members of this fungal group are ubiquitously widespread and have adopted many different lifestyles. Black fungi are amongst the most predominant rock settlers and are often observed in association with lichens, with which specific interactions, although they probable [15,53], have not been described yet [62,66,89]. Specialised niches, including both natural environments like ant nests [147], and man-made ones like salterns [17,65] and dishwashers [160], are known.

Some black fungi are frequently isolated from hydrocarbon-polluted sites [104,122] and pathogenic members of the group have been described [33]. In humans, pathogenic black fungi like *Exophiala dermatitidis* cause phaeohyphomycosis (i.e. cutaneous, subcutaneous or systemic infections of the brain and the lungs) and are amongst the most devastating infectious agents known to date, showing opportunistic lifestyle but able to infect immunocompetent individuals [29,81,82,161]. For these fungi, melanins are virulence factors which allow penetration into host cells or tissues and evasion of the host immune system [44,77,115,162]. It has been proposed that extremotolerance (melanisation, oligotrophism, tolerance to salt stresses and temperature fluctuations) as well as ability to assimilate hydrocarbons (see below, *Section 1.2.2*) are acquired traits which predisposed them toward pathogenic lifestyle [27,32,104].

Recently, phylogenetic studies with modern molecular techniques enabled a detailed analysis of members of the black fungi, confirming the enormous differences amongst them [43,63,64,110,116]. Black fungi are polyphyletic and found mainly in the orders *Capnodiales*, *Dothideales*, *Pleosporales* (class *Dothideomycetes*) and *Chaetothyriales* (class *Eurothiomycetes*). Phylogenetic knowledge allowed a rough ecological classification of pathogenic and lichen-associates black fungi into the *Chaetothytriales* and of environmentally relevant and extremotolerant ones into the other three orders. Nevertheless, exceptions are common. For example, the genus *Lichenotelia* (*Dothideomycetes*) forms border-line lichens [89], the salt-tolerant *Hortaea werneckii* (*Dothideomycetes*, *Capnodiales*) is pathogenic [65] and many chaetothyrialean black fungi are environmental isolates [56]. Among black fungi, rock-inhabiting lifestyle has emerged more often than pathogenic one and much earlier in the *Dothideomycetes* than the *Eurothiomycetes* [63,129]. Rock-inhabiting fungi (RIF) are widespread in all orders and form an early-diverging group from which pathogenic and lichenised lifestyles emerged [64]. Hence, the study of RIFs is of interest to investigate evolution of pathogenesis and symbiosis in fungi.

Convergent evolution at the morphological level camouflaged the extensive ecological and phylogenetic variety of black fungi [111]. Recent studies clarified their ecology and their phylogenetic relationship as well as the molecular mechanisms underlying extremotolerance [61,63,64,71,110,135]. Nevertheless, physiology and nutritional modes of black fungi, and RIFs in particular, are still less described.

1.2.2 Fasting, feasting, eating air?

Although physiology of black fungi has been investigated by classical tests [28,29,126,140], open questions on metabolism of rock-inhabiting microorganism remains, not least since sources of nutrients on rocks are barely known.

Rock surfaces are oligotrophic niches in which, except for inorganic nutrients, factors required for growth (primary nutrients and auxotrophic substances) are scarce [47,52]. Thriving of black fungi in such ecosystems is possible by their marked oligotrophism and extremely reduced growth rates [62,114]. Recently, the phenomenon of "radiotropism" has been observed in black fungi, i.e. the enhancement of growth upon exposure to ionising radiation, and it was proposed that melanins are directly involved in the storage of energy to support growth [25,26,109]. Thus, melanised cell wall would not simply confer passive resistance toward stress, but also help explain oligotrophic lifestyle of black fungi.

On the other hand, some nutrients might be present in non-limiting amounts. On rocks, organic carbon might be endogenously present in the form of dead or fossil organic biomass [125], as well as synthesised by photoautotrophic (lichens, algae or cyanobacteria) or lithoautotrophic settlers [52,54,66]. Organic nitrogen is also probably present, either provided by nitrogen-fixing (diazotrophic) bacteria or abiotically reduced in the atmosphere [47,54]. In addition to nutrients synthesised by primary producers, co-occurring heterotrophs might burst and release intracellular substances suitable for growth. Thus, rock-inhabiting species might be occasionally confronted with a wealth of nutrients and growth factors.

Apart from autochthonous sources, nutrients on rock surfaces are air-borne and exogenously introduced in the ecosystem as dust particles, rainfall deposits and animal droppings [21,97,125]. Interestingly, black fungi are known, since some years, to assimilate volatile organic compounds (aliphatic or aromatic hydrocarbons) as sole carbon and energy source [5,103,104,122,163]. This trait allows them to colonise specialised niches [147] or predominate in polluted urban environments [132], and confers them industrial potential for bioremediation purposes [101,104].

1.3 Aim of this study

Despite major advancements in the last years [34,36], several questions regarding biology of black fungi still remain open, in particular concerning their specialised lifestyle, nutritional modes and stress-resistance mechanisms. Further, even though the Black Yeast Community is rapidly growing and consistent advancements have been presented [151,152], a consensus on cultivation and analyses of meristematic fungi has not yet been reached, among others due to their peculiar growth behaviour.

The present thesis aims to establish the previously described strain *K. petricola* A95 as model microorganism to investigate rock-inhabiting black fungi [56,91]. Several approaches were undertaken to thoroughly characterise the strain and compare it with other black fungi. Phenotype microarray technology was employed to investigate growth requirements and nutritional metabolism in a high-throughput manner; a new synthetic medium for cultivation of black fungi was developed and used for build-up experiments; molecular

methods were adapted from standard protocols for genomic analyses; cell-wall mutants were isolated and described; and a distantly-related black fungus, *Coniosporium apollinis* [63,110,128], which origin as rock inhabitant has been estimated to be separated from those of *K. petricola* A95 by ca. 72 million years of evolutionary branching [63,128], was included in the analysis to dissect differences between morphologically undistinguishable but phylogenetically different rock-inhabiting strains. To investigate life development on rocks, oligotrophic mechanisms of *K. petricola* A95 were studied and preliminary results on the model subaerial biofilm composed of the black fungus and *N. punctiforme* ATCC 29133 were presented [54,86].

2 MATERIALS AND METHODS

2.1 Chemicals, solutions and growth media

Reagents (chemical grade) were provided by AppliChem GmbH, Merck KGaA, Carl Roth GmbH or Sigma-Aldrich (Germany). Further details, when relevant, are given throughout the text. Solutions and media were prepared with double-distilled water (Milli-Q Water Purification System from Merck Millipore, United States) and were sterilised either by autoclaving for 15 min at 121 °C and ca. 210 kPa in a Systec VX-75 autoclave (Systec GmbH, Germany) or, if specifically indicated, by filtration with 0.2 μm cellulose acetate filters (VWR Sterile Syringe Filter from VWR International, United States).

Composition of solutions and growth media is reported below.

ASM (A95-Specific Medium)[a]

D-Mannitol	100 mM
$NaNO_3$	80 mM
KH_2PO_4	5 mM
Na_2SO_4	2 mM
Citric acid (anhydrous)	20 mM
Stock solution 1 (100X)[b]	dilute 1/100
Stock solution 2 (2'500X)[c]	dilute 1/2'500
Stock solution 3 (1'000X)[d]	dilute 1/1'000
pH[e]	pH 5

[a] For solid ASM, medium was solidified with 20 g/L agar (Agar-Agar Kobe I, #5210.2 from Carl-Roth GmbH) and as carbon source 100 mM D-(+)-sucrose (# A4743 from AppliChem GmbH) was used instead of D-mannitol
[b] $MgCl_2$ 500 mM, KCl 500 mM (added before autoclaving)
[c] $Fe(NO_3)_3$*$9H_2O$ 2.5 mM, Na_2MoO_4*$2H_2O$ 2.5 mM, $MnCl_2$ 5 mM, $ZnCl_2$ 7.5 mM (added before autoclaving)
[d] Thiamine hydrochloride 10 mM, choline chloride 10 mM, N-acetyl-D-glucosamine 10 mM (filter-sterilised, added after autoclaving)
[e] Set to pH 5 with 5 M KOH

CTAB Buffer

Hexadecyltrimethylammonium bromide[a]	20 g/L
5 M NaCl	280 mL/L
0.5 M EDTA pH 8	40 mL/L
1 M Tris-HCl pH 8	100 mL/L

[a] CTAB, #52365 from Sigma-Aldrich

Haematoxylin Solution

Haematoxylin[a]	6 g/L
Sodium iodate	0.6 g/L
$Al_2(SO_4)_3$	52.8 g/L
Ethylene glycol	250 mL/L
Acetic acid	60 mL/L

[a] #CI 75290 from AppliChem GmbH

MEA (malt-extract agar) or MEB (malt-extract broth)

Malt extract[a]	20 g/L
D-(+)-Glucose[b]	20 g/L
Casein-digested peptone[c]	1 g/L
Agar[d]	20g/L

[a] #1.05391 from Merck KGaA
[b] #1.04074 from Merck KGaA
[c] #1.02239 from Merck KGaA
[d] Agar-Agar Kobe I, #5210.2 from Carl-Roth GmbH; omitted from MEB

Mineral Medium MM[a]

NH_4Cl	2 g/L
$MgSO_4*7H_2O$	0.1 g/L
K_2HPO_4	1.15 g/L
KH_2PO_4	5.91 g/L
Yeast extract[b]	200 mg/L
$FeCl_3$	0.24 mg/L
H_3BO_3	0.1 mg/L
$CuSO_4*5H_2O$	0.02 mg/L
KI	0.02 mg/L
$MnSO_4*H_2O$	0.09 mg/L
$Na_2MoO_4*2H_2O$	0.04 mg/L
$ZnSO_4*7H_2O$	0.15 mg/L
$CoCl_2*6H_2O$	0.1 mg/L
$AlK(SO_4)_2*12H_2O$	0.04 mg/L
$CaCl_2*2H_2O$	26.5 mg/L
NaCl	20 mg/L

[a] Prepared according to Prenafeta-Boldú *et al.*, 2001 [103]. Acidity of the medium was determined by the phosphate buffer (pH 6, buffer strength 50 mM). Mineral salts were added from a 500X stock solution.
[b] #103753 from Merck KGaA

10X MOPS[a]

3-(N-morpholino)propanesulfonic acid[b]	200 mM
Sodium acetate	20 mM
EDTA pH 8	10 mM

[a] In DEPC-treated ddH_2O; filter-sterilised with 0.45 μm filter and stored in the dark
[b] MOPS, #A1077 from AppliChem

PEG-NaCl Solution

Polyethylene glycol 8000[a]	200 mL/L
NaCl	146.1 g/L

[a] PEG, #P5413 from Sigma-Aldrich

0.1 M Phosphate Buffer pH 7.2

1 M K_2HPO_4 solution	71.5 mL/L
1 M KH_2PO_4 solution	28.5 mL/L

Protein Resuspension Buffer

Tris-HCl pH 7.5	20 mM
NaCl	20 mM
$MgCl_2$	10 mM

Protoplast Buffer

Tris-Base	10 mM
$MgSO_4*7H_2O$	10 mM
KCl	1 M
pH[a]	pH 7

[a] Set to pH 7 with 3 M HCl

SDS-PAGE Loading Dye

0.5 M Tris-HCl pH 6.8	1.25 mL
Glycerol	2.5 mL
10 % w/v SDS	2 mL
0.5 % w/v Bromphenol blue	200 μL
9.5 M Dithiothreitol	50 μL
ddH_2O	3.5 mL

Stacking Gel for SDS-PAGE

30 % v/v Acrylamide:Bisacrylamide 37.5:1	4 mL
1.5 M Tris-HCl pH 8.8	2.5 mL
10 % w/v Sodium dodecyl sulphate (SDS)	100 µL
Tetramethylethylenediamine (TEMED)	5 µL
10 % w/v Ammonium persulphate (APS)	50 µL
ddH_2O	3.3 mL

Resolving Gel for SDS-PAGE

30 % v/v Acrylamide:Bisacrylamide 37.5:1	2 mL
0.5 M Tris-HCl pH 6.8	2.5 mL
10 % w/v Sodium dodecyl sulphate (SDS)	100 µL
Tetramethylethylenediamine (TEMED)	20 µL
10 % w/v Ammonium persulphate (APS)	100 µL
ddH_2O	5.3 mL

10X TAE Buffer

Tris base	48.4 g/L
Glacial acetic acid	11.4 mL/L
0.5 M EDTA pH 8	20 mL/L

10X TBE Buffer

Tris base	108 g/L
Boric acid	55 g/L
0.5 M EDTA pH 8	40 mL/L

2.2 Microorganisms

The rock-inhabiting black fungus *Knufia petricola* (former *Sarcinomyces petricola*) strain A95 [56,91,148,156] was the main object of this study. This environmental, relatively fast-growing strain is easily handled in the laboratory [56,148] and is a non-pathogenic, pigment- and mycosporine-rich strain isolated in 1996 from a marble stone surface in Athens, Greece (Anna A. Gorbushina) [148,149]. *Knufia petricola* A95 belongs to an early-diverging lineage of the pathogen-rich ascomycetes order *Chaetothyriales* (class *Eurotiomycetes*) from which symbiotic lifestyle (lichenisation) has evolved [64], and it belongs to the same order as the well-studied pathogenic black fungus *Exophiala dermatitidis* [22,29,64,133]. Recently, the genome of *K. petricola* A95 has been sequenced in the framework of the Black Yeast Sequencing Project (Black Yeast Database, www.broadinstitute.org; annotation in progress).

For these reasons, the strain represents an excellent candidate model microorganism to study biology of rock-inhabiting black fungi.

The rock-inhabiting melanised fungus *Coniosporium apollinis* [110,128] was included in some of the experiments for a direct comparison with *K. petricola* A95. The strain was also isolated from a marble surface in Athens, Greece, and has similar ecology and morphology as *K. petricola* A95, but belongs to a different class of filamentous ascomycetes (*Dothideomycetes*). *Coniosporium apollinis* is also part of the Black Yeast Sequencing Project.

Several spontaneous, pink/orange mutants of A95 – likely deficient in cell-wall biogenesis – were isolated during this study and characterized further. They were named A95pm and numbered in chronological order according to isolation date.

Other microorganisms were included in some of the experiments, either as positive control strains or as additional object of this study (*Tab. 1*).

All strains are maintained at the Fungal Biodiversity Centre (CBS-KNAW, The Netherlands), the German Collection of Microorganisms and Cell Cultures (DSMZ, Germany) or the American Type Culture Collection (ATCC, United States) as well as at the BAM culture collection (Berlin, Germany).

Table 1. Microorganisms used in this study

Strain	Collection number	Description	Refs.
Knufia petricola A95	CBS 123872	Rock-inhabiting black fungus (*Eurotiomycetes*, *Chaetothyriales*); suitable model microorganism for RIFs	This study; [56,91]
A95pm1	n/a	Pink mutant of *K. petricola* A95, isogenic with the wild type	This study
A95pm2	n/a	Pink mutant of *K. petricola* A95, isogenic with the wild type	This study
A95pm3	n/a	Pink mutant of *K. petricola* A95, isogenic with the wild type	This study
Coniosporium apollinis	CBS 100218	Rock-inhabiting black fungus (*Dothideomycetes*, order not defined)	This study; [110,128]
Trametes versicolor	DSM 3086	White-rot basidiomycetes; positive control for laccase assay	[141]
Cladophialaphora psammophila	CBS 110553	Black fungus (*Eurotiomycetes*, *Chaetothyriales*); positive control for VOC-utilisation assay[a]	[5]
Fonsecaea spp.	n/a	Uncharacterized black-fungal strain (*Eurotiomycetes*, *Chaetothyriales*); tested in the VOC-utilisation assay	This study
Nostoc punctiforme	ATCC 29133	Symbiotic cyanobactierum; phototrophic partner in subaerial model biofilm	[54,86]

[a] The strain is able to grow on toluene as sole energy and carbon source (see *Section 3.II.4*).

2.3 Microbiological methods

2.3.1 Handling of fungal strains

Fungal strains were routinely grown on malt-extract broth or agar (MEB or MEA) for several days or weeks with (in liquid cultures) or without (on plates) shaking at 100 rpm. For all the experiments shown throughout the thesis, cells were grown at 25 °C, if not explicitly mentioned (e.g. *Section 2.3.5*). Liquid cultures were grown in 20 mL medium filled in 100 mL Erlenmeyer flasks by 1/100 inoculation of start cultures. Start cultures were obtained by growing the strains into the stationary phase. Growth on solid media was observed by spreading 100 μL of an appropriate dilution using a Drigalski spatula or streaking an undiluted culture with an inoculation loop on Petri dishes.

Prior to any analysis or inoculation, macroscopic cellular clumps were disrupted by pouring liquid cultures in metal beakers provided with eight stainless steel beads (ca. 5 mm diameter) and vigorous shaking (10 min at 30 Hz) in a MM400 Retsch Mixer Mill (Retsch Laborgeräte GmbH, Germany).

Cells were washed by removing spent media and at least two resuspending steps in physiological saline solution (0.9 % w/v NaCl) after centrifugation for 5 min at 7'000 rpm (#5430R table-top centrifuge from Eppendorf GmbH, Germany).

Axenic conditions were ensured by sterile work under a safety cabinet (SafeFlow 1.8 by BioAir, Euroclone S.p.A., Italy).

For long-term storage, strains were streaked on MEA slant agar and maintained at 4 °C.

2.3.2 Generation and isolation of protoplasts

Protoplasts were generated for the indicated purposes (e.g. karyotyping, see *Section 2.4.7*) with shaken MEB liquid cultures [16]. Cells in the early stationary phase were shaken (10 min at 30 Hz), washed with physiological solution, resuspended in 1/10 volume of Protoplast Buffer with 10 mg/mL "Lysing Enzymes from *Trichoderma harzianum*" (#L1412 from Sigma-Aldrich, United States) and incubated for 1-2 d at 27 °C, 100 rpm. Protoplasts were washed with Protoplast Buffer at 4 °C without exceeding 4'000 × *g* and concentrated 5-10X by resuspending in a 5-10X lesser volume of Protoplast Buffer.

Protoplasts were isolated by gradient centrifugation after adapting existing protocols [98,112]. Four millilitres of protoplast suspension thus generated were carefully laid on top of 44 mL 0.8 M sucrose with ca. 1.5 % w/v Ficoll (prepared by mixing 32 mL 1.2 M sucrose with 12 mL Histopaque-1077 from Sigma-Aldrich). Cells were centrifuged in a swinging bucket rotor for 10 min at 4'000 × *g* and 4 °C (Avanti J-26 XP centrifuge from Beckman Coulter Inc., United States) allowing intact cells and protoplasts to separate. Cells in the interphase were collected and counted with the Haemocytometer (using the same protocol as during the generation of growth curves; see below).

Identity, integrity and purity of protoplasts were verified under light microscope (Zeiss Primo Star from Carl Zeiss AG, Germany).

2.3.3 Generation of growth curves

Growth curves were generated with standardized shaken cultures by:

(i) viable count by plating on MEA expressed in colony-forming units per millilitre (CFU/mL),
(ii) microscopical cell count using a Haemocytometer (Neubauer Improved cell counting chamber from Hecht-Assistent, Germany) under light microscope (Zeiss Primo Star from Carl Zeiss AG, Germany), and
(iii) light-scattering measurements at 660 nm (Abs_{660nm}) using a UV-Vis spectrophotometer (NanoDrop 2000/2000c from Thermo Fisher Scientific, United States).

In (ii), residual cell clumps were defined as five or more cells clustering together and expressed as clumps/mL. In all cases appropriate dilutions in physiological solution were produced to obtain 30-300 colonies on MEA, count 20-200 cells + clumps under microscope and measure absorbance values between 0.2-0.6 to avoid re-scattering.

Generation time g [80] during exponential growth was calculated with the formula

$$g = t/n$$

with

t duration of exponential growth [h],
n number of generations or cell divisions [dimensionless].

Basing on the relationships

$$N(t_2) = N(t_1) \times 2^n$$

and

$$t = t_2 - t_1$$

with

$N(t_1)$, $N(t_2)$ cell population at time t_1, t_2 [CFU/mL]

we thus have

$$n = \log \frac{N(t_2)}{N(t_1)} \Big/ \log 2$$

and

$$g = t \times \log 2 \Big/ \log \frac{N(t_2)}{N(t_1)}.$$

Maximal increases in viable cells were calculated between inoculation and maximal CFU values.

2.3.4 Phenotypic analyses with the Biolog

Broad physiological characterisation of fungal strains for up to ca. 1'150 different growth conditions was performed using 96-well Phenotype MicroArray (PM) plates PM1-5 and PM9-16 developed by Biolog Inc. (Unites States) [10-12]. Briefly, phenotypic analyses with the Biolog System is done by inoculating cells in commercially available microtiter plates with wells each having a different chemical environment. Cellular activity and/or biomass accumulation is then evaluated to obtain insights into preferred growth conditions. The protocol includes a colourless, tetrazolium-based substrate that becomes purple upon active cell respiration (reduction of dye) [10].

Since black fungi do not form spores, rather than with them as recommended by the manufacturer, inocula were prepared with shaken cell suspensions. Shaken start cultures were washed and inoculated 1/100 or 1/1'000 in the viscous Phytagel-based FF-IF fluid (#72106 from Biolog Inc.) supplemented as required[1]. The commercially-available Redox Dye Mix E (100X, #74225 from Biolog Inc.) was added 1/100 to the inoculating fluid FF-IF to detect cellular metabolism, and plates were inoculated with 100 µL cell suspension in every well. Plates were sealed with parafilm and incubated at 25 °C for the desired time. An overview of the PM plates used as well as supplementation, inoculation and incubation time is given in *Tab. 2*.

[1] Supplementation according to the manufacturer's instructions (see *Tab. 2* for details). The different chemical environment in the wells is created by freeze-dried chemicals already present in each well upon purchase of Phenotype MicroArray plates.

Table 2. Biolog's Phenotype MicroArray plates and conditions used

Plate (Cat. No.)	Description	Supplementation[a]	Inoculum	Incubation[b]
PM1-2 (#12111-2)	C metabolism	FF-IF buffered at pH 5 with 20 mM citric acid[c]	1/100	11 d
PM3 (#12121)	N metabolism	100 mM D-(+)-glucose, 5 mM KH_2PO_4, 2 mM Na_2SO_4[d]	1/100	7 d
PM4 (#12131)	P and S metabolism	100 mM D-(+)-glucose[e]	1/1'000	5 d
PM5 (#12151)	Effect of growth factors	100 mM D-(+)-glucose, 5 mM KH_2PO_4, 2 mM Na_2SO_4[f]	1/1'000	11 d[g]
PM9-16 (#12161-2, 12211-6)	Effect of salts, pH or drugs	100 mM D-(+)-glucose, 6.7 g/L yeast nitrogen base[h]	1/100	7 d

[a] Additionally, all plates were supplemented with Redox Dye Mix E (1 % v/v)
[b] Optimal incubation time for phenotypic analyses of *K. petricola* A95 as determined experimentally for each plate; incubation time varied for other strains and is indicated in the figure captions (see *Section 3.II.3*)
[c] Trace elements as well as nitrogen, phosphorus and sulphur sources were already provided in the wells
[d] Trace elements were already provided in the wells
[e] Trace elements as well as nitrogen and either sulphur (to test phosphorus catabolism) or phosphorus (to test sulphur catabolism) sources were already provided in the wells
[f] Trace elements and nitrogen source were already provided in the wells
[g] For experiment with 1 μM thiamine (*Fig. 11*), incubation time was reduced to 7 d since stronger background growth was observed
[h] #239210 from Difco BD & Co. (United States)

Growth and reduction of tetrazolium dye was monitored spectroscopically as recommended by the manufacturers with the MicroStation™ System and MicroLog™ Software (Release 4.2 from BIolog Inc.), as well as with the Synergy™ HT microplate reader and Gen5™ 2.0 Software (from BioTek Instruments Inc., United States). Spectroscopic measurements were done at 490 nm (Abs_{max} of reduced tetrazolium dye) and 750 nm (Abs_{max} of fungal mycelia) and metabolic activity was calculated by subtracting values

$$\Delta Abs = Abs_{490nm} - Abs_{750nm}.$$

Eventually, since spectroscopic measurements did not give the expected results (see *Section 3.II.3*), analysis of growth was performed by visual inspection of biomass formation. Visual inspection of growth was done by at least two persons independently by using an *ad hoc* scoring system and each plate type was inoculated at least three times. Growth in each well was compared with those in negative control well (i.e. for plates PM1-4 without nutrient source, for plate PM5 without growth factors) and scored with:

2 for strong growth,
1 for growth,
0 for no growth (or no difference with negative control in case of background growth),
b for borderline growth (unsure between 0 and 1).

In case of multiple assignments of the value "b" (i.e. by more than one person for the same well), growth was scored with 0.5, otherwise with 0. When poor overall growth (i.e. on the whole plate) or strong background growth (i.e. in the negative control well) were observed, plates were incubated longer or shorter, respectively. If the problem of strong background growth could not be circumvented, scoring with "2" was omitted.

Plates with salt, pH or drug gradients (PM9-16) were evaluated as illustrated above but using additionally:

1.5 for medium strong growth, and
0.5 for poor growth.

In such a way numerical values reflecting physiological preferences under the various growth conditions were obtained, allowing the generation of broad phenotypic profiles for the analyzed strains.[2] Results are shown as charts, presented as median with first and third quartiles calculated for at least six growth analyses (at least three repetition and at least two independent evaluations each); minimum and maximum values are also shown.

2.3.5 Temperature-optimum profiles

Temperature-optimum profiles were generated by growing fungal strains on solid media and inspecting increases in colony size. Hereby, 100 µL of start culture (1/10'000 dilution) were plated (in duplicate) on agar media and incubated for up to 4 weeks at 5 to 35 °C with 5 °C step-wise temperature increase.

Total projected surface area of colonies was determined with the Java image processing software ImageJ, version 1.47 (32-bit) developed by the National Institute of Health (NIH, United States) using 8-bit TIFF images of whole plates taken from above and manually selecting ROIs (regions of interest, i.e. colonies) on the plates with Wand Tool with tolerance of 50 pixels. Average colony size expressed in mm^2 was calculated by dividing the total area by number of colonies.

2.3.6 Growth experiments

Experiments were carried out to analyze response of black fungi to different media, growth conditions or stress stimuli. Strains were subjected to diverse conditions and effects were assessed by visual inspection of growth, viable counting (expressed as CFU/mL), colony size (expressed in mm^2, see *Section 2.3.5*) and/or dry weight measurements after desiccating the biomass for ca. 16 h at 70 °C in a Memmert ICP 600 Incubator (Memmert GmbH, Germany).

[2] Even if spectroscopical measurements were not performed, tetrazolium dye was added since it was helpful to recognize clumps in wells, especially upon poor growth.

Resistance toward ultraviolet irradiation was assessed immediately after plating strains on MEA (dilution 1/1'000) by treatments for the indicated time with germicidal 254-nm UVC (#G40T10 40W lamp from Sankyo Denki Co. Ltd., Japan) under a safety cabinet or with environmental 340-nm UVA at 50 W/m^2 (UVA-340 Sunlamp Fluorescent from Q-Lab GmbH, Germany)[3] in a weathering chamber (Global UV Test 200 from Weiss Umwelttechnik GmbH, Germany).

Effects of nutrient limitation were observed in oligotrophic media, i.e. the defined medium ASM deprived of primary nutrients (C, N, P or S), as well as in pure water – both liquid and solidified with agar. Dead fungal biomass, prepared as indicated in *Tab. 3*, was added to the oligotrophic media as nutrient supplement (10 % v/v) to discern its putative growth-enhancing properties.

Table 3. Preparation of dead fungal biomass as nutrient supplement in oligotrophic media

Biomass	**Preparation**[a]
Autoclaved biomass	Wash and resuspend in the original volume of saline solution, autoclave (15 min at 121 °C, ca. 210 kPa)
Ethylene-oxide biomass	Wash in saline solution, centrifuge and remove supernatant, lyophilise (*Section 2.5.1*), sterilize by treatment with ethylene oxide (cold-sterilisation method), resuspend in the original volume of saline solution
Autoclaved cell fragments	Lysis with French© Press (*Section 2.5.1*), wash and resuspend cell fragments in the original volume of saline solution, autoclave
Autoclaved protoplasts	Generate protoplasts (*Section 2.3.2*), wash in Protoplast Buffer and resuspend cells in the original volume of saline solution, autoclave
Intracellular fraction	Wash and resuspend in the original volume of saline solution, lyse with French© Press (*Section 2.5.1*), sterile-filter supernatant with 0.2 μm filters

[a] As starting material, *K. petricola* A95 was grown for 1 w in MEB (stationary phase, ca. 2.69 × 10^7 cells+clumps/mL, see *Fig. 7*) and shaken as reported in *Section 2.3.1.*

2.4 Molecular biology methods

2.4.1 Nucleic acid extractions

DNA was extracted from stationary-phase liquid cultures. Circa 250 mg biomass (fresh weight) was filled in 1.5 mL screw-cap tubes with 1 g glass pearls (0.5 mm^2 diameter, #N030.1 from Carl Roth GmbH, Germany), 600 μL CTAB buffer and 600 μL Phenol:Chloroform:Isoamyl acohol 25:24:1 solution (#P2069 from Sigma-Aldrich). Cells were lysed by vigorous shaking for 60 s at 5 m/s in Hybaid RiboLyser (#FP120 from Hybaid GmbH, Germany). Following centrifugation (15 min at 12'300 rpm, 4 °C), the liquid phase was transferred into a microcentrifuge tube and the identical volume of Chloroform:Isoamyl alcohol 24:1 (#C0549 from Sigma-Aldrich) was added; DNA was centrifuged again (10 min at 12'300 rpm, 4 °C), liquid phase was collected in a fresh tube and double volume of PEG-NaCl

[3] Petri dishes were incubated with lid to avoid contamination resulting to a 10-20 % shielding of UVA irradiation and thus to ca. 40 W/m^2 (Volker Wachtendorf, personal communication).

Solution was added, followed by 2 h incubation at 4 °C. DNA was pelleted by centrifugation (30 min at 12'300 rpm, 4 °C) and the supernatant was discarded, then pellet was washed with 70 % v/v ethanol and air dried for 20 min at 25 °C. DNA was resuspended in 30-50 µL ddH_2O and stored at -20 °C.

Total RNA was extracted either by single-step or on-column isolation methods depending on the downstream application. Particular care was taken with regard to RNase contaminations by treating solutions with diethylpyrocarbonate (add 0.1 % v/v DEPC, incubate 1 h at 37 °C, autoclave), by baking lab equipments (at least 4 h at 180 °C) and by safe laboratory work on ice.

For lab-scale analyses, cells from 10 mL exponential-phase culture (2 d at 25 °C in MEB) were lysed in 1 mL TRIzol® Reagent (#15596 from Life Technologies, United States) with ca. 0.1 g silica beads (0.1 mm^2 diameter) for 60 s at 5 m/s in Hybaid RiboLyser. Ribonucleid acids were isolated with 1 mL TRIzol® Reagent according to the manufacturer's instructions and resuspended in 50 µL DEPC-treated ddH_2O.

To obtain large amounts of RNA for genome annotation, RNA was extracted using RNeasy Midi Kit (#75144 from Qiagen, Germany). Cells were collected at different growth conditions to broadly activate gene expression (*Tab. 4*). Ribonucleic acid transcription was interrupted by adding 1/8-volume of pre-chilled Stop Solution (5 % water-saturated phenol in ethanol) and, after washing twice, cells were resuspended in 10 mL RLT lysis buffer (#79216 from Qiagen) with 1 % v/v β-mercaptoethanol (#4227 from Carl Roth GmbH). Cellular lysis was achieved in metal beakers with ca. 8 mL glass pearls (0.5 mm^2 diameter) by vigorous shaking (10 min at 30 Hz) in MM400 Retsch Mixer Mill. Supernatant was collected and RNA was isolated by column purification according to the manufacturer's instructions and eluted in 500 µL DEPC-treated ddH_2O.

2.4.2 Quality of nucleic acids

Concentration and purity of nucleic acids were determined by spectrophotometric measurements (NanoDrop 2000/2000c from Thermo Fisher Scientific) at 260 nm in 1 mM NaH_2PO_4 and calculation of absorbance ratio at 260 nm vs. 280 nm (Abs_{260nm}/Abs_{280nm} ratio). Quality of total RNA was assessed by agarose gel electrophoresis (see *Section 2.4.5*) or, for sensitive downstream applications (i.e. genome annotation), by formaldehyde agarose gel electrophoresis as well as with Agilent 2100 BioAnalyzer on RNA Nano LabChips (RNA Series II Kit from Agilent Technologies Inc., United States) according to the manufacturer's instructions with 1 µL samples (diluted to 50 ng/µL).

Table 4. Growth conditions for RNA isolation from* Knufia petricola *A95 for genome annotation

No.	Growth conditions	Details
1	Early-exponential phase, complex medium (liquid)	16 h at 25 °C in 300 mL MEB
2	Late-exponential phase, complex medium (liquid)	4 d at 25 °C in 100 mL MEB
3	Stationary phase, complex medium (liquid)	8 d at 25 °C in 60 mL MEB
4	Late-stationary phase, complex medium (liquid)	2 w at 25 °C in 60 mL MEB
5	Complex medium (solid)	2 w at 25 °C on MEA[a]
6	As on 2, with cell-wall stress	4 d at 25 °C in 100 mL MEB + 0.5 % v/v CMC[b]
7	Late-exponential phase, defined medium (liquid)	4 d at 25 °C in 100 mL ASM[c]
8	As on 7, at low temperature	4 d at 16 °C in 120 mL ASM
9	As on 7, at high temperature	4 d at 30 °C in 120 mL ASM
10	Defined medium with salt stress (liquid)	11 d at 25 °C in 200 mL ASM + 6 % w/v NaCl
11	Defined medium at low pH (liquid)	7 d at 25 °C in 200 mL ASM pH 3.5
12	Defined medium under nutrient deprivation (liquid)	5 d at 25 °C in 500 mL ASM-S[d]

In samples 10-12, culture volume and incubation time were increased to counteract poor growth yield.
[a] To collect biomass, cells were grown after plating (100 µL shaken start culture + 900 µL MEB) on nitrocellulose membrane (#HP40.1 Roti-NC membrane from Carl Roth GmbH) laid on MEA. Filter was soaked in 17.5 mL ddH_2O + 2.5 mL Stop Solution (5 % water-saturated phenol in ethanol) to collect biomass.
[b] Carboxymethylcellulose sodium salt (low viscosity, #C5678 from Sigma-Aldrich)
[c] A95-Specific Medium (see *Section 3.II.5*)
[d] A95-Specific Medium deprived of sulphur

2.4.3 Manipulation of nucleic acids

For lab-scale analyses (i.e. to detect activity of laccase genes, see below), RNA samples were prepared as following. DNA was removed from RNA samples (5-10 µg total RNA) by digesting with 2 U recombinant DNase I (#BP3226 from Thermo Fisher Scientific) with the corresponding 10X buffer in 10 µL reaction volume for 30 min at 37 °C. DNase I was inactivated by incubating 10 min at 70 °C. Complementary DNA (cDNA) synthesis was carried out with DNase I-digested total RNA (ca. 0.5 µg) using 2 µL iScript™ Reverse Transcriptase Supermix for RT-qPCR (#170-8840 from Bio-Rad Laboratories, Unites States) in 10 µL reaction volume at the following sequential temperature steps: 5 min at 25 °C, 30 min at 42 °C, 5 min at 85 °C. After each treatment, quality of RNA samples was verified by spectrophotometric measurements (NanoDrop 2000/2000c from Thermo Fisher Scientific).

DNA was sequenced by the Sequencing Service Company at the Humboldt University of Berlin by capillary electrophoresis using the chain-termination method (Dr. Martin Meixner).

2.4.4 Polymerase chain reactions and oligonucleotides

Polymerase chain reactions (PCRs) were run in C1000 Thermal Cycler (Bio-Rad Laboratories) with 1.0-2.5 U DNA *Taq* Polymerase and 10X *Taq* buffer (#EP0401 from Thermo Fisher Scientific), 0.5 µL dNTP mix (10 mM each, #R0142/-52/-62/-72 from Thermo Fisher Scientific), 1 µL suitable primers at 20 pmol/µL (synthesized by *biomers.net* GmbH,

Germany) and ca. 100-200 ng template DNA in 25 µL reaction volume. Thermal cycles (repeated 35-40X between T_{den} and T_{el}) were set up as following:

T_{in}	95 °C	5 min	Initial denaturation step
T_{den}	95 °C	1 min	Denaturation of dsDNA segments
T_{ann}	Variable[a]	1 min	Annealing of primers
T_{el}	72 °C	Variable[b]	Elongation of complementary DNA
T_{end}	72 °C	10 min	Finish synthesis of incomplete amplicons
T_{fin}	4 °C	∞	Storage temperature

[a] Primer specific (usually 5 °C less than primers' melting temperature T_{melt})
[b] Depending on amplicon size (usually 1 min for each kb)

Oligonucleotides are reported in *Tab. 5*. Primers sequences were reported in previous studies or designed with PrimerSelect™ from LaserGene® (DNASTAR Inc., United States).

Table 5. Oligonucleotides used in this study

Name	Sequence (5' to 3')	T_{melt} (°C)	Purpose	Amplicon size (nt)	References[a]
ITS-1	TCCGTAGGTGAACCTGCGG	65.0	Amplification of ITS[b] region; sequencing of amplicon (forward)	ca. 700	[78,154]
ITS-4	TCCTCCGCTTATTGATATGC	58.0	Amplification of ITS[b] region (reverse)		
ITS-Int	TAATCAAGTACATTCAGACG	54.0	Sequencing of ITS[b] region (internal reverse primer)	n/a	*Section 3.I.3*
00745fw	ACAGCCAACGGTCGATAACTCTC	56.2	Amplification of putative laccase gene 00745 (forward)	109	*Section 3.IV.3*
00745rev	GGGCGGTCTGTACATCTTTCCTT	57.4	Amplification of putative laccase gene 00745 (reverse)		
09127fw	CGCGGACGCCCTTATCTTGAA	60.8	Amplification of putative laccase gene 09127 (forward)	108	*Section 3.IV.3*
09127rev	CCTGCGCCGTTGGTGAGTTTG	62.2	Amplification of putative laccase gene 09127 (reverse)		
09687fw	GCCAATATCCCGGACTCAGACCTC	60.8	Amplification of putative laccase gene 09687 (forward)	144	*Section 3.IV.3*
09687rev	AGTGCCAGCGCCGATCATAAAGTA	60.7	Amplification of putative laccase gene 09687 (reverse)		
04700fw	CAAGGCGAGACGTCCAACTGCT	60.2	Amplification of putative laccase gene 04700 (forward)	149	*Section 3.IV.3*
04700rev	ATCTGCCGGCCGCTCCAATA	61.2	Amplification of putative laccase gene 04700 (reverse)		
03963fw	ACATTGACCTCGGGCCACTTTTAC	59.2	Amplification of putative laccase gene 03963 (forward)	132	*Section 3.IV.3*
03963rev	CTTTGCCGTTGATGAGGTTGTTGT	59.0	Amplification of putative laccase gene 03963 (reverse)		
01838fw	ACAAAGAATGACACGAGCGAAAAT	56.0	Amplification of putative laccase gene 01838 (forward)	144	*Section 3.IV.3*
01838rev	AAAAGTGGCGTTGGGCAGAGAA	59.6	Amplification of putative laccase gene 01838 (reverse)		
04147fw	CACGGCCATGACTTCTCGCTCCTC	64.8	Amplification of putative laccase gene 04147 (forward)	100	*Section 3.IV.3*
04147rev	CTGTGTCACGTCGCATTGGGTTGT	62.6	Amplification of putative laccase gene 04147 (reverse)		
08679fw	CGAGCCGGCAGCCACTAACTTT	61.3	Amplification of putative laccase gene 08679 (forward)	109	*Section 3.IV.3*
08679rev	GGAGGAGCTTGAGCCGCCATTCTT	64.5	Amplification of putative laccase gene 08679 (reverse)		
09945fw	CCGTCAGGGTGGGCCGTTATTAG	62.2	Amplification of putative laccase gene 09945 (forward)	145 (254)[c]	*Section 3.IV.3*
09945rev	TCGACCCCACCGTACTTATCATTC	57.9	Amplification of putative laccase gene 09945 (reverse)		
09443fw	GGGGTCGGGTGAAGGCGTGTT	63.7	Amplification of putative laccase gene 09443 (forward)	106	*Section 3.IV.3*
09443rev	CGGTGGCAAATCTATGGTGTCTCG	61.3	Amplification of putative laccase gene 09443 (reverse)		

[a] Text references (this study) are indicated
[b] Internal transcribed spacer
[c] Amplicon size of putative laccase gene 09945 in brackets refers to genomic DNA (with intron sequences)

2.4.5 Agarose gel electrophoresis

Agarose gel electrophoreses [112] to separate nucleotides by size were performed with 1.0-2.5 % w/v agarose (#11404 from SERVA Electrophoresis GmbH, Germany) in 0.5X TAE buffer at the specified conditions using MUPID-exU device (#MU-0040 from Eurogentec, Belgium). As size marker, 100 bp GeneRuler DNA Ladder with the corresponding 6X DNA Loading Dye (#SM0241 and #R0611, both from Thermo Fisher Scientific) was used. Gels were stained for 15 min in 3X gel red staining solution (105 μL 10'000X gel red, #M3199 from Genaxxon BioScience GmbH, Germany, in 350 mL 0.1 M NaCl solution). Bands were visualized by UV transillumination with ChemiDoc™ XRS+ System and ImageLab Software (#170-8265 from Bio-Rad Laboratories).

2.4.6 Formaldehyde agarose gel electrophoresis

Formaldehyde gel electrophoreses [112] with 1.5 % w/v agarose were performed to verify quality of total RNA samples. Formaldehyde gels (2.2 M) were prepared by dissolving 1.5 g agarose in 72 mL ddH_2O with 10 mL 10X MOPS buffer and 18 mL 39 % w/v (12.3 M) formaldehyde (#20910 from VWR International GmbH, Germany). Up to 2 μg total RNA were mixed with 2X RNA Loading Dye (#R0641 from Thermo Fisher Scientific), denaturated 10 min at 70 °C and loaded on the gels (final volume 20 μL). RiboRuler High Range RNA Ladder (#SM1821 from Thermo Fisher Scientific) was used as size marker (4 μL mixed with 4 μL 2X RNA Loading Dye). Gels were run in 1X MOPS for 1-2 h at 100 V. Bands were visualized as for standard agarose gel electrophoreses (no staining needed since RNA Loading Dye contains ethidium bromide).

2.4.7 Rotating field gel electrophoresis (karyotyping)

Pulsed-field gel electrophoresis (PFGE) was chosen as method to karyotype black fungi [112,117]. Rotating-field gel electrophoresis (ROFE), a type of PFGE allowing versatility in electric field separation angle, was set up with Rotaphor 6.0 System, the corresponding software, and the provided accessories (Biometra GmbH, Germany).

Protoplasts at the desired cellular concentration (isolated as described above) were melted in plugs of 1 % w/v low melting point agarose (#A9414 from Sigma-Aldrich) in 0.125 M EDTA pH 7.5 within the provided moulds. Plugs were submerged in 0.5 EDTA + 7.5 % v/v β-mercaptoethanol and incubated 16 h at 37 °C to disrupt cell membranes and digest cellular debris; they were then submerged in DNSK (0.5 M EDTA + 1 % w/v N-laurylsarcosine + 0.5 mg/mL Proteinase K from AppliChem) and incubated 16 h at 50 °C to digest proteins. Plugs were washed twice in 0.5 M EDTA and stored at 4 °C.

Gels were casted in the provided 20 × 20 cm^2 frame with 1 % w/v UltraPure Agarose (#16500 from Life Technologies) in 0.5X TBE buffer. Separation of DNA fragments was achieved in 2.4 L 0.5X TBE buffer (adapted from [68,112]). Optimal electrophoretic

conditions were determined experimentally basing on the existing literature or using Biometra pre-set programs (details indicated in *Figs. 44-45*). Constant temperature (14 °C) was ensured with thermostat MultiTemp II (#LKB2219 from GE Pharmacia, United States). Chromosomal DNA from *Saccharomyces cerevisiae* (#170-3605 from Bio-Rad Laboratories) and *Schizosaccharomyces pombe* (#170-3633 from Bio-Rad Laboratories) were used as size markers. For DNA staining, gels were submerged for 15 min in 1 μg/mL ethidium bromide (#M3178 from Genaxxon BioScience GmbH) in ddH_2O and then washed for 15 min in ddH_2O. Bands were visualized as for standard agarose gel electrophoreses.

2.4.8 Bioinformatics

Genomic sequences of black fungi were retrieved from the National Center for Biotechnology Information (NCBI, Unites States, www.ncbi.nlm.nih.gov) or the Black Yeast Database (Black Yeast Sequencing Project, Broad Institute of Harvard and MIT, Unites States, www.broadinstitute.org). Nucleotide sequences were analyzed *in silico* with Clone Manager (Version 8.04 from Sci-Ed Software, United States). Multiple sequence alignments were performed with ClustalW2 tool (http://www.ebi.ac.uk/Tools/msa/clustalw2/) from the European Bioinformatics Institute at EMBL (United Kingdom).

Putative laccase genes were identified based on the draft sequence of *K. petricola* A95 (Black Yeast Database of the Broad Institute, www.broadinstitute.org, not yet publicly available).[4] Further candidate genes were selected by BLAST algorithms (BLASTn and BLASTp) using putative laccases from the better characterized black fungus *E. dermatitidis* as query.[5]

2.5 Biochemical and analytical methods

2.5.1 Preparation of biomass

When biomass needed further treatment, cells were treated as described below.

Biomass was preserved for downstream applications (e.g. carotenoid analysis) by snap-freezing in liquid nitrogen and storage in -80 °C.

Cells were mechanically lysed after washing in saline solution at 18'000 psi for 3 times using French© Press (Model F-10 HTU-DIGI-F-Press from G. Heinemann, Germany). Successful lysis was verified under light microscope (Zeiss Primo Star). Supernatant was separated from cell debris and intact cells by centrifugation (6'800 × *g* for 10 min at 4 °C) and stored at 4 °C.

Lyophilisation (after spreading washed cells on a Petri dish to maximize surface-to-volume ratio) was achieved at 0.25 mbar and -50 °C for 24 h using Gamma 1-20 freeze-dryer (from

[4] February 2014.

[5] Putative *Exophiala dermatitidis* laccases: HMPREF1120_05645.1, HMPREF1120_02828.1, HMPREF1120_02754.1, HMPREF1120_00199.1, HMPREF1120_04510.1, HMPREF1120_05865.1, HMPREF1120_04578.1, HMPREF1120_08564.1

Christ Gefriertrocknungsanlage GmbH, Germany). Cells were collected by scraping with a sterile scalpel and stored at -80 °C.

2.5.2 Laccase (oxidase) assays

Presence of laccase(s) (EC1.10.3.2) was screened on chromogenic medium supplemented with 0.03 % w/v ABTS (2,2'-azino-bis(3-ethylbenzothiazoline-6-sulphonic acid), #A1088 from AppliChem). In liquid media, presence of laccase(s) was assessed by development of purple colour in the supernatant; on plates, 10 µL of a shaken start cultures (undiluted and diluted 1/10, 1/100 and 1/1'000) were inoculated (by dropping, without spreading) and formation of halos around the biomass was observed after incubation of cells. To gain insight into oxidative activity, absorbance in chromogenic liquid cultures was measured by spectrophotometric measurement of supernatants at 420 nm (Abs_{420nm}) with the NanoDrop 2000/2000c (Thermo Fisher Scientific). *Trametes versicolor* DSM 3086 was used as positive control in both cases.

2.5.3 Gas chromatographies and hydrocarbon-utilisation assay

Assimilation of volatile organic compounds (VOCs) benzene, toluene and pentane as sole carbon and energy source was tested as described in Badali *et al.*, 2011 [5]. *Cladophialophora psammophila*, which grows on toluene as sole nutrient source, was used as positive control. Hydrocarbon-utilisation assay was performed in 250 mL Boston flasks sealed with Mininert Teflon valves (from Phase Separation, The Netherlands) to prevent VOC leakage. Flasks were filled with 25 mL buffered Mineral Medium MM and injected using a syringe with 10 µL benzene, toluene or pentane resulting in an initial concentration in the liquid phase of ca. 1.52 mM for benzene, 1.11 mM for toluene and 7.24 µM for pentane.[6] The experimental set-up also included the controls:

(i) without any added C source (negative control to determine endogenous respiration),
(ii) with D-(+)-glucose instead of VOC (700 mg/L, i.e. ca. 3.89 mM; positive control), and
(iii) with both D-(+)-glucose and VOC (700 mg/L; co-metabolism and toxicity control).

After gas-liquid substrate equilibration, ca. 100 µg (defined with viable counting at ca. 1-40 × 10^4 CFU) black-fungal biomass grown on MEA was resuspended in 1 mL ddH_2O and inoculated in the media. Flasks were incubated at 25 °C under static conditions. Abiotic controls (two Boston flasks with all three VOCs together but without fungal cells) were

[6] At equilibrium. Concentrations in the liquid phase are calculated basing on the known Henry's Law constants for benzene (H_C = 4.6) toluene (H_C = 3.8) and pentane (H_C = 0.019) at 25 °C [2]. 10 µL hydrocarbons were added according to a previous study on toluene assimilation by *C. psammophila* [5]. Pentane, which has much lower H_C value and lower solubility, was added in excess.

included in the analysis and measured twice to rule out substrate leakages and validate analytic measurements.

Growth and substrate consumption were assessed by gas-chromatographic analyses by measuring increase in carbon dioxide and decrease in substrate concentrations, respectively. Headspace measurements were done over a period of ca. 5 w. For CO_2, 200 µL gas sample was injected into Varian chromatograph (model CP-3800 by Agilent Technologies) provided with Hayesep Q 80-100 column (Agilent Technologies) and Thermal Conductivity Detector (GC-TCD). Helium at a flow rate of 45 mL/min was the carrier gas and temperatures of column and detector were 90 °C and 180 °C, respectively. Concentration of VOCs was determined in 100 µL headspace by injection into ThermoQuest chromatograph (model GC Trace 2000 from CE Instruments Ltd., United Kingdom) provided with TRB 624 column and Flame Ionization Detector (GC-FID). Helium at a flow rate of 2 mL/min was the carrier gas and measurements (split-less, isothermal) were carried out at column and detector temperatures of 180 °C and 250 °C, respectively. Amount of carbon dioxide and hydrocarbons in the gas phase were extrapolated based on calibration curves with defined CO_2 and VOC concentrations to convert peak integration areas in gas chromatographs into substance concentrations (*A.5 Supplementary data*).

Concentration of hydrocarbon in the gas and liquid phases were inferred with the Henry's Law. The Henry's Law for gaseous substances is defined as

$$p = H_C \times c$$

with

p	partial pressure of solute in the gas phase [atm],
c	concentration of solute in the liquid phase [mol/L],
H_C	Henry's Law constant [atm × L/mol].

Hence, it follows that

$$H_C = p/c.$$

The Henry's Law constant H_C is also defined as the water-air distribution ratio[7] and can be expressed as

$$H_C = c_{aq}/c_g \text{ [dimensionless]}$$

[7] H_C values at 25 °C are reported in the literature for several volatile compounds [2].

with

c_{aq}	concentration of chemical in the liquid phase [g/L or mol/L],
c_g	concentration of chemical in the gas phase [g/L or mol/L].

For volatile compounds at equilibrium between liquid and gas phases apply the formula

$$M_{tot} = c_{aq} \times V_{aq} + c_g \times V_g$$

with

M_{tot}	total amount of chemical in the system [g or mol],
c_{aq}	concentration of chemical in the liquid phase [g/L or mol/L],
c_g	concentration of chemical in the gas phase [g/L or mol/L],
V_{aq}	volume of chemical in the liquid phase [L],
V_g	volume of chemical in the gas phase [L].

Therefore the two-equation system

$$\begin{cases} M_{tot} = c_{aq} \times V_{aq} + c_g \times V_g \\ H_C = c_{aq}/c_g \end{cases}$$

is obtained, from which it is possible to calculate c_{aq} and c_g values for a given chemical with known H_C constant at equilibrium.

During fungal growth and substrate consumption, it is possible to determine experimentally concentration of substrate in the gas phase c_g by gas chromatography (headspace measurements) and thus extrapolate concentration in the liquid phase c_{aq} using the formulae expressed above. Assuming substrate equilibrium between gas and liquid phase, a pre-requisite for the calculation, is acceptable for slow-growing microorganisms since substrate consumption rates are lower than those required to restore equilibrium. A negative control without added substrate to measure endogenous respiration is however needed in the experimental set-up.

Concentration of carbon dioxide was only calculated in the gas phase since CO_2 reacts with water, and thus Henry's Law does not apply. The amount of CO_2 in the liquid phase was neglected since the medium was buffered at acidic pH and thus the equilibrium was shifted toward the gas phase.

Carbon mass balances and mineralisation of substrates were calculated as the amount of carbon recovered in the headspace as CO_2 after subtraction of endogenous respiration from

negative controls. Percent (w/w) mineralisation of substrates was calculated using the relation

$$[\text{mg-C}(CO_2,\text{substrate})_{fin} - \text{mg-C}(CO_2,\text{control})_{fin}]/\text{mg-C}(\text{substrate})_{in} \times 100\ \%$$

with

$\text{mg-C}(CO_2,\text{substrate})_{fin}$	final amount of carbon (CO_2) in the flask with substrate [mg],
$\text{mg-C}(CO_2,\text{control})_{fin}$	final amount of carbon (CO_2) in the flask without substrate [mg],
$\text{mg-C}(\text{substrate})_{in}$	initial amount of carbon (substrate) in flask with substrate [mg].

Aside from gas-chromatographic measurements, formation of biomass was constantly inspected visually and cultures were further incubated (up to three months) to monitor the lag phase in the onset of growth.

2.5.4 Protein precipitation and SDS-PAGE

Extracellular proteins in growth media supernatant (1 mL) were precipitated by ammonium-sulphate precipitation. An equal volume of saturated $(NH_4)_2SO_4$ solution (766.8 g ammonium sulphate in 1 L ddH_2O; set to pH 7.0 with 5 M NaOH) was added drop-wise to the samples, vortexed, and incubated 1 h on ice, vortexed again and spun for 5 min at 13'200 rpm, 4 °C. The resulting pellet was resuspended in 20 µL Protein Resuspension Buffer and stored at 4 °C.

Proteins – either from growth medium supernatant or precipitated samples – were separated by size by SDS-PAGE. A 10 µL aliquot was mixed with 10 µL SDS-PAGE Loading Dye, heated for 5 min at 95 °C to denature proteins and loaded into the Stacking Gel. Proteins were resolved in Resolving Gel for 1-2 h at 130 V in 1X Running Buffer (25 mM Tris-Base, 200 mM glycine, 0.1 % w/v SDS in 1 L ddH_2O). Protein size marker was SDS-PAGE Molecular Weight Standard Broad Range (#161-0318 from Bio-Rad Laboratories). Protein bands were stained either by coomassie (Roti®-Blue, #A152 from Carl Roth GmbH) or silver staining (Roti®-Black P, #L533 from Carl Roth GmbH) according to the manufacturer's instructions.

2.5.5 Extraction of intracellular pigments

Extraction of carotenoids and other intracellular pigments was performed for *K. petricola* A95 and its isogenic mutants A95pm1 and A95pm2. Fungal colonies (500 mg fresh biomass) grown on MEA plates for 2 w at 25 °C, or grown on MEA plates for 2 w at 25 °C and then incubated for 2 w at 4 °C, were weighted in 1 mL Eppendorf® tubes and dried for ca. 16 h at 70 °C in a Memmert ICP 600 Incubator. After biomass lyophilisation, pigments were extracted with 100 % acetonitrile and separated by high-performance liquid chromatography

(HPLC) with Dionex UltiMate 3000 LC Systems (Thermo Fisher Scientific) on Nucleosil® RP C_{18} column 300-5, 250 mm × 4 mm (CS Chromatographic Service GmbH, Germany). In the mobile phase, a mixture of eluent A (80 % acetonitrile and 20 % ddH_2O) and eluent B (100 % ethyl acetate) was used according to *Tab. 6*. Separations were performed for 30 min at a flow of 0.8 mL/min. Pigments were identified basing on standard separation curves.

Table 6. Eluents used for HPLC

Time (min)	Eluent A	Eluent B
0.0	60 %	40 %
7.0	50 %	50 %
17.0	40 %	60 %
21.0	30 %	70 %
28.5	20 %	80 %
29.5	10 %	90 %

2.5.6 Chlorophyll *a* extraction

Chlorophyll (Chl) *a* was extracted from *Nostoc* cells using existing protocols.[8] A representative sample of cyanobacterial culture (shaken for 5 min at 25 Hz with four stainless steel beads as described for fungal strains, see *Section 2.3.1*)[9] was filled in an Eppendorf® tube (1 mL) or a 15 mL Falcon™ tube (2 mL or more). Cells were collected by centrifugation (2 min at 7'000 × *g*), resuspended by vortexing in the same volume[10] of 90 % v/v methanol and Chl *a* was extracted for 5 min in the dark. Methanolic extract was separated from cells by centrifugation (2 min at 7'000 × *g*) and quantified by spectroscopic measurements at 665 nm (Abs_{665nm}) in 1 cm cuvettes against a 90 % v/v methanol blank (NanoDrop 2000/2000c from Thermo Fisher Scientific with baseline correction at 750 nm). Chlorophyll *a* concentrations (in μg/mL) were calculated basing on its extinction coefficient of 78.74 mL/mg cm in 90 % v/v methanol [87] with the formula

$$\frac{1}{78.74\ \text{mL/mg cm}} \times \frac{10^3\ \mu\text{g}}{1\ \text{mg}} \times \frac{Abs_{665nm}}{1\ \text{cm}} = 12.7\ \mu\text{g/mL} \times Abs_{665nm}.$$

[8] Research group homepage of Prof. John C. Meeks, University of California (Unites States): http://microbiology.ucdavis.edu/meeks/ (retrieved on February 2014).

[9] This shaking condition to obtain homogeneous samples does not result in lysis of cyanobacteria as determined by comparing Chl *a* values of shaken vs. non-shaken samples (not shown).

[10] In case a smaller/bigger volume of methanol was used for extraction, Chl *a* concentrations obtained after calculation were adjusted by multiplying/dividing Chl *a* values by the volume factor.

Extractions were performed in duplicate and viable cells (cells/mL) were calculated by dividing obtained Chl *a* concentration by the relation

$$\frac{1.75 \times 10^{-7}\ \mu g\ Chl\ a}{viable\ cell}$$

according to [24].

In the analysis of the model biofilm (*Section 3.IV.5*), different amounts of *K. petricola* A95 cells (determined under microscope as for the generation of growth curves; *Section 2.3.3*) in three growing phases (5×10^6, 1×10^7 or 5×10^7 cells in the lag, exponential or stationary phase) were added to *N. punctiforme* ATCC29133 after growth for ca. 2 w in liquid BG11. Then, Chl *a* was extracted in 1 mL or a higher volume of 90 % v/v methanol and the obtained values were compared with the control extractions without fungal cells.

2.6 Microscopical and histological methods

2.6.1 Microscopy

Microscopical observations were done under optical microscope (Zeiss Primo Star) as reported above or with fluorescent microscope Polyvar 2 from Leica Biosystems GmbH with PLAN FLUOR APO interference contrast objectives (4X, 10X, 25X, 40X or 100X magnification; from Nikon Corp., Japan).

Squash preparations were observed under optical microscope after removing a colony growing on solid medium, laying it on a microscope slide, overlaying with 10-20 μL saline solution and gently pressing a cover slip on top.

Histological sections of fungal colonies were observed with the VHX-1000 digital microscope using VH-Z20W and VH-Z250W objectives (150X, 200X, 500X and 1'000X magnification; Keyence Corp., Japan).

2.6.2 Embedding of fungal colonies

Structure of *K. petricola* A95 colonies grown for 2 w, 3 w and 4 w on MEA, ASM, ASM deprived of primary nutrients (ASM-C, -N, -P or -S) and water-agar was analyzed after embedding in HEMA-based resin Technovit® 7100 (#64709003 from Heraeus Kulzer GmbH, Germany) [48,49]. A chunk of agar with a single colony was cut from solid media and submerged in 4 % v/v glutaraldehyde in 0.1 M Phosphate Buffer pH 7.2. Fixation was achieved in a desiccator for 2 h under vacuum (pump model RV8 from Edwards, United Kingdom). Colonies were washed in 0.1 M Phosphate Buffer pH 7.2 (four times for 10 min), then dehydrated for 30 min in increasing ethanol concentrations ("ethanol series": 30 %, 50 %, 70 %, 80 %, 90 % and 100 % v/v ethanol). A pre-infiltration step (Technovit® 7100:Ethanol 1:1, 1 h under vacuum), was followed by infiltration with Preparation Solution (100 mL

Technovit® 7100 + 1 g Hardener I, 1 h under vacuum) before embedding in Embedding Solution (Preparation Solution + 6.7 % v/v Hardener II, 15 min under vacuum then 16 h at room temperature to complete hardening). For this last step 22 × 22 × 20 mm^3 Embedding moulds (#18646A from Polysciences Inc., United States) were used. All steps were done at 25 °C.

2.6.3 Histological sections

Histological sections of fungal colonies along the x-axis (around the colony middle section) were prepared using a sledge microtome (Microm HM440E from Microm GmbH, Germany) [90]. Samples embedded in Technovit® 7100 were roughly cut with a 20 cm hacksaw near the colony mid section and inserted into the microtome. Cuts of about 20 μm thickness were produced with 16 cm knife, wedged profile (type C), from Leica Biosystems GmbH (Germany) using a declination angle of 135° and an inclination of 6 μm. Histological sections were mounted on glass slides with 70 % v/v ethanol and allowed to adhere by heating at 60 °C.

2.6.4 Staining

Histological slides were subjected to Periodic acid-Schiff (PAS) staining to detect polysaccharides by glycol cleavage [90]. After submersion for 30 min in 70 % v/v ethanol, cuts were treated for ca. 5 min with 0.75 % w/v periodic acid (#375810 from Sigma-Aldrich) in ddH_2O, then washed for 5 min with 70 % v/v ethanol and 5 min with water. Slides were coloured for some seconds to 2 min with Schiff's Reagent (#S5133 from Sigma-Aldrich) until a recognizable red colour developed, and treated twice with Sulphite Solution (0.6 % w/v Na_2SO_3 in ddH_2O:HCl 1 M 95:5) for 3 min, then washed for 10 min with water and re-mounted on glass slides with 70 % v/v ethanol as above.

Counterstaining was performed by haematoxylin (#C.I. 75290 from AppliChem GmbH) with a modified Haematoxylin-Eosin protocol [48,49,90]. Slides were stained for 15 min with Haematoxylin Solution and washed for 10 min with water, then cleared with twice with some drops of xylene, and re-mounted on glass slides as with 70 % v/v ethanol as above.

2.7 Statistical analyses

To ensure robustness of results, data are represented throughout the monograph as average with standard error (Microsoft Excel 2007 from Microsoft Office, United States) or as median with first and third quartiles (Origin 9.0G 32-bit from OriginLab, United States) from at least three independent repetitions except for few cases (indicated). Unless clearly stated, it was not discriminated between technical and biological replicates.

Significance analysis was done using Student's *t*-test (unpaired two-sample *t*-test, two-tailed) with Microsoft Excel 2007 (Microsoft Office). Significance thresholds were set at $p < 0.05$ (*) and $p < 0.01$ (**).

Table 7. Summary of experiments conducted in this study in relation to fungal strains

Experiment	*K. petricola* A95	A95pm1	A95pm2	A95pm3	*C. apollinis*	Text Refs.
Growth and physiological analyses						
Effect of shaking	Yes	No	No	No	No	*Section 3.I.1*
Generation and isolation of protoplasts	Yes	Yes	Yes	No	Yes	*Section 3.I.2*
Growth curves in liquid media	Yes	Yes	Yes	Yes	No	*Sections 3.II.2, 3.II.5*
Phenotypic characterisation (Biolog)	Yes	Yes	Yes	No	Yes	*Section 3.II.3*
Utilisation of hydrocarbons[a]	Yes	Yes	No	No	Yes	*Section 3.II.4*
Temperature-optimum profile	Yes	Yes	Yes	No	No	*Section 3.II.6*
Description of mutant phenotype	n/a	Yes	Yes	No	n/a	*Section 3.II.7*
Resistance toward UV irradiation	Yes	Yes	Yes	No	No	*Section 3.II.8*
Growth in oligotrophic media	Yes	No	No	No	No	*Sections 3.III.1-3*
Molecular analyses						
ITS sequencing	Yes	Yes	Yes	Yes	No	*Section 3.I.3*
Nucleic acid extractions	Yes	Yes	Yes	Yes	No	*Section 3.I.3*
RNA extraction for genome annotation	Yes	No	No	No	No	*Section 3.IV.1*
Karyotyping (ROFE)	Yes	Yes	Yes	No	Yes	*Section 3.IV.2*
Biochemical analyses						
Laccase assay[b]	Yes	Yes	Yes	Yes	Yes	*Section 3.IV.3*
Protein precipitation and SDS-PAGE	Yes	Yes	Yes	No	Yes	*Section 3.IV.3*
Intracellular pigment analysis	Yes	Yes	Yes	No	No	*Section 3.IV.4*
Chlorophyll *a* extraction	n/a[c]	n/a	n/a	n/a	n/a	*Section 3.IV.5*
Microscopical analyses						
Histology	Yes	Partly	No	No	No	*Section 3.III.2*

[a] The strain *C. psammophila* was used as positive control; an uncharacterized *Fonsecaea* spp. was investigated as well.
[b] *Trametes versicolor* DSM3086 was used as positive control
[c] Chlorophyll *a* extraction was performed from *Nostoc* cells in association with *K. petricola* A95 (model biofilm)

Summarizing table

Table 7 gives a summary of the methods and strains used in this study. All experiments were designed with and conducted on the model microorganism *K. petricola* A95, while depending on the purpose other strains were included as well. Even though the data in *3 RESULTS* are presented to follow a logical rather than a chronological order, some temporal aspects had an influence on the overall experimental set-up of this thesis (e.g. the fact that some mutants were isolated toward the end of this work and could not be included in the analyses). *Table 7* is aimed at giving an overview and is conceived as navigation help throughout the data presented in the next chapter.

3 RESULTS

PART I – Preliminary results

Some preliminary observations and experiments were fundamental for ensuing analyses of black fungi. *PART I – Preliminary results* shows data that are prerequisite for experiments presented in the next subchapters.

3.I.1 Shaking did not have deleterious effects on *Knufia petricola* A95

Diffuse patterns of inhomogeneous, clump-like growth (both in liquid and on solid media) is an inherent peculiarity of black fungi (*Fig. 1*). Thus, disruption of clumps in black-fungal cultures is a prerequisite for basic experimental work, e.g. pipetting and inoculation of fresh cultures or reliable viable counting.

The method of choice – vigorous shaking using a cell mill – could entail mechanical damages or even cell lysis. This possibility was investigated by comparing growth of shaken vs. non-shaken *Knufia petricola* A95 cultures (dry weight after 1 w), as well as those of shaken/non-washed vs. shaken/washed samples (both dry weight and viable count after 1 w; *Fig. 2*). Samples were collected from 10 mL liquid cultures at different growth phases to exclude a time-dependent susceptibility toward mechanical damages. These were lag (12- to 16-h-old cultures), exponential (3- to 4-d-old) and stationary phases (7- to 8-d-old) according to *Fig. 7* (see below). Higher growth in shaken/non-washed samples in comparison to non-shaken ones was not observed for shaken/washed samples (no significant increases in dry weight or viable count values). Thus, the phenomenon is not due to release of growth-enhancing substances from putatively lysed cells upon shaking, but probably to an evenly spreading of cells on plates following disruption of clumps. After shaking, *K. petricola* A95 cells look intact under optical microscope (e.g. see *Fig. 3*) and several passages – i.e. repeated cycles of cultivation into the stationary phase, shaking, and inoculation – do not decrease cell viability (see *Fig. 28D*), both of which are further validations of absence of cellular damages.

Altogether, the data indicate that shaking does not have a deleterious effect on *K. petricola* A95 cells.

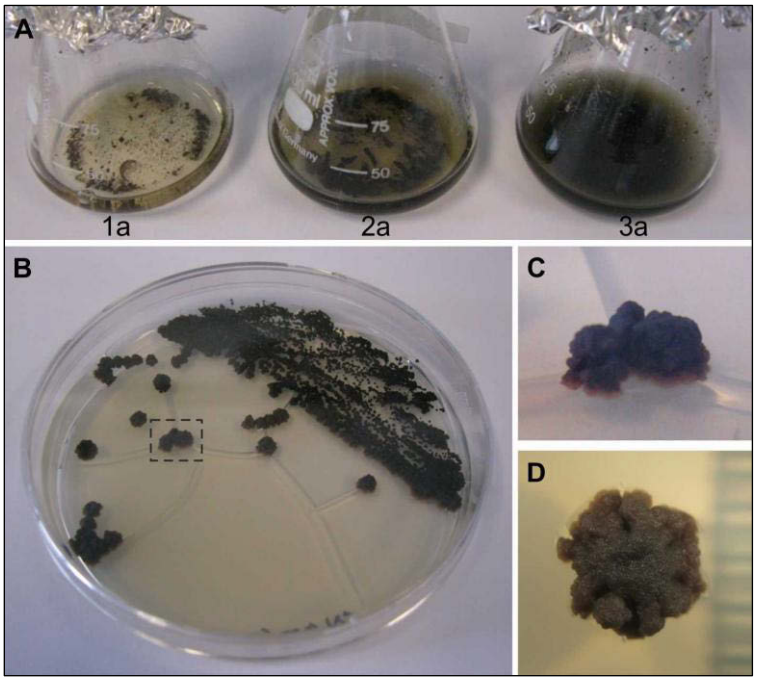

Figure 1. Clump- and cauliflower-like growth of* Knufia petricola *A95

(A) Growth in liquid malt-extract broth (MEB) after **(1a)** 3 d, **(2a)** 8 d and **(3a)** 10 d of incubation (here, as well as throughout the thesis if not otherwise indicated, at 25 °C). **(B-D)** Growth on solid malt-extract agar (MEA) after ca. 3 w of incubation. Dotted square in **(B)** is the single colony in **(C)** magnified to show thickness of colonies. Remarkably, upon prolonged incubation on rich media *K. petricola* A95 is growing along the z-axis reaching heights of up to 1-1.5 cm (e.g. see *Fig. 39, Section 3.III.2*).

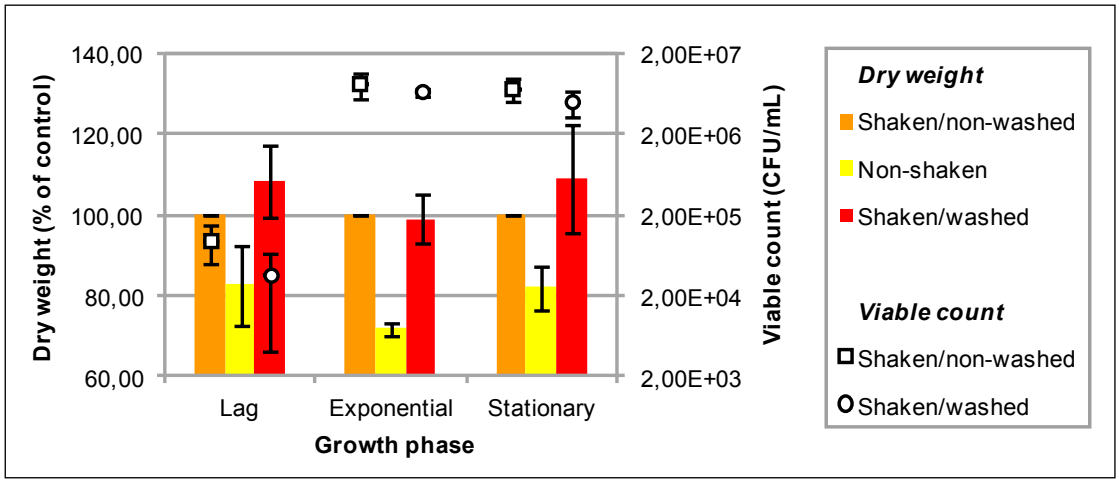

Figure 2. Growth of* Knufia petricola *A95 after mechanical disruption of clumps

Growth was assessed by dry weight measurements (bars) and, for shaken samples, viable counting (squares and circles). Growth in shaken/non-washed samples was considered as control (set at 100 % for dry weight values) and compared with the other treatments. (Modified from Nai *et al.*, 2013 [91].)

3.I.2 Protoplasts of *Knufia petricola* A95 cells were efficiently isolated

Removal of cell wall from *K. petricola* A95 cells is essential to several purposes, as for example the successful transformation of the strain [Steffi Noack-Schönmann, Nicole Knabe and Anna A. Gorbushina, unpublished]. Whereas protoplasts could be efficiently generated with existing protocols using a mixture of lytic enzymes (β-glucanase, cellulase, protease and chitinase, resulting in about 60 % protoplast yield) [16], some techniques like pulsed-field gel electrophoresis (PFGE, see *Section 3.IV.2*) required separation of them from intact cells. Isolation of protoplasts by sucrose-Ficoll gradient centrifugation yielded a solution of pure protoplasts (*Fig. 3*).

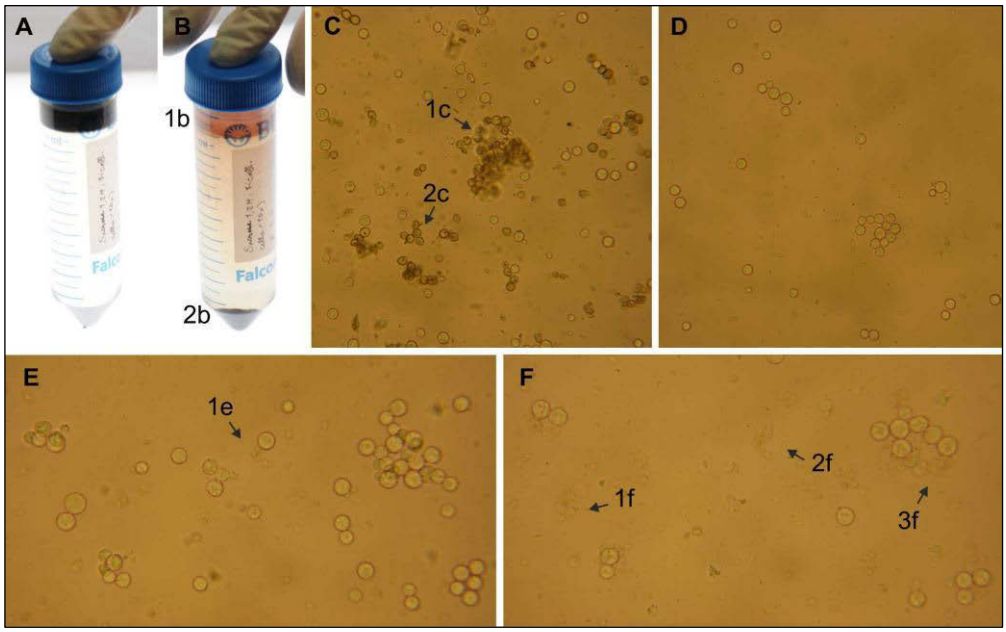

Figure 3. Isolation of* Knufia petricola *A95 protoplasts by gradient centrifugation

(A-B) Protoplast suspension **(A)** before and **(B)** after gradient centrifugation [with **(1b)** interphase (protoplasts) and **(2b)** pellet (intact cell and clump fractions)]. **(C-D)** Microscopic observations of protoplast suspension **(C)** before centrifugation [with **(1c)** clumps and **(2c)** intact cells] and **(D)** after centrifugation. **(E-F)** Verification of protoplast identity by lysis control **(E)** ca. 1 min and **(F)** ca. 2 min after addition of ddH_2O [with **(1e**, **1-3f)** bursting protoplasts].

3.I.3 Mutants of *Knufia petricola* A95 were isogenic with the wild type

During the course of this work, several pink/orange colonies derived from *K. petricola* A95 were observed (*Fig. 4*). These spontaneous, constitutive mutants were obtained by routinely growing A95 on malt-extract agar (MEA) and had stable phenotypes (i.e. maintained upon several cell passaging). Mutants analysed in this study were named A95pm1 and A95pm2. A later pink mutant, A95pm3, was also included in some of the experiments.

Preliminary observations could be drafted by visual inspection of colonies. As evident from the altered pigmentation, both mutants were probably affected in synthesis of melanised cell wall. Pink/orange colouration was due to "unmasking" of internal carotenoids ([56] and see also *4 DISCUSSION*). Distinct pigmentation was observed between A95pm1 and A95pm2 whereas for each strain similar pigmentation was observed either in liquid or solid cultures; pink mutant A95pm1 formed smaller colonies than wild-type strain (*Fig. 4*).

Prior to any further experiment, identity of mutants needed to be verified. This was done by ITS analyses (PCR with primer pair ITS-1 and ITS-4, sequencing with forward primer ITS-1 and reverse primer ITS-Int) and comparison with ITS region of *K. petricola* A95. Sequence comparisons revealed that all mutants were isogenic with the wild-type strain. Multiple ITS sequence alignment is shown in *A.5 Supplementary data* (*Suppl. Figs. 1-2*).

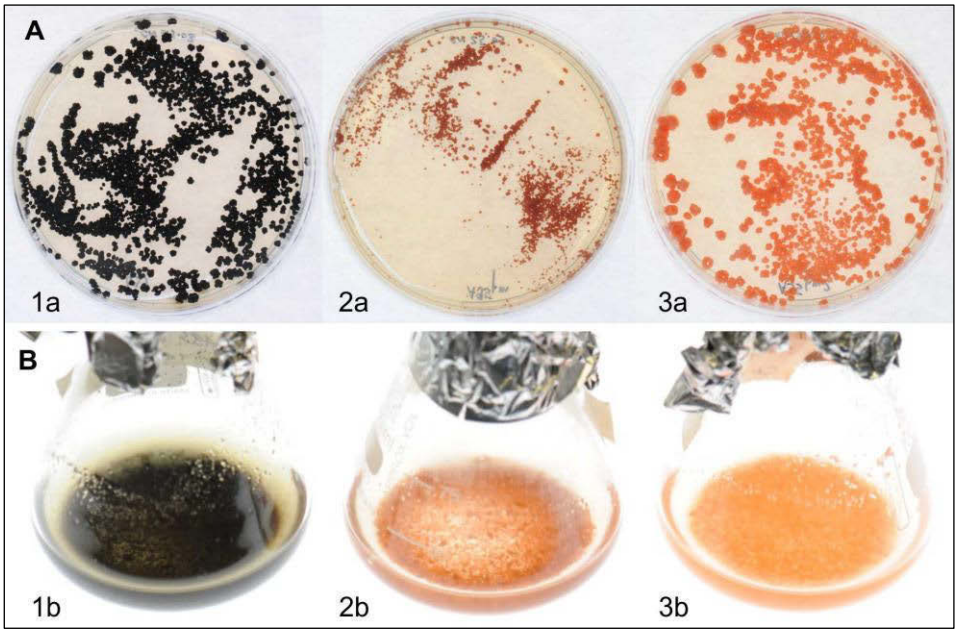

Figure 4. Growth of* Knufia petricola *A95 and spontaneous pink mutants on malt-extract media
(A) Growth of **(1a)** wild type, **(2a)** A95pm1, and **(3a)** A95pm2 on malt-extract agar after 3 w of incubation. **(B)** Growth of **(1b)** wild type, **(2b)** A95pm1, and **(3b)** A95pm2 in malt-extract broth after 1 w of incubation.

PART II – Phenotypic characterisation of black fungi

In this main subchapter (*PART II – Phenotypic characterisation of black fungi*) black-fungal strains were characterized regarding morphology, growth rate in different media, growth preferences, auxotrophic requirements, utilisation of nutrients, growth-temperature optimum and stress tolerance. All experiments were performed with the rock-inhabiting fungus *K. petricola* A95 (*Fig. 5*), which was validated as a suitable model to study environmental black yeasts (see *4 DISCUSSION*), while in some of them additional strains were included.

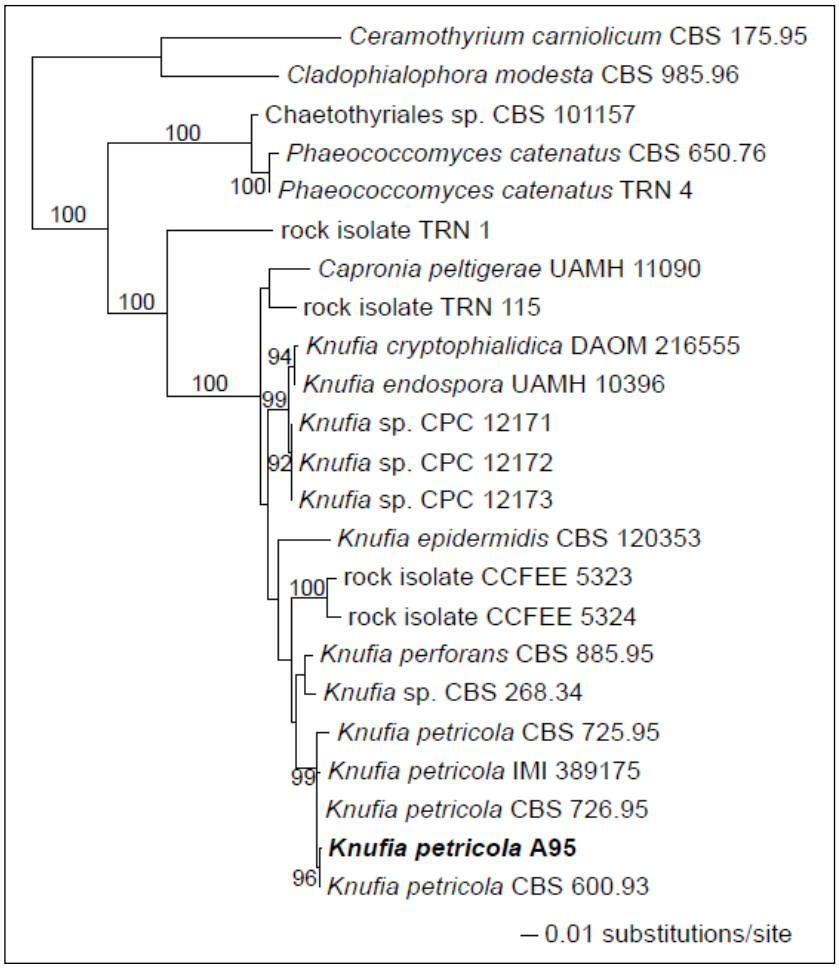

Figure 5. Phylogenetic tree of* Knufia petricola *A95

Phylogenetic placement of *K. petricola* A95 as previously reported in the literature (Adopted from Nai *et al.*, 2013 [91].)

3.II.1 Morphology of *Knufia petricola* A95

Morphology is one of the basic phenotypic traits of any organism. Even if members of the black-fungal group are rather undifferentiated in this regard [111,126], morphological observations allow a rough differentiation between strains, which, when combined with phylogenetic analyses (*Fig. 5*), is premise to thorough taxonomic classifications [64]. A recent study described the model microorganism *K. petricola* A95 and renamed it from the basionym *Sarcinomyces petricola* A95 [91,139]. Morphology of *K. petricola* A95 is shown in *Fig. 6*.

3.II.2 Growth curves in complex medium

Another primary phenotypic trait of (micro-)organisms is growth. Observing growth behaviours and determining such parameter as generation time *g* in culture media is thus not only a fundamental knowledge, but also a crucial prerequisite for further experimental analyses.

As such, growth curves in the complex – i.e. undefined – malt-extract broth (MEB), a standard liquid culture medium in mycology, were generated. Along with the wild-type strain *K. petricola* A95, growth of the pink mutants A95pm1, A95pm2 and A95pm3 in liquid culture was investigated and is shown in *Fig. 7*.

Knufia petricola A95 is a relatively fast-growing black fungus, reaching stationary phase after ca. four days of incubation and with generation time *g* = 13.0 h (considering exponential growth between days 1 and 4). A maximal log increase of 2.15 was calculated. Increases in optical densities at stationary phase probably reflect melanisation at later time points (*Fig. 7A*). This observation was validated by visual inspections of both liquid cultures (i.e. blackening of cells and growth medium supernatant, *Fig. 1A*) and colonies on agar (not shown). The overall growth trend is nearly identical for the mutants. Very similar results were calculated for growth parameters of mutants in liquid medium (*Fig. 7B-D*). For A95pm1, generation time *g* = 13.8 h and log $increase_{max}$ = 2.08 were obtained; for A95pm2, *g* = 16.0 h and log $increase_{max}$ = 2.01; and for A95pm3, *g* = 12.6 h and log $increase_{max}$ = 1.91.

Growth curves for *Coniosporium apollinis* could not be generated with same method (see *4 DISCUSSION*).

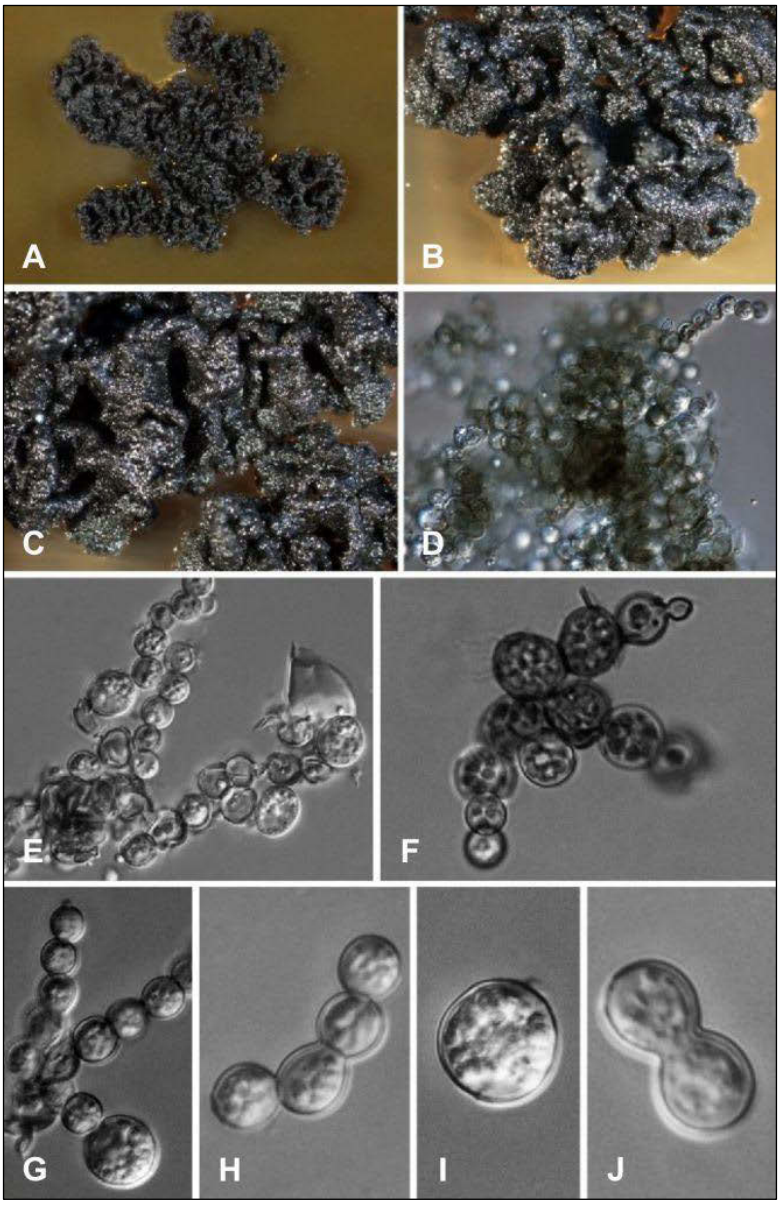

Figure 6. Morphology of* Knufia petricola *A95 on malt-extract agar

(A-C) Black, thick and cerebriform colonies, with rough, shiny and wet surface, branched in large, irregularly shaped lobes. **(D-E)** Thallus composed of melanised and meristematically dividing clusters of cells, occasionally branching into short torulose hyphae. **(F-I)** Cells ca. 5 μm in diameter, but reaching 15 μm when old and full of granules. **(J)** Yeast-like growth only rarely observed. (Adopted from Nai *et al.*, 2013 [91].)

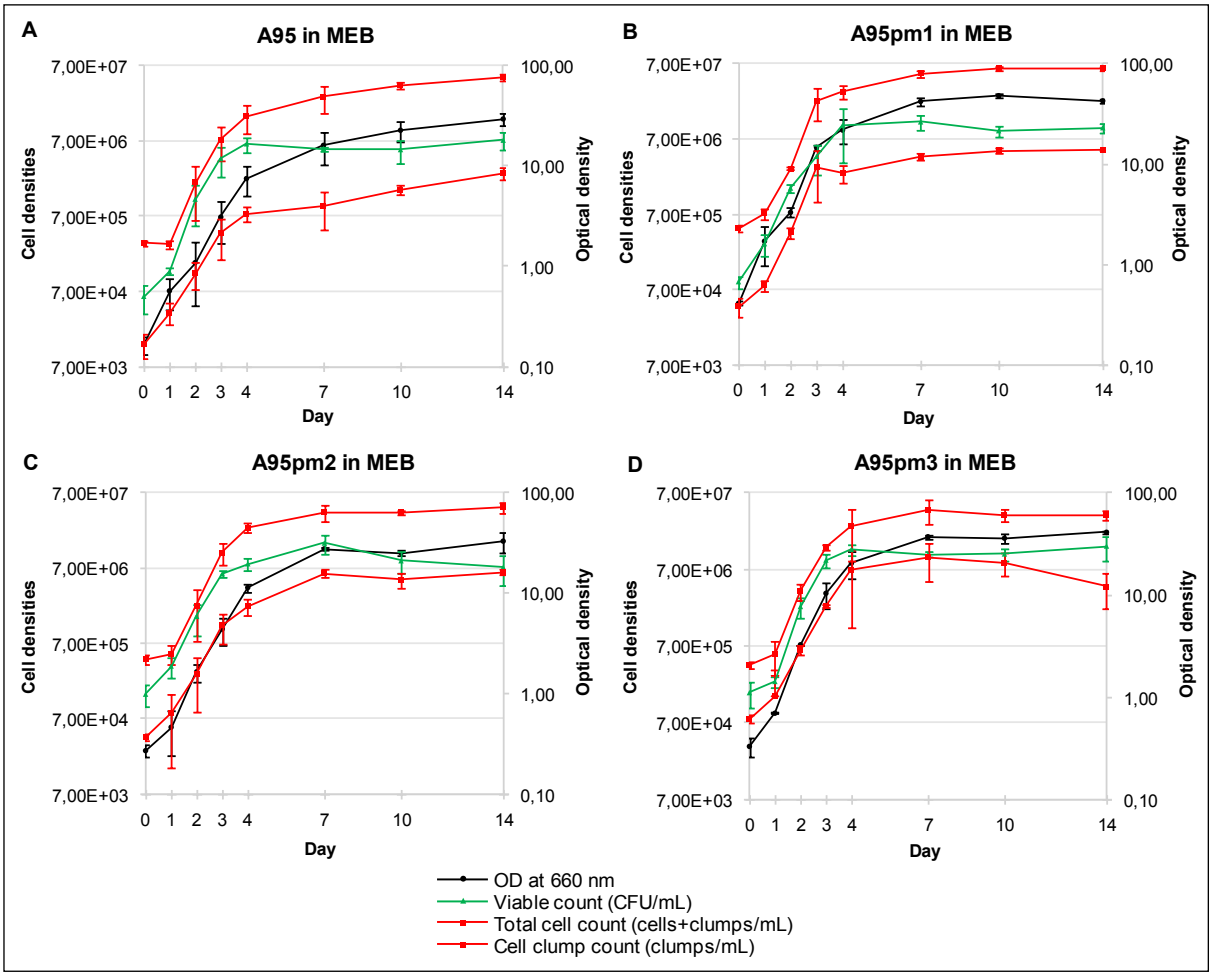

Figure 7. Growth of* Knufia petricola *A95 and its isogenic mutants in malt-extract broth

Data, obtained as exposed in *Section 2.3.3*, are shown from at least three repetitions, except for mutant A95pm3 (two repetitions only). (Expanded from Nai *et al.*, 2013 [91].)

3.II.3 Physiological characterisation (1) – Biolog's Phenotype MicroArrays

Morphological descriptions are fundamental for the characterisation of any species, but for black fungi knowledge thus gathered is rather trivial, since the microorganisms have undifferentiated cells and, on solid media, similar microcolonial growth patterns. Similarly, knowledge of growth behaviour in complex liquid MEB is important but uninformative with regard to real growth preferences. Thus, an approach with phenotype microarrays was undertaken which allowed the parallel and miniaturized growth analysis in hundreds of different chemical environments [10].

Fungal strains were inoculated in Biolog's Phenotype MicroArray (PM) plates as described above and growth preferences were monitored spectroscopically. However, even though both growth and tetrazolium dye reduction were observed, the value ΔAbs could not be calculated since:

(i) black-fungal cultures are highly inhomogeneous and thus Abs_{750nm} values were not reproducible, and
(ii) after reduction tetrazolium dye associates with cells and thus Abs_{490nm} values were almost identical to Abs_{750nm} values.[11,12]

Nonetheless, as shown in *Fig. 8*, patterns of *K. petricola* A95 growth in PM plates were easily distinguishable (as well as reproducible; not shown). Therefore, responses to different chemical environments were evaluated by eye with a scoring system as exposed in *2.3.4 Phenotypic analyses with the Biolog*.

Optimal incubation time to recognize different growth patterns were determined experimentally for each different PM plate and adopted for the repetition experiments. Oligotrophic and prototrophic character of black fungi resulted often in growth in negative controls (wells without nutrient source or without growth factors, see e.g. *Fig. 8E-G*); this background growth was minimized by reducing inoculum densities, cultivating strain at suboptimal conditions or reducing incubation time.[13]

Since microtiter plates were differently inoculated and/or incubated for different times, cross-plate analyses were difficult and data are presented for single plates to extrapolate preferred chemical environments or nutrient sources. Details of inoculation and incubation conditions are reported in *Tab. 2* (*2 MATERIALS AND METHODS*), whereas when necessary further relevant details are provided throughout the text or in the figure captions. First, results with for the model strain *K. petricola* A95 are shown (*Subsection* Knufia petricola

[11] Observation also corroborated by centrifugation, resulting in colourless supernatant.
[12] Other Biolog's Redox Dye Mixes were tested without different results (Mix D, #74225, and Mix G, #74227).
[13] Due to this phenomenon, some chemicals inhibitory for growth were identified (less biomass formation than negative control, see e.g. *Fig. 8F, wells B1-2*). When such chemicals were identified, this is indicated throughout the text.

A95).[14] Then, in the following subsections, growth of pink mutants A95pm1 and A95pm2 as well as *C. apollinis* in selected PM plates was compared with those of the model organism. Figures with Biolog results are clustered together at the end of each subsection.

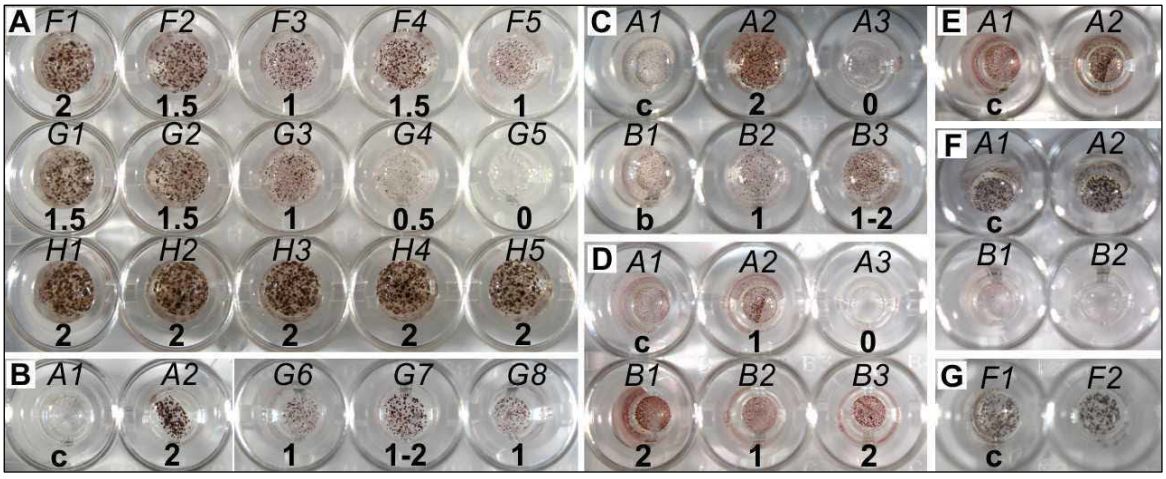

Figure 8. Growth of* Knufia petricola *A95 in Biolog's Phenotype MicroArray (PM) plates

(A) With gradients of osmotically active compounds in PM9; **(B)** with selected growth factors in PM5 (wells A1/2: negative/positive control; wells G6-8: with thiamine derivatives); **(C)** with diverse carbon sources in PM1; **(D)** with diverse nitrogen sources in PM3; **(E-G)** Oligotrophic growth upon prolonged incubation **(E)** without nitrogen in PM3 (well A1), **(F)** without phosphorus in PM4 (well A1) or **(G)** without sulphur in PM4 (well F1). Scores were assigned as illustrated in *Section 2.3.4* (0-2, reported at the bottom of each well). Well coordinates are reported on top of each well in italics. **(b)** Borderline result; **(c)** Negative control well. (Modified from Nai *et al.*, 2013 [91].)

[14] Results for chemical sensitivity tests with plates PM11-16 are not shown for *K. petricola* A95 alone but only in comparison with its isogenic mutants in the *Subsection* Knufia petricola *A95 versus isogenic mutants*.

Knufia petricola A95

Knufia petricola A95 is halotolerant and pH optimum for growth is at around pH 5. To begin with, general growth requirements of *K. petricola* A95 were determined with PM9-10. These plates are provided with osmotically active salts at increasing concentrations (PM9) or different pH environments (PM10), and the cells are inoculated in a complete medium with all primary nutrients and supplemented with yeast nitrogen base, which is rich in vitamins and growth factors.

As shown in *Fig. 9*, *K. petricola* A95 is halotolerant and grows best at around pH 5. Charts with values for *K. petricola* A95 in plates PM9-10 are shown in *Fig. 10*. Most osmotically active chemicals were well tolerated at high concentrations (e.g. sodium chloride, potassium chloride, sodium sulphate, ethylene glycol, ammonium sulphate and sodium nitrate), while few were either mildly tolerated (e.g. urea, sodium lactate and sodium phosphate) or inhibitory at low concentrations (e.g. sodium salts of formate, benzoate and nitrite). None of the putative compatible solutes boosted growth on 6 % w/v NaCl (*Fig. 10*, left panel). A growth preference at acidic pH could be ascertained, with optimum at around pH 5 and ability to grow between pH 3.5 and pH 7. While some chemicals had a deleterious effect at pH 4.5 (i.e. isoleucine, leucine, tryptophane, *o*-/*p*-aminobenzoate, norleucine, norvaline, cysteic acid, α-aminobutyric acid and urea), none had a positive effect at basic pH (wells E1-G12). Similarly, no growth was recognizable with 5-bromo-4-chloro-3-hydroxyindole derivatives (wells H1-12) (*Fig. 10*, right panel).

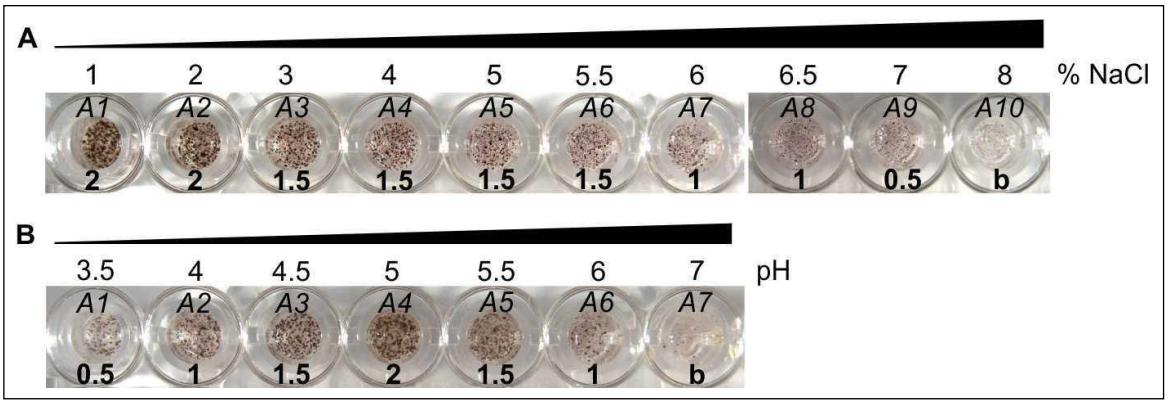

Figure 9. **Knufia petricola *A95 is halotolerant and has growth optimum at around pH 5***

Growth of *K. petricola* A95 in **(A)** plate PM9 and **(B)** plate PM10 after 7 d. Upon prolonged incubation (ca. 2 w) some basal growth was observed with up to 10 % w/v NaCl and up to pH 8.5 (not shown). Assigned score (0-2; bold) is reported on the bottom, well coordinates (in italics) on top of each well. **(b)** Borderline result. (Adopted from Nai *et al.*, 2013 [91].)

Thiamine enhances growth of *Knufia petricola* A95 at suboptimal growth conditions. Besides determining tolerance toward salt stresses and pH preferences, requirement of growth factors and vitamins was assessed with plate PM5. As opposed to growth in richly supplemented medium as above, the strain was inoculated in a medium with primary

nutrients but without nutrient supplements. Biomass formation in distinct wells provided with putative growth-enhancing substances was then assessed to identify factors and vitamins able to stimulate *K. petricola* A95's growth.

Upon dilution of cells 1/100 in the inoculating fluid, however, growth could be observed in every well after few days, including negative control well (A1, no supplements; not shown). A stronger dilution (1/1'000) to achieve suboptimal conditions was then used, which, as shown in *Fig. 8B*, minimized growth in negative control while resulting in clump formation in positive control well A2, which is supplemented with a rich peptone mixture [Barry Bochner; personal communication]; additionally, growth was clearly observed in wells G6-8, containing thiamine derivatives (inosine + thiamine, thiamine and thiamine pyrophosphate, respectively). A slightly positive effect upon prolonged incubation (ca. 2-3 w) could be also observed with choline, D,L-mevalonic acid and D-biotin (not shown).

Since growth in positive control seemed to be stronger than with thiamine derivatives (*Fig. 8B*), additive effect of growth supplements were investigated by diluting cells 1/1'000 in inoculating fluid supplemented with 1 μM thiamine and inoculating a fresh PM5 plate anew (*Fig. 11*). In such a way, stronger growth in A2 was abolished, and further growth-enhancing substances could be identified. These were adenine, threonine, cytosine, cytidine, 2'-deoxyuridine, N-acetyl-D-glucosamine and tween 20, and to a lesser extent phenyalalanine, valine, ornithine, pyridoxamine, *p*-aminobenzoate and menadione.

Knufia petricola A95 is selective in the utilisation of carbon compounds. Carbon metabolism of *K. petricola* A95 was studied using plates PM1-2. Here, cells were inoculated in a defined medium supplemented with trace elements and all nutrients but carbon, which is instead provided in the wells. Being each well amended with a different carbon source, by observing fungal biomass formation is thus possible to discern which nutrient is able to support growth.

Initially, poor growth was generally observed due to buffering of plates at pH 7 with high concentrations of sodium phosphate [Barry Bochner; personal communication]. Inoculating fluid was thus acidified at pH 5 with 20 mM citric acid as buffer to counteract high concentrations of sodium phosphate and achieve pH optimum for the model microorganism. In such a way carbon metabolism profile of *K. petricola* A95 could be generated as shown in *Fig. 12*. To facilitate analysis, nutrients were grouped into major fungal metabolic pathways [7,45,70,155].

Most pathways supported growth, except from fatty acid, purine, pyrimidines and glyoxylate/dicarboxylate metabolic pathways (median and max values = 0 for all compounds; omitted from *Fig. 12*). Remarkably, the strain showed limited ability to catabolise metabolic intermediates. For example, good growth was observed on L-arabinose and D-xylose from the pentose catabolic pathway, but poor to no growth was observed on L-arabitol and

xylitol, the next intermediates in the pathway. The same held true for glycolytic (growth on D-glucose, D-mannose and D-fructose, none on D-glucose-1-phosphate), galactose (good growth on galactose but poor on galactitol) and glycerol pathways (growth on glycerol much better than on glycerol-3-phosphate; in *Fig. 12* under "compatible solutes"). Accordingly, poor growth was scored on intermediates of the citric acid cycle and pyruvate metabolism. Poor growth was also observed on most amino acids, with the exception of L-Pro, L-Asn, L-Gln, L-Arg and L-Phe. Against the expectations, *K. petricola* A95 is selective concerning utilisation of carbon source and many compounds were not used. Out of 190 compounds only 63 allowed biomass formation (median ≠ 0), and, with only 23 of these, good growth was scored (media > 1). Carbohydrates (simple sugars to complex polysaccharides), in particular those found in nature (e.g. D- rather than L-enantiomers) were preferred carbon sources. No clear preference was however observed either for C5 vs. C6 sugar or for furanoses vs. pyranoses. Carbohydrates were followed by other species like amino acids, amino sugars, nucleosides, etc., which were generally poorly or not used at all. *Meso*-erythritol however, a signature sugar for black fungi, did not support growth of *K. petricola* A95. Out of the rather few compounds efficiently catabolised, particular intriguing is strong growth on *p*-hydroxybenzoic acid. This aromatic acid is of central importance to metabolism of aromatic compounds [88,104] and is linked to degradation of lignin [3]. Both ability to grow on selected volatile aromatic compounds and presence of oxidative enzymes associated with degradation of lignin were further studied (see *Sections 3.II.4 and 3.IV.3*).

Knufia petricola A95 is less selective in the utilisation of other primary nutrients and growth under nutrient deprivation is more pronounced. Catabolism of nitrogen, phosphorus and sulphur compounds was investigated in *K. petricola* A95 using plates PM3-4 with the same principle exploited for utilisation of carbon sources.

In negative control well without nitrogen (plate PM3), background growth was pronounced (see *Fig. 8D-E*, well A1). Therefore, for utilisation of nitrogen sources, growth was analyzed in unbuffered inoculating medium (i.e. without addition of citric acid and acidification of pH 5) after shorter incubation than for PM1-2. As shown in *Fig. 13* – with substances grouped into chemical classes rather than metabolic pathways – *K. petricola* A95 is much less selective in the utilisation of nitrogen sources. Out of 95 compounds, 71 supported growth, most of whom efficiently (median > 1). Preferred nitrogen sources were, in order, amino acids (especially L-isomers) and their derivatives (including dipeptides), simple nitrogenous compounds (ammonia, nitrate, urea), primary amines, amides, and some nucleobases and derivatives. Poor or inert nitrogen sources were amino sugars, aminated alkyl carbohydrates and the remaining simple sugars nitrite and biuret (with few exceptions, e.g. butyric acid derivatives or aminated alkanes were good N sources). Upon prolonged incubation (ca. 2-3

w) hydroxylamine, xanthine and D,L-α-aminocaprylic acid were toxic (less growth than negative control).

Growth in wells without phosphorus or sulphur in plate PM4 (*Fig. 8F-G*) was yet stronger than those in control without nitrogen. To circumvent this drawback both inoculum density and incubation time were further reduced (1/1'000 dilution and 5 d, respectively). Whereas utilisation profile of phosphorus sources could be generated – although without scoring with "2" – (*Fig. 14*), growth upon sulphur deprivation was still sustained and no increases were observed with sulphur compounds. Additional experiments (e.g. further reduction in initial cell load) strongly delayed growth in all wells, hampering analyses of S catabolism. Therefore, utilisation of sulphur compounds could not be studied with the Biolog System.

About half of the phosphorus compounds supported growth of *K. petricola* A95. Preferred phosphorus sources were ubiquitous phosphorylated molecules (e.g. phosphoenolpyruvate, glycerol-3-phosphate), non-cyclic nucleotides (but not their cyclic counterparts) and phosphorylated amino acids, followed by PO_4^{3-}-derivatives, phosphosugars and phosphonates. Upon prolonged incubation (ca. 2-3 w) some compounds were toxic (less growth than negative control, see e.g. *Fig. 8F, wells B1-2*), i.e. thiophosphate, dithiophosphate and 2-aminoethylphoshonic acid.

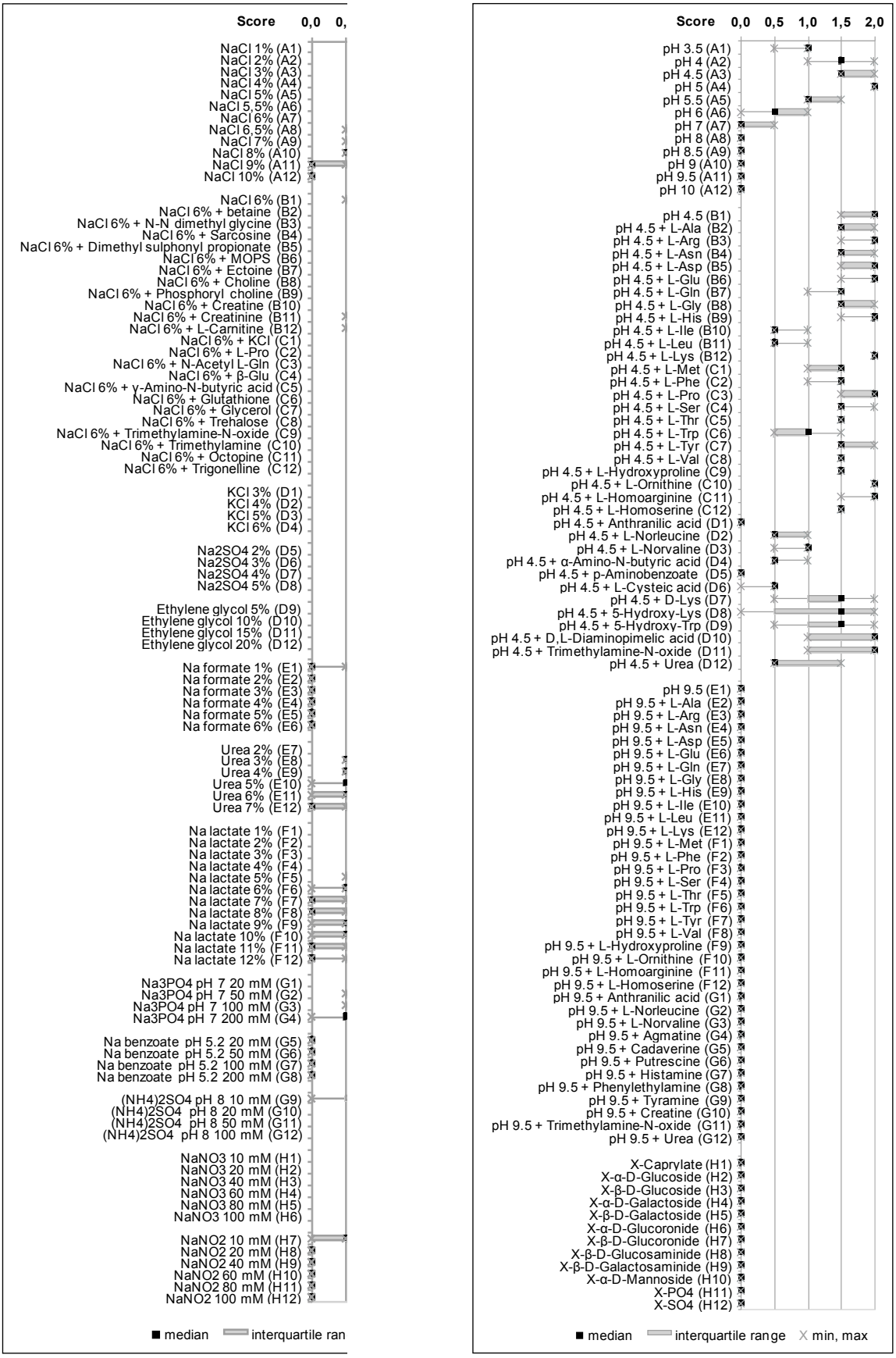

Figure 10. Growth of* Knufia petricola *A95 under osmotic stress (left panel) and different pH values (right panel) (Biolog's plates PM9-10)

Strain was inoculated 1/100 and plates incubated for 7 d. (Modified from Nai *et al.*, 2013 [91].)

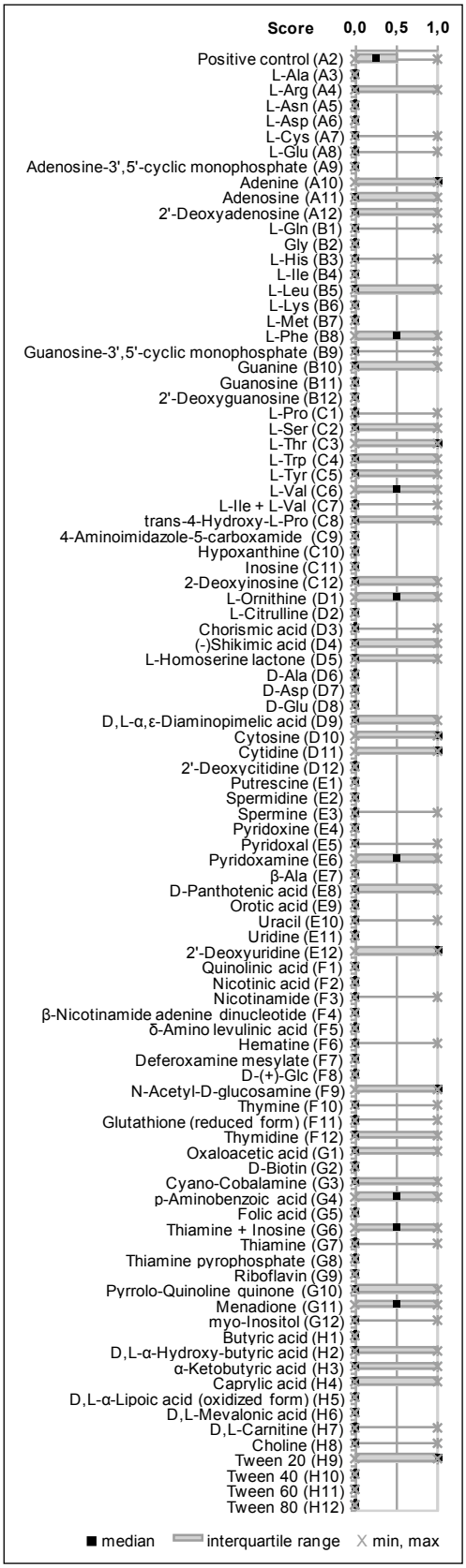

Figure 11. Growth of* Knufia petricola *A95 in Biolog's plate PM5 with 1 μM thiamine

Strain was inoculated 1/1'000 in inoculating fluid (supplemented as reported in *Tab. 2*) additionally amended with 1 μM thiamine, and plate was incubated for 7 d. Relative strong background growth in negative control well due to thiamine made the assignment of the score "2" not possible. (Adopted from Nai *et al.*, 2013 [91].)

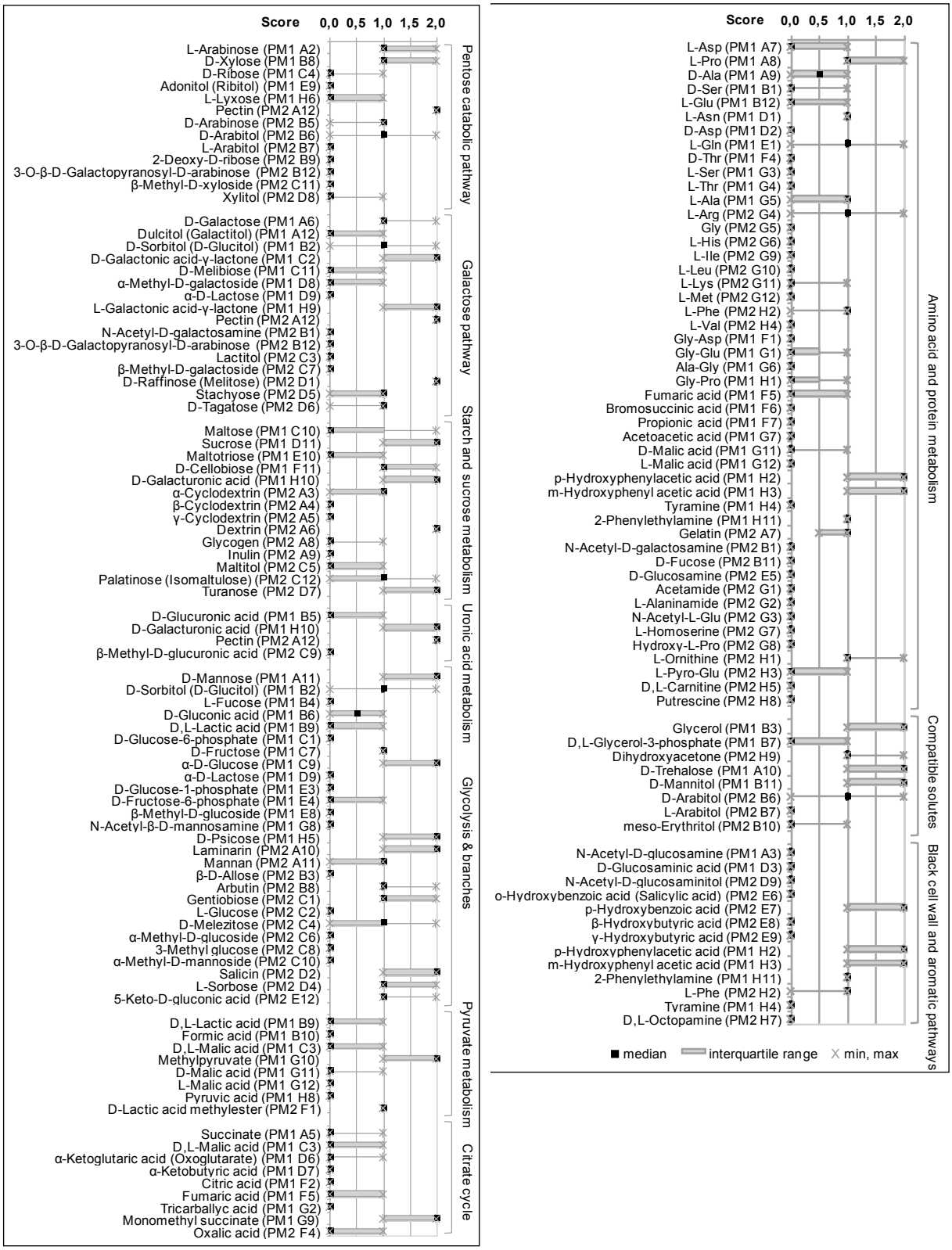

Figure 12. Growth of* Knufia petricola *A95 with different carbon sources (Biolog's plates PM1-2)

Strain was inoculated 1/100 (inoculating fluid buffered with 20 mM citric acid and acidified at pH 5) and plates were incubated for 11 d. Carbon sources are grouped into major fungal metabolic pathways. Additional carbon sources, which are not shown here, are reported in *Suppl. Fig. 3* in *A.5 Supplementary data*. (Adopted from Nai *et al.*, 2013 [91].)

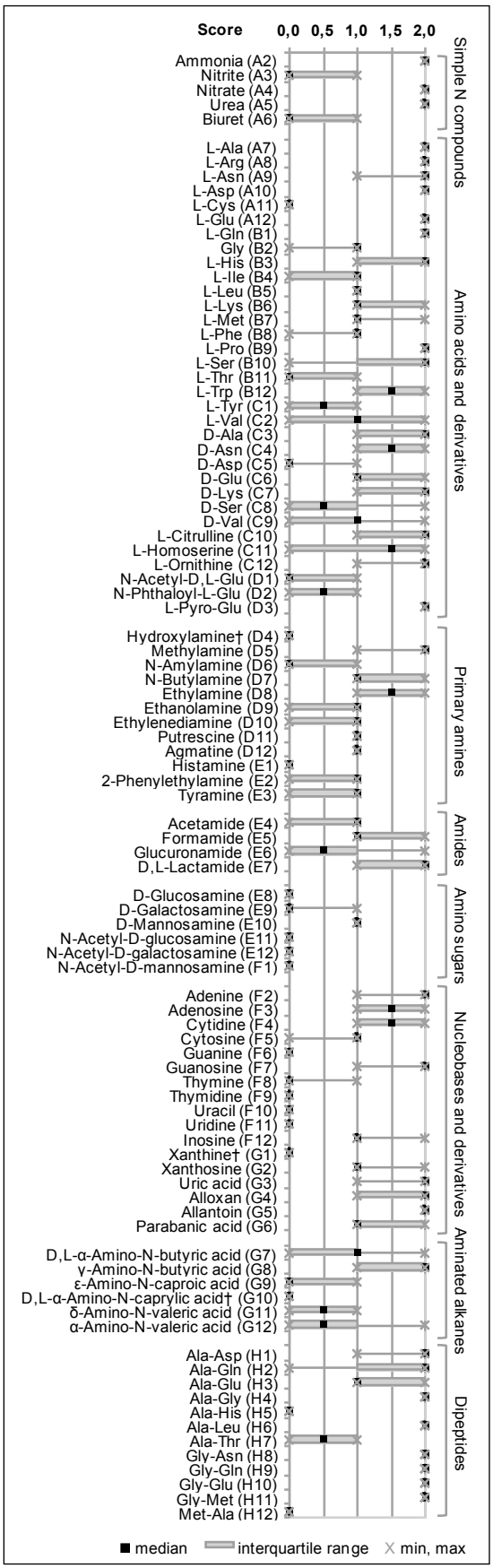

Figure 13. Growth of* Knufia petricola *A95 with different nitrogen sources (Biolog's plate PM3)
Strain was inoculated 1/100 and plate was incubated for 7 d. Nitrogen sources are grouped into chemical classes. † Toxic (less growth than negative control). (Adopted from Nai *et al.*, 2013 [91].)

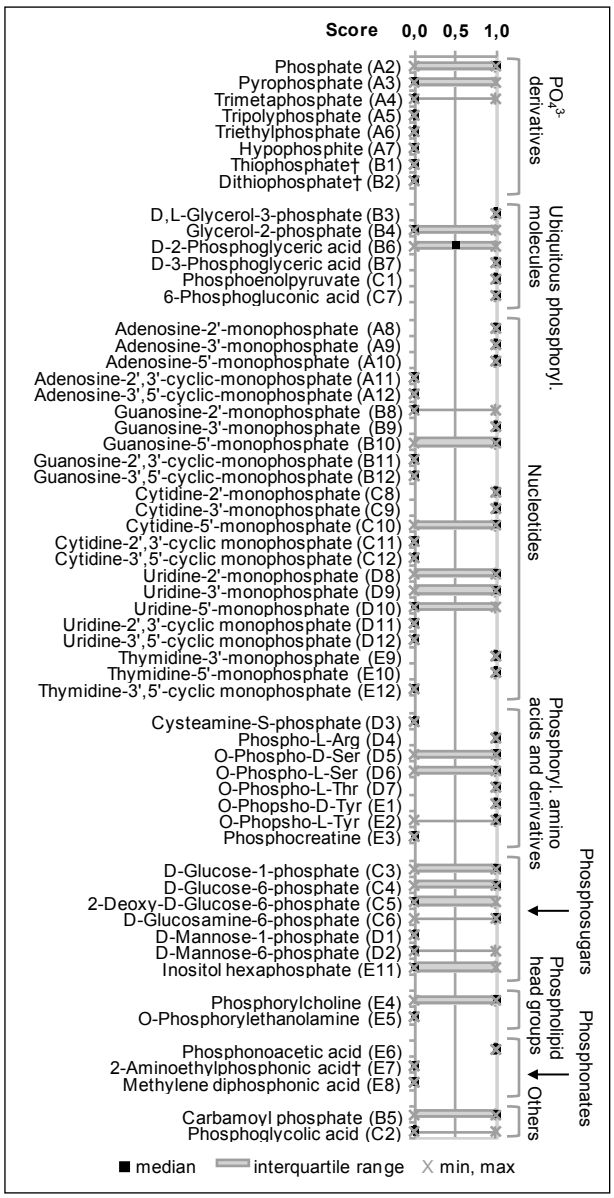

Figure 14. Growth of* Knufia petricola *A95 with different phosphorus sources (plate PM4)

Strain was inoculated 1/1'000 and plate was incubated for 5 d. Phosphorus sources were grouped into chemical classes. Relative strong background growth in negative control well due to oligotrophism made the assignment of the score "2" not possible. † Toxic (less growth than negative control). (Adopted from Nai *et al.*, 2013 [91].)

Knufia petricola A95 versus isogenic mutants A95pm1 and A95pm2

To investigate differences between *K. petricola* A95 and its isogenic mutants at the physiological level, strains A95pm1 and A95pm2 were characterized as reported above, and results were compared with those obtained for the wild type. The analysis included growth of mutants in plates PM9-10 (salt tolerance and pH profile) and PM1-3 (utilisation of carbon and nitrogen sources), as well as PM11-16 (drug plates to assess different sensitivity toward chemicals).[15] Plate PM4 (phosphorus and sulphur metabolism) was omitted given the difficulties encountered with *K. petricola* A95.

For both mutant strains, general growth requirements (plates PM9-10) were very similar to those of wild type (*Figs. 15-16*). A slightly increased tolerance to NaCl was observed for both (10 % w/v NaCl well tolerated). This was unexpected, since melanised cell wall is an efficient protection against osmotic stress [65,99]. The growth pattern was almost identical for the three strains upon presence of salt species other than NaCl. As for the wild-type strain, tolerance toward 6 % w/v NaCl was not improved by compatible solutes (no higher scores in comparison to "control" score with 6 % w/v NaCl).

A shift in pH optimum was observed for both mutants in comparison to the wild type (toward basic pH for A95pm1 and toward acidic pH for A95pm2). Compared with *K. petricola* A95 at pH 4.5, norleucine, norvaline and urea was not inhibitory for pink mutant A95pm1 and several amino acids (e.g. Arg, Glu, Gly, Met) had a beneficial effect on growth; cysteic acid and urea were not inhibitory for A95pm2 while trimethylamine-*N*-oxide was.

Analyses of carbon and nitrogen metabolism of pink mutants are shown in *Figs. 17-19*. For both strains, growth upon absence of carbon or nitrogen in negative controls was more pronounced than the wild type (not shown). Therefore, the score "2" could not be assigned.

Regarding carbon metabolism, both mutants showed differences with the parental strain, however, such differences seemed to be restricted to some compounds and not clustered into specific metabolic pathways or group of chemicals (*Figs. 17-18*). Importantly, almost absolute overlapping was observed in the group "Black cell wall and aromatic pathways."

Differences also emerged in the analysis of nitrogen metabolism, although, for chemical groups, preferential utilisation was similar in the three strains (i.e. simple nitrogenous compounds, amino sugars, nucleobases and derivatives, dipeptides; *Fig. 19*). Mutants showed most differences in the utilisation of amino acids and derivatives and were less able to grow on primary amines; pink mutant A95pm1 was apparently using amides and aminated alkanes more efficiently than *K. petricola* A95 (*Fig. 19*, left panel), whereas the same was not true for A95pm2 (*Fig. 19*, right panel).

[15] Due to a shortage of plates, in some cases less than three replicates were run. These were PM1, PM2, PM11 and PM14 for A95pm1 (two replicates); PM1, PM2, PM3 and PM14 for A95pm2 (two replicates) and PM11 for A95pm2 (one replicate only). Growth in PM15-16 was not reproducible for any strain and the results were not considered.

Susceptibility of *K. petricola* A95 and pink mutants toward drugs is shown in *Fig. 20*. Several substances were able to halt growth of wild-type and mutant strains (median ≤ 0.5), in particular salts of transition metals (e.g. nickel, chromate, cobalt, copper, cadmium, vanadate), quaternary ammonium salts (e.g. benzethonium chloride, dequalinium, sanguinarine), inducers of stringent response (e.g. D,L-serine hydroxamate, L-aspartic acid-β-hydroxamate) and nucleic acid inhibitors (e.g. nalidixic acid, novobiocin). Others active compounds included the antifungal acriflavine, the β-lactame nafcillin, as well as the pyrimidine analogue 5-fluorouracil and its pro-drug 5-fluoroorotic acid.

Pairwise comparisons with the wild type showed increased susceptibility of both mutants toward several drugs (median difference ≥ 1), in particular β-lactame antibiotics (e.g. ampicillin, azlocillin, cefuroxime, geneticin, moxalactam) and aminoglycosides (e.g. sisomicin, tobramycin, spectinomycin). In no case, a chemical active against *K. petricola* A95 was more tolerated by the mutants than the parental strain.

Figure 15. Growth of pink mutant A95pm1 versus* Knufia petricola *A95 under osmotic stress (left panel) and different pH values (right panel) (Biolog's plates PM9-10)

Pink mutant A95pm1 was inoculated 1/100 and plates were incubated for 7 d. Data are shown as in *Fig. 10* for *K. petricola* A95. Median values for *K. petricola* A95 (open green squares) are reported for direct comparison.

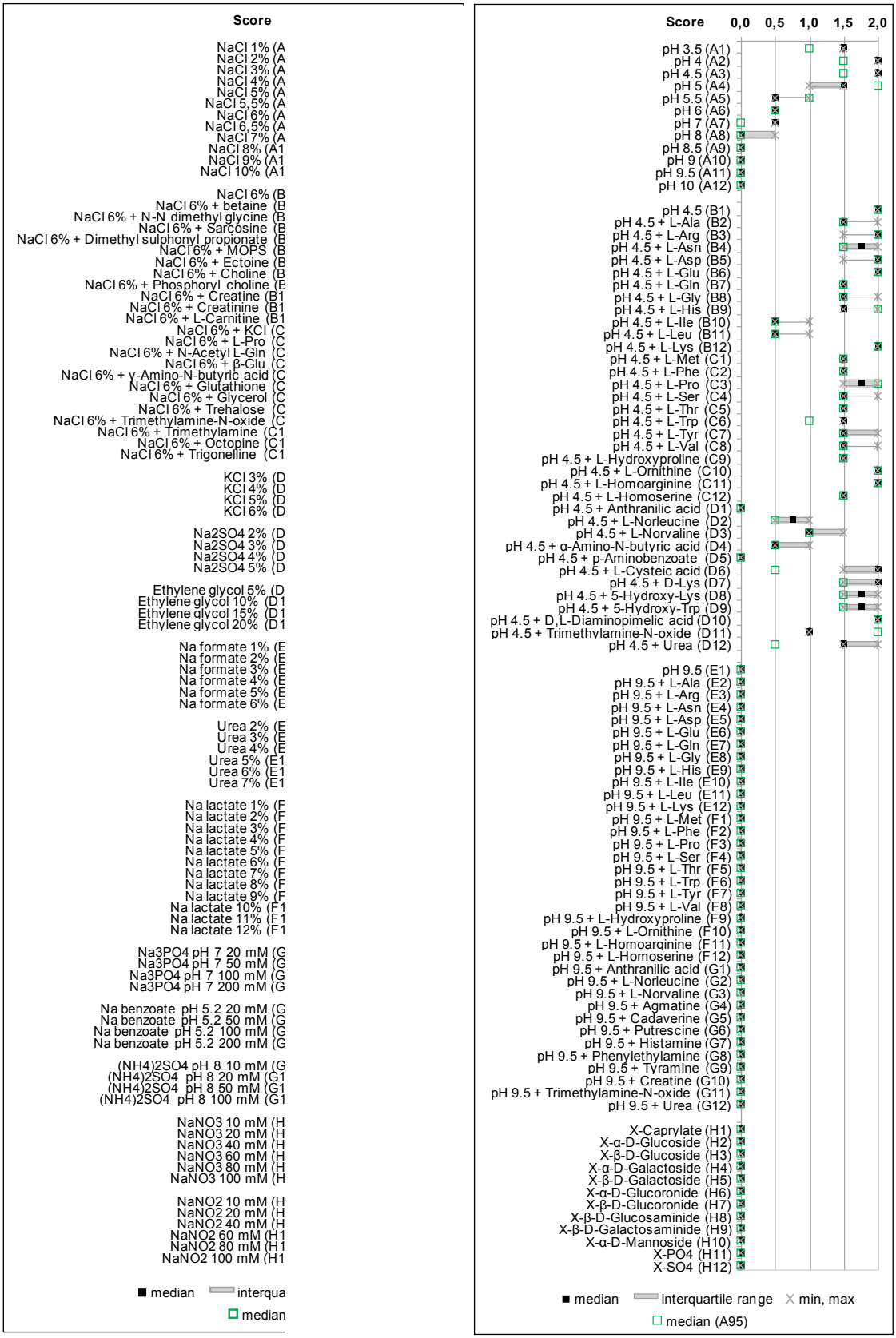

Figure 16. Growth of pink mutant A95pm2 versus* Knufia petricola *A95 under osmotic stress (left panel) and different pH values (right panel) (Biolog's plates PM9-10)

Results for pink mutant A95pm2 in PM9-10 were generated as illustrated for A95pm1 in *Fig. 15*.

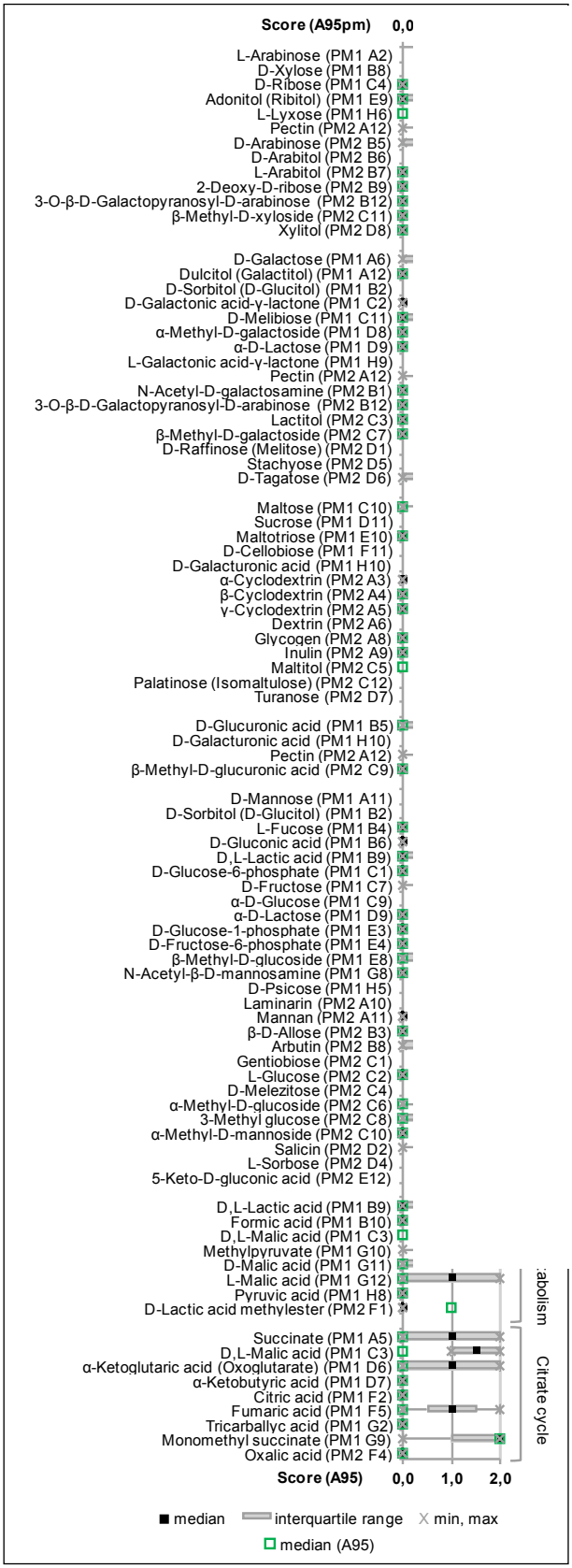

Figure 17. Growth of pink mutant A95pm1 versus* Knufia petricola *A95 with different carbon sources (Biolog's plates PM1-2)

Pink mutant A95pm1 was inoculated 1/100 (inoculating fluid buffered with 20 mM citric acid and acidified at pH 5) and plates were incubated for 11 d. Data are shown as in *Fig. 12* for *K. petricola* A95 (with additional carbon sources reported in *Suppl. Fig. 3*). Median values for *K. petricola* A95 (open green squares) are reported for direct comparison.

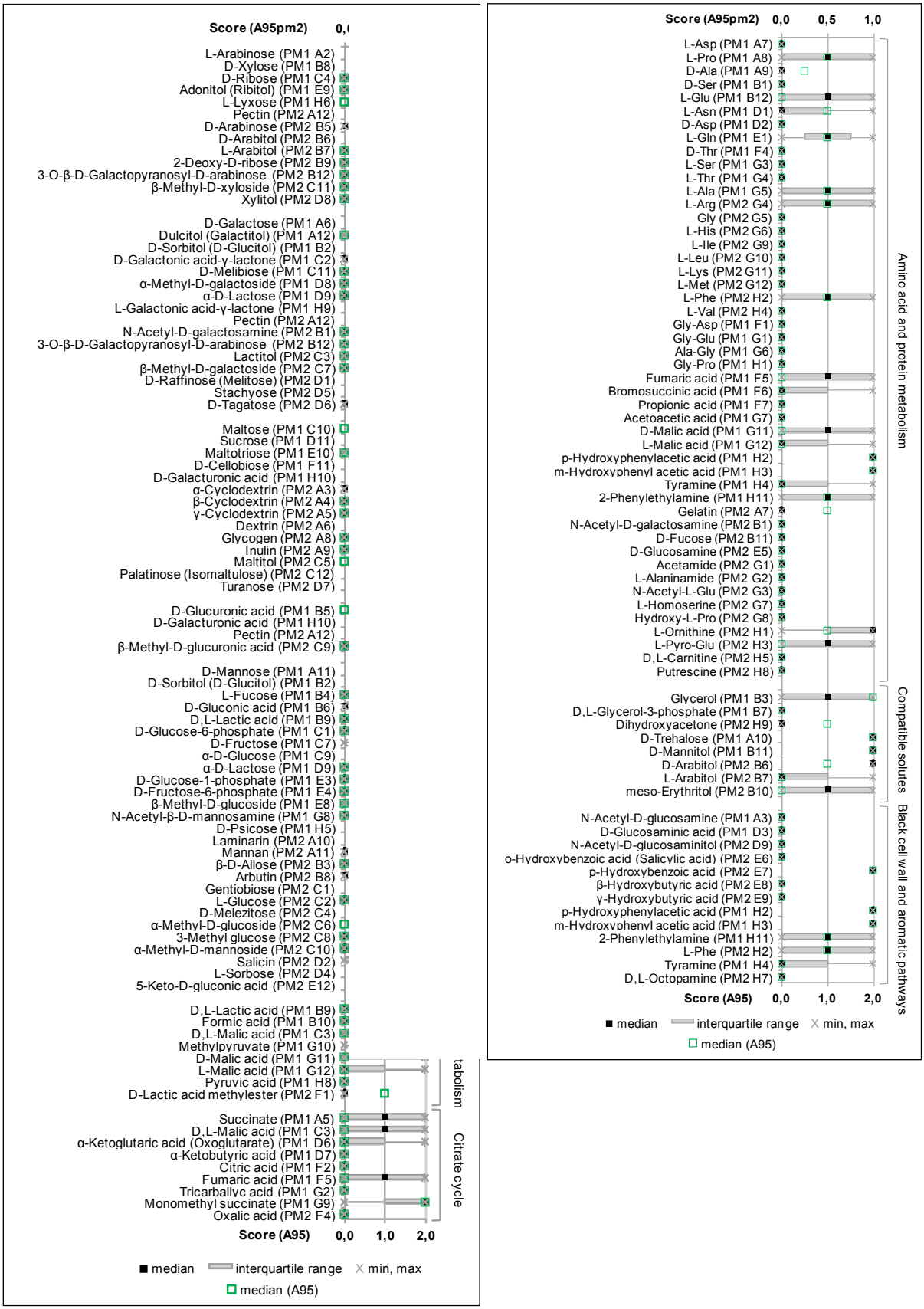

Figure 18. Growth of pink mutant A95pm2 versus* Knufia petricola *A95 with different carbon sources (Biolog's plates PM1-2)

Results for pink mutant A95pm2 in PM1-2 were generated as illustrated for A95pm1 in *Fig. 17*.

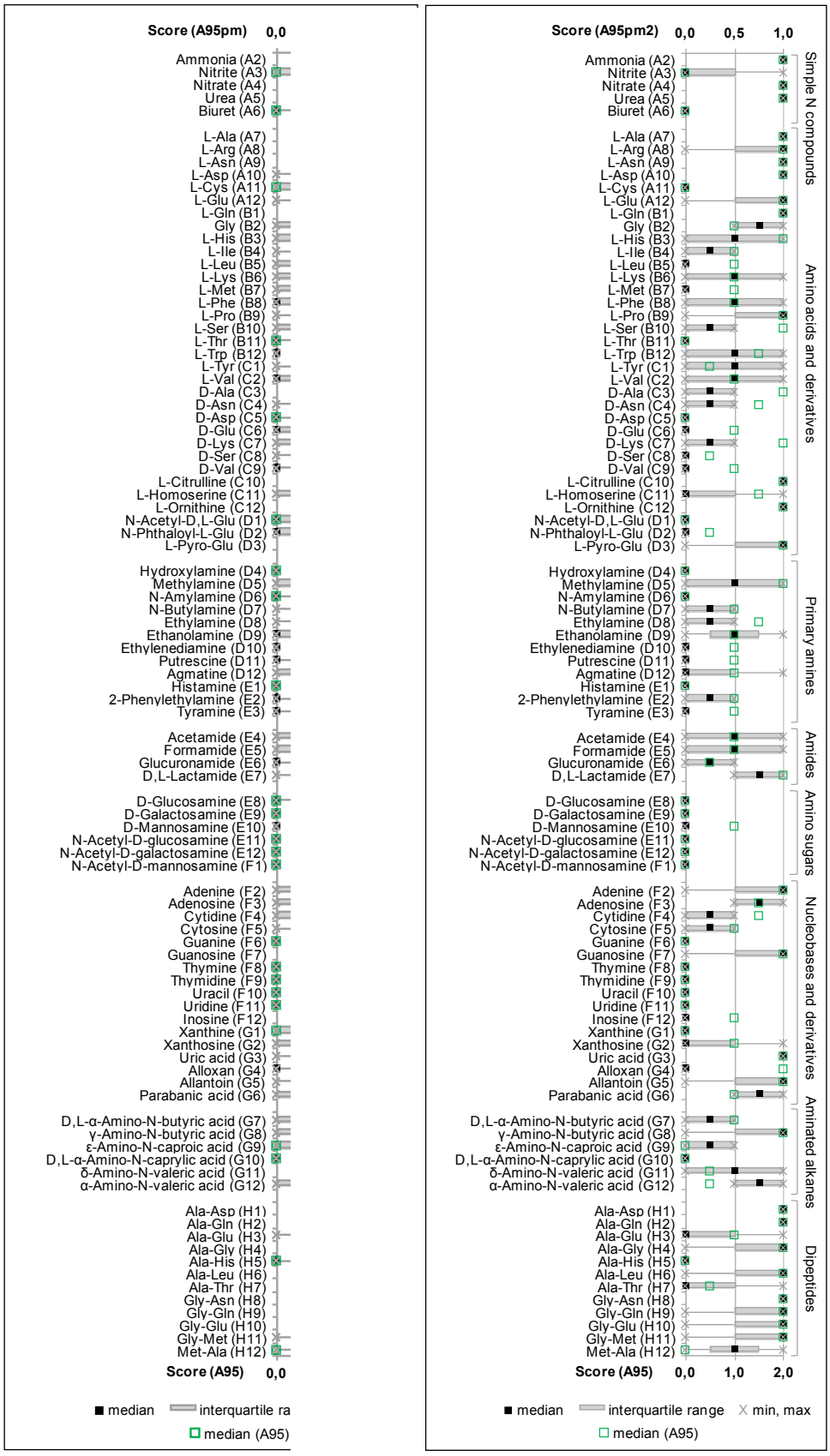

Figure 19. Growth of pink mutants A95pm1 (left panel) and A95pm2 (right panel) versus* Knufia petricola *A95 with different nitrogen sources (Biolog's plate PM3)

Pink mutants A95pm1 and A95pm2 were inoculated 1/100 and plates were incubated for 7 d. Data are shown as in *Fig. 13* for *K. petricola* A95. Median values for *K. petricola* A95 (open green squares) are reported for direct comparison.

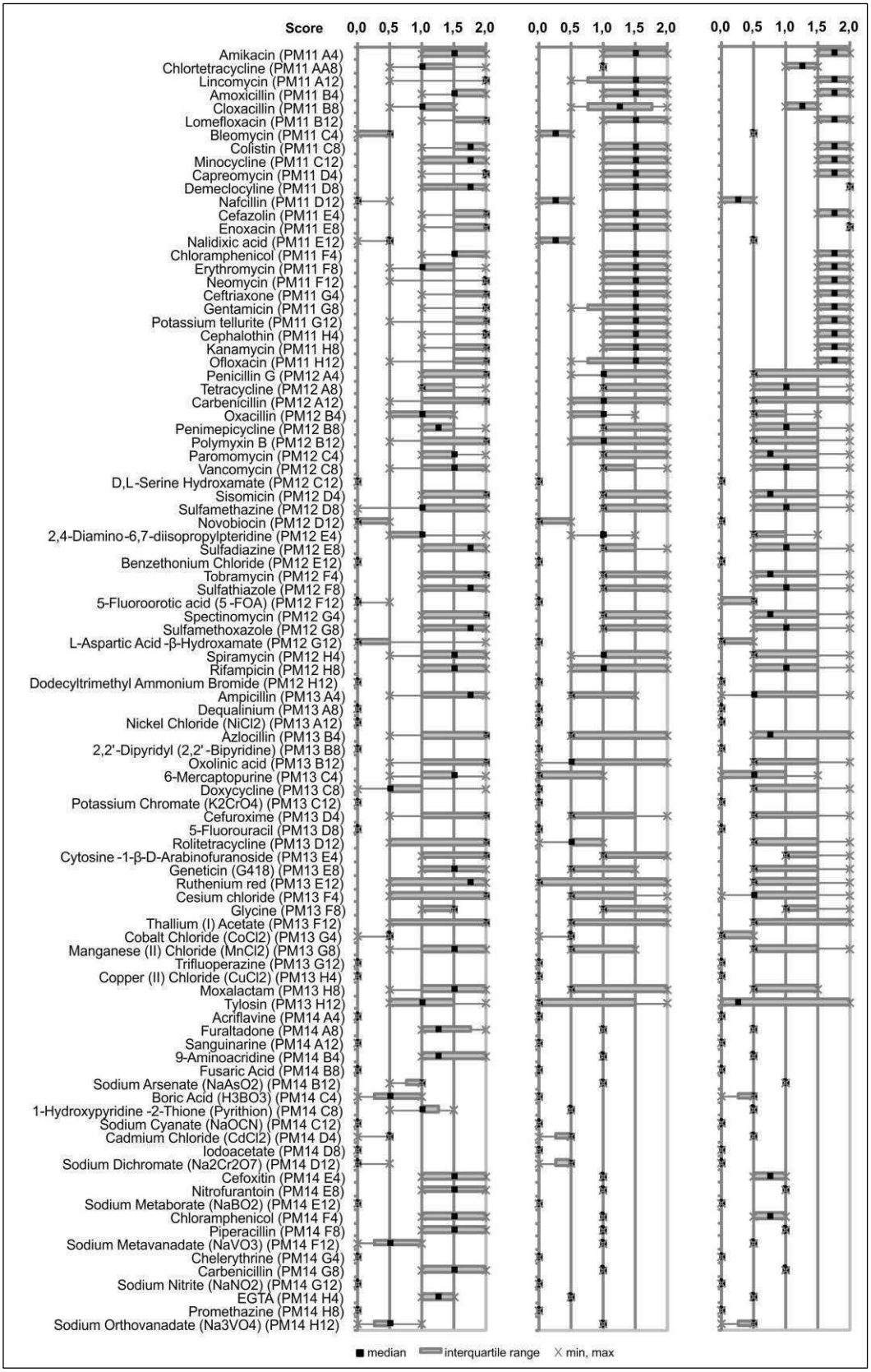

Figure 20. Growth of* Knufia petricola *A95 and pink mutants A95pm1 and A95pm2 with growth-inhibiting drugs (Biolog's plates PM11-14)

All strains (*K. petricola* A95, left; A95pm1, centre; A95pm2, right) were inoculated 1/100 and plates were incubated for 7 d. Every chemical is present in four wells at increasing concentrations (values not disclosed by Biolog Inc.). For sake of simplicity, only results for each fourth well is shown, i.e. those with highest drug concentrations.

Knufia petricola A95 versus *Coniosporium apollinis*

The strains *K. petricola* A95 and *C. apollinis* share the same ecological niche and lifestyle as well as – like many black fungi – similar morphological traits, but belong to two different classes of ascomycetes. Comparing their phenotypes is therefore of interest to share light into diversification and specialized lifestyle of rock-inhabiting black fungi. Broad physiological profile of *C. apollinis* was generated as presented above for *K. petricola* with Biolog's plates PM9-10 (salt tolerance and pH profile) and PM1-3 (utilisation of carbon and nitrogen sources). As for the mutants, analysis using plate PM4 was omitted.

As observed under salt stress (PM9), *C. apollinis* is less osmotolerant than *K. petricola* A95 (*Fig. 21*, left panel). No biomass formation could be recognized from 5 % w/v NaCl (vs. 9 % w/v for *K. petricola* A95). This taken into consideration, the general trend is the same as for *K. petricola* A95 (same salt species are tolerated but growth is reduced at lower concentrations, and putative compatible solutes are ineffective also for *C. apollinis*). An exception is represented by ammonium sulphate (more inhibitory) and sodium phosphate (less inhibitory). This last, however, is as observed on pH plate (PM10) probably a pH effect. In comparison to *K. petricola* A95, growth was possible over a broader pH range (pH 4.5 to pH 9.0 with some basal growth at more alkaline conditions), and a shift toward basic values was observed (*Fig. 21*, right panel). Growth optimum was less stringent and distributed between pH 5.0 and pH 6.0. Some compounds were inhibitory at pH 4.5 similarly as for *K. petricola* A95 (i.e. isoleucine, leucine, tryptophane and *o*-/*p*-aminobenzoate) but, given reduced growth for *C. apollinis* at acidic conditions, some amino acids (especially polar uncharged as well as some hydrophobic ones) could be identified as able to increase growth.

Analyses of carbon and nitrogen metabolism are shown in *Figs. 22-23*. Also for *C. apollinis*, as for the mutants, background growth in negative control wells deprived of carbon or nitrogen was stronger than for *K. petricola* A95 (not shown), and the score "2" was omitted.

The black fungus is even more selective in the utilisation of carbon sources than *K. petricola* A95, with 160 out of 190 compounds (ca. 84 %) unable – or very poorly able – to support growth (median = 0; *Fig. 22*). Major differences for *C. apollinis* in comparison to *K. petricola* A95 were observed in the pentose catabolic pathway (growth on the intermediates adonitol, L-arabitol, xylitol), the galactose pathway (no growth D-galactose and thus seemingly not active)[16], the starch and sucrose metabolic pathway (more active with maltose, maltotriose, maltitol, the plant disaccharide D-cellobiose and the polysaccharide of animal or fungal origin glycogen supporting strong growth) and the aromatic pathway (inactive). The remaining metabolic pathways were poorly active or inactive in both strains. Another main discrepancy between the two black fungi was that sugar alcohols (adonitol, L-arabitol, xylitol, D-sorbitol, maltitol, glycerol, mannitol, dihydroxyacetone) were good carbon

[16] Growth on D-sorbitol, D-melibiose and stachyose is not supportive of activity of galactose pathway since D-sorbitol is also in the glycolytic pathway and the two oligosaccharides are composed of glucose, which is probably responsible for growth.

sources for *C. apollinis* but not used by *K. petricola* A95 (except for *meso*-erythritol, not used by *C. apollinis* as well).

Also in the utilisation of nitrogen compounds (*Fig. 23*), *C. apollinis* is more selective than *K. petricola* A95, with only 35 out of 95 compounds supporting growth. For all chemical but few exceptions, less (or occasionally same) growth was observed. Higher median was calculated with the purine base xanthine, the aminated alkane δ-amino-*N*-valeric acid and the dipeptide methionine-alanine. With regard to chemical classes, similar responses were observed for simple nitrogenous compounds and amino sugars. However, neither D-amino acids nor primary amines (except tyramine) could support growth of *C. apollinis* even though they were relatively good nitrogen sources for *K. petricola* A95.

Figure 21. Growth of* Coniosporium apollinis *versus* Knufia petricola *A95 under osmotic stress (left panel) and different pH values (right panel) (Biolog's plates PM9-10)

Coniosporium apollinis was inoculated 1/100 and plates were incubated for 14 d. Data are shown for *C. apollinis* as in *Fig. 10* for *K. petricola* A95. Median values for *K. petricola* A95 (open green squares) are reported for direct comparison.

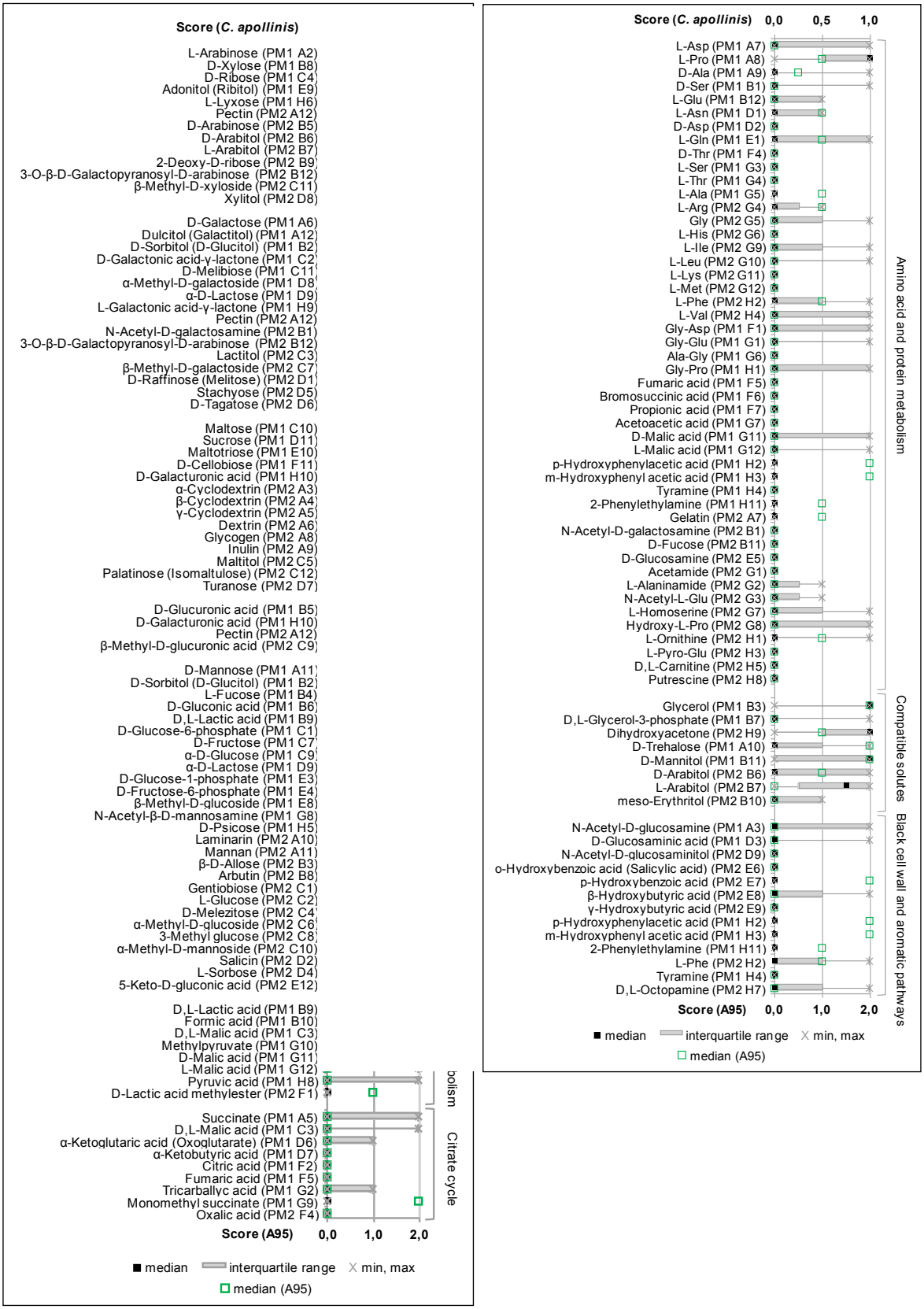

Figure 22. Growth of* Coniosporium apollinis *versus* Knufia petricola *A95 with different carbon sources (Biolog's plates PM1-2)

Coniosporium apollinis was inoculated 1/100 (inoculating fluid buffered with 20 mM citric acid and acidified at pH 5) and plates were incubated for 11 d. Data are shown as in *Fig. 12* for *K. petricola* A95 (with additional carbon sources reported in *Suppl. Fig. 3*). Median values for *K. petricola* A95 (open green squares) are reported for direct comparison.

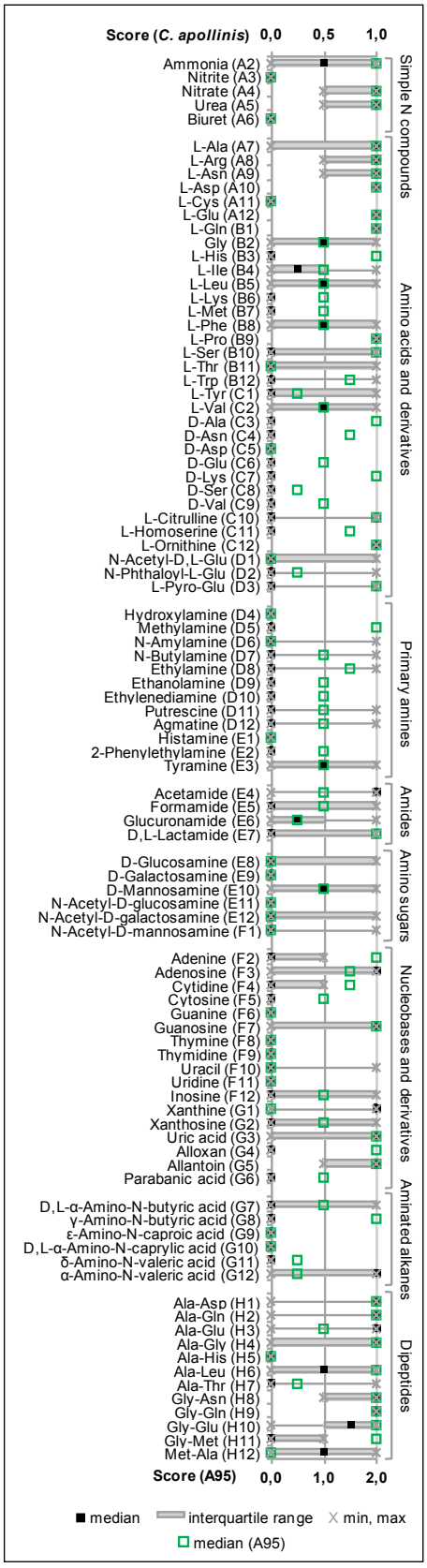

Figure 23. Growth of* Coniosporium apollinis *versus* Knufia petricola *A95 with different nitrogen sources (Biolog's plate PM3)

Coniosporium apollinis was inoculated 1/100 and plate was incubated for 7 d. Data are shown as in *Fig. 13* for *K. petricola* A95. Median values for *K. petricola* A95 (open green squares) are reported for direct comparison.

3.II.4 Physiological characterisation (2) – Assimilation of hydrocarbons

A restricted group of black fungi colonizes niches rich in hydrocarbons and is able to assimilate them as sole carbon and energy source [5,103,104,132,147,163]. Although high-throughput analysis of black-fungal metabolism was possible with Biolog's Phenotype MicroArrays, assessment of hydrocarbon utilisation was limited. Promisingly, *p*-hydroxybenzoic acid, a molecule central to metabolism of aromatic compounds – including hydrocarbons – in fungi [104], was one of the few excellent carbon sources for *K. petricola* A95 and its mutants, even if not used by *C. apollinis* (*Figs. 12, 17-18, 22*).

Selected black-fungal strains were tested for ability to utilize benzene, toluene and pentane as sole carbon and energy source as described above (*Section 2.5.3*). These volatile organic compounds (VOCs) are among the simplest hydrocarbons (benzene: unsubstituted monoaromatic molecule; toluene: mono-substituted alkyl-derivative of benzene; pentane: short-chained alkane [2]). While ability to metabolize them is a proof of hydrocarbon assimilation, the contrary would at the same time speak against utilisation of more complex ones.

Another candidate molecule to test usage of hydrocarbons was phenol. This less-volatile, mono-substituted benzene derivative is composed of a single aromatic ring with one hydroxyl group [2]. Phenol is a simple molecule which is catabolised through pathways distinct from those of simple volatile organic compounds [104]. Thus, testing utilisation of phenol as sole carbon and energy source in black fungi is complementary to the VOC-utilisation assay. Moreover, many natural-occurring molecules of plant origin are composed of phenol [3,6,141] and it is known that microorganisms (e.g. some actinobacteria) are able to metabolise it [107].

None of the selected black fungi was able to assimilate volatile organic compounds

Strains *K. petricola* A95, its isogenic pink mutant A95pm1 and *C. apollinis* were tested for usage of all three volatile organic compounds; for growth on toluene an uncharacterized *Fonsecaea* spp. was included in the experiment, while *Cladophialophora psammophila* was used as positive control strain [5]. Growth was assessed by gas-chromatographic measurements of carbon dioxide (CO_2) increases vs. VOC decreases over ca. 5 w of incubation. First, results for the control flasks without hydrocarbons are presented, i.e. CO_2 increases in flasks either with or without glucose (positive and background respiration controls, respectively; *Fig. 24*). Then, carbon dioxide production in flasks provided with hydrocarbons is shown (*Fig. 26*) and carbon balance for the positive control was calculated to validate the experimental results (*C. psammophila* growing on toluene; *Fig. 25*). Summarizing tables with VOC (initial and final values) and CO_2 concentrations (final values) are reported (*Tabs. 8-9*). Complete gas-chromatographic measurements of VOCs as well as calibration curves are reported in *Suppl. Figs. 4-5*.

In glucose flasks and background respiration controls, CO_2 values between 0.20-0.49 mM (8.9-21.6 mg/L) and between 1.19-1.69 mM (52.4-74.5 mg/L) were observed, respectively (*Fig. 24*). Once evolution of CO_2 concentrations in controls was determined, values for flasks provided with hydrocarbons were examined. Only for the positive control strain *C. psammophila* incubated with toluene, either with or without glucose, an increase in CO_2 concentration was observed (*Fig. 26A*). This increase was combined with a decrease in hydrocarbon and thus reflected substrate assimilation (*Tab. 8*).[17] For the other strains, no increases in CO_2 were observed in presence of hydrocarbons alone, but only when glucose was present. Low final CO_2 values in control flasks with both toluene and glucose (*Fig. 26A*) indicated toxicity at the used concentration, while no toxicity was observed for benzene or pentane (*Fig. 26B-C*). In abiotic controls (flasks without biomass) a reduction in toluene and benzene was observed probably due to leakage (*Tab. 8*). Reductions in VOC concentration in comparison to abiotic controls for *K. petricola* A95 (pentane) and for pink mutant A95pm1 (toluene) were observed, but these were not in concurrence with CO_2 increases in comparison with background respiration controls (*Figs. 24, 26* and *Tab. 8*). They should thus be considered artefacts (see *4 DISCUSSION*).

Carbon balance for *C. psammophila* growing on toluene was reproducible with previous results [5], indicating correct experimental set-up and execution (*Fig. 25*). Mineralisation values for toluene and glucose were calculated (ca. 66 % w/w and ca. 53 % w/w, respectively). The latter is lower probably because the sugar is a better carbon source and thus more efficiently incorporated into anabolic pathways.

Gas-chromatographic measurements for the hydrocarbon-utilisation assay were performed only once. All flasks were incubated further (up to three months) and biomass formation was visually assessed. In none a delay in the onset of growth could be observed. Inability of strains to grow on toluene as sole carbon and energy source, as opposed to growth inhibition due to toxicity, was confirmed by repeating the experiment with 5 µL toluene instead of 10 µL (0.55 mM in the liquid phase at equilibrium). By visual inspection, growth was observed in the control flasks with both toluene and glucose (indicating no toxicity), but not in the flasks with toluene only [Francesc Prenafeta; personal communication], thus confirming that the selected black fungi are unable to assimilate volatile organic compounds.

[17] It was also noted, only for *C. psammophila* growing on toluene, a biomass formation at the gas-liquid interphase attached to the flasks interior, indicative of utilisation of volatile compound (not shown).

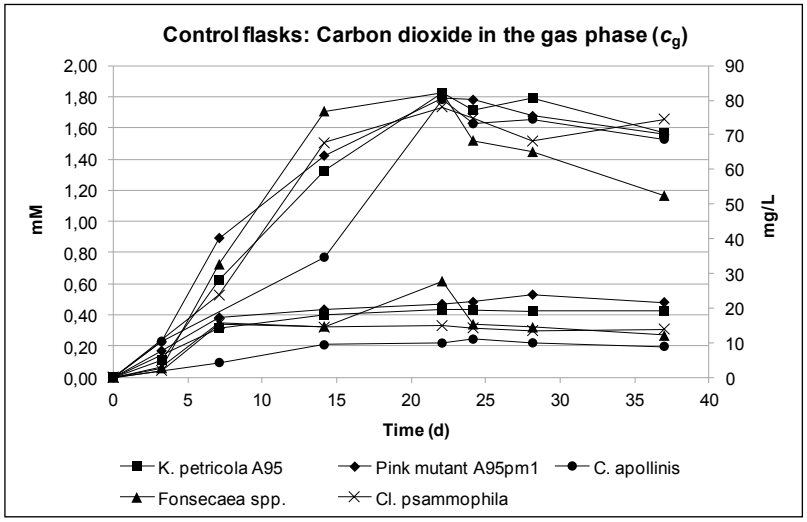

Figure 24. Carbon dioxide increases in control flasks of hydrocarbon-utilisation assay

CO_2 concentrations for control flasks without hydrocarbon and with glucose (solid lines) or without any carbon source (background respiration controls, dashed lines). Data were determined by GC-TCD measurements in the gas phase over 37 d of incubation. Some early measurements (between 0-7 d) were missing and are omitted from the chart.

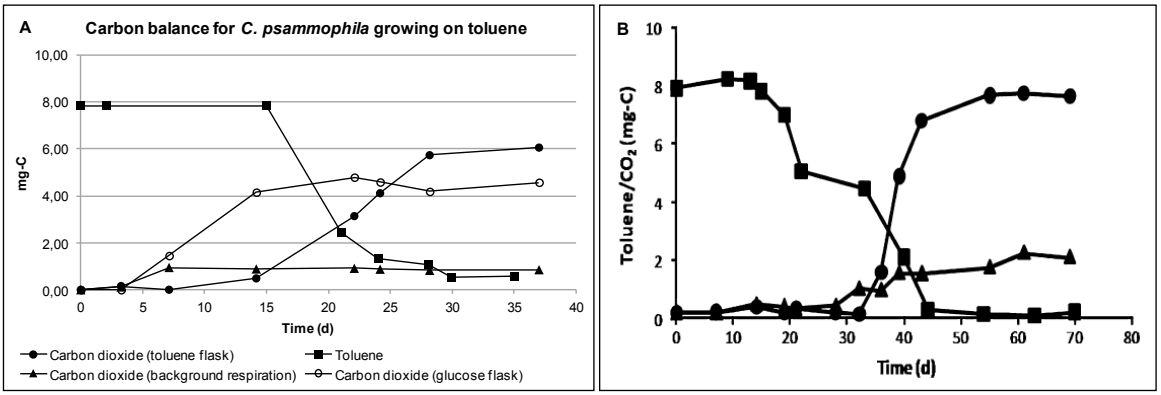

Figure 25. Carbon balance for* Cladophialophora psammophila *growing on toluene

(A-B) Carbon balance (in mg-carbon) for *C. psammophila*: Toluene consumption (squares) vs. CO_2 generation (circles) in flask with VOC; CO_2 generation in control flasks without carbon (background respiration control, triangles) or with glucose alone (open circles). **(A)** Chart generated in this study with GC-TCD and GC-FID data for *C. psammophila*. Values of VOC at day 0, day 2 and day 15 are theoretical (calculated) values since measured values were outliers (see *Suppl. Fig. 5*). **(B)** Assimilation of toluene by *C. psammophila* as previously reported (Badali *et al.*, 2011 [5]). Earlier onset of growth in **(A)** compared to **(B)** was due to different supplementation of Mineral Medium MM (0.02 % w/v yeast extract vs. 0.01 % w/v in Badali *et al.*, 2011 [5]).

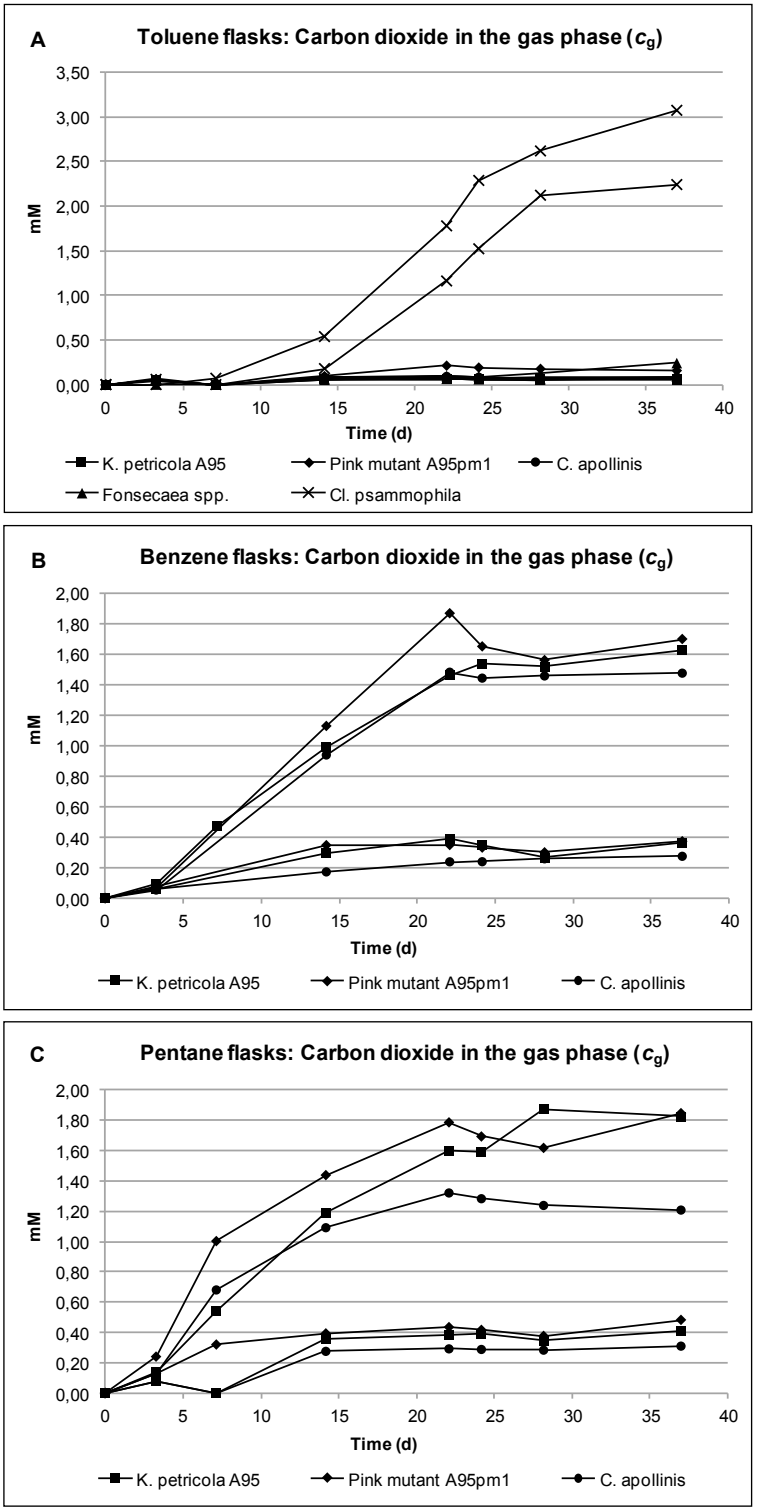

Figure 26. Only* Cladophialophora psammophila *showed respiration upon incubation with volatile organic compounds (toluene)

(A-C) Carbon dioxide concentrations in flasks with VOC and glucose (co-metabolism/toxicity controls, solid lines) or with VOC alone (dashed lines). Data were determined by GC-TCD in the gas phase over 37 d of incubation. **(A)** Toluene flasks: CO_2 increases were observed for *C. psammophila* growing on toluene, both without and with glucose, but not for the other strains, whereas no respiration in flasks amended with glucose indicated toxicity of toluene at the used concentrations. **(B-C)** Benzene and pentane flasks: CO_2 increases were observed only in flasks with VOC supplemented with glucose and not in flasks with VOC alone, indicating no toxicity by benzene and pentane but no ability to catabolise them. In **(B)**, data for day 7 were missing and were therefore omitted (except for *K. petricola* A95 in control flasks amended with glucose).

Table 8. Hydrocarbon and carbon dioxide concentrations in the hydrocarbon-utilisation assay (gas phase)[a]

Strain	Initial VOC conc. (mM)[b]			Final VOC concentration (mM)									Final CO_2 concentration (mM)					
	T	B	P	T	T+G	T(AC)[c]	B	B+G	B(AC)[c]	P	P+G	P(AC)[c]	T	T+G	B	B+G	P	P+G
K. petricola A95				0.16	0.16		0.22	0.25		**0.26**	0.39		0.05	0.06	0.36	1.63	0.41	1.83
A95pm1		0.33	0.38	**0.07**	0.14		0.18	0.25	0.23	0.40	0.43	0.35	0.16	0.08	0.37	1.70	0.48	1.85
C. apollinis	0.29			0.14	0.13	0.13	0.25	0.21		0.38	0.39		0.08	0.06	0.27	1.48	0.31	1.21
Fonsecaea spp.[d]		n/a	n/a	0.12	0.13		n/a	n/a	n/a	n/a	n/a	n/a	0.24	0.09	n/a	n/a	n/a	n/a
C. psamm.[d]		n/a	n/a	**0.02**	**0.03**		n/a	n/a	n/a	n/a	n/a	n/a	**2.24**	**3.07**	n/a	n/a	n/a	n/a

T: toluene; B: benzene; P: pentane; +G: control with glucose (co-metabolism/toxicity control); AC: abiotic control flasks (without biomass). In bold are highlighted decreases in VOC concentrations relative to abiotic controls and increases in CO_2 concentrations similar to those observed in the positive controls (see *Fig. 24*). Both were registered only for *C. psammophila* incubated with toluene.

[a] Measured by gas chromatography (GC-FID or GC-TCD) after ca. 5 w of incubation

[b] Initial values were calculated in the gas phase at equilibrium for flasks both with or without glucose as reported in *Section 2.5.3* [2]

[c] Abiotic control: reported is the average value of four measurements (two flasks and two measurements each)

[d] For *C. psammophila* (positive control strain) and *Fonsecaea* spp., only utilisation of toluene was tested.

Table 9. Hydrocarbon concentrations in the hydrocarbon-utilisation assay (liquid phase)[a,b]

Strain	Initial VOC conc. (mM)[c]			Final VOC concentration (mM)								
	T	B	P[d]	T	T+G	T(AC)[e]	B	B+G	B(AC)[e]	P	P+G	P(AC)[e]
K. petricola A95				0.61	0.61		1.02	1.15		**4.90×10^{-3}**	7.46×10^{-3}	
A95pm1		1.52	7.24×10^{-3}	**0.25**	0.53		0.83	1.15	1.06	7.55×10^{-3}	8.11×10^{-3}	6.66×10^{-3}
C. apollinis	1.11			0.52	0.50	0.48	1.14	0.98		7.21×10^{-3}	7.50×10^{-3}	
Fonsecaea spp.[f]		n/a	n/a	0.47	0.50		n/a	n/a	n/a	n/a	n/a	n/a
C. psamm.[f]		n/a	n/a	**0.08**	**0.11**		n/a	n/a	n/a	n/a	n/a	n/a

T: toluene; B: benzene; P: pentane; +G: control with glucose (co-metabolism/toxicity control); AC: abiotic control flasks (without biomass). In bold are highlighted decreases in VOC concentrations relative to abiotic controls.

[a] Inferred in the liquid phase from concentrations in the gas phase (*Tab. 8*) as reported in *Section 2.5.3* with known H_C values [2]

[b] Concentrations of CO_2 in the liquid phase were not calculated since the gas reacts with water and Henry's Law does not apply

[c] Initial values were calculated in the liquid phase at equilibrium for flasks both with or without glucose as reported in *Section 2.5.3* [2]

[d] Pentane has a much lower H_C value than toluene or benzene, and therefore smaller concentrations in the liquid phase were obtained

[e] Abiotic control: reported is the average value of four measurements (two flasks and two measurements each)

[f] For *C. psammophila* (positive control strain) and *Fonsecaea* spp., only utilisation of toluene was tested.

Screening for phenol utilisation gave negative results

Utilisation of phenol as sole nutrient source by *K. petricola* A95, its isogenic mutants A95pm1 and A95pm2 and *C. apollinis* was screened in the defined medium ASM (see below, *Section 3.II.5*) deprived of carbon. Phenol was added at concentrations ranging from 1 nM to 10 mM. For all strains, no positive effects (judged by eye by biomass formation) were observed as compared to the negative control without phenol, and high concentrations seemed to be inhibitory (*Fig. 27*). Small-scale growth of *C. apollinis* in ASM was scarce and therefore it was not possible to draw any conclusions (omitted from figure). The screening was repeated only once.

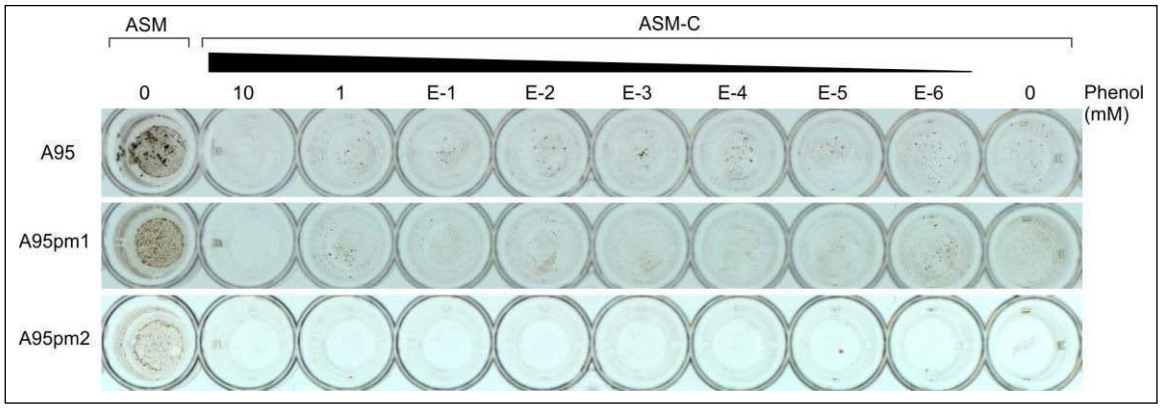

Figure 27. Phenol did not support growth of* Knufia petricola *A95 and its isogenic mutants
Growth of *K. petricola* A95 and its isogenic mutants A95pm1 and A95pm2 in microtiter plates in the defined medium ASM (see *Section 3.II.5*) or ASM without carbon (ASM-C) without or with increasing concentrations of phenol. Plate was incubated for up to 7 w.

Summary of results (Part II – first half)

In the first half of *PART II – Phenotypic characterisation of black fungi*, knowledge was gathered on the model microorganism *K. petricola* A95, with focus on morphology and physiology. Growth curves in liquid complex medium and broad phenotypic profiles with Biolog's Phenotype MicroArray plates were generated for a total of ca. 1'150 different conditions (including salt and pH tolerance, growth factor requirement, nutrient metabolism and resistance to drugs). Assimilation of selected hydrocarbons – benzene, toluene, pentane and phenol – was tested.

Other black-fungal strains were analyzed in some of the experiments for direct comparisons with *K. petricola* A95, namely pink mutants A95pm1 and A95pm2 (growth curves in MEB; ca. 850 conditions tested by phenotype microarrays; usage of hydrocarbons) and the rock-inhabiting fungus *C. apollinis* (ca. 500 conditions tested by phenotype microarrays; usage of hydrocarbons).

Data presented here are a prerequisite for experiments and results shown below in the second half of *PART II – Phenotypic characterisation of black fungi*.

Main findings are summarized as following:

- *K. petricola* A95 showed typical microcolonial traits
- The model strain was characterized as relatively fast-growing and halotolerant, with growth optimum around pH 5, and prototroph (yet stimulated by thiamine)
- Analysis of nutrient metabolism showed the activity of most metabolic pathways concomitant with selectivity in the utilisation of C sources (only ca. 33 % supporting growth)
- The strain was less selective in the utilisation of N and P sources (ca. 75 % and 50 % supporting growth, respectively)
- Several chemicals inhibitory for *K. petricola* A95 growth were identified

- In complex MEB, growth of pink mutants was comparable to those of wild type
- Pink mutants were slightly more tolerant toward osmotic stress than *K. petricola* A95, but similar pH preferences were observed; no major differences in nutrient metabolism of pink mutants were observed in comparison to the wild type
- β-Lactame antibiotics and aminoglycosides were more effective against pink mutants than the parental strain

- *C. apollinis* was less tolerant toward osmotic stress than *K. petricola* A95 and growth at alkaline conditions was favoured
- *C. apollinis* was more selective in the utilisation of C and N compounds than *K. petricola* A95; sugar alcohols were better C sources

- Volatile organic compounds (benzene, toluene, pentane) were not assimilated by *K. petricola* A95, pink mutant A95pm1 and *C. apollinis*
- Phenol did not not support growth of *K. petricola* A95 and pink mutants

- For all strains, marked oligotrophism was observed

3.II.5 A new synthetic growth medium for black fungi

As opposed to complex, nutrient-rich media where the exact formulation is not known and might vary from one batch to another (e.g. when using different lots of the same nutrient mixture), defined – i.e. synthetic – growth media are prepared from single substances and thus their chemical composition is fully known [80]. Such media allow standardization of experiments and the conception of further ones, as for example the analysis of growth rate and cellular morphology after varying the composition of the medium by depriving one (or more) single components or supplementing it with others. Commonly, their composition is simplified and they can thus be regarded as minimal media. Availability of suitable synthetic media is an essential tool in microbiology [80]. However, defined media specific for the cultivation of black fungi have not yet been developed and known recipes like Czapek Dox are unsatisfactory to obtain high biomass yields [118].

Based on the data presented above regarding growth physiology of *K. petricola* A95 in Phenotype MicroArray plates (*Section 3.II.3*), a new synthetic medium specific for the cultivation of the strain was designed [91]. As primary nutrients, those that supported high growth were chosen, i.e. D-mannitol,[18] nitrate and phosphate (C, N and P source, respectively; *Figs. 12-14*), while sulphate was selected as S source. Nutrients were added at non-limiting concentrations and high amounts of $NaNO_3$ (80 mM, well tolerated as shown in *Fig. 10*) were used to confer to the medium selective properties. Acidity was set at pH optimum (pH 5; *Fig. 9B*) with 20 mM citric acid as buffer, which is not used as C source (*Fig. 12*). As growth supplements thiamine was added (*Fig. 8B*) along with choline and *N*-acetyl-D-glucosamine. Minerals and trace elements (Mg, Cl, K, Fe, Mo, Mn and Zn) were reduced to the minimum and selected based on pre-experiments with known supplements and Biolog data (see *Suppl. Tab. 1* for details). This *ad hoc* medium was named ASM (for A95-Specific Medium) and its detailed composition is reported in *Subchapter 2.1 (2 MATERIALS AND METHODS)*.

Growth of the model organism in the new defined medium ASM (both liquid and solid) was tested (*Fig. 28*). On solid medium, colonies were easily recognizable after one week of incubation and were about half the size of those on MEA (*Fig. 28A-B*). In liquid medium, generation time g = 17.4 h and maximal log increase of 1.72 were obtained (*Fig. 28C*). In comparison to growth in MEB (see *Fig. 7A*), a delay in the onset of exponential-growing phase (ca. 24 h) as well as lower final cell densities after 2 w of incubation (ca. 5.7- to 6.8-fold differences) were observed. To rule out that such lower biomass yields were due to an improper medium formulation or that growth was enhanced by internally stored resources, final cell densities (after 2 w of incubation) were determined after up to three consecutive

[18] On solid ASM, D-(+)-sucrose was used instead of D-mannitol as carbon source since it supported better growth for unknown reasons.

passages, resulting in stable values (*Fig. 28D*). Thus, ASM is a suitable defined medium for cultivation of *K. petricola* A95 [91].

Preliminary observations showed that the new synthetic medium is able to support growth of *Capronia*, *Cladophialophora*, *Exophiala* and *Phialophora* spp., thus making ASM a suitable candidate medium for cultivation of other black-fungal strains (data not shown).

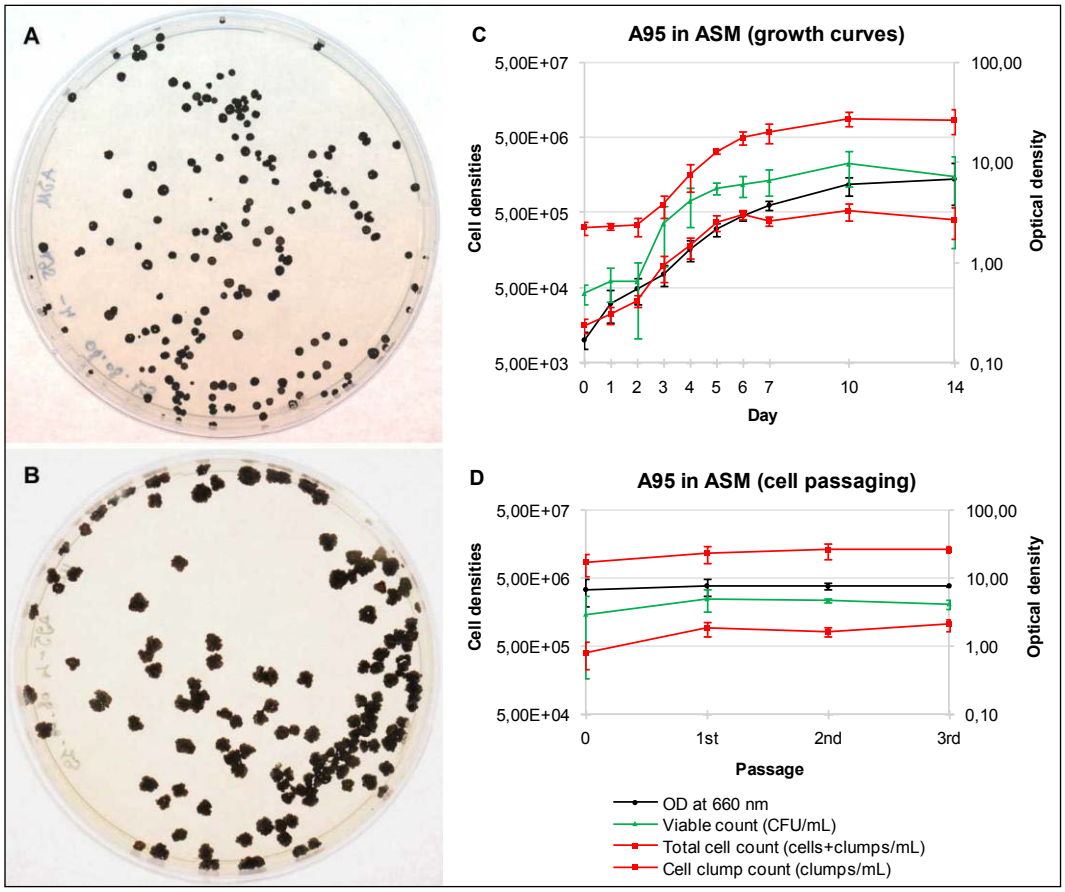

Figure 28. Growth of* Knufia petricola *A95 in the new synthetic medium ASM

(A-B) Growth of *K. petricola* A95 on **(A)** ASM and **(B)** MEA after ca. 2w. **(C)** Growth curves of *K. petricola* A95 in ASM. **(D)** Cell densities and absorbance values of *K. petricola* A95 in ASM after up to three consecutive passages (determined after 2 w of incubation). (Expanded from Nai *et al.*, 2013 [91].)

3.II.6 Temperature-optimum profiles

Even though black fungi are extremely stress-tolerant microorganisms, they usually have growth optima at mesophilic temperatures [124,126]. To determine experimentally T_{opt} of *K. petricola* A95, temperature-optimum profiles on both MEA and ASM after 4 weeks of incubation were generated. Since – aside from the obvious colour differences – only minor phenotypic differences were ascribed to the mutants in comparison with their parental strain (see above), A95pm1 and A95pm2 were also included in the analysis (*Fig. 29*).

Growth-temperature optimum of wild type was around 25 °C (*Fig. 26A*), corresponding to the temperature at which *K. petricola* strains are routinely incubated [56,156]. On ASM, colonies were about 2-3 times smaller than on MEA, although the difference was abrogated at 30 °C, probably indicating a medium-dependent temperature-optimum shift toward higher temperatures. On both media, negligible growth was achieved at 10 °C (surface area < 0.5 mm^2), while none was observed at 5 °C or 35 °C (omitted from figure). For A95pm1, growth on MEA was strongly impaired (see also *Fig. 4A*) and colonies reached an average surface area < 1 mm^2 but, strikingly, growth on ASM was comparable with those of wild type (same colony size and T_{opt} around 25-30 °C, *Fig. 29B*). In contrast, nearly identical profiles were obtained for A95pm2 and the wild type on both media (*Fig. 29C*).

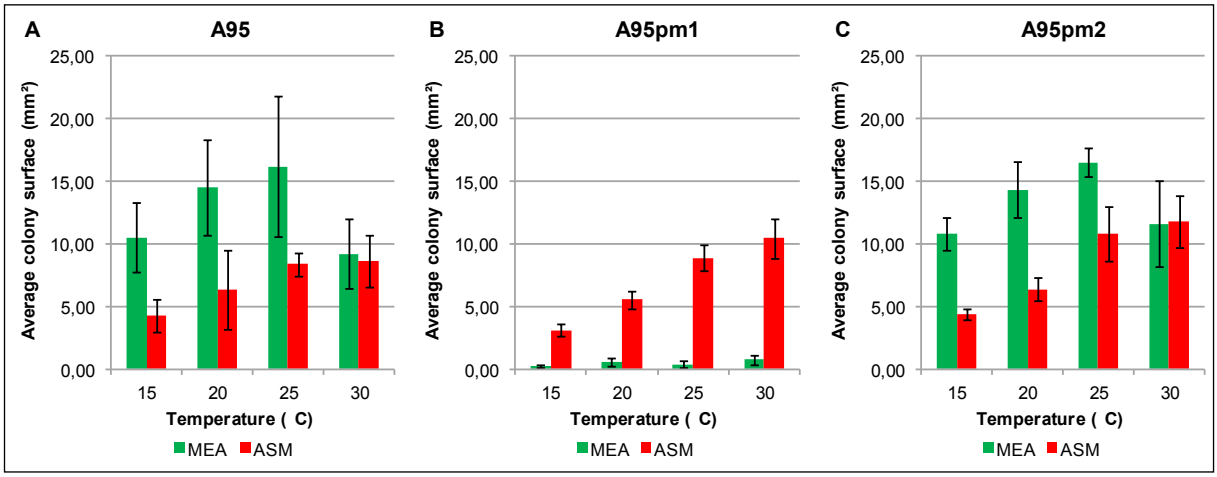

Figure 29. Temperature-optimum profiles of* Knufia petricola *A95 and pink mutants A95pm1 and A95pm2.

(A-C) Average colony surfaces in relation to incubation temperatures, obtained as illustrated in *Section 2.3.5*, for the three strains growing on malt-extract agar (MEA) and solid A95-Specific Medium (ASM). Plates were incubated for 4 w. Incubation at temperatures of 5 °C, 10 °C and 35 °C resulted in negligible growth (data omitted). Data were calculated from at least three independent replicates.

3.II.7 Description of mutants

During generation of temperature-optimum profiles, specific phenotypes of the isogenic mutants of *K. petricola* A95 were observed.

For pink mutant A95pm1 on ASM, aside from colony sizes similar to those of wild type (*Fig. 29B*), dark phenotype was restored, even though pigmentation was less pronounced than in the wild type (*Fig. 30A-C*). The same observation was not true for A95pm2 (*Fig. 30D*).

Although pink mutant A95pm2 was not affected upon incubation on different media, colonies became darker during incubation at low temperatures, suggesting that the strain is a temperature-sensitive mutant (*Fig. 31A*). The same phenomenon was not observed for A95pm1 (*Fig. 31D*).

Specific phenotypes of A95pm1 and A95pm2 were thus identified, which allowed a deeper characterisation of the mutants.

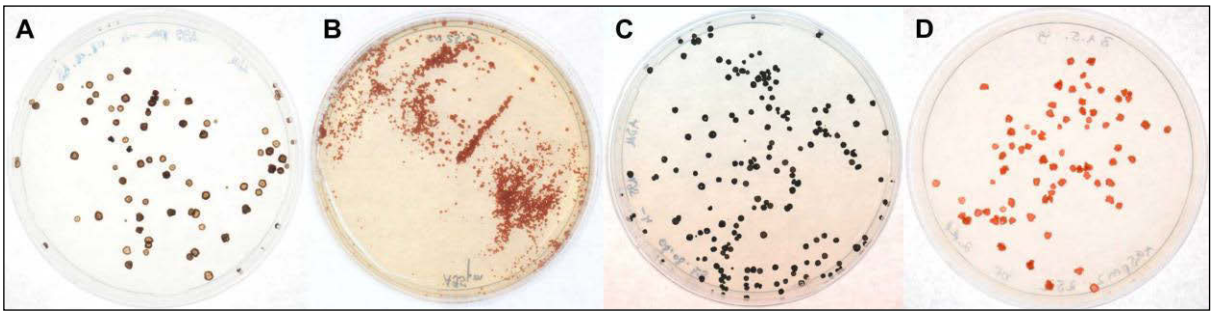

Figure 30. Phenotype of pink mutant A95pm1 on solid media

(A-B) Pink mutant A95pm1 on **(A)** ASM and **(B)** MEA. **(C)** *Knufia petricola* A95 on ASM. **(D)** Pink mutant A95pm2 on ASM. Plates were incubated for ca. 2 w, except for A95pm1 on MEA (ca. 3 w).

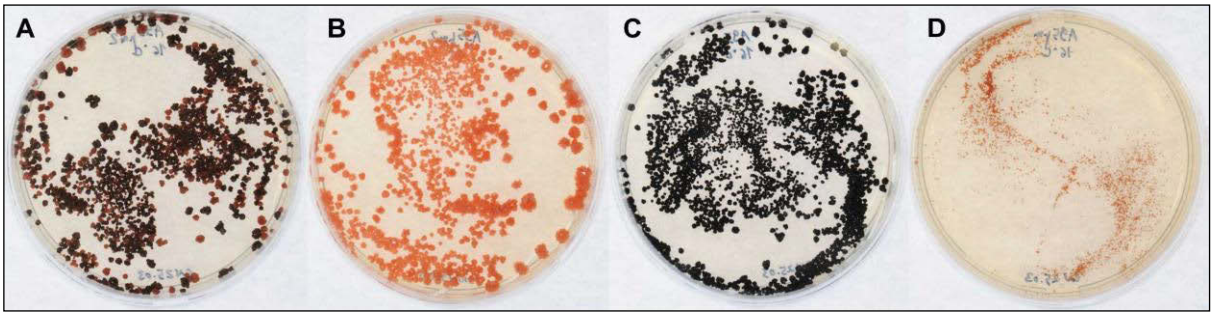

Figure 31. Phenotype of pink mutant A95pm2 at low temperature

(A-B) Pink mutant A95pm2 at **(A)** 15 °C or **(B)** 25 °C. **(C)** *Knufia petricola* A95 at 15 °C. **(D)**Pink mutant A95pm1 at 15 °C. All plates (MEA) were incubated for 4 w.

Chloride anions restored both colony size and dark phenotype in pink mutant A95pm1

Data presented above for growth of pink mutant A95pm1 on solid media (*Fig. 30*) suggested that:

(i) some component(s) of MEA was inhibitory for growth of A95pm1, or
(ii) some component(s) of ASM was able to restore the phenotypical growth defect of A95pm1 observed on MEA.

These hypotheses were investigated by supplementing MEB with chemicals from ASM (see ASM composition in *Subchapter 2.1*). Nutrients were excluded, since both media were provided with them at non-limiting concentrations, but stock solutions and citric acid were taken into consideration as candidate components responsible for the phenotypic effect. A growth enhancement similar to growth on ASM was observed for A95pm1 on MEA with Stock solution 1 ($MgCl_2$ and KCl; 5 mM each) and, to a minor extent, also with 20 mM citric acid (medium acidity adjusted to pH 5 with KOH as in ASM). In both cases, though, black pigmentation was not restored. No effects were observed with Stock solutions 2 and 3. By contrast, ASM components had no effect on colony size of wild type growing on MEA (*Fig. 32*).

Following this result, both Stock solution 1 and 20 mM citric acid were further considered. First, they were added to MEA together to investigate a putative additive effect for growth and/or pigmentation of pink mutant A95pm1. This was not the case (not shown). Next, components of Stock solution 1 were added singularly to discern which of them increased size of A95pm1 colonies on MEA. Both $MgCl_2$ and KCl restored growth defect of mutant on MEA, although to a lesser extent than when added jointly (*Fig. 33*). This observation suggested that:

(i) chloride anions were responsible for restoration of wild-type phenotype, and/or
(ii) the effect was achieved by salts in a dose-dependent manner.

The assumptions were examined by observing growth of A95pm1 on MEA supplemented with increasing concentrations of KCl, NaCl or Na_2SO_4 (from 1.6 mM up to 405 mM). According to Biolog's results, these salts are well tolerated (*Fig. 10*, left panel) and thus suitable to use as additives in the assay. With increasing concentrations of KCl and NaCl (around 15-45 mM), A95pm1 colonies reached sizes observed for wild type colonies. At higher concentrations (> 135 mM), both KCl and NaCl restored dark pigmentation of A95pm1, even though the salts became inhibitory for both A95pm1 and wild type in term of colony size. Only minor growth effects, without restoring dark phenotype, were observed with Na_2SO_4 (*Fig. 34*). Thus, it was concluded that chloride anions restored, on solid media,

wild-type phenotype in A95pm1 in a dose-dependent manner. This phenomenon could help explain increased salt tolerance of A95pm1 as observed with the Biolog System (*Fig. 15*, left panel).

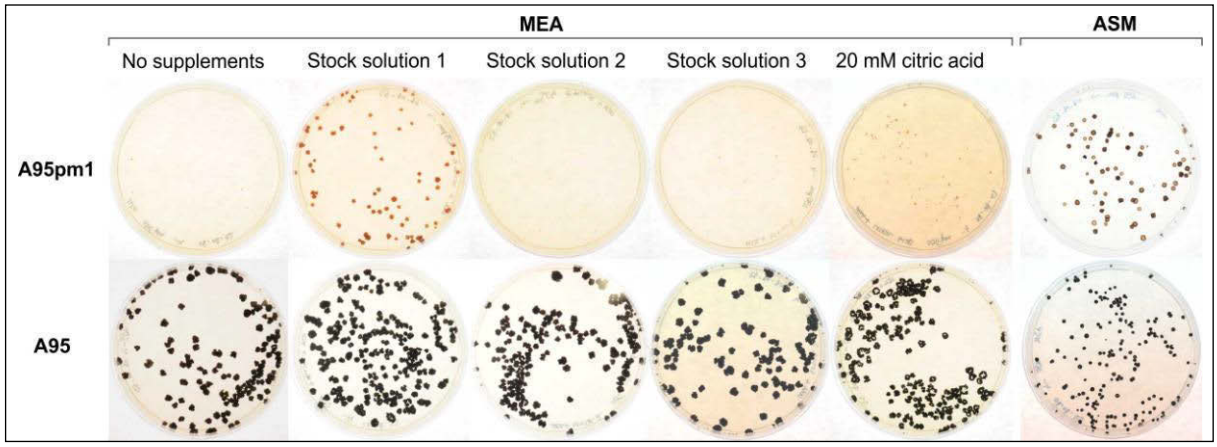

Figure 32. Single components of ASM restored growth defect of pink mutant A95pm1

Growth of pink mutant A95pm1 and *K. petricola* A95 on MEA supplemented with ASM components (Stock solutions or 20 mM citric acid). For A95pm1, growth enhancements were observed with Stock solution 1 and, to a lesser extent, with with 20 mM citric acid. Colony size was not affected for wild type on MEA upon supplementation. Plates were incubated for ca. 2 w.

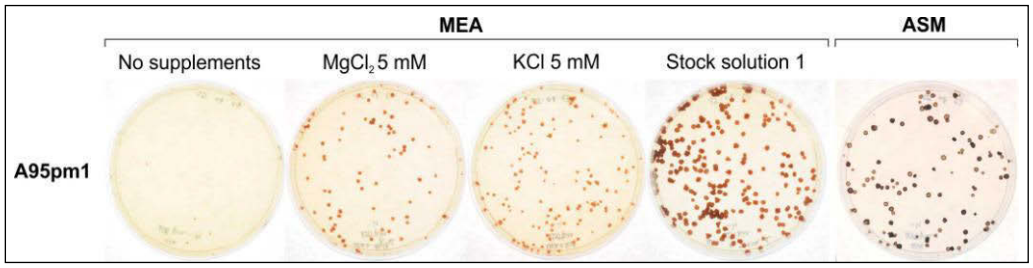

Figure 33. $MgCl_2$ and KCl restored growth defect of pink mutant A95pm1 in synergistic fashion

Growth of pink mutant A95pm1 on MEA supplemented with ASM components (Stock solution 1 or its components alone). Growth enhancements were observed with Stock solution 1 and, to a lesser extent, with its single components (5 mM $MgCl_2$ and 5 mM KCl). Plates were incubated for ca. 2 w. Following results in *Fig. 32*, wild-type strain was not included in the analysis.

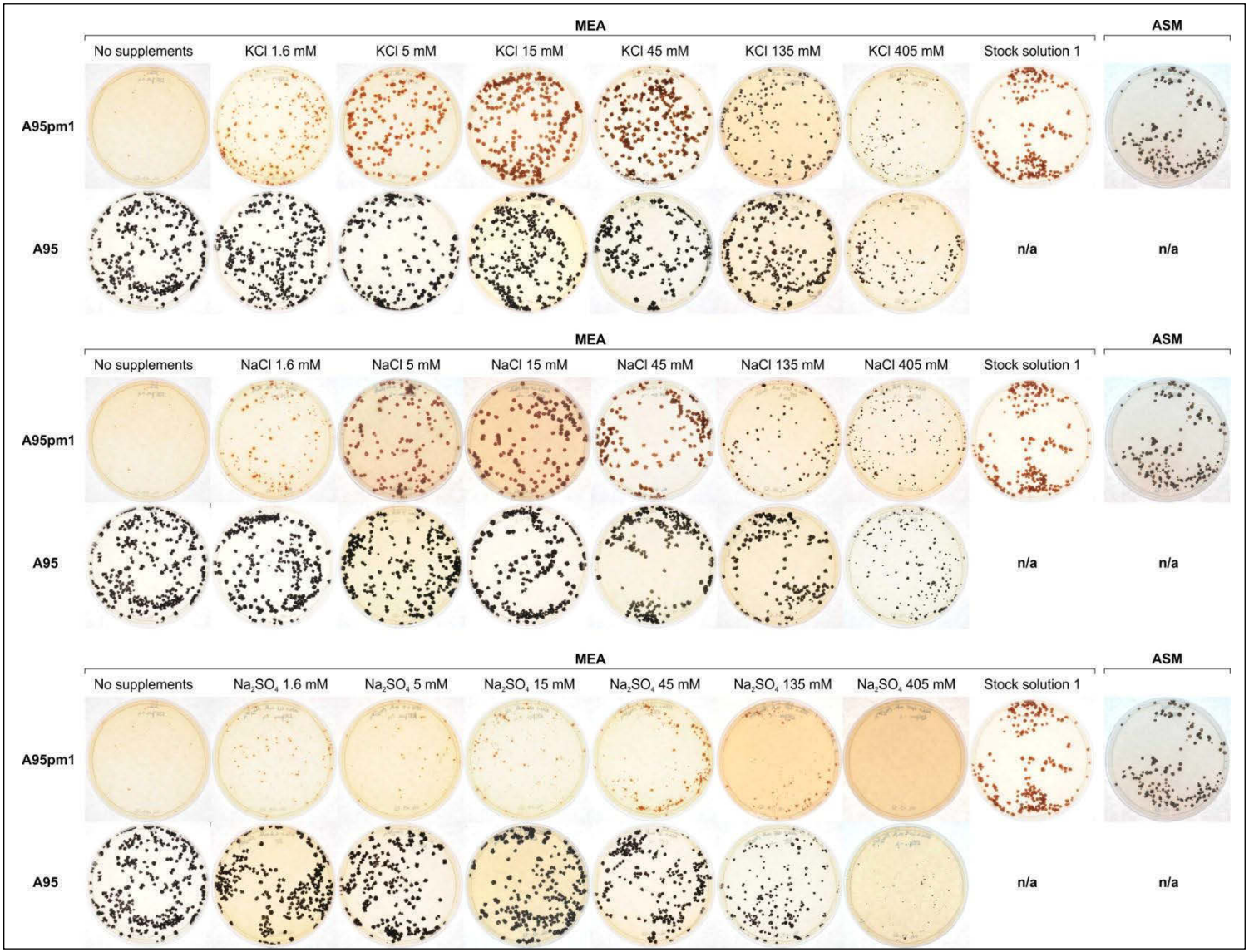

Figure 34. Chloride anions restored growth and pigmentation defects of pink mutant A95pm1 in a dose-dependent manner

Growth of pink mutant A95pm1 and *K. petricola* A95 on MEA supplemented with KCl, NaCl or Na_2SO_4 (1.6 mM to 405 mM) For A95pm1, growth enhancements were observed with KCl and NaCl (increases in colony size and darker pigmentation). Plates were incubated for ca. 2 w.

Low temperatures restored dark phenotype in pink mutant A95pm2

As observed during generation of temperature-optimum profiles, colonies of pink mutant A95pm2 became increasingly brown at low temperatures (*Fig. 31*). The same observation was noticed upon storage of plates at 4 °C, even though cells in liquid cultures did not undergo the same colour shift (*Fig. 35A-E*). Thus, the phenomenon was growth-independent and occurring only on solid medium. To investigate if colour shift of A95pm2 at low temperatures was reversible, a dark colony of A95pm2 (i.e. a colony from a plate stored at 4 °C) was streaked along with a pink colony (i.e. one from a plate incubated at 25 °C) and grown at 25 °C. After growth, pink phenotype was observed in both streaked samples, and upon storage at 4 °C colonies became darker again (*Fig. 35F-G*). This observation was validated upon reiterating of the experiment up to three times (not shown), indicating that pink mutant A95pm2 is a stable and reversible temperature-sensitive mutant.

Colour shift in A95pm2 at low temperatures was further considered by pigment analysis of black-fungal strains, showing that intracellular pigments were not responsible for it (see *Section 3.IV.4*).

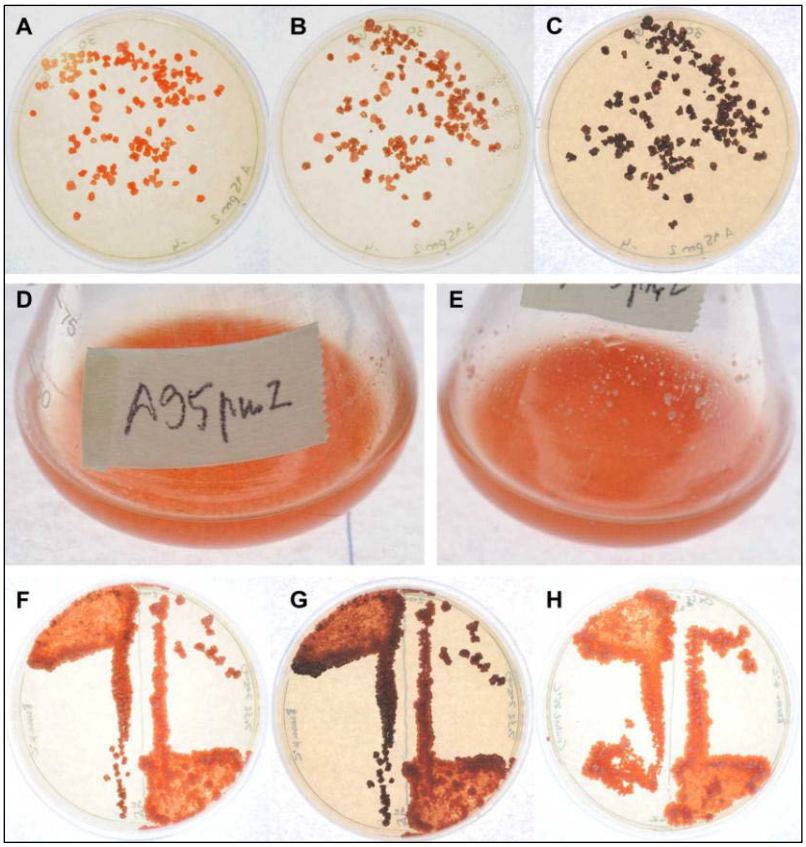

Figure 35. Pink mutant A95pm2 is a stable and reversible temperature-sensitive mutant

(A-C) Pink mutant A95pm2 (grown for 1 w on MEA at 25 °C) **(A)** before storage at 4 °C and **(B-C)** after storage at 4 °C [5 d in **(B)** and 9 d in **(C)**]. **(D-E)** Liquid cultures of A95pm2 (grown for 2 w at 25 °C in MEB) **(D)** after incubation at 25 °C or **(E)** after incubation at 4 °C. **(F-H)** Colonies of pink mutant A95pm2 on MEA (left half of plates: streak of a dark colony; right half of plates: streak of a "regular" mutant colony) **(F)** after growth for 1 w at 25 °C and **(G)** after incubation for 2 w at 4 °C. **(H)** Control for **(F-G)**, i.e. incubation of a plate for 2 w at 25 °C instead of at 4 °C.

3.II.8 Resistance toward ultraviolet irradiations

Melanised cell wall of black fungi is an effective barrier to ultraviolet (UV) stress [18,126]. To investigate putative differences in stress response between *K. petricola* A95 and its isogenic mutants, the strains were subjected to germicidal or environmental UV irradiations after plating on MEA; effects were analysed by viable counting after colony formation and compared with the control (no UV treatment).

All strains responded to both UVC and UVA treatments, upon increases in irradiation times (up to 5 min for germicidal UVC, up to 4 h for environmental UVA), with gradual viability decreases, resulting in comparable CFU values. A more severe reduction in viability (in comparison to the wild type) seemed to be observed for pink mutant A95pm1 after 2 min UVC irradiation; however, the effect was not corroborated by treatments with environmental UVA. Thus, the data suggest that all strains are similarly affected by UV stress (*Fig. 36*).

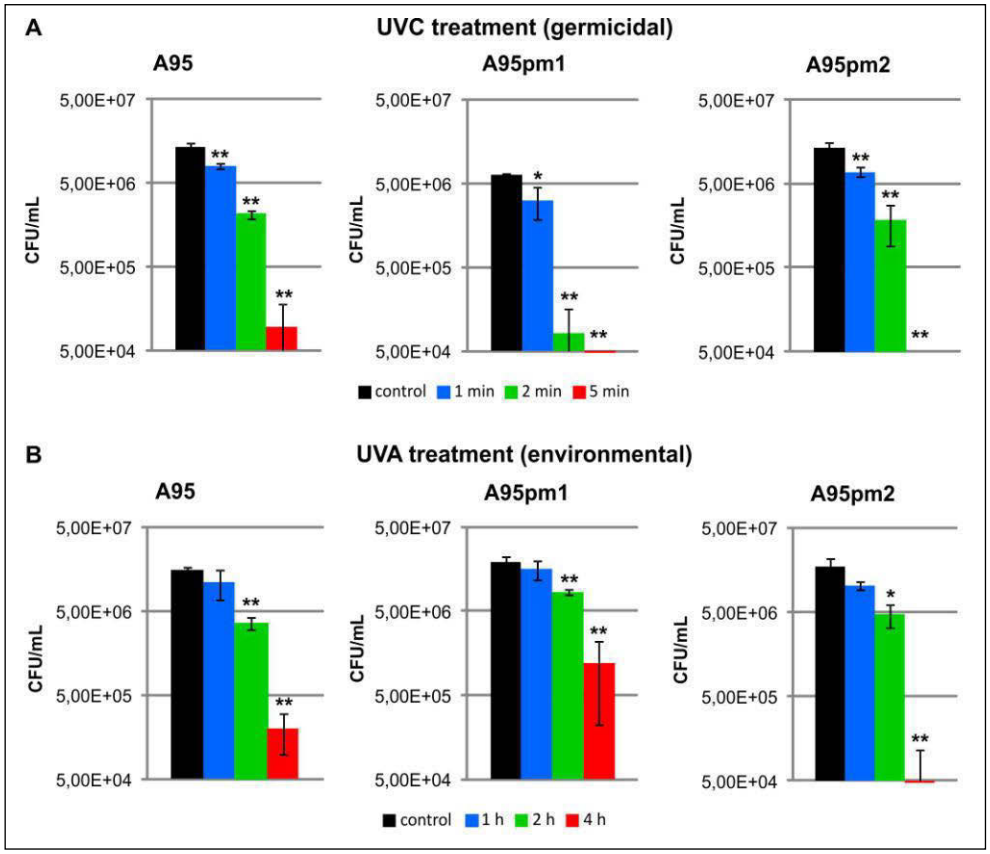

Figure 36. Viable count of* Knufia petricola *A95 and pink mutants after ultraviolet irradiation
(A-B) Viability (in CFU/mL) after irradiation for the indicated time with **(A)** germicidal UVC or **(B)** environmental UVA. Data are calculated from three independent replicates. For significance analysis, data are compared pairwise with the controls (no irradiation). * $p < 0.05$, ** $p < 0.01$.

Summary of results (Part II – second half)

In this second half of *PART II – Phenotypic characterisation of black fungi*, the focus was directed toward the in-depth characterisation of fungal strains, in particular aimed at highlighting differences between *K. petricola* A95 and its isogenic mutants A95pm1 and A95pm2. Growth on differently supplemented solid media, at different temperatures and after ultraviolet irradiation was analysed. Most of the build-up experiments were carried out with the newly developed synthetic medium ASM, which was as well used for further analysis of *K. petricola* A95 as shown in *PART III – Growth in oligotrophic media*.

Main findings are summarized as following:

- A new defined medium for black fungi was developed
- Temperature-optimum profiles were generated
- Specific phenotypes of pink mutants were described
- Wild-type phenotypes in mutants were restored by growth experiments, indicating that A95pm1 and A95pm2 are conditional mutants
- Ultraviolet irradiations resulted in similar effects for the three strains

PART III – Growth in oligotrophic media

In this subchapter growth of the black fungus *Knufia petricola* A95 in nutrient-deprived media was investigated. First, growth in oligotrophic media was quantified, followed by descriptive observations of colonies on nutrient-deprived solid media (macroscopic and microscopic analyses, including histological sections and cellular staining). Finally, oligotrophism was investigated by supplementing nutrient-deprived media with dead fungal biomass and analysis of putative beneficial effects by growth experiments.

3.III.1 Oligotrophism of *Knufia petricola* A95

Previously reported oligotrophism of black fungi [62,114] and pronounced biomass formation in control wells without primary nutrients in Biolog's Phenotype MicroArrays (*Fig. 8E-G*) prompted the analysis of growth in oligotrophic media. This was possible by cultivating *K. petricola* A95 in the defined medium ASM (both liquid and solid, *Section 3.II.5*) deprived of carbon, nitrogen, phosphorus or sulphur source (ASM-C, -N, -P, -S) as well as in pure water. As direct comparison, ASM was also included. Growth in such media was quantified as described previously by:

(i) viable counting in CFU/mL (incubation for 1 w in oligotrophic liquid media, followed by plating on MEA for colony counting), and
(ii) average colony size in mm^2 (incubation for 2-4 w on oligotrophic solid media with concomitant determination of colony surface area).

When colonies formed filaments (e.g. on ASM-N or water-agar, see *Fig. 38*) they were not considered for measurement of surface area.

In all liquid media, including pure water, formation of biomass could be observed upon 1 w of incubation and, after plating on MEA, retrieved CFU/mL values exceeded initial (inoculated) values of ca. 5×10^4 CFU/mL. In all nutrient-deprived media, significant decreases in growth were observed when compared with the defined ASM (*Fig. 37A*). In comparison to ASM (2.39×10^6 CFU/mL), reduction in cell viability was most dramatic in ASM-S (1.05×10^5 CFU/mL, ca. 23-fold decrease) and less marked in ASM-P (5.61×10^5 CFU/mL, ca. 4-fold decrease). In ASM-C, ASM-P and pure water, ca. 9- to 13-fold reductions were calculated (*Fig. 37A*).

On all nutrient-deprived solid media, fungal colonies could be recognized after few weeks of incubation (*Fig. 37B-D*). On ASM, average colony area of ca. 2.9 mm^2, 8.6 mm^2 and 13.9 mm^2 after 2 w, 3 w and 4 w of incubation were observed. Colony formation on oligotrophic media was most compromised on ASM-N (reaching 0.3-0.4 mm^2 after 2-4 w, ca. 11- to 35-fold reduction in comparison to ASM) and H_2O-agar (0.2-0.4 mm^2, ca. 15 to 37-fold reduction). Circa 5- to 10-fold reductions were observed on both ASM-C and ASM-P (0.4-1.7

mm^2) and only up to 3-fold reduction on ASM-S (2.5-5.5 mm^2), arguably due to a contamination of agar with sulphur sources. On all solidified nutrient-deprived media, colony sizes were significantly smaller than on ASM (*Fig. 37B-D*).

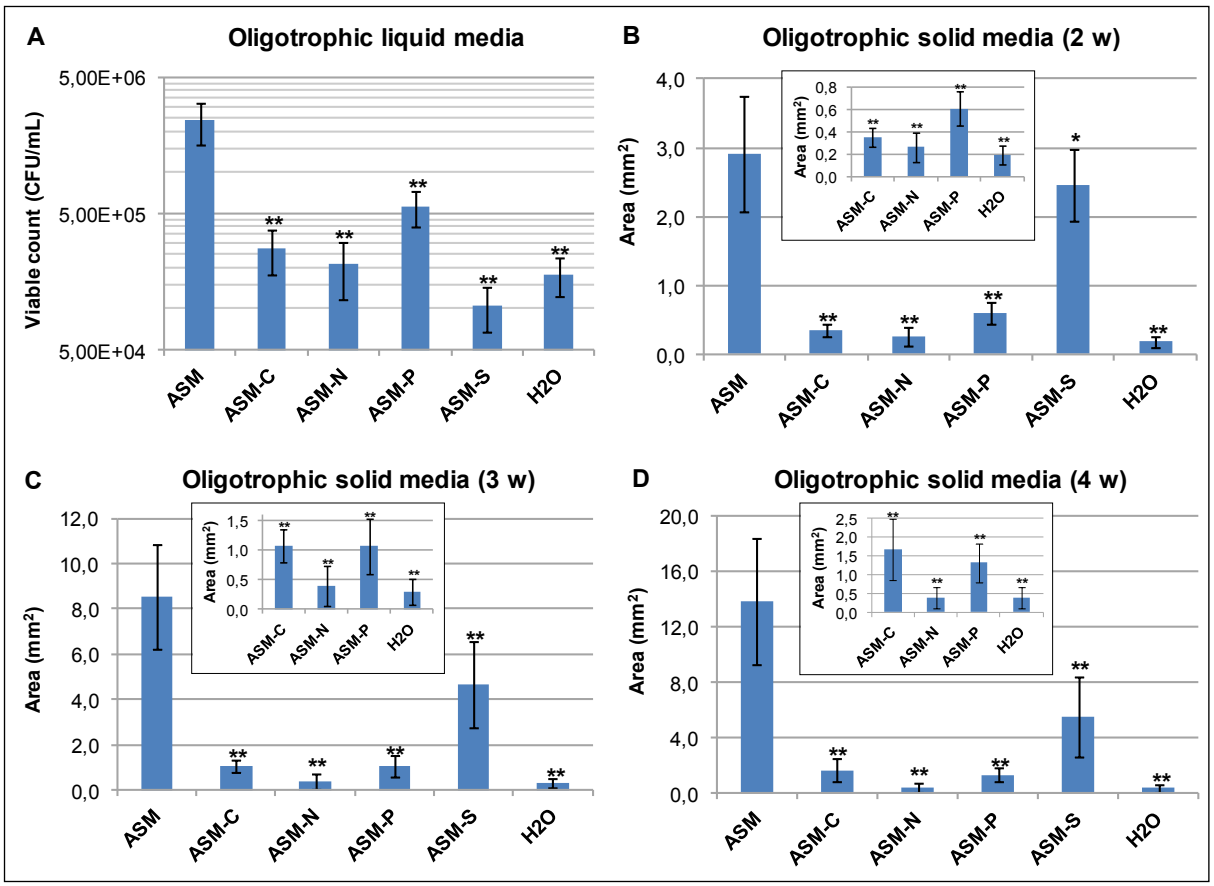

Figure 37. Growth of* Knufia petricola *A95 in nutrient-deprived media (I) – Quantification of growth

(A-D) Growth of *K. petricola* A95 in oligotrophic media. **(A)** Growth in nutrient-deprived liquid media (1 w of incubation in oligotrophic media followed by viable counting after plating on MEA); **(B-D)** Growth on nutrient-deprived solid media after **(B)** 2 w, **(C)** 3 w and **(D)** 4 w of incubation on oligotrophic plates (quantified by calculation of average colony size in mm^2). Frames in **(B-D)** show basal growth on ASM-C, -N, -P and H_2O-agar. Data are calculated from ca. 20-30 repetitions using the negative controls in *Fig. 41* (oligotrophic media supplemented with 1/10 volume of saline solution, see *Section 3.III.3*). For significance analysis, data in nutrient-deprived media are compared with data in ASM. * $p < 0.05$, ** $p < 0.01$. ASM: A95-Specific Medium; ASM-C, -N, -P, -S: ASM deprived of carbon, nitrogen, phosphorus or sulphur source. Area: Average projected colony surface area, in mm^2.

3.III.2 Macroscopic and microscopic observations of fungal colonies

Growth on nutrient-deprived media was investigated by observing phenotypes on MEA, ASM, ASM-C, ASM-N, ASM-P, ASM-S and H_2O-agar after 2-4 w of incubation. Both macro- and microscopic observations of whole colonies and of squash preparations (*Fig. 38*) were performed, as well as microscopic analyses of histological sections (*Fig. 39*).

Remarkably, colony phenotypes differed depending on the nutrient deprivation. On media supporting maximal growth (MEA, ASM and ASM-S) colony margins were irregularly shaped,

while on the other media colonies were mostly round-shaped. Of those, especially on the media supporting less biomass formation (ASM-N, and H_2O-agar), colonies formed filaments expanding into the surrounding agar. Under microscope, filaments and oblong cells on ASM-N and H_2O-agar could be observed; clump-like growth was observed on MEA, ASM and ASM-S, while less dense cellular aggregations were seen on ASM-C and ASM-P (*Fig. 38*).

As observed by histology, on complex MEA colonies grew healthy and three-dimensional, with heights reaching diameter of projected surface area, although extensive voids in the colony interior were observed. By contrast, growth on ASM and ASM-S was mostly two-dimensional, with flat colonies and cells forming a layer localised at the colony borders only; on media supporting poor growth (ASM-C, -N, -P and H_2O-agar), filaments infiltrated into the agar. To observe structures in more detail, histological sections were visualised with higher magnification and differences within or between colonies were inspected by staining protocols. In contrast with growth on MEA, more localised biomass formation could be observed in colonies on ASM, with cells organized in a thicker layer. After PAS carbohydrate staining, all cells within colonies reacted overall similarly, but a difference between colonies could be observed, insofar starved cells on ASM-N, ASM-P and H_2O-agar seemed to colour less intensively, possibly indicating lesser carbohydrate storage (*Fig. 39*). Haematoxylin counterstaining to visualize cell nuclei overshadowed PAS staining resulting in dark images, and was thus not pursued. Vital staining to further highlight putative differences within colonies, e.g. with propidium iodide, was not suitable in combination with histology (fixation and embedding of colonies required).

Histological sections of the pink mutant A95pm1 on the same media were generated, resulting in overall very similar patterns as described for the wild type (not shown). Therefore, pictures were omitted.

3.III.3 Supplementation of oligotrophic media with dead fungal biomass

Sustained growth of *K. petricola* A95 in oligotrophic media (*Fig. 37*) indicated that the black fungus can rely on low-level traces of nutrients and/or is able to recycle stored compounds. A preliminary experiment showed that autoclaved fungal biomass had, in comparison to the control (saline solution), a beneficial growth effect in liquid as well as on solid nutrient-deprived media (*Fig. 40*).

This effect was further analyzed in all nutrient-deprived media as well as in ASM and malt-extract media (controls). Dead fungal biomass was generated by different means. To exclude artefacts by autoclaving (e.g. formation of non-naturally occurring chemical bonds or degradation of heat-sensitive substances), a cold-sterilisation method was introduced (gas-phase sterilisation of lyophilized biomass by ethylene oxide). As an attempt to localize putative nutrient sources, biomass was fractionated to generate (i) cell-wall and cell-membrane fragments, (ii) protoplasts, and (iii) intracellular fraction. An overview of the

biomass used in the experiment is given in *Tab. 3* (*2 MATERIALS AND METHODS*). The experiment was performed in both liquid and solid oligotrophic media. Results are plotted in *Fig. 41* and numerical values are reported in *Suppl. Tabs. 2-3*.

In liquid nutrient-deprived media, autoclaved biomass had a beneficial effect upon deprivation of nitrogen, phosphorus or sulphur, while ethylene-oxide-sterilised biomass increased growth in all oligotrophic media, thus suggesting that a putative carbon source was heat-sensitive. Fragmentation experiments indicated that putative N sources were cell-wall associated (positive effect, in ASM-N, with autoclaved cell fragments, but not with autoclaved protoplasts or intracellular fraction), while P sources were associated with cell wall and cell membrane (effect, in ASM-P, with autoclaved cell fragments and, to a lesser extent, protoplasts); S sources were probably intracellular (effect, in ASM-S, with autoclaved protoplasts and intracellular fraction, but not with autoclaved cell fragments;[19] *Fig. 41A*). Neither intracellular (filter-sterilised) fraction, nor ethylene-oxide-sterilised cell fragments or protoplasts, had a beneficial effect in liquid ASM-C (*Suppl. Tab. 2*). Similar results were observed on solid media, with both autoclaved and ethylene-oxide-sterilised cells boosting growth on all oligotrophic media and effect on ASM-C reduced upon autoclaving. The effect on ASM-S was difficult to recognize due to sustained growth on solid medium deprived of sulphur (*Fig. 36B-D*)[20]. Localization experiment yielded similar observations for media deprived of phosphorus, although on ASM-N the results obtained in liquid media could not be replicated. Putative heat-sensitive carbon source is probably intracellular (effect, on ASM-C, with intracellular fraction) as well as cell-wall and/or cell-membrane associated (effect with ethylene-oxide-sterilised cell fragments/protoplasts; *Fig. 41B* and *Suppl. Tab. 3*). Dead fungal biomass did not enhance growth in both liquid and solid malt-extract media (not shown).

Thus, from the data emerged that *K. petricola* A95 mobilized internal resources and/or re-cycled some yet-to-be-defined cell components as a mechanism to cope with nutrient paucity.

[19] This statement is hardly recognizable from *Fig. 41A*, where for sake of simplicity the average of all negative controls was plotted as in *Fig. 37*. Significant increases in viability with autoclaved protoplasts and intracellular fraction, but not with autoclaved cell fragments, were calculated with the corresponding saline control plates. See *Suppl. Tab. 2* in *A.5 Supplementary data* for numerical values.

[20] Nonetheless, an effect was observed with ethylene-oxide-sterilised cells on solid ASM-S ($p < 0.01$). The effect could not be recognized in *Fig. 41B* for the same reason exposed in the previous footnote. See *Suppl. Tab. 3* in *A.5 Supplementary data* for numerical values.

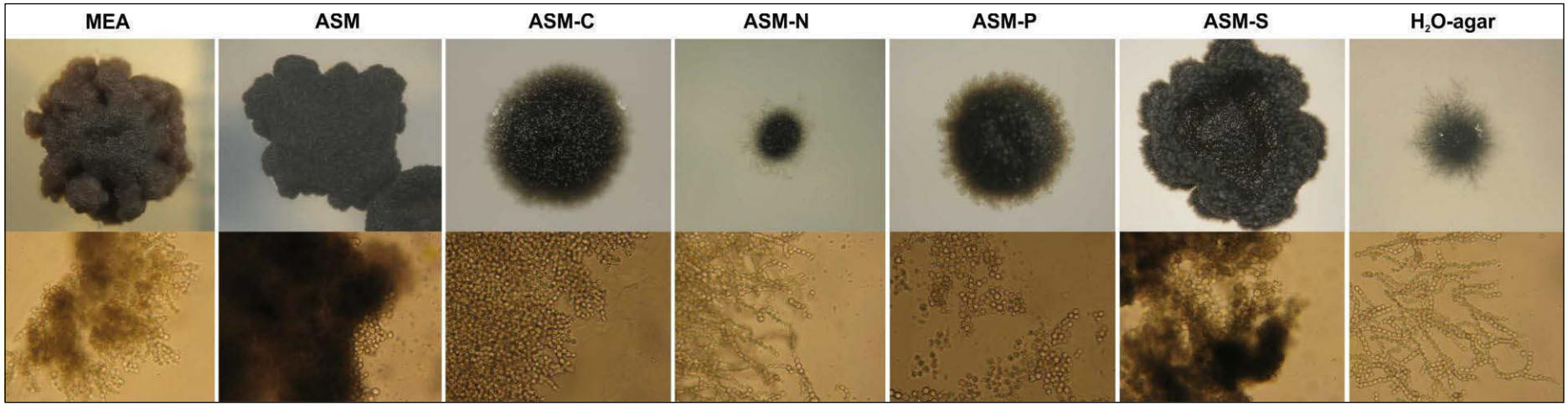

Figure 38. Growth of* Knufia petricola *A95 on nutrient-deprived media (II) – Colony morphologies and squash preparations

See next page for figure legend

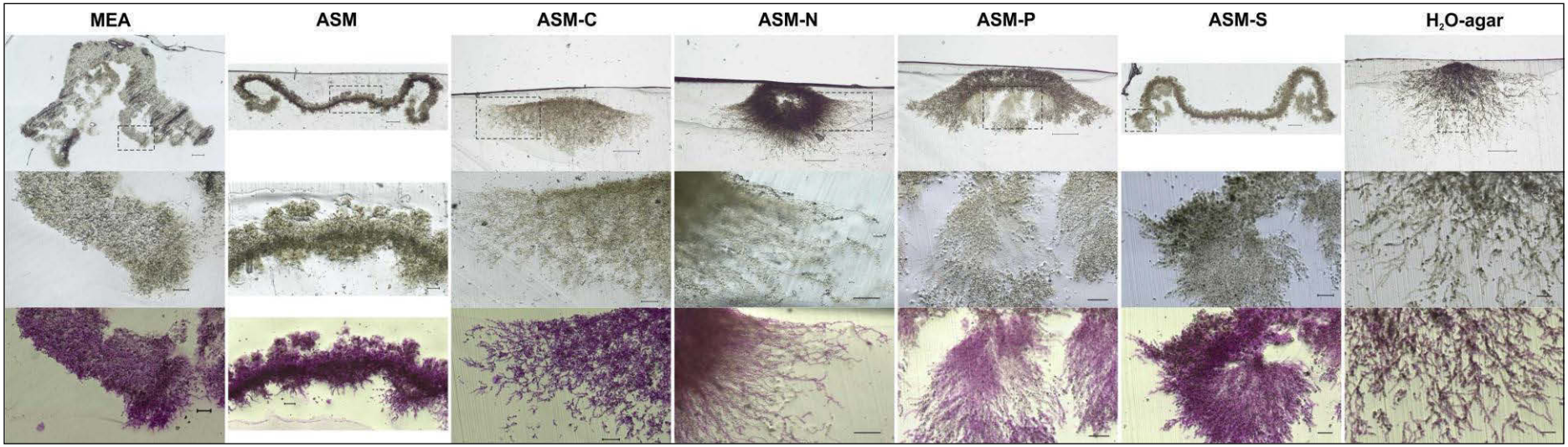

Figure 39. Growth of* Knufia petricola *A95 on nutrient-deprived media (III) – Histological section of colonies

See next page for figure legend

Figure 38 (previous page). Growth of* Knufia petricola *A95 on nutrient-deprived media (II) – Colony morphologies and squash preparations

(Upper panels) Colony phenotypes on different oligotrophic media after 3 w of incubation. **(Lower panels)** Microscopic observation of squash preparations (magnification ca. 100X). ASM: A95-Specific Medium; ASM-C, -N, -P, -S: ASM deprived of carbon, nitrogen, phosphorus or sulphur source. Pictures are not in scale (for colony size, please refer to *Fig. 37B-D*; for scale bar in microscopic pictures, see *Fig. 39*).

Figure 39 (previous page). Growth of* Knufia petricola *A95 on nutrient-deprived media (III) – Histological section of colonies

(Upper panels) Histological sections of whole colonies after 3 w of incubation (magnification 200X). **(Middle and lower panels)** Particulars of colonies without or with PAS staining (magnification 500-1'000X). ASM: A95-Specific Medium; ASM-C, -N, -P, -S: ASM deprived of carbon, nitrogen, phosphorus or sulphur source. For sake of illustration, pictures are not in scale but provided with scale bar (400 µm upper panels, 40 µm middle and lower panels). Dotted squares in upper panels: particular of colonies shown in middle and lower panels. Histological sections of colonies grown for 2 w and 4 w are shown in *Suppl. Figs. 6-7* in *A.5 Supplementary data*.

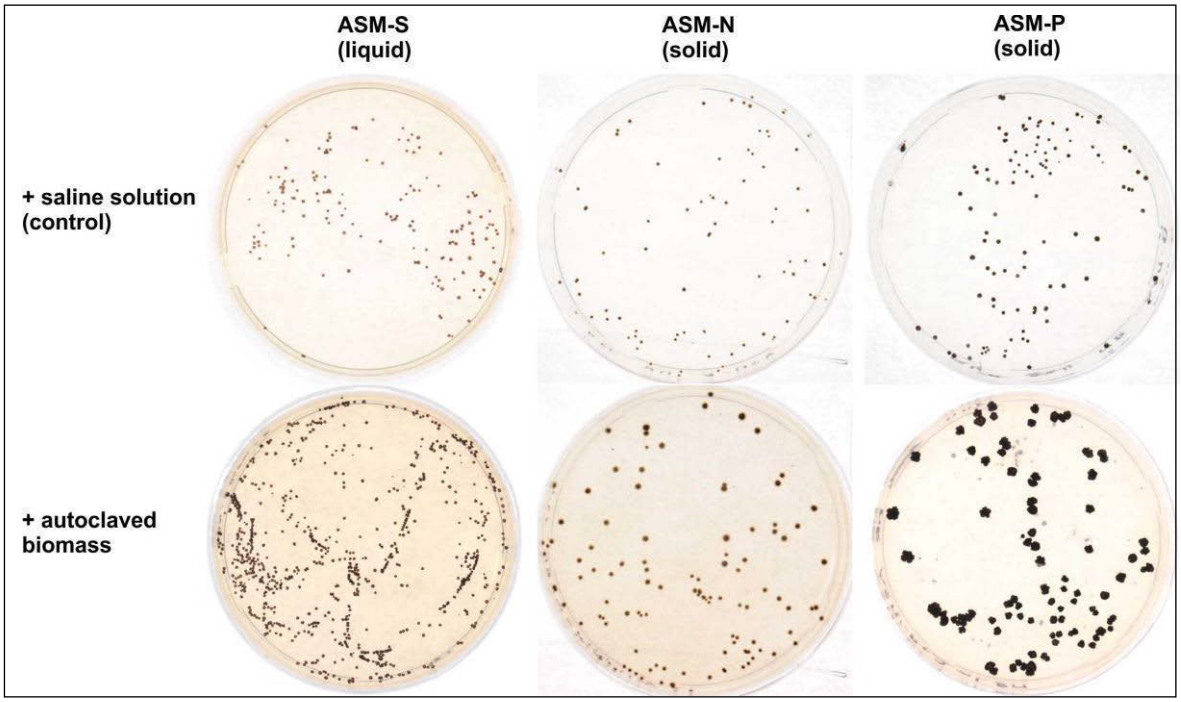

Figure 40. Dead fungal biomass enhanced growth of growth of* Knufia petricola *A95 in nutrient-deprived media (I) – pre-experiment

Knufia petricola A95 was cultivated in liquid ASM-S (left plates), on solid ASM-N (middle plates) or on solid ASM-P (right plates). Nutrient-deprived media were supplemented by adding 10 % v/v dead fungal biomass (lower plates) or the same volume of saline solution (controls, upper plates). (Autoclaved biomass was obtained as reported in *Tab. 3*.) Oligotrophic media were inoculated with a washed start culture. Growth in liquid oligotrophic media was evaluated by inoculating a start culture (1/100 dilution) in the media, followed by 1 w incubation and plating on MEA for viable counting; on solid oligotrophic media by plating a start culture (100 µL of dilution 1/10'000) on the media and determining average colony size after 3 w of incubation. In both liquid and solid nutrient-deprived media, growth enhancements were observed upon supplementation of dead biomass (i.e. increases in CFU values and colony sizes, respectively).

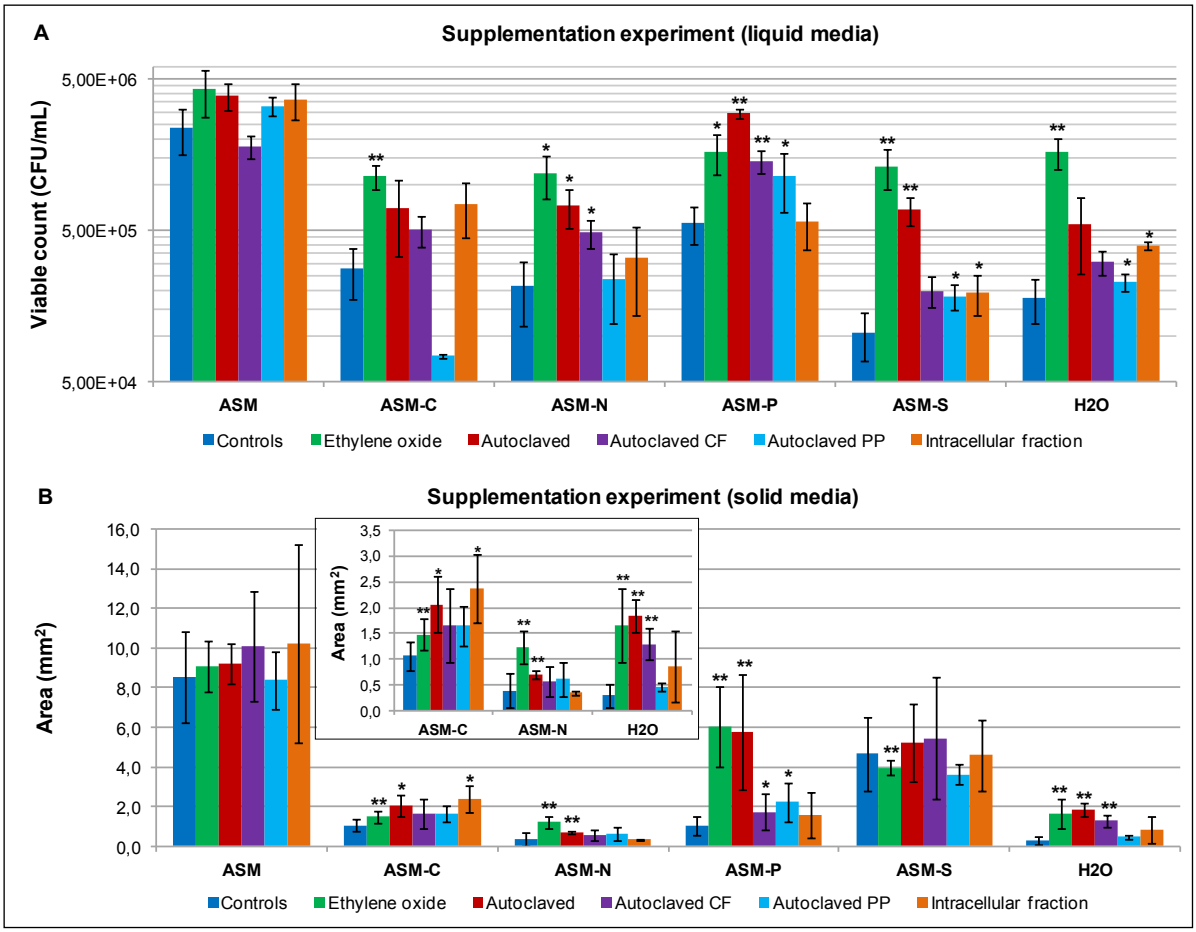

Figure 41. Dead fungal biomass enhanced growth of growth of* Knufia petricola *A95 in nutrient-deprived media (II)

(A-B) Growth of *K. petricola* A95 in **(A)** liquid or **(B)** solid oligotrophic media supplemented with dead fungal biomass (10 % v/v). Biomass was prepared as illustrated in *Tab. 3* (CF: cell fragments; PP: protoplasts). Growth was quantified as explained above (*Fig. 40*) by viable counting after 1 w of incubation (in CFU/mL, liquid media) or average colony size after 3 w of incubation (in mm^2, solid media). Frame in **(B)** show growth on ASM-C, -N and H_2O-agar. Data are calculated from at least three repetitions. For sake of simplicity, negative controls plotted in the figure (supplementation with 1/10 volume of saline solution) are mean and average of all saline controls in a given nutrient-deprived medium (ca. 20-30 in total) but, for significance analysis, data are compared with the corresponding saline controls. * $p < 0.05$, ** $p < 0.01$. ASM: A95-Specific Medium; ASM-C, -N, -P, -S: ASM deprived of carbon, nitrogen, phosphorus or sulphur source. See *Suppl. Tabs. 2-3* in *A.5 Supplementary data* for numerical values.

Summary of results (Part III)

In *PART III – Growth in oligotrophic media*, oligotrophism of the model strain was quantified and descriptive analyses of black-fungal colonies on nutrient-deprived media were performed. Semi-qunatitative supplementation experiments with dead fungal biomass showed that the strain was able to rely on its own cell components to counteract starvation; putative nutrient sources were localized to cellular fractions.

Main findings are summarized as following:

- *K. petricola* A95 was able to grow on nutrient-deprived media including pure water
- Different colony structures were formed on different media
- Three-dimensional colonies with extensive voids were formed on MEA; colonies on defined ASM were flat
- A correlation could be drawn between nutrient limitation, colony size and formation of filaments as nutrient-searching structures formed on media supporting growth poorly
- Dead fungal biomass was able to support growth upon nutrient limitation
- Putative nutrient sources were localized in the cell wall (N source), cell wall and cell membrane (P source) or intracellularly (S source); putative C source was heat-sensitive but seemingly ubiquitous

PART IV – Biochemical and molecular biology results

Several data are jointly presented in this subchapter *PART IV – Biochemical and molecular biology results*. The results, even though not linked thematically, are grouped here for sake of simplicity. Connections with relevant results presented in other subchapters are mentioned throughout the text or in *4 DISCUSSION*.

3.IV.1 Quality of ribonucleid acids was suitable for downstream analyses

To support genome annotation of *K. petricola* A95, total RNA isolation was performed for subsequent cDNA generation from mRNA templates. Different growth conditions were chosen as reported in *Tab. 4* to activate a broad range of genes (e.g. growth-phase specific or stress-induced).

Ribonucleic acids were isolated on-column starting from large biomass samples to obtain high yields. As determined by spectrophotometric measurements, yields between 65 ng/µL and 1'100 ng/µL were obtained and Abs_{260nm}/Abs_{280nm} ratios in 1 mM NaH_2PO_4 were in the expected range of around 2.1 (*Tab. 10*). Quality of RNA samples was verified by formaldehyde agarose gel electrophoresis and, since messenger RNA (mRNA) is poorly visualized on gels, by on-chip analysis. After electrophoretic separation, three major bands corresponding to ribosomal RNAs (rRNAs) were observed for all but three samples. For sample 4 (late-stationary phase in MEB), 10 (growth in ASM under salt stress) and 12 (growth under sulphur deprivation in ASM-S), RNA bands were either absent or faint and coupled with an increased smear signal (*Fig. 42*). Results obtained on formaldehyde agarose gel were confirmed on RNA Nano LabChips with the BioAnalyzer. Even though, for all samples, both 28S/18S rRNA ratio and RNA integrity numbers[21] were lower than the expected values (2 and 10, respectively), extensive patterns of RNA degradation were absent. Overall quality of RNA samples was thus considered suitable for downstream analysis, except for conditions 4, 10 and 12 (*Fig. 42*). The reason for this could be either due to inefficient cell lysis (sample 4) or to poor growth (samples 10 and 12). For all other samples, an aliquot (20-40 µL) was send to the DNA-sequencing company Fasteris SA (Switzerland) for mRNA isolation, generation of cDNA libraries and next-generation sequencing.

[21] RIN, see http://www.chem.agilent.com/Library/applications/5989-1165EN.pdf (retrieved on February 2014).

Table 10. Isolation of total RNA from* Knufia petricola *A95 for genome annotation

Sample	Growth conditions[a]	Yield (ng/µL)	Abs_{260nm}/Abs_{280nm}
1	Early-exponential phase (MEB)	100	2.07
2	Late-exponential phase (MEB)	870	2.35
3	Stationary phase (MEB)	410	2.15
4	Late-stationary phase (MEB)	65	2.20
5	Solid medium (MEA)	130	2.21
6	Growth under cell-wall stress (MEB + CMC)	475	2.14
7	Late-exponential phase (ASM)	300	2.14
8	Growth at low temperature (ASM)	245	2.13
9	Growth at high temperature (ASM)	725	2.17
10	Growth under salt stress (ASM)	433	2.22
11	Growth at acidic pH (ASM)	1’100	2.20
12	Growth under nutrient limitation (ASM-S)	117	2.11

[a] See *Tab. 4* for details on growth conditions

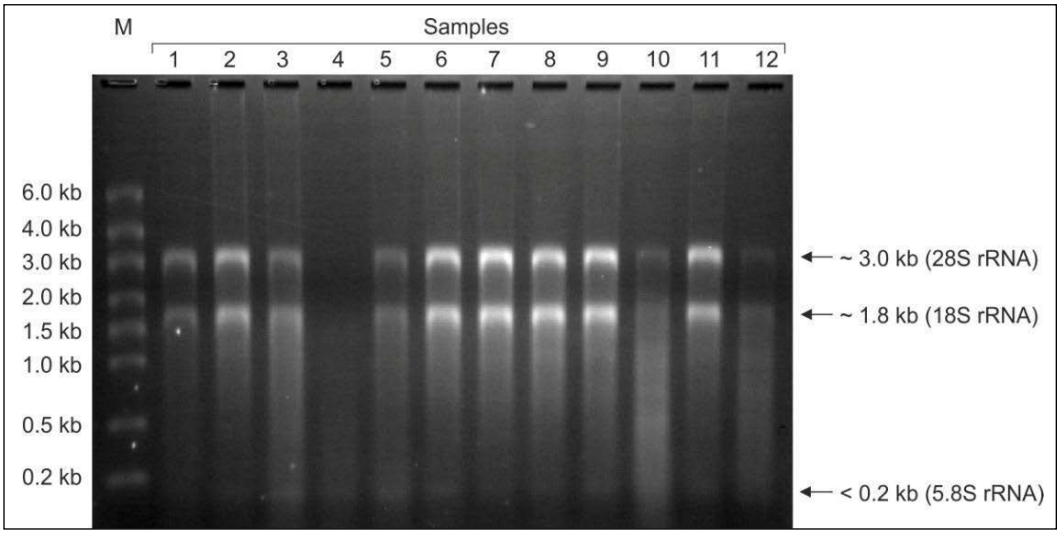

Figure 42. Analysis of total RNA samples from* Knufia petricola *A95 by formaldehyde agarose gel electrophoresis

Total RNA samples (*Tab. 10*) were separated by formaldehyde agarose gel electrophoresis, resulting in three major bands corresponding to fungal rRNAs. Faint signal for 5.8 S rRNA was due to column purification using RNaesy Midi Kit (elution of small nucleic acid fragments). M: RNA size marker (RiboRuler High Range RNA ladder, size indicated in kilobases).

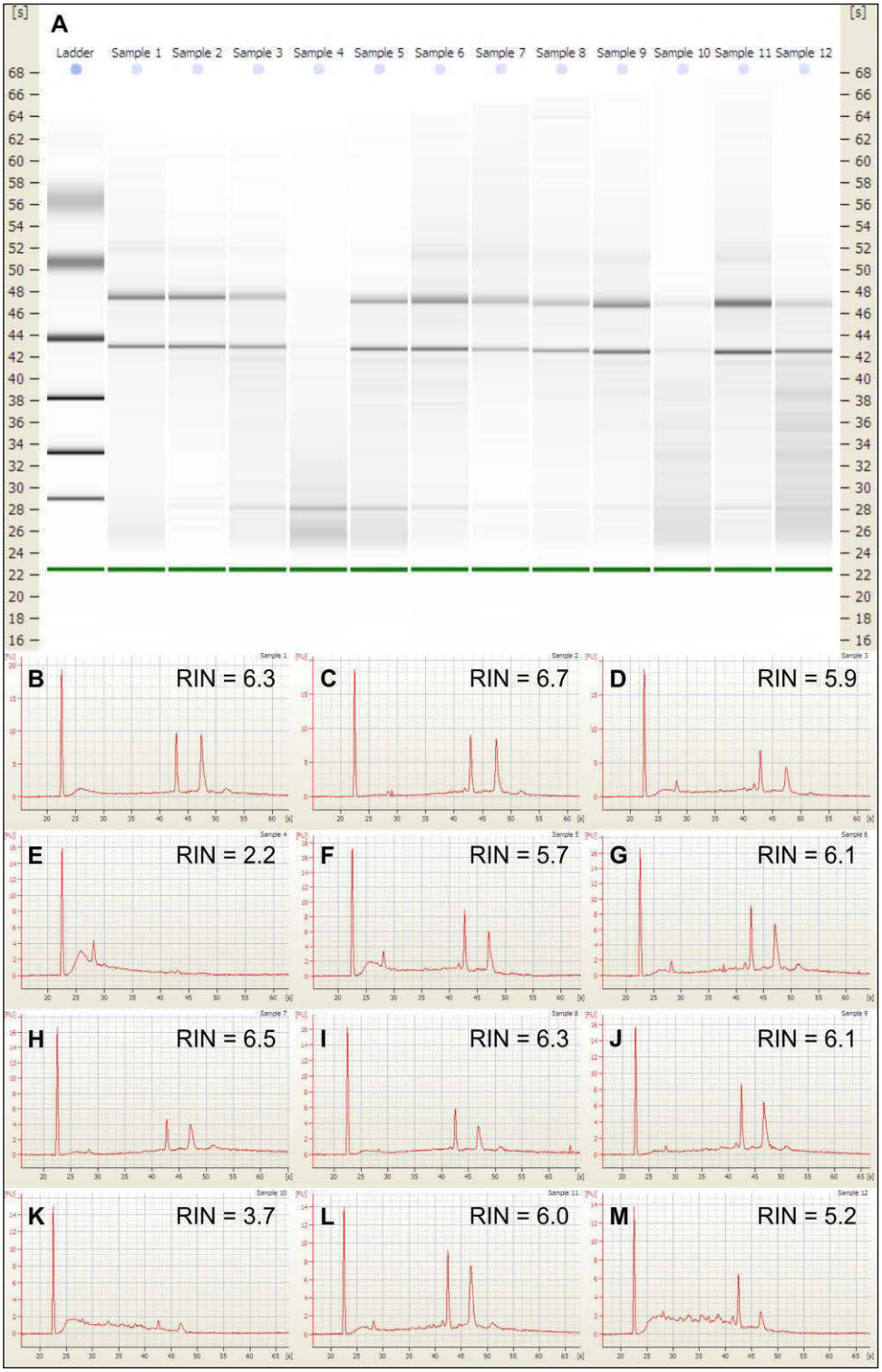

Figure 43. Analysis of total RNA samples from* Knufia petricola *A95 with the BioAnalyzer

(A-M) Quality of total RNA samples (*Tab. 10*) was further validated with the more sensitive BioAnalyzer. **(A)** Electrophoretic separation of RNA samples (Ladder: 25 nt, 200 nt, 500 nt, 1'000 nt, 2'000 nt, 4'000 nt and 6'000 nt); **(B-M)** Electorpherograms for samples 1-12 showing peaks at 25 nt (marker), ca. 1.8 kb (18S rRNA) and ca. 3.0 kb (28S rRNA). Narrow peaks, acceptable RIN numbers and absence of pattern of RNA degradation were observed for all samples except 4, 10 and 10. RIN: RNA Integrity Number.

3.IV.2 Karyotyping of black-fungal strains

Another way to support genome annotation is by karyotyping, i.e. the determination of number and size of chromosomes in an organism. Karyotyping is used in systematics but is also aimed at supporting modern genome analysis [13,68]. During generation of draft genome sequences, contigs – i.e. overlapping regions of DNA sequences – are produced which might, however, significantly exceed the actual number of chromosomes [79]. By experimentally determining chromosome number and size, thus, knowledge complementary to and supportive of *in silico* genome assembly is gathered [68]. Since separation of nucleic acids fragments bigger than ca. 40 kb by regular one-dimensional electrophoretic protocols is not possible, karyotyping of the two recently sequenced strain *K. petricola* A95 and *C. apollinis*, as well as the mutants A95pm1 and A95pm2, was performed by rotating-field gel electrophoresis (ROFE), a variation of the more common pulsed-field gel electrophoresis (PFGE) [112,117].

First, optimal DNA load was determined for karyotyping of *K. petricola* A95 genome. Protoplast (PP) concentrations in the range of ca. 2×10^5 to 1×10^7 were loaded in each well and subjected to electrophoretic separation. At the load of 1×10^7 PP/well, a genomic DNA concentration of ca. 1-2 µg is estimated according to the relation in Herschleib *et al.*, 2007 [68] for both *K. petricola* A95 and *C. apollinis* (genome sizes of ca. 27.2 Mb and ca. 28.7 Mb, respectively; Black Yeast Database of the Broad Institute, www.broadinstitute.org). Although running front of DNA reached only ca. 1/3 of the gel, with the chosen electrophoretic conditions discrete chromosomal bands could be recognized. A relative good balance between sharp, recognizable bands and absence of smear was observed at around 6×10^6 PP/well (*Fig. 44*). Following this result, a longer run was performed with 5×10^6, 5×10^7 and 1×10^8 PP/well (with same electrophoretic conditions as in *Fig. 44* but for 96 h instead of 48 h). Again, best results were generated with a load of ca. 5×10^6 PP/well, and 7-8 bands were recognized ranging between ca. 2.1-5.5 Mb for an estimated size of 29.4 Mb (*Fig. 45A*). Different electrophoretic conditions aimed at visualisation of putative chromosomes smaller than 2 Mb were applied (i.e. higher voltage and/or short time switch), but the signal localized around the gel top, indicating absence of small chromosomes (not shown). Karyotypes of pink mutants A95pm1 and A95pm2 were similar to those of *K. petricola* A95, thus indicating absence of large-scale reduction of genome size (not shown). However, given the size of *K. petricola* A95 chromosomes, losses of DNA fragments in the range of hundreds kb cannot be identified by ROFE.

Subsequently, the same protocol as in *Fig. 45A* was adopted for *C. apollinis* with a similar protoplast load. No bands were recognizable and signal was localized around the running front of the gel (not shown). Different electrophoretic conditions were adopted aimed to resolve smaller fragments and twelve discrete bands could be thus observed ranging from 0.65-2.1 Mb for an estimated size of ca. 14.3 Mb (*Fig. 45B*). Since this result was in strong

disagreement with the genome size estimated by the Broad Institute, two further conditions divergent from those in *Fig. 45A* were adopted to resolve putative bigger chromosomes and thus obtain a karyotypic estimation closer to the annotation result. However, in neither protocol chromosomes bigger than 2.2 Mb could be visualized (*Fig. 45C-D*).

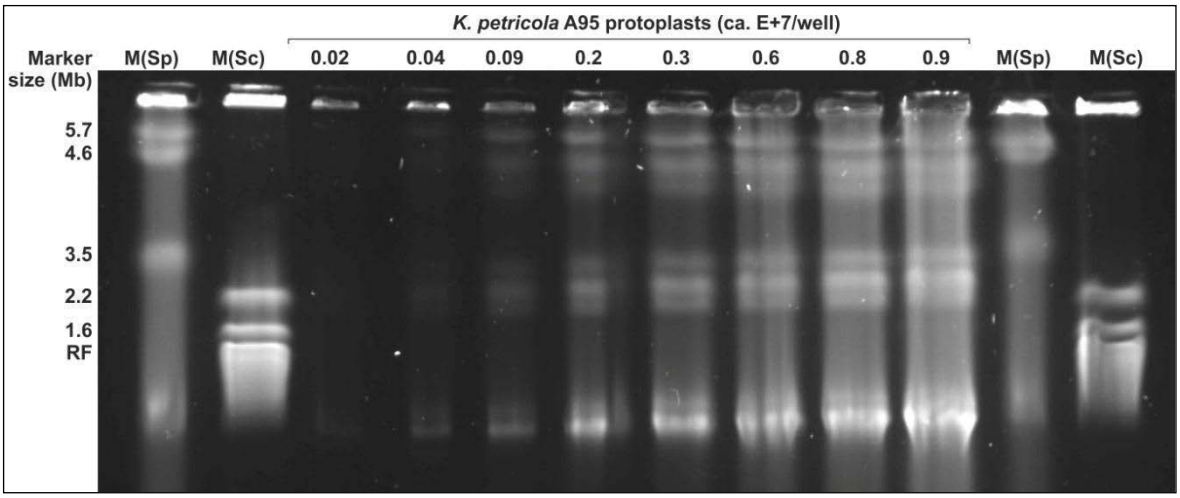

Figure 44. Rotating Field Gel Electrophoresis with* Knufia petricola *A95 protoplasts to determine suitable loading concentrations

Knufia petricola A95 protoplast (PP) concentrations in the range of ca. 2×10^5 to 1×10^7 PP/well were loaded into the gel. Electrophoretic separation by rotating-field electrophoresis (ROFE) was performed for 48 h at 70 V, 20 min to 30 min linear time switch, angle 106°. M(Sp): Marker, Chromosomal DNA from *Schizosaccharomyces pombe*; M(Sc): Marker, Chromosomal DNA from *Saccharomyces cerevisiae*; Mb: Megabases; RF: Resolving front of marker (size undefined). Since some bands are hard to recognize, a negative image of the same figure is presented in the appendix (*Suppl. Fig. 8*).

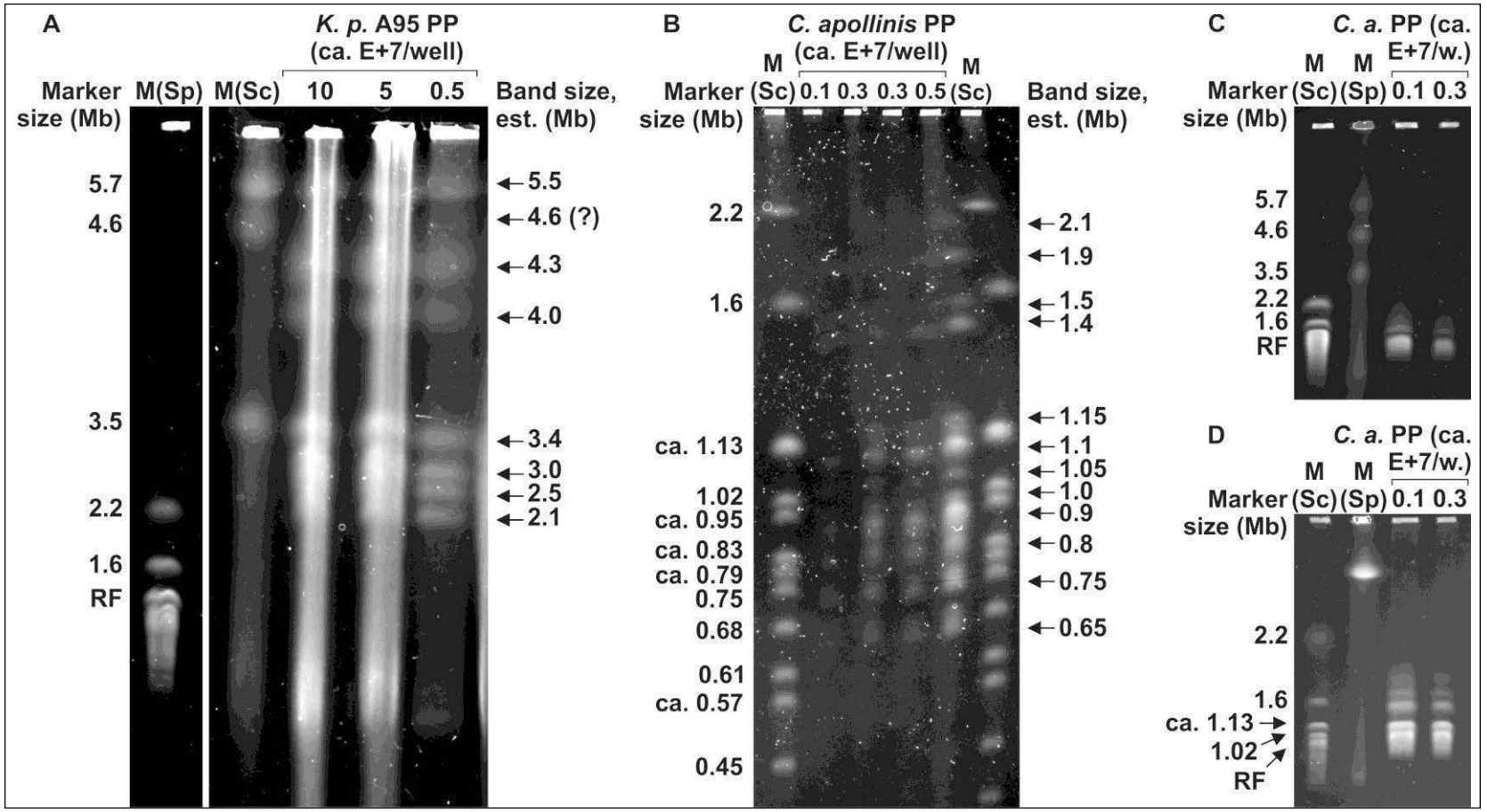

Figure 45. Karyotyping of* Knufia petricola *A95 and* Coniosporium apollinis *by Rotating Field Gel Electrophoresis

(A) Karyotyping of *K. petricola* A95. Protoplast (PP) concentrations of ca. 1×10^8, 5×10^7 and 5×10^6 PP/well were loaded into the gel. Electrophoretic separation by rotating-field electrophoresis (ROFE) was performed for 96 h at 70 V, 20 min to 30 min linear time switch, angle 106°. **(B-D)** Karyotyping of *C. apollinis*. **(B)** Electrophoretic separation by ROFE for 48 h at 180 V, 150 s to 30 s logarithmic time switch, 130° to 115° linear angle switch (protoplast concentrations of ca. 1-5 × 10^6 PP/well). **(C)** Electrophoretic separation by ROFE for 120 h at 50 V to 45 V linear voltage switch, 83.3 min to 16.7 min logarithmic time switch, 110° to 100° linear angle switch (protoplast concentrations of ca. 1-3 × 10^6 PP/well). **(D)** Electrophoretic separation by ROFE for 144 h at 50 V, 20 min to 30 min linear time switch, 106° (protoplast concentrations of ca. 1-3 × 10^6 PP/well). M(Sp): Marker, Chromosomal DNA from *Schizosaccharomyces pombe*; M(Sc): Marker, Chromosomal DNA from *Saccharomyces cerevisiae*; Mb: Megabases; RF: Resolving front of marker (size undefined); Band size, est. (Mb): Estimated chromosome size, in megabases. See *Suppl. Fig. 9* for negative images of the figure.

3.IV.3 Laccase (oxidase) activity of black-fungal strains

Fungal laccases (EC1.10.3.2) are extracellular phenol oxidases best characterized in white-rot fungi (basiodiomycota) like *Botrytis cinerea* and *Trametes versicolor*, where they are involved in the degradation of complex biopolymers like lignin [6,113]. However, in some ascomycetes the enzymes are involved in the synthesis of melanins [8,18,136] and it has been shown that a laccase secreted by the fungal phytopathogen *Gaeumannomyces graminis* is able to polymerize the melanin precursor 1,8-DHN *in vitro* [42]. Oxidative activity of fungal strains is routinely tested with a marker substance ABTS, which is reacting with laccases and/or other oxidative enzymes. The ABTS oxidation is catalyzed in two sequential single-electron transfers, resulting in a green or a purple substance (monoradical and fully oxidised ABTS, respectively) [136].

Ability to oxidise ABTS was screened for the black-fungal strains on both liquid and solid chromogenic media, including *T. versicolor* DSM3086 as positive control. Since phenotypic appearance of pink mutants hinted that the strains were impaired in the synthesis of melanised cell wall, and thus possibly in the activity of laccase(s), strains A95pm1, A95pm2 and A95pm3 were included into the analysis. Interestingly, all strains resulted positive in both liquid and solid chromogenic media, except the two mutants A95pm1 and A95pm3; *C. apollinis* seemed able to oxidise ABTS but much less effectively than the other strains tested positive (*Fig. 46A-C*). Restoration of pink mutant A95pm1's dark phenotype on solid ASM (*Fig. 30*) indicated a medium-dependent formation of melanin and suggested an inducible expression of the responsible enzyme(s). The assay was repeated on the defined medium; nonetheless, also on ASM, mutant A95pm1 was unable to oxidise ABTS (*Fig. 46D*). To obtain an indirect measure of their oxidative activity, black-fungal strains were cultivated up to 7 d in chromogenic MEB and Abs_{420nm} of supernatants was determined at defined time intervals. Results mirrored the data presented in *Fig. 46*, except for *C. apollinis*, for which no increases in Abs_{420nm} values could be determined (*Fig. 47*).

The results for the mutants A95pm1 and A95pm3 suggested that either the strains do not posses the responsible enzyme for oxidation of ABTS, or the enzyme(s) is inactive. Presence of laccase proteins was investigated for all strains tested in *Fig. 46* by SDS-PAGE analysis of growth medium supernatant (either unprocessed or after protein precipitation). After both coomassie and silver staining, no specific band differences could be observed between the strains (not shown). A more sensitive analysis by Western blotting was not possible due to unavailability of specific laccase antibodies. Thus, a molecular approach was adopted to detect transcription of putative laccase genes from *K. petricola* A95 and mutants A95pm1 and A95pm2.

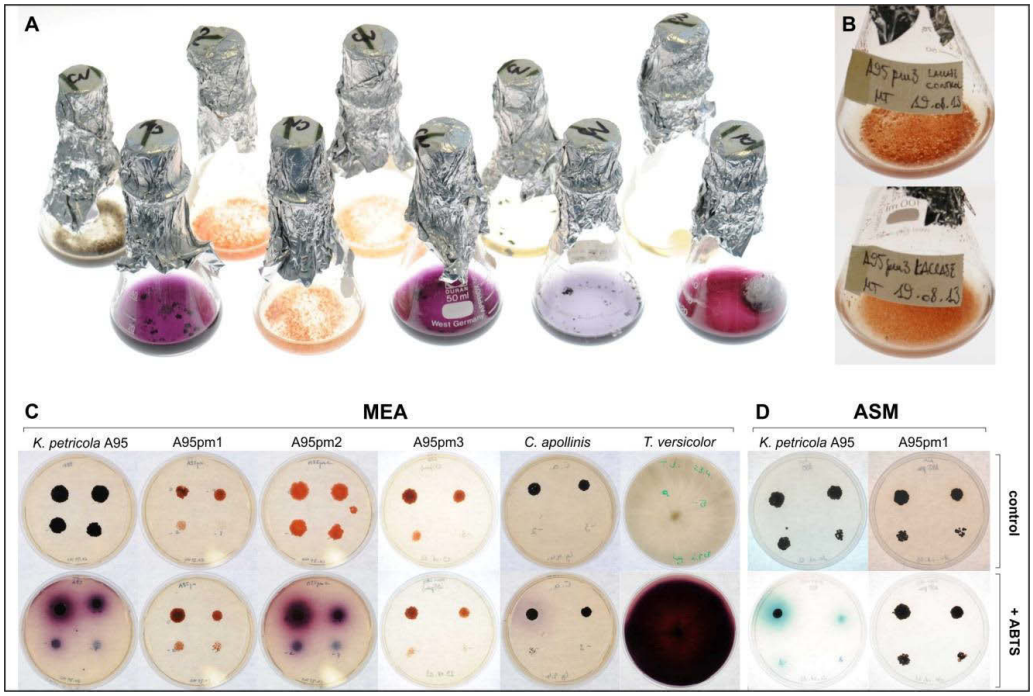

Figure 46.* Knufia petricola *A95 and* Coniosporium apollinis *are laccase (oxidase) positive, but not some of the pink-mutant strains (A95pm1 and A95pm3)

(A-B) Laccase assay in liquid chromogenic medium. **(A)** *Knufia petricola* A95, pink mutants A95pm1 and A95pm2, *C. apollinis* and *T. versicolor* in MEB (back row) or MEB + ABTS (front row) after ca. 5 d of incubation. **(B)** Pink mutants A95pm3 in MEB (upper panel) or MEB + ABTS (lower panel) after ca. 7 d of incubation. **(C-D)** Laccase assay on solid chromogenic medium. **(C)** The strains were spotted undiluted or diluted 1/10, 1/100 and 1/1'000 on MEA (upper panels) or MEA + ABTS (lower panels) and incubated for 1-2 w. **(D)** *Knufia petricola* A95 and pink mutant A95pm1 were spotted on ASM (upper panels) or ASM + ABTS (lower panels) and incubated for 1-2 w.

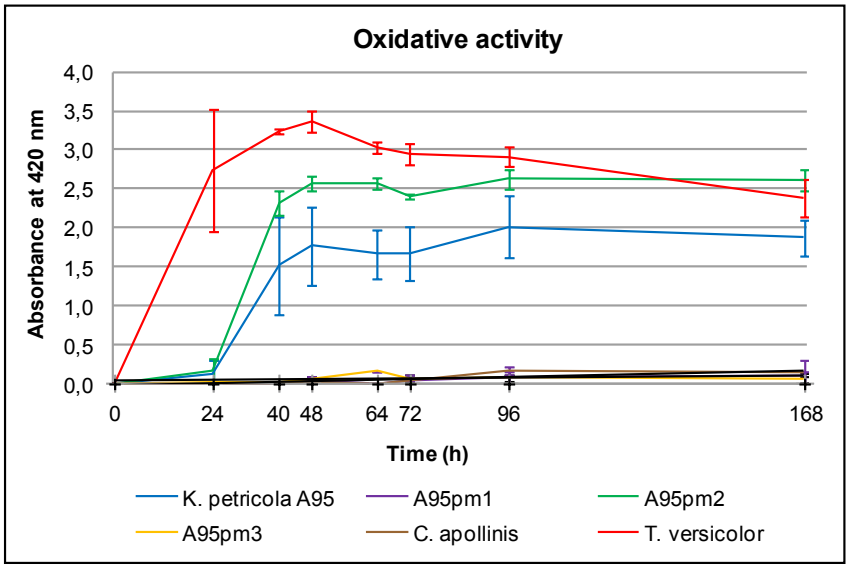

Figure 47. Absorbance (Abs_{420nm}) of culture supernatants in liquid chromogenic medium as an indirect measure of oxidative activity

An aliquot of supernatant of black-fungal cultures in liquid chromogenic medium was removed at the indicated time and absorbance at 420 nm was determined as indication of oxidative activity. Data were generated from three independent repetitions.

In total, ten *K. petricola* A95 laccases were identified by bioinformatics, all provided with multicopper oxidase domain (*Tab. 11*). Total RNA was extracted from the three strains during exponential-growth phase, followed by DNase I digestion and cDNA generation. Specific primers were designed to specifically bind to cDNA and amplify 100-150 nt of each gene. For gene H314_09445, primer pair 09954fw, 09954rev was designed to bind at the border of a region encompassing two introns and thus discriminate between genomic and complementary DNA. First, primers were tested on genomic DNA to validate thermal protocol (annealing temperature 55 °C, elongation time 30 sec, 35X cycles) and primer binding specificity. All primer pairs generated an amplicon of the expected size (*Tab. 5*), even though band for gene H314_08679 was faint (*Fig. 48*). Next, the same PCR protocol was adopted using cDNA as template with 40X thermal cycles to increase signal for gene H314_08679. For gene H314_09945, a spiked sample was included (i.e. a sample with both gDNA and cDNA). By PCR with cDNA as template, all genes except H314_00745 were amplified, and no differences were observed between the three strains. For gene H314_09945 (unspiked tube), a faint upper band of the size of the spiked-tube amplicon was generated, possibly indicating gDNA contamination in cDNA samples (*Fig. 49*). A new PCR was run for all three strains with primer pair 09954fw, 09954rev using cDNA, gDNA or spiked samples. Same amounts of cDNA and gDNA were added (ca. 100-200 ng/µg). With cDNA template, a major band at 145 nt was observed, as well as a faint upper one at 245 nt. With gDNA and spiked samples, only upper band was observed (*Fig. 50*).

Despite this, several observations speak against a contamination of cDNA samples with gDNA, that is:

(i) gene H314_00745 was not amplified from cDNA samples (*Fig. 49*), although in gDNA samples a clear signal was observed (*Fig. 48*);
(ii) in spiked samples, with primer pair 09954fw, 09954rev only upper gDNA band is amplified (*Fig. 50*);
(iii) quality of cDNA samples was verified by qPCR and contamination with gDNA was not observed [Nicole Knabe, personal communication].

The experiment was repeated several times with different protocols to reduce a putative gDNA contamination (fresh RNA extraction, prolonged or reiterated DNase I digestion and/or new cDNA synthesis with less total RNA template); however, a faint upper band with cDNA and primer pair 09954fw, 09954rev was always observed. Thus, the double band for gene H314_09954 is probably due to the chosen reverse-transcription protocol; in fact, using iScript™ Reverse Transcriptase Supermix, cDNA could be produced from non-spliced mRNAs [Bio-Rad Laboratories; personal communication]. Altogether, these observations suggest that results shown in *Fig. 49* are genuine data obtained from cDNA samples and all putative

laccase genes except H314_00745 are constitutively active (i.e. transcribed into mRNA) in all three strains. Deficiency in laccase (oxidase) activity in strain A95pm1 (and A95pm3), thus, must be explained otherwise (see *4 DISCUSSION*).

Table 11. Putative laccase genes in* Knufia petricola *A95

Locus	Description (gene family)	Domains	Comments
H314_00745	Hypothetical protein	Multicopper oxidase	Putative laccase (Broad Institute annotation)
H314_09127	Hypothetical protein (laccase TilA)	Multicopper oxidase	Putative laccase (Broad Institute annotation)
H314_09687	Hypothetical protein (laccase TilA)	Multicopper oxidase	Putative laccase (Broad Institute annotation)
H314_04700	Hypothetical protein	Multicopper oxidase	Putative laccase (Broad Institute annotation)
H314_03963	Hypothetical protein	Multicopper oxidase	Putative laccase (Broad Institute annotation)
H314_08679	Hypothetical protein	Multicopper oxidase	Query with *E. dermatitidis* laccases, 9 hits[a]
H314_01838	Hypothetical protein (ferrooxidoreductase Fet3)	Multicopper oxidase	Query with *E. dermatitidis* laccases, 9 hits[a]
H314_04147	Hypothetical protein	Multicopper oxidase	Query with *E. dermatitidis* laccases, 8 hits[a]
H314_09945	Hypothetical protein	Multicopper oxidase	Query with *E. dermatitidis* laccases, 4 hits[a]
H314_09443	Hypothetical protein	Multicopper oxidase	Query with *E. dermatitidis* laccases, 2 hits[a]

[a] BLASTn and/or BLASTp hits

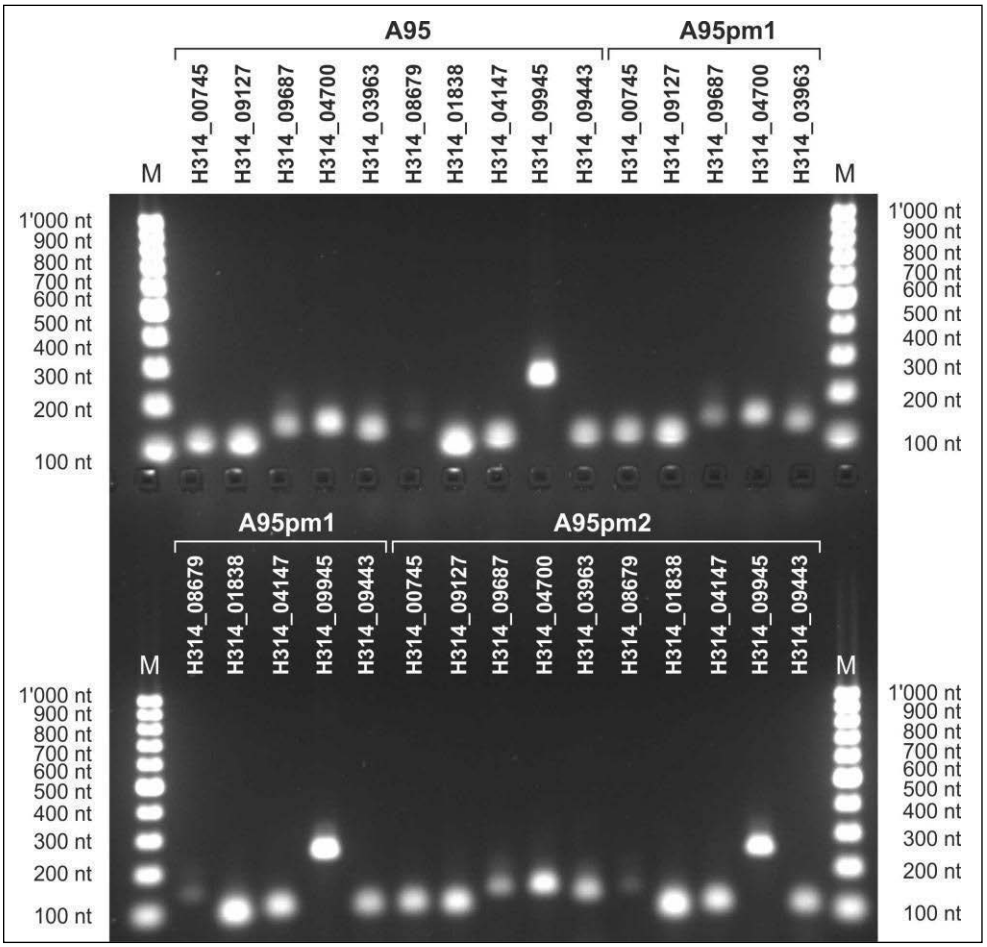

Figure 48. Amplification of putative black-fungal laccase genes from genomic DNA

Putative laccase genes from *K. petricola* A95 and pink mutants A95pm1 and A95pm2 (*Tab. 11*) were amplified from gDNA templates with specific primers (*Tab. 5*) by 35X thermal cycles (annealing temperature 55 °C, elongation time 30 sec) and separated by 2 % w/v agarose gel electrophoresis (45 min at 100 V). M: DNA size marker (100 bp GeneRuler DNA Ladder, size indicated in nt).

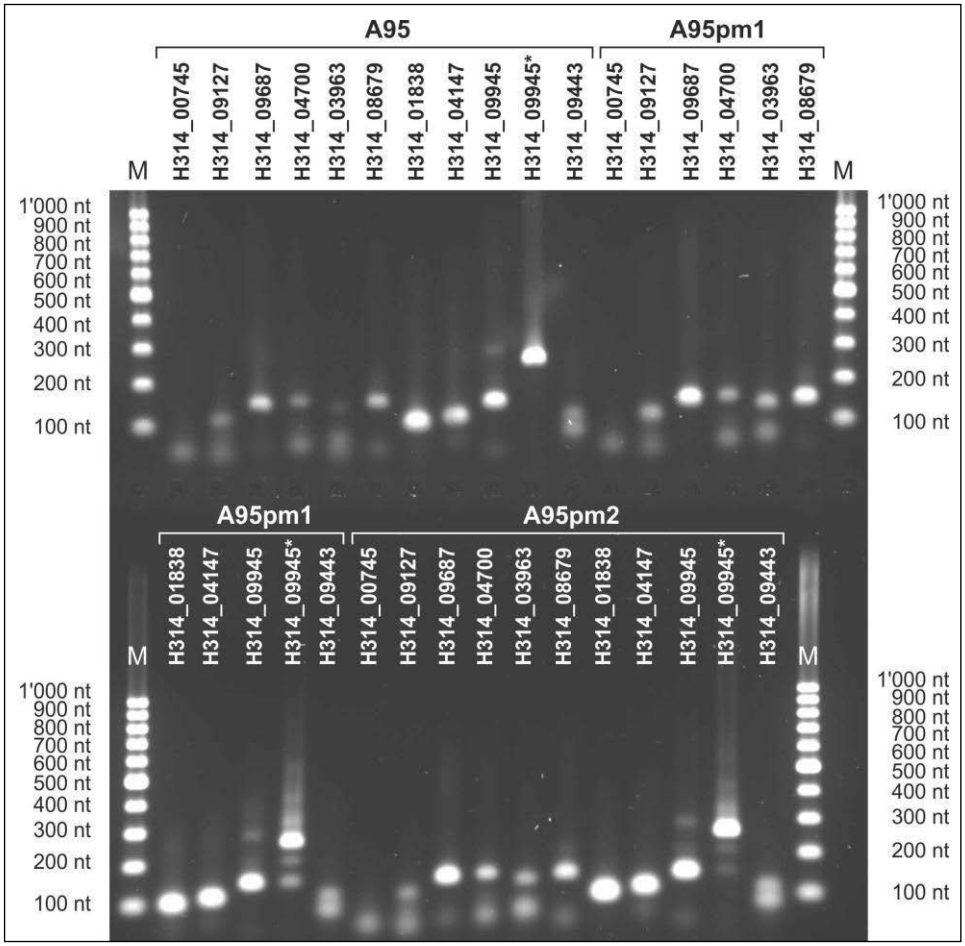

Figure 49. Amplification of putative black-fungal laccase genes from complementary DNA

Putative laccase genes from *K. petricola* A95 and pink mutants A95pm1 and A95pm2 (*Tab. 11*) were amplified from cDNA templates with specific primers (*Tab. 5*) by 40X thermal cycles (annealing temperature 55 °C, elongation time 30 sec) and separated by 2 % w/v agarose gel electrophoresis (45 min at 100 V). M: DNA size marker (100 bp GeneRuler DNA Ladder, size indicated in nt); H314_09945*: spiked templates (cDNA + gDNA).

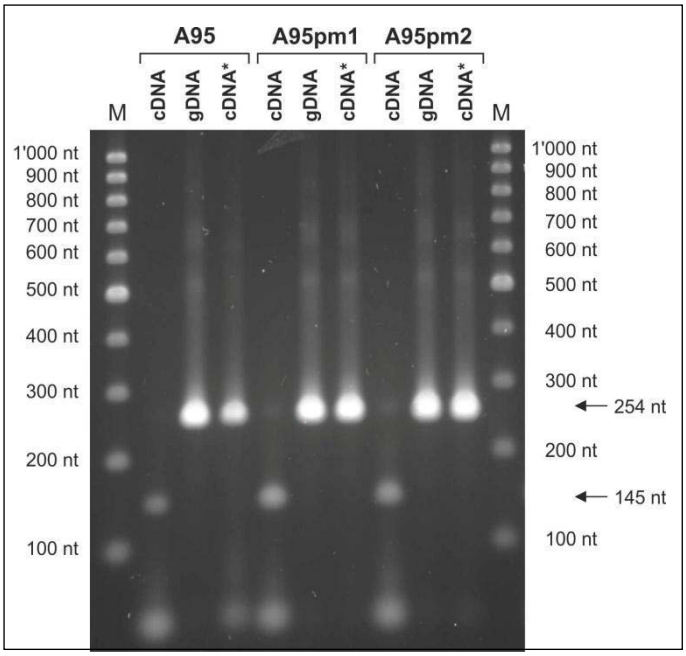

Figure 50. Amplification of gene H314_09945 from complementary and genomic DNA

Putative laccase gene H314_09945 from *K. petricola* A95 and pink mutants A95pm1 and A95pm2 (*Tab. 11*) was amplified from cDNA, gDNA or spiked templates with primer pair 09954fw, 09954rev (*Tab. 5*) by 40X thermal cycles (annealing temperature 55 °C, elongation time 30 sec) and separated by 2.5 % w/v agarose gel electrophoresis (2 h min at 70 V). M: DNA size marker (100 bp GeneRuler DNA Ladder, size indicated in nt); cDNA*: spiked templates (cDNA + gDNA).

3.IV.4 Pigment analysis of *Knufia petricola* A95 and its isogenic mutants

Carotenoids and other pigments present in *K. petricola* A95 and its isogenic mutants A95pm1 and A95pm2 were analyzed by HPLC. Fungal colonies growing on MEA were collected as starting material. To investigate if colour shift observed in A95pm2 at low temperatures (*Fig. 35*) was due to an alteration of pigment composition, pigments were extracted from colonies incubated at 4 °C for 2 w and compared with results for plates not subjected to cold storage (i.e. kept at the table top; *Tab. 12*). Several pigments were identified similarly to results presented in Gorbushina *et al.*, 2008 [56], i.e. lycopene and its derivatives dihydrolycopene and didehydrolycopene, torulene, γ-/β-carotene and torularhodin. As shown in *Tab. 12*, the pigment profiles of all three strains were overall very similar, and upon cold incubation significant increase in some pigments (didehydrolycopene, torulene and others) were observed only for A95pm1 (bold in *Tab. 12*). Thus, it is concluded that colour shift observed in pink mutant A95pm2 at low temperatures was not due to intracellular pigments.

Table 12. Intracellular pigments in* Knufia petricola *A95 and its isogenic mutants[a]

Pigment	A95		A95pm1		A95pm2	
	4 °C	control	4 °C	control	4 °C	control
Lycopene	55.7 ± 13.0	71.7 ± 8.4	81.7 ± 14.7	71.7 ± 14.6	104.0 ± 18.9	102.2 ± 11.1
DL[b]	14.3 ± 0.9	16.2 ± 2.3	18.7 ± 1.9	26.4 ± 4.6	14.5 ± 1.9	14.2 ± 0.2
DDL[c]	137.9 ± 28.3	141.8 ± 2.7	**134.6 ± 10.6**	77.8 ± 8.3	177.3 ± 31.6	168.3 ± 14.2
Torulene	46.8 ± 10.1	47.3 ± 0.8	**50.0 ± 7.0**	31.0 ± 3.8	56.3 ± 10.6	51.7 ± 2.5
γ-Carotene	12.8 ± 4.1	15.4 ± 3.5	10.6 ± 4.6	9.6 ± 3.1	19.9 ± 4.7	19.6 ± 2.7
β-Carotene	15.7 ± 3.2	15.6 ± 1.9	15.2 ± 3.6	14.0 ± 4.1	27.0 ± 5.1	22.3 ± 4.8
Torularhodin	4.5 ± 7.7	3.0 ± 5.2	n/a	n/a	9.6 ± 10.4	0.7 ± 1.2
Others	2.1 ± 3.6	5.7 ± 5.4	**9.3 ± 2.1**	1.3 ± 1.3	25.4 ± 13.7	140.4 ± 197.5

[a] Concentrations are given in mAu*min/g dry weight (average ± error) due to inavailability of calibration curves; bold: significant increases upon storage at 4 °C
[b] Dihydrolycopene
[c] Didehydrolycopene

3.IV.5 Analysis of the model subaerial biofilm

Microorganisms colonising rock surfaces are exposed to harsh environmental conditions and, under such circumstances, antibioses are less often observed than cooperative interplays [47,52]. Many microbial rock dwellers interact in a symbiotic fashion to cope with stress, resulting in complex consortia as lichens or so-called subaerial biofilms (SABs) [1,52,54]. To study development and establishment of SABs in the laboratory, a model biofilm composed of the black fungus *K. petricola* A95 and the well-characterized cyanobacterium *Nostoc punctiforme* ATCC29133 was investigated [54,86]. The model biofilm is regarded as a basic SAB unit in which both partners profit by each other's presence; mutualistic interactions are expected upon unfavourable growth conditions, as for example intense ultraviolet irradiation (protective action by melanins – black fungus' contribution) and nutrient paucity (reduction of inorganic carbon – cyanobacterium's contribution). Previously, it has been shown that the microorganisms form complex three-dimensional patterns, indicative of specific interactions and symbiotic association [54].

A simple way to study the association of *K. petricola* A95 with *N. punctiforme* ATCC29133 is by performing growth experiments under various environmental conditions and comparing responses of both microorganisms when cultivated either alone or in combination with the other partner. Accumulation of SAB biomass is indicative of mutualism, but less informative about the growth rate of the single organisms. Therefore, a way to discriminate between growth responses of the symbiotic microorganisms *per se* is prerequisite to understand establishment of the model biofilm. Growth of fungal and cyanobacterial partner could be analyzed by viable counting and chlorophyll (Chl) *a* extraction, respectively. Cyanobacterial cells do not grow on malt-extract media, thus by plating samples on MEA and determining CFU values of *K. petricola* A95 fungal growth can be assessed. On the other hand, since *K. petricola* A95 does not possess photosynthetic pigments, Chl *a* content is a direct measure of

viable *N. punctiforme* ATCC29133 cells. However, it was not known if presence of fungal cells interferes with Chl *a* extraction. This was assessed in liquid media by growing cyanobacteria, adding fungal cells and extracting Chl *a*. Disregarding from the fungal growth phase, moderate cell loads (5×10^6 and 1×10^7 cells) had a minor effect on Chl *a* content, while presence of 5×10^7 fungal cells resulted in ca. 20 % reduction in Chl *a* values (*Fig 51A*). To validate the result, the same amount of stationary-phase fungal cells as in *Fig. 51A* were added to cyanobacterial cultures, but Chl *a* extractions were performed in increasing volumes of 90 % v/v methanol (1, 5 or 10 mL). Starting from 5 mL methanol, results obtained with 1×10^7 or 5×10^7 fungal cells were indistinguishable and identical to control values (*Fig. 51B*). Thus, it was concluded that high loads of *K. petricola* A95 cells can compromise output of Chl *a* extraction from *N. punctiforme* ATCC29133 in the model biofilm, but the effects can be abrogated by performing extractions in higher volumes of methanol so that fungal cells does not exceed densities of 1×10^7 cells/mL.

Preliminary results with the model biofilm showed that both partners benefit from their association and can actively influence the substrates they colonize, thus confirming that the experimental object is a good candidate to study interactions of microorganisms on and with rock and material surfaces [Franz Seiffert *et al.*, unpublished].

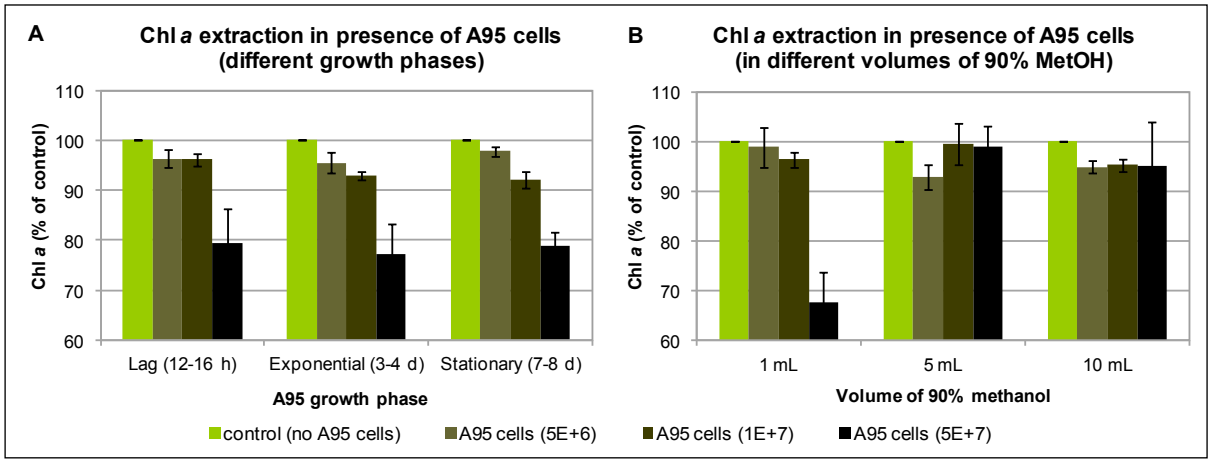

Figure 51. **Knufia petricola *A95 biomass does not interfere with chlorophyll a extraction from* Nostoc punctiforme *ATCC29133***

(A-B) Chlorophyll (Chl) *a* extractions from *N. punctiforme* ATCC29133 liquid cultures (ca. 2 w in liquid BG11) in presence of *K. petricola* A95 cells. **(A)** Extractions in 1 mL 90 % v/v methanol with 5×10^6, 1×10^7 or 5×10^7 fungal cells in the lag, exponential or stationary phase. **(B)** Extractions in 1 mL, 5 mL or 10 mL methanol (MetOH) with 5×10^6, 1×10^7 or 5×10^7 fungal cells in the stationary phase. Results show the average of at least three repetitions.

Summary of results (Part IV)

Diverse results regarding biochemical and molecular characterisation of black-fungal strains were presented together in *Part IV – Biochemical and molecular biology results*. The data were aimed at supporting genome analysis, determining further differences between *K. petricola* A95 and its isogenic mutants and investigating the model biofilm in association with *Nostoc punctiforme* ATCC 29133.

Main findings are summarized as following:

- Ribonucleid acid isolation protocols were established for *K. petricola* A95; resulting RNA quality was suitable for downstream applications (generation of cDNA libraries)
- *K. petricola* A95 and *C. apollinis* were karyotyped by rotating field gel electrophoresis; chromosomes of *K. petricola* were much bigger than those of *C. apollinis*; estimation of genome size correlated well with draft genome data of *K. petricola*, but not of *C. apollinis*
- All fungal strains oxidised ABTS, except for pink mutants A95pm1 and A95pm3; however, this could not be linked with deficiency in expression of laccase(s)
- Intracellular pigments were quantified in *K. petricola* and pink mutants A95pm1 and A95pm2; in A95pm2, no differences were observed upon storage at 4 °C in comparison to the control sample
- Chlorophyll *a* extraction was suitable to monitor growth of *N. punctiforme* ATCC29133 in a model biofilm with *K. petricola* A95

4 DISCUSSION

Biology of black yeasts presents us with a multitude of questions which are still to be answered, e.g. regarding the mechanisms underlying:

(i) ubiquitous distribution and colonisation of unfavourable niches,
(ii) stress tolerance,
(iii) colonisation of materials,
(iv) symbiotic interactions with co-occurring (autotrophic) organisms, and
(v) pigmentation (melanisation).

This heterogeneous group of filamentous fungi is geographic widespread and relevant for many fields of application, yet relatively poor understood. For this purpose, the rock-inhabiting strain *Knufia petricola* A95 was investigated and confirmed as suitable model microorganism. A broad spectrum of experimental methods was designed with and conducted on the strain, in particular:

(i) growth experiments (e.g. phenotype microarrays, growth curves, determination of colony size upon variation in external conditions, etc.), and
(ii) molecular biology and biochemical methods (e.g. nucleic acid isolation, gene-expression analysis, karyotyping, determination of laccase activity, etc.).

Additional methods (e.g. histological sections and microscopic observations of colonies, gas-chromatographic assay, etc.) were adopted to gain further knowledge on the strain, in particular regarding its nutritional modes and growth under nutrient limitation. Many protocols needed to be established, and thus the thesis concentrated on the development of novel experimental approaches to study black fungi.

Growth – e.g. differences in viability or colony size – was often evaluated to discern nutritional preferences, consider effects of environmental conditions or assess resistance toward stress stimuli. This primary phenotypic trait is a good parameter for slow-growing organism and was easily quantified by cultivation methods.

Black fungi are present in different taxa of ascomycetes. Their striking similarities regarding survival strategies and morphology thus developed independently. For this reason, comparative analysis of black fungi from different phylogenetic groups are necessary. The black fungus *Coniosporium apollinis* [110,128] and isogenic mutants of *K. petricola* A95 were included in a part of the experiments when a direct comparison was sought after. Comparative analysis with *C. apollinis* are of interest since the two strains show remarkable ecologic and morphologic similarity but are distantly related [64]. Genomes of both, along

with other species, are currently investigated in the framework of the Black Yeast Sequencing Project of the Broad Institute (www.broadinstitute.org).

Data shown in the thesis are discussed in details below in subchapters roughly following the order in which results were presented. First, phenotypic data are discussed; then, oligotrophic growth of the model microorganism is considered; a subchapter is devoted to the pink mutants of *K. petricola* A95; finally, data on black-fungal genomes are developed. Results for *C. apollinis* are not grouped into a separate subchapter but are compared throughout the text with the data obtained for *K. petricola* A95.

Data which are not mentioned in this chapter are considered in *5 CONCLUSIONS AND OUTLOOK* where a final overview and future developments are proposed.

4.1 Phenotypic characterisation of black fungi

The model microorganisms *K. petricola* A95 was studied with regard to morphology, growth in different liquid media, growth preferences, nutrient metabolism and temperature-growth optimum. Based on the data, a defined medium for black fungi was developed (*3 RESULTS – PART II*).

4.1.1 Growth in complex medium

At first, primary parameters such as growth rate and generation time *g* were defined to allow standardisation of experiments. Although the protocol needed some modifications (e.g. the shaking step to disrupt cell aggregations or the arbitrary definitions of clumps as a group of five or more cells), black-fungal liquid cultures could be characterised by absorbance measurements, viable counting by plating and cell counting under microscope as normally performed for bacteria and yeasts [80]. This was possible due to the restricted, meristematic growth of the black fungus (no hyphal growth and no formation of filaments).

With generation time g = 13.0 and onset of stationary phase after ca. 4 d after inoculation, *K. petricola* A95 grows, probably, faster than any other black fungus described so far (*Fig. 7*). Data presented in *Fig. 7A* can be regarded as a standard growth curve and, since the shaking step did not have deleterious effect neither on cell viability nor on integrity in none of the growth phases (*Fig. 2*), were used to prepare inocula with defined cell density and/or isolate cells at the desired growth phase. By using a treated culture of a certain age, it was thus possible to rely on inocula of standard quality.

No growth curves for *C. apollinis* could be generated, as it was impossible to obtain standard propagation units. After shaking cultures as reported in *Section 2.3.1*, cells looked intact under microscope (not shown) and liquid culture could be successfully inoculated but, after plating on MEA, viable counting gave non-reproducible results. After mitigation of shaking conditions (fewer beads, less frequency and/or shorter shaking time), cultures remained clumpy and thus difficult to handle and grow on plates as single colonies. For *C.*

apollinis, thus, presence of clumps for growth on solid media might be more crucial than for *K. petricola* A95. Despite this observation is difficult to interpret, importance of cell clusters as "propagation and survival units" has been proposed as a fundamental growth mechanisms of black fungi, even upon favourable culture conditions [51]. This further confirms the choice of *K. petricola* A95 as a suitable model strain.

Analysis of growth on solid media showed that *K. petricola* A95 is mesophilic with growth-temperature optimum at around 25 °C (*Fig. 29*), validating previous observations that black fungi can withstand, but not grow at, temperature extremes [56,124]. For average colony size, big fluctuations in the results should be interpreted as experimental artefacts (*Figs. 29*, *37B-D* and *41B*). By plating highly diluted samples (1/10'000), for example a 2-fold increase in colony numbers did not affect final CFU values much, while having a more drastic reduction in average colony size. This phenomenon has been previously observed [Anna A. Gorbushina; personal communication] and might be explained in several ways. Upon strong growth, colonies could grow adjoining and compete for limited space, and thus inhibit each other. Similarly, nutrients might be consumed, resulting in a growth slow-down. However, the phenomenon has also been observed with sufficient spacing among single colonies, thus suggesting a chemical signalling mechanism, which could link population density with growth inhibition as observed in quorum-sensing population control. This last speculation needs to undergo further investigations.

4.1.2 Phenotype microarrays and nutritional physiology

To test growth on multiple substances and conditions, a miniaturised, high-throughput approach was chosen. Commercially-available Biolog's Phenotype MicroArrays allow parallel analysis of growth upon hundreds of different conditions and are well-established in microbiology [11]. Apart from the presence of genes responsible for utilisation of a given compound, for example, active metabolism in its presence needs to be proven experimentally. Thus, phenotypic tests are an important compendium to genome analyses [9,10]. By presence of the tetrazolium dye, metabolic activity could be uncoupled from biomass accumulation, which is especially alluring for microorganism difficult to cultivate (e.g. slow growing and VBNC cells). Main purposes of phenotypic microarrays are to determine growth preferences of uncharacterized microorganisms [41], support genome annotation [9], differentiate metabolism of related species or mutant strains [12,38,41,134] and develop media for growth of non-culturable species [93]. To different extent, all these goals were pursued in this thesis following phenotypic characterisation of the model organism *K. petricola* A95. This was, to the best of knowledge, the first time that Biolog's Phenotype MicroArrays were used to characterize rock-inhabiting black fungi, although the method was already applied to other filamentous species [38,41,46,108,134].

Several obstacles were encountered and circumvented accordingly. Primarily, clump formation and association of reduced dye with cells did not allow spectroscopic measurements. To obtain numerical values, biomass accumulation in plates was evaluated by eye using an *ad hoc* scoring system not dissimilar from those used in classical physiological screenings [28,140,142,156], yet still taking advantage of miniaturised Biolog's MicroArrays. To ensure robust results, each plate type was inoculated at least three times and analysed by at least two persons independently. Reliability of data was indicated by statistical analyses (e.g. values bigger than one integer were rarely observed for differences between minimum and maximum scores, and for interquartile ranges in less than one percent of the results) and by comparison with data from previously characterised *K. petricola* strains using classical physiological test [91,156].

Despite the advantages of Biolog's Phenotype MicroArrays plates to characterise phenotype, a drawback was that comparisons between plate types were impossible due to different (and undisclosed) supplementation. For example PM1-2 plates were buffered with high concentration of phosphate buffer, but not the others; PM1-2 were provided with sulphur source, while PM3 needed supplementation of it in inoculating fluid; positive control well in PM5 was provided with an unknown supplement (Barry Bochner, personal communication). This resulted in different growth patterns and in different incubation times. Marked oligotrophism of strains also forced the visual inspection after few days of incubation to reduce background growth. This was especially critical for analysis of sulphur metabolism, which could not be performed with Biolog's Phenotype MicroArrays. A comparison between strains was possible but given a – putative – more marked oligotrophism *in C. apollinis* and pink mutants A95pm1 and A95pm2 (as observed by pronounced background growth in negative control wells), highest score was omitted in the evaluation of nutrient plates.

Since the measured output of Biolog's microarrays is growth and/or cellular respiration, a distinction between nutrient import and assimilation is rarely possible. That is, a compound which supports growth is surely both imported and assimilated, while, for one which does not, it cannot be determined if either transport or metabolism is affected (or both). Rarely encountered nutrients could have degenerated transport systems, even though the enzymatic machineries to catabolise them might be active; similarly, complex substances might not be taken up although the corresponding monomers might be assimilated. All this disadvantages notwithstanding, broad phenotypic profiles the strains were generated (*Section 3.II.3*).

Osmo- and desiccation tolerance of *K. petricola* A95 confirmed it as a typical rock dweller. Osmotolerance (*Fig. 9*) is distinctive for black fungi and rock-inhabiting species, which thrive on niches subjected to desiccation and local solute increases [56]. As observed here,

osmotolerance is not restricted to some salt species; this trait is passively conferred by melanins and intracellular solutes (e.g. glycerol), which counteract deleterious effects of high solute concentrations [65,73,75,99]. The model strain tolerates a relatively broad spectrum of pH values, although the optimum at acidic pH is typical for most black fungi. Effect of growth factors – arguably not abundant on rocks – was negligible upon "regular" inoculation (dilution of cell 1/100 in inoculating fluid) but discernible upon lower cell load. Biomass accumulation in control well without primary nutrients validated oligotrophism of black fungi, which is an important adaptive mechanism for the colonisation of nutrient-scant niches. However, the strain was rather selective in the utilisation of nutrients (in particular carbon sources). Especially in oligotrophic niches, utilisation of a broad spectrum of compounds should be of advantage to boost metabolism upon nutrient availability; on the other hand, strains might lose ability to import and/or assimilate rarely encountered chemicals.

Carbon metabolism was analysed by grouping compounds into major fungal metabolic pathways (*Fig. 12*). Some were not easily linked to known pathways and were not considered in the analysis (reported in *Suppl. Fig. 3* in *A.5 Supplementary data*). Despite the fact that only ca. 33 % supported growth (of which only ca. 37 % efficiently with median > 1), most pathways seemed to be active. Many intermediates of metabolic pathways did not support growth of *K. petricola* A95 while the upstream molecule did (e.g. growth on L-arabinose and D-glucose, but not on L-arabitol and D-glucose-1-phosphate), thus indicating that defect in uptake rather than assimilation. It is argued that in stressed ecosystems as rock surfaces, passive diffusion must be avoided to prevent leakage of intracellular substances and thus transport should be tightly regulated [91]. Due to the symbiotic character of rock inhabitants, which co-habit the same niche in a facultative consortium of microorganisms, competition for short-lived molecules like sugar alcohols is probably fierce and thus it is not in the interest of slow growing organism to compete for them. Restricted ability to import metabolic intermediates was previously observed in other filamentous fungi [38,41]. In this light, nutritional strategy of *K. petricola* A95 is to selectively import carbon sources while at the same time retain major fungal pathways active so that a broad spectrum of substances can still enhance metabolism. Alternatively, it could be argued that carbon is not a limiting nutrient on rock surfaces, where autotrophic settlers and fossil organic material might be abundant [52,125]. Preferential use of certain compounds was observed for carbohydrates of plant and microbial origin (pectin, dextrin, D-enantiomers of monosaccharides, etc.).

Nitrogen and phosphorus sources were used less selectively than carbon ones (ca. 75 % and ca. 50 % able to support growth, respectively) and nutrients were grouped into chemical groups rather than into metabolic pathways (*Figs. 13-14*). As for carbon molecules, preferences could be ascertained (e.g. amino acids as N source and ubiquitous

phosphorylated molecules as P source). Interestingly, little overlapping was observed between nutrient groups; for example, nucleobase derivatives were good P sources but poor C and N ones, while amino acids derivatives were good N sources but poor C and P ones. This could be a mechanism for species growing in nutrient-limited niches to devote certain chemicals to feed into specific metabolic pathways. Due to pronounced oligotrophism without any sulphur source, S metabolism could not be analysed. Many attempts to reduce growth in negative control well either did not had the desired effect or slowed down metabolism excessively (i.e. dilution of cells 1/10'000, reduction of incubation time, or supplementation with 1 mM D-(+)-glucose instead of 100 mM or pre-cultivation in sulphur-deprived media to deplete putative intracellular reserves).

Comparison with phenotype microarrays data for *C. apollinis* showed differences between the two organisms.[22] Growth in negative control wells without nutrients was even stronger than for *K. petricola* A95, thus the score "2" (defined as strong growth in relation to negative control) was omitted. The dothideomycetes *C. apollinis* was less tolerant to salt stresses and had a broader pH optimum (shifted toward alkaline conditions; *Fig. 21*), and was even more selective in the utilisation of nutrients (ca. 16 % of carbon sources and ca. 37 % of nitrogen sources supporting growth; *Figs. 22-23*). Except for the starch and sucrose metabolic pathway, which seemed to be more active in *C. apollinis*, most of the others were less active. Regarding N metabolism, reduced utilisation was observed for some chemical classes like D-amino acids and primary amines.

Down-regulation of metabolism as stress-resistance mechanism is a feature of rock-inhabiting fungi, and as shown by proteome analysis seems to be particularly pronounced in dothideomycetes [71,159]. Thus, increased selectivity for *C. apollinis* could be a result of metabolic down-regulation. Remarkably, and in contrast with *K. petricola* A95, metabolic intermediates such as sugar alcohols were efficient C sources (e.g. adonitol, L-arabitol, xylitol, D-sorbitol, etc.). Polyols are synthesised by lichens, as well as intracellularly present in free-living fungi, and therefore autochthonous on rocks. However, *C. apollinis* has never been isolated from lichens, and it has never been reported that dothideomycetes are more associated with them than eurothiomycetes [Lucia Muggia, personal communication].

Knowledge on physiology and nutritional modes of black-fungal strains will support comparative genome analysis of these organisms, e.g. during metabolic pathway predictions, gene annotation and function assessment of hypothetical proteins. All experiments were performed at "standard" conditions. Effect of further environmental factors on nutrient metabolism or salt resistance might be investigated to increase knowledge on the model strain (e.g. incubate plates at different temperatures, use another

[22] See *Subchapter 4.3* for comparisons with pink mutants.

carbon source instead of glucose to analyse nitrogen metabolism and thus investigate co-ordination of N and C metabolism, etc.).

4.1.3 Utilisation of hydrocarbons

Ability to grow on hydrocarbons as sole nutrient and energy source was previously reported for black fungi, in particular some specialized member of this group belonging to the family *Herpotrichiellaceae* (order *Chaetothyriales*), notably *Exophiala* spp. and *Cladophialophora* spp. [5,32,104]. This hydrocarbonoclastic trait is appealing for bioremediation purposes for the degradation of hazardous industrial pollutants like BTEX (benzene, toluene, ethylbenzene and xylene) [101]. Even though fungal assimilation of hydrocarbons outside the *Herpotrichiellaceae* is not known, a *Knufia* spp. (family *Chaetothyriaceae*) has been recently isolated from a hydrocarbon-polluted environment [72], possibly indicating resistance toward and/or biodegradation of such compounds. Absence of hydrocarbons in Biolog's Phenotype MicroArrays prompted the analysis by other means. Simple volatile organic compounds (toluene, benzene and pentane) as well as phenol were chosen as candidate molecules to test utilisation by black-fungal strains (*Section 3.II.4*). Selection of monoaromatic and short-chained hydrocarbons had the advantage of:

(i) narrowing the range of molecules to test, and
(ii) eliminating redundant molecules, since simple compounds are intermediates during degradation of complex hydrocarbons [104].

As of today, fungi able to assimilate benzene (unsubstituted monoaromatic) are not known, and fungal strains (*K. petricola* A95 and its mutant A95pm1, an uncharacterized *Fonsecaea* spp. as well as *C. apollinis*) were incubated with the VOC. Gas-chromatographic methods to monitor decreases in VOCs coupled with increases in CO_2 were performed as proof of assimilation, since microorganisms might be able to degrade them without showing actual cell respiration [103]. Utilisation of phenol was tested in microtiter plates in ASM deprived of carbon. Phenol is less volatile [2] and thus a complex set-up was not necessary; nonetheless, the simplified experiment should be considered as a preliminary screening only.

All selected strains resulted negative in the utilisation of the tested hydrocarbons, except for the control strains *C. psammophila* incubated with toluene. Results were reproducible with data from the literature [5,100,102,103,105], thus validating set-up and execution of the experiment (*Fig. 25*). Reaching of a plateau in CO_2 levels is indicative of full biodegradation of substrate. Gas-chromatographic assay included abiotic controls to validate analytic measurements and exclude VOC leakage; flasks amended with glucose as sole carbon source (positive controls for growth); flasks without any carbon (background respiration controls);

and flasks amended with both VOC and glucose (both co-metabolism and toxicity controls). In these latter, no CO_2 production by a given strain – concomitant with CO_2 production for the same strain in positive controls – meant that the corresponding VOC was toxic; on the other hand, since hydrocarbon utilisation is often co-metabolic [103], CO_2 production coupled with VOC decrease in those flasks only – and not in flasks with VOC alone – meant that the hydrocarbon could be degraded, but not assimilated. Toluene was toxic at the used concentration (ca. 1.15 mM in the liquid phase); this was unexpected on the basis of previous experiments [103] and was indicative of inability to assimilate this compound. This was verified with lower concentrations of toluene (ca. 0.55 mM) and observation of biomass formation in co-metabolism controls [Francesc Prenafeta; personal communication]. In this validation experiment, chromatographic measurements were not performed since using small concentration of substrate is critical for oligotrophic strains due to high background respiration in control flasks without carbon source. Some data reported in *Tabs. 8-9* – e.g. the reduction of toluene with strain A95pm1 and pentane with *K. petricola* A95 – should be considered artefacts, since concomitant CO_2 increases were not observed.

Interestingly, there were no indication of an active aromatic pathway in *C. apollinis* (Biolog results; *Fig. 22*), while *K. petricola* A95 showed activity in the pathway (*Fig. 12*). In *K. petricola* A95, *p*-hydroxybenzoic acid was amongst the preferred carbon sources. The monoaromatic compound is linked to metabolism of aromatic acids, including lignin, which is a natural substrate abundant in the environment [3,88,104]. However, all strains resulted unable to assimilate the VOCs and these differences in metabolism of aromatic carbon compounds as observed with the Biolog System were not mirrored in the results of the hydrocarbon-utilisation assay.

Despite the fact that the organisms did not assimilate the hydrocarbons, these data add further knowledge on the black-fungal strains and confirm the observation that the hydrocarbon metabolism is probably restricted to certain members of the *Herpotrichiellaceae*. The results, along with phenotype microarrays data, might support the identification of genes responsible for hydrocarbon assimilation – e.g. when comparing genome sequences of *K. petricola* A95 and *C. apollinis* with the hydrocarbonoclastic fungus *C. psammophila*.

4.1.4 Development and testing of A95-Specific Medium

As a direct output of the knowledge of phenotype, the new synthetic medium ASM (A95-Specific Medium) was formulated. Preferred (i.e. with highest median in Biolog's PM plates), commercially cheap and non-pyrolysing (upon autoclaving) nutrients were chosen; preferred pH was set; well-tolerated mineral salts were added as stock solutions; and growth-enhancing factors were selected from Phenotype MicroArray plate PM5. Of these, thiamine

had a clear positive effect (*Fig. 8B*), while choline and *N*-acetyl-D-glucosamine were included in the attempt to boost growth further (a comparison of growth in ASM with or without these last two growth factors was, however, not done). As carbon source for liquid ASM, D-mannitol was added, but, surprisingly, on solid ASM the compound was less suitable for strong biomass formation for unknown reasons (not shown); thus, D-(+)-sucrose was used instead. Different nutritional preferences on solid/liquid media could not be addressed by analysing growth in Phenotype MicroArray due to the viscous character of the inoculating fluid.

Growth rates and final cell densities in liquid ASM were reduced in comparison to the complex MEB (*Figs. 7, 28*); however, aside from a delay in the onset of exponential-growth phase, similar patterns were observed (i.e. ratio between total and viable cells, increase in Abs_{660nm} values during stationary phase and length of exponential phase; *Fig. 28C*). Repeated inoculation in ASM showed that viability did not decrease, thus corroborating correct medium formulation (*Fig. 28D*). On solid ASM, colonies were easily recognizable after 1-2 w, resulting in an average surface area of up to ca. 8.4 mm^2 (*Fig. 29A*). Preliminary experiments showed that other black fungi were also capable of growth in ASM (not shown), thus making the medium alluring to investigate this group of microorganisms.

The new synthetic medium ASM was suitable for cultivation of *K. petricola* A95 even though it did not support growth as efficiently as the complex malt-extract medium. Yet, the appeal of defined media in microbiology is not necessarily to obtain high biomass yields, but the ability to design further experiments – as for example the analysis of growth in nutrient-deprived media as discussed in the next subchapter.

4.2 Growth of *Knufia petricola* A95 in oligotrophic media

Oligotrophism – i.e. ability to grow upon nutrient limitation – is well known for black fungi [62,114]. Data shown in *3 RESULTS – PART III* focused on the analysis of growth of *K. petricola* A95 in nutrient-deprived media, including pure water. The aim was to characterise growth of the model microorganism further and to investigate possible mechanisms responsible for the phenotype. Descriptive (macro- and microscopic) observations were performed and supplementation experiments with dead fungal biomass were designed to asses growth in a semi-quantitative way and investigate mechanisms of oligotrophism.

Increases in viability and biomass could be quantified in both liquid and on solid media (*Fig. 37*). Differences between liquid and solid oligotrophic media were observed, most dramatically upon sulphur limitation (low viability in liquid ASM-S but big colonies on ASM-S); this was probably to ascribe to a contamination of agar with sulphur compounds. However, there are probably intrinsic differences in surface versus submerged growth, especially for organisms which have adapted to grow at the solid-atmosphere interface. This

was clear in the preference, on solid ASM, for D-(+)-sucrose as carbon source instead of D-mannitol in liquid ASM. Analysis of phenotype with the Biolog was not of help in this regards, since the viscous Phytagel-based inoculating fluid (FF-IF), recommended for characterisation of filamentous fungi, had semi-solid character. Conclusive information about growth preferences in liquid or on solid media could not be gathered by using Biolog's Phenotype MicroArrays plates. Analysis of oligotrophic growth of *K. petricola* A95 was done in parallel in both liquid and solid media.

Growth was quantified by viable counting or by calculation of average colony size by image processing as reported in *Section 2.3.5*. Projected surface area was a suitable quantification method on solid media (easily performed, reproducible) and, in this way, numerical values could be obtained. Upon plating of a shaken, washed start culture, colony count was similar on all media, including H_2O-agar, and only size of colonies was affected. Thus, average colony size was used as direct measure of growth. Radial expansion on solid media is often used in mycology to quantify growth of fungi (see e.g. [106]), although in this thesis a modified protocol including image analysis with the software ImageJ was adopted to calculate average colony size. As opposed to flat, mat-like growth in filamentous fungi, for *K. petricola* A95 microcolonial, cauliflower-like patterns were observed on MEA (*Fig. 1*); this was however not the case on the defined ASM, where colonies were flat (*Fig. 39*). By calculating projected surface area, three-dimensional growth of the strain resulted thus in an underestimation of biomass on MEA in comparison to ASM. Calculation of colony volumes was in principle possible, but much more laborious by image processing as done in this thesis; volume of colonies was further not in correlation with biomass yields due to extensive presence of voids on all media supporting good growth. Quantification by other means like dry weight would have been a direct measure of growth, although unreliable upon low biomass yields on oligotrophic media. Apart from these limitations, by supplementation experiments beneficial effects on nutrient-deprived media were immediate (*Fig. 40* and see discussion below). In no cases, upon presence of dead fungal biomass, two-dimensional growth on oligotrophic media became three-dimensional, and thus no false negative results were observed.

Remarkably, colony morphologies varied upon cultivation on different media (*Figs. 38-39*). Filamentous colonies were observed upon poor growth on nutrient-deprived media, especially ASM-C, ASM-N and H_2O-agar. Formation of "exploration hyphae" has been previously reported in both yeast-like and filamentous fungi upon starvation [50,146]. PAS staining of histological sections did not show major differences among colonies grown on different media, apart from a lighter colouration of starved cells. Invesitgation of putative differences in viability of cells from different regions within a three-dimensional colony would have been an interesting issue, but, unfortunately, the question could not be addressed by histological analyses (fixation step required).

To investigate mechanism of oligotrophism, growth in nutrient-deprived media supplemented with dead fungal biomass was quantified (*Fig. 41*). For this purposes, different sterilisation methods (autoclaving vs. ethylene-oxide sterilisation) were utilised to rule out artefact – e.g. formation of non-natural occurring chemical bonds – and/or degradation of substances; also, fractionation of cells was performed as an attempt to localize putative nutrient sources.

A beneficial effect was evident in both liquid and solid oligotrophic media (*Figs. 40-41*). It is argued that dead fungal biomass can be utilised by the fungus to support growth, meaning that internal/cell-associated molecules are mobilised upon nutrient shortage. This phenomenon could help explain marked oligotrophism of black-fungal strains. Basal growth without exogenously added nutrients (*Fig. 37*) could thus be due to mobilisation of substances; however, contamination of media with traces of chemicals could not be excluded (e.g. tenside residues on glass flasks or dust particles introduced during media preparation). To avoid this, meticulous care should be paid and special equipments used during media preparation (e.g. working under controlled atmosphere and/or special hoods, cleaning of glassware with acids, wearing of a dust mask, etc.); however, the required laboratory facility was not available.

Localisation experiments showed that putative nutrient sources were probably localized in the cell wall (N source), both the cell wall and the cell membrane (P source), the cytoplasm (S source) or all compartments (C source; probably heat-sensitive). Based on this preliminary screening, the precise nature of nutrients could be identified more easily. As starting material, standardised amount of cells were used (stationary-phase culture of *K. petricola* A95 in MEB, ca. 2.5-3.0 $\times 10^7$ cells+clumps/mL according to *Fig. 7*); a more precise biomass quantity (e.g. in mg/mL) should be used for further experiments.

4.3 Description of mutants

Spontaneous mutant colonies arose during cultivation of the black fungus *K. petricola* A95. Mutant strains were isolated and characterised in *3 RESULTS – PARTS I, II and IV*.

The strains were isogenic with the parental strain (*Suppl. Figs. 1-2*) and showed remarkable colouration (*Fig. 4*). Pink/orange phenotypes were most probably due to unmasking of internal pigments, which are abundant in *K. petricola* A95 [56]. Pigment analysis showed no major differences between wild type and mutants (*Tab. 12*); thus, cell-wall biosynthesis was likely affected and responsible for the phenotypes. Emergence of spontaneous albino mutants by repeatedly sub-culturing black fungi has been previously observed [162]. Pink mutants of *K. petricola* A95 represented excellent candidates to study effect of melanisation on growth and stress resistance.

Overall, striking similarities were observed between the parental strain and the mutants. Apart from the obvious colour differences, growth in complex medium was, in liquid MEB, almost identical (*Fig. 7*) and, exclusively for pink mutant A95pm1, reduced on solid MEA (*Figs. 4, 29*); colony morphologies were not affected (not shown); growth-temperature optima were the same (*Fig. 29*); tolerance to salts and pH was comparable (although mutants seemed to have slightly increased osmotolerance; *Figs. 15-16*); phenotype microarray data showed similar results for nutritional metabolism (no pathway or chemical group comprehensively affected; *Figs. 17-19*) and resistance toward drugs (apart from β-lactame antibiotics and aminoglycosides, more effective against mutants; *Fig. 20*); viability after ultraviolet stress was not compromised more than in the wild type (*Fig. 36*); and no differences in karyotype could be observed (not shown; see also *Subchapter 4.4*).

Nonetheless, during generation of temperature-optimum profiles interesting observations could be drawn that were investigated to describe phenotype of mutants further (*Sections 3.II.6-7*). Growth of pink mutant A95pm1 was compromised on solid MEA but unaffected on ASM (*Figs. 29-30*). This medium-dependent restoration of colony size and pigmentation was further analysed by growing A95pm1 on MEA supplemented with ASM components, showing that chloride anions were responsible for restoring wild-type phenotype in a specific and dose-dependent manner (*Figs. 32-34*). The phenomenon could also help explain increased tolerance toward certain salt species observed with phenotype microarrays (*Fig. 15*). Restoration of both pigmentation and colony size on modified solid medium hints toward a link between melanisation and growth; however, such a link is not known [18]. Alternatively, the mutant might have multiple mutations associated with either phenotypes (either colour change or growth defect), and thus a link might not exist. At best of knowledge, biosynthesis of 1,8-DHN melanins has never been associated with presence of exogenously-added anions and this could thus be the first time that such a link is established [8,18,19,77]. On the other hand, cations are enriched in melanised cell walls, and copper ions might increase melanin synthesis [18] and are known co-factors for laccases [136], which are involved in the biosynthesis of melanins [77,137]. Fungal melanins are a heterogeneous group of substances formed by oxidative polymerisation of monomers including phenols [77]. The chemical structure of melanins are not fully known and the synthetic pathways not entirely characterised, but black fungi produces 1,8-DHN melanins and the final oxidation step involves laccases [18,137]. Although they are also found intracellularly, such enzymes are mostly extracellular or associated with the cell wall and are probably responsible for the final polymerisation of 1,8-DHN monomers [18,138]. Interestingly, pink mutant A95pm1 resulted negative in laccase screenings, but ability to oxidise ABTS was not restored on ASM (*Fig. 46*). Thus, a link between chloride ions and oxidation of ABTS could not be established. At the gene-expression level, no differences between wild type and mutants in transcription of putative laccase genes could be

ascertained (*Fig. 49* and see also *Subchapter 4.4*). Colour development in presence of ABTS could be due to presence of oxidative enzymes other than laccases; alternatively, the observed phenotype for A95pm1 could be due either to mutations in the coding region of putative laccase genes or to decreased enzymatic activities. These assumptions require further validation. Similarly, phenotype in pink mutant A95pm1 needs further analyses to investigate the link, if any, between growth defect, melanisation and chloride ions and to characterise at the biochemical and/or molecular level the enzyme(s) affected.

Growth of pink mutant A95pm2 was not compromised on solid MEA and pigmentation was not medium-dependent (*Figs. 29-30*). However, during generation of temperature-optimum profiles it was observed that darker colonies appeared upon growth at lower temperatures (10-15 °C; *Fig. 31*). The phenomenon was growth-independent (i.e. also observed upon storage of plates at 4 °C), reversible (i.e. darker colonies became again pink upon incubation at 25 °C) and reproducible, indicating a stable, temperature-sensitive mutation (*Fig. 35*). As for pink mutant A95pm1, this phenomenon is difficult to explain but could nevertheless help dissect biogenesis of black-fungal cell walls – e.g. by transcriptome analysis of A95pm2 colonies grown at 15 °C or at 25 °C to identify differentially expressed genes involved in the phenotype. Genome sequencing of mutants is not ongoing but, in the future, could help shed light on melanisation.

Based on the observations presented above, the mutants A95pm1 and A95pm2 described in this thesis should be thus considered conditional mutants. By cultivating the strains at different conditions, availability of such mutants will help investigate synthesis of melanins by black fungi and its participation in stress tolerance.

4.4 Genome analysis of black-fungal strains

Molecular biology experiments were aimed at supporting genome analyses of black-fungal strains. Main experiments involved isolation and analysis of nucleic acids, gene-expression analysis by PCR and karyotyping by pulsed-field gel electrophoresis (*3 RESULTS – PART IV*). Some of the protocols, although well established in microbiology, have rarely before been applied to black fungi.

Isolation of nucleic acids from thick-walled black fungi is an established protocol, though not standardised between laboratories, among other due to different cell-lysis methods. Ribonucleid acids were gained at satisfactory quality and quantity. Currently, the cDNA-sequencing data obtained in collaboration with Fasteris SA (see *Section 3.IV.1*) are – along with phenotype microarray results – used by the Broad Institute in the framework of the Black Yeast Sequencing Project (www.broadinstitute.org).

Small-scale RNA samples were used to verify expression of ten putative laccase genes annotated in the draft genome sequence of *K. petricola* A95 and investigate differences with the mutant strains A95pm1 and A95pm2 (*Figs. 48-50*). As nine of ten genes were constitutively expressed by all three strains, inability to oxidise ABTS by A95pm1 cannot be explained by differences in gene activity. Double band for DNA-contamination sample (PCR with primer pair 09954fw, 09954rev) was likely due to the chosen cDNA-generation protocol; an mRNA-enrichment step, e.g. with Oligo-d(T) columns, would be recommended to ensure reverse-transcription solely of spliced mRNA. In principle, the methods could be used to investigate differences between wild type and mutants in the expression of other genes as well. For quantification of mRNA, qPCR analysis of black-fungal transcripts is currently being established (Nicole Knabe, ongoing project).

Determining chromosome number can support genome sequencing e.g. for the assembly of contigs [68,79]. Currently, results on karyotyping of black fungi by pulsed-field gel electrophoresis have never been published, mostly due to the difficulty of removing melanised cell walls [158]. Protoplasting of *K. petricola* A95 cells has been previously described with a yield of ca. 60 % protoplasts [16]. An isolation step to remove intact cells was therefore required before starting electrophoresis to avoid clogging of gel. A separation step by gradient centrifugation was developed here (*Section 3.I.2*). The same method worked for *C. apollinis*, but not for the black yeast *Cryomyces antarcticus* CBS 116301 (not shown). With some limitations, karyotyping could be performed and discrete bands were observed for *K. petricola* A95, its isogenic mutants and *C. apollinis* (*Figs. 44-45*). Electrophoretic conditions were determined experimentally based on pre-set protocols and the available literature [68,112]. A balance between protoplast loads and ability to visualize bands was difficult to achieve: Smear as well as jagged running front was indicative of gel overloading; by reducing cell load, however, bands became faint. Sometimes DNA seemed to remain stuck into the wells, apparently with no correlation to protoplast loads (e.g. no DNA in well with ca. 6×10^6 PP/well in *Fig. 44*, but DNA in well with the same load in *Fig. 45A*).

For *K. petricola* A95, seven or eight discrete bands were observed for a total size of ca. 27-29 Mb, which was in good correlation with the genome size as obtained by sequencing. No differences in number and size of chromosomes were observed between wild type and pink mutants (not shown), although genomic losses in the range of several hundreds kb are not recognizable by PFGE. *Coniosporium apollinis* chromosomes are much smaller, yet the strain has more chromosomes than *K. petricola* A95, and its estimated genome size (ca. 14 Mb) did not correspond to data from the Broad Institute. A chromosomal damage upon the chosen conditions could be excluded, since a smear was not observed (*Fig. 45B*) and results were reproducible upon repeated protoplast generation and electrophoresis (not shown). This discrepancy could be explained either by an underestimation of genome size by karyotyping

or by co-migrating chromosomes. In any cases, chromosomes of *C. apollinis* were remarkably smaller than those of *K. petricola* A95, which is a further difference between these ecological and morphological indistinguishable species.

5 CONCLUSIONS AND OUTLOOK

Several black fungi were characterised in this thesis, in particular the rock inhabitant *K. petricola* A95 [56,91,156]. Recent advancements in the study of black fungi have been possible thanks to the introduction of model microorganisms like the human pathogen *E. dermatitidis* or the halotolerant *Hortaea werneckii* to investigate pathogenesis [22,44] and extremotolerance [65]. The introduction of *K. petricola* A95 as model to study rock-inhabiting black fungi was confirmed. The strain was validated as a suitable model microorganism to investigate biology of RIFs for several reasons. First, it is easily cultivated and handled in the laboratory, growing both in complex and defined media, and standardised inocula could be prepared by mechanical disruption of clumps. The fungus is relatively fast-growing, reaching stationary phase in complex liquid medium after ca. four days after incubation, which is appealing for experimental design. Typical microcolonial traits were observed by morphological and physiological analyses, e.g. melanisation, restricted meristematic growth, osmotolerance, oligotrophism and mesophily. Thus, the strain is expected to behave representatively for other rock-inhabiting members of the black-fungal group. The strain belongs in an ancient clade, together with other RIFs, from which diverse lifestyles emerged [63,64,110] and is thus attractive to investigate emergence of both symbiotic behaviour and virulence in related black fungi. Abundant presence of caroteinoids and mycosporines [56,149] make the strain further appealing to investigate influence of pigments and intracellular solutes for rock-inhabiting lifestyle. Recently, manipulation of its genome by plasmid-mediated transformation has been successful [Noack-Schönmann *et al.*, manuscript in preparation].

Results gathered here – e.g. development of a new synthetic medium, dissection of nutrient metabolism, investigation of mechanisms of oligotrophy and genome analyses – further deepened knowledge on the strain and are currently integrated into the Black Yeast Sequencing Project for the annotation of its genome. Parallel analysis of the rock-inhabiting fungus *C. apollinis*, also part of the Black Yeast Sequencing Project, allowed a direct comparison between the two strains. Isolation and description of two conditional mutants of *K. petricola* A95 affected in cell-wall biosynthesis will help investigate melanin biogenesis and its contribution to stress resistance.

5.1 Black to the future

This thesis aimed to contribute to the growing corpus of knowledge on black fungi. Due to their slow growth, the difficulty to isolate them and their low incidence as pathogens in the population, black fungi has been often overlooked in the past [31]. Their interest for microbiology has experienced a revival in the last few decades and black fungi are increasingly considered relevant in a number of basic and applied disciplines like microbial ecology, phylogenetics, medicine, biotechnology, bioremediation, material preservation and

astrobiology (e.g. [39,61,62,64,94,104,109,110,135,143,160,161]). Several black-fungal genomes have been sequenced and are currently comparatively annotated by the Broad Institute (Black Yeast Sequencing Project, www.broadinstitute.org) [22]. The Black Yeast Community[23] is blossoming and the future of black fungi is, indeed, bright [34,36,151,152].

5.2 Celebrating differences – A wealth of mutants

Availability of isogenic strains with different phenotypes is valuable to study biology of black fungi, especially whereas the microorganisms show strikingly phylogenetic and ecological variability while having undifferentiated morphology.

Apart from the conditional mutants characterised in this thesis, other yet uncharacterised, isogenic pink strains were observed and isolated (A95pm4 and A95pm5). The strain A95pm3 was partly characterized here (e.g. *Figs. 7, 46*) and seemed overall very similar to A95pm1 (not able to oxidise ABTS and affected in growth on solid media). Double mutants were observed by plating A95pm3 on complex MEA (*Fig. 52*). The three double mutants (named A95pm3A, A95pm3B and A95pm3C) were yet pink, but seemed to have restored colony size and were thus putative growth revertants. Further investigations with A95pm3 and its double-mutants might help define a link, if any, between growth defect and melanisation as observed for A95pm1. The fact that the fast-growing double mutants have same colouration as A95pm3, however, seems to rule out the presence of such a link.

Future experiments with isogenic mutants of *K. petricola* A95 will include analysis of cell wall (e.g. observation of ultrastructures by transmission electron microscopy, biochemical characterisation of cell-wall fractions) and response to stress. In this thesis, exposure to ultraviolet irradiation was chosen as paradigmatic stressor encountered by rock-inhabiting black fungi and counteracted by melanised cell walls, but no differences could be observed between wild type and mutants. Influence of cell wall as protective barrier to environmental stresses is currently investigated by exposing cell to hydrogen peroxide and monitor gene expression by qPCR (Nicole Knabe, ongoing project).

5.3 Team play – Analysis of the model subaerial biofilm

Works on the model SAB composed of *K. petricola* A95 and the cyanobacterium *N. punctiforme* ATCC 29133 will help clarify symbiotic interactions between microorganisms growing on rock and material surfaces. In this thesis, it was shown that presence of the black fungus does not interfere with Chlorophyll *a* extraction from *N. punctiforme* ATCC 29133 as a method to quantify growth of the cyanobacterium. Preliminary results indicated that co-cultivation of the strains has mutual benefit for both upon unfavourable conditions like nutrient limitation (not shown). A more detailed analysis of the model biofilm was beyond

[23] Webpage: http://www.blackyeast.org/ (retrieved on February 2014).

the goal of this thesis but, recently, the subaerial model biofilm has been validated has a suitable tool to investigate effects of microorganisms on material surfaces [92]. Mutualistic interactions of the model SAB and its effects on rock substrates are currently investigated in detail (Franz Seiffert, Ph.D. Thesis, in preparation).

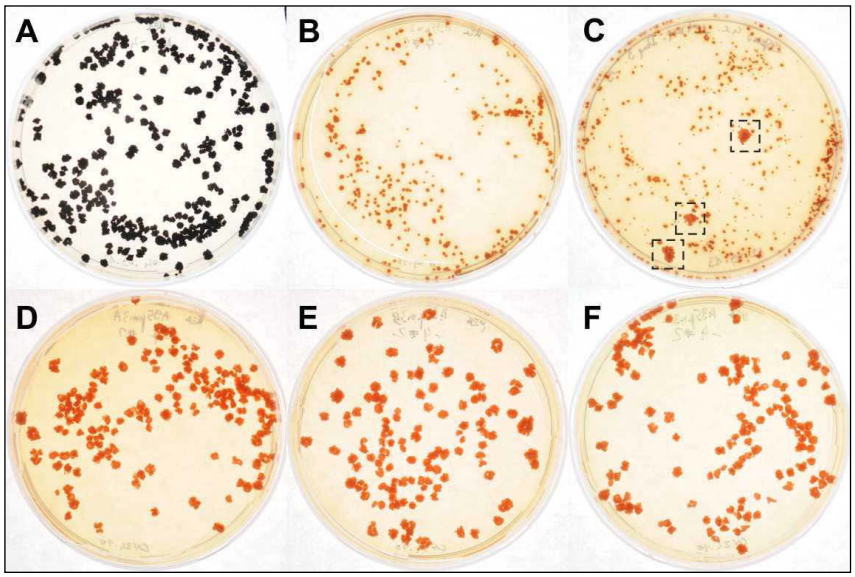

Figure 52. Isolation of pink double mutants (putative growth revertants of A95pm3)

(A-F) Growth of *K. petricola* A95 and isogenic mutants on MEA plates incubated ca. 2 w. **(A)** *Knufia petricola* A95. **(B-C)** Pink mutant A95pm3. **(D-F)** Growth reveratants of A95pm3 **(D)** A95pm3A, **(E)** A95pm3B, and **(F)** A95pm3C after isolation and plating. Dotted squares in **(C)** are the double mutants in **(D-F)**.

LITERATURE

[1] Ahmadjian V (1992). *Basic mechanism of signal exchange, recognition and regulation in lichens*. In *Algae and Symbioses: Plants, Animals, Fungi, Viruses, Interaction Explored*, Reisser W (Ed.). Biopress Limited (Bristol, England): 675-697.

[2] Amoore JE and Hautala E (1983). *Odor as an aid to chemical safety: Odor thresholds compared with threshold limit values and volatilities for 214 industrial chemicals in air and water dilution.* Journal of Applied Toxicology **3**(6): 272-90.

[3] Arun A and Eyini M (2011). *Comparative studies on lignin and polycyclic aromatic hydrocarbons degradation by basidiomycetes fungi.* Bioresource Technology **102**(17): 8063-8070.

[4] Badali H, Gueidan C, Najafzadeh MJ, Bonifaz A, van den Ende AH and de Hoog GS (2008). *Biodiversity of the genus Cladophialophora.* Studies in Mycology **61**: 175-91.

[5] Badali H, Prenafeta-Boldú FX, Guarro J, Klaassen CH, Meis JF and de Hoog GS (2011). *Cladophialophora psammophila, a novel species of Chaetothyriales with a potential use in the bioremediation of volatile aromatic hydrocarbons.* Fungal Biology **115**(10): 1019-1029.

[6] Baldrian P (2006). *Fungal laccases - occurrence and properties.* FEMS Microbiology Review **30**(2): 215-242.

[7] Battaglia E, Benoit I, Gruben BS and de Vries RP (2010). *Plant cell wall derived sugars as substrates for fungi and industry*. In *The sugar industry and cotton crops*, Jenkins PT (Ed.). Nova Science Publishers, Inc. (New York, US): 65-94.

[8] Bell AA and Wheeler MH (1986). *Biosynthesis and Functions of Fungal Melanins.* Annual Review of Phytopathology **24**: 411-451.

[9] Bochner B (2011). *Phenomics and phenotype microarrays: Applications complementing metagenomics*. In *Handbook of molecular microbial ecology I: Metagenomics and complementary approaches,*, Bruijn FJ (Ed.). John Wiley and Sons Inc. (New Jersey, US): 533-540.

[10] Bochner BR (2003). *New technologies to assess genotype-phenotype relationships.* Nature Review Genetics **4**(4): 309-14.

[11] Bochner BR (2009). *Global phenotypic characterization of bacteria.* FEMS Microbiology Review **33**(1): 191-205.

[12] Bochner BR, Gadzinski P and Panomitros E (2001). *Phenotype microarrays for high-throughput phenotypic testing and assay of gene function.* Genome Research **11**(7): 1246-55.

[13] Boekhout T, Renting M, Scheffers WA and Bosboom R (1993). *The use of karyotyping in the systematics of yeasts.* Antonie Van Leeuwenhoek **63**(2): 157-63.

[14] Bogomolova EV and Minter DW (2003). *A new microcolonial rock-inhabiting fungus from marble in Chersonesos (Crimea, Ukraine).* Mycotaxon **86**: 195-204.

[15] Brunauer G, Blaha J, Hager A, Turk R, Stocker-Worgotter E and Grube M (2007). *An isolated lichenicolous fungus forms lichenoid structures when co-cultured with various coccoid algae.* Symbiosis **44**(1-3): 127-136.

[16] Buś T (2011). *Etablierung eines geeigneten Transformationsprotokolls für Sarcinomyces petricola Stamm A95*. Bachelor Thesis. Fachhochschule Jena, Germany.

[17] Butinar L, Sonjak S, Zalar P, Plemenitas A and Gunde-Cimerman N (2005). *Melanized halophilic fungi are eukaryotic members of microbial communities in hypersaline waters of solar salterns.* Botanica Marina **48**(1): 73-79.

[18] Butler MJ and Day AW (1998). *Fungal melanins: A review.* Canadian Journal of Microbiology **44**(12): 1115-1136.

[19] Butler MJ, Gardiner RB and Day AW (2009). *Melanin synthesis by Sclerotinia sclerotiorum.* Mycologia **101**(3): 296-304.

[20] Campbell EL and Meeks JC (1989). *Characteristics of hormogonia formation by symbiotic Nostoc spp in response to the presence of Anthoceros punctatus or its extracellular products.* Applied and Environmental Microbiology **55**(1): 125-131.

[21] Cary SC, McDonald IR, Barrett JE and Cowan DA (2010). *On the rocks: The microbiology of Antarctic Dry Valley soils.* Nature Reviews Microbiology **8**(2): 129-138.

[22] Chen Z, Martinez DA, Gujja S, Sykes SM, Zeng Q, Szaniszlo PJ, Wang Z and Cuomo CA (2014). *Comparative genomic and transcriptomic analysis of Wangiella dermatitidis, a major cause of phaeohyphomycosis and a model black yeast human pathogen.* G3: Genes Genomes Genetics (Epub ahead of print, DOI 10.1534/g3.113.009241).

[23] Cohen MF and Meeks JC (1997). *A hormogonium regulating locus, hrmUA, of the cyanobacterium Nostoc punctiforme strain ATCC 29133 and its response to an extract of a symbiotic plant partner Anthoceros punctatus.* Molecular Plant-Microbe Interactions **10**(2): 280-289.

[24] Cohen MF, Wallis JG, Campbell EL and Meeks JC (1994). *Transposon mutagenesis of Nostoc sp. strain ATCC 29133, a filamentous cyanobacterium with multiple cellular differentiation alternatives.* Microbiology **140**: 3233-3240.

[25] Dadachova E, Bryan RA, Huang XC, Moadel T, Schweitzer AD, Aisen P, Nosanchuk JD and Casadevall A (2007). *Ionizing radiation changes the electronic properties of melanin and enhances the growth of melanized fungi.* PLoS One **2**(5).

[26] Dadachova E and Casadevall A (2008). *Ionizing radiation: How fungi cope, adapt, and exploit with the help of melanin.* Current Opinion in Microbiology **11**(6): 525-531.

[27] de Hoog GS (1993). *Evolution of black yeasts: Possible adaptation to the human host.* Antonie Van Leeuwenhoek **63**(2): 105-9.

[28] de Hoog GS, Gerritis van den Ende AH, Uijthof JM and Untereiner WA (1995). *Nutritional physiology of type isolates of currently accepted species of Exophiala and Phaeococcomyces.* Antonie Van Leeuwenhoek **68**(1): 43-9.

[29] de Hoog GS and Haase G (1993). *Nutritional physiology and selective isolation of Exophiala dermatitidis.* Antonie Van Leeuwenhoek **64**(1): 17-26.

[30] de Hoog GS and Rubio C (1982). *A new dematiaceous fungus from human skin.* Sabouraudia **20**(1): 15-20.

[31] de Hoog GS, Vicente VA and Gorbushina AA (2013). *The bright future of darkness - The rising power of black fungi: Black yeasts, microcolonial fungi, and their relatives.* Mycopathologia **175**(5-6): 365-368.

[32] de Hoog GS, Zeng JS, Harrak MJ and Sutton DA (2006). *Exophiala xenobiotica sp. nov., an opportunistic black yeast inhabiting environments rich in hydrocarbons.* Antonie Van Leeuwenhoek **90**(3): 257-68.

[33] de Hoog SG (1999). *Atlas of clinical fungi*. In *Black yeasts and their relatives*, de Hoog SG, et al. eds, 3rd Edition. Centraalbureau voor Schimmelcultures (Utrecht, The Netherlands): 374-380.

[34] de Hoog SG and Grube M, eds (2008). *Black fungal extremes*. Studies in Mycology (special issues) **61**: 1-194.

[35] de Hoog SG and Hermanides-Nijhof EG (1977). *The black yeast and allied hyphomycetes.* Studies in Mycology **15**: 1-222.

[36] de Hoog SG, Vicente VA and Gorbushina AA, eds (2013). *The bright future of darkness - The rising power of black fungi*. Mycopathologia (special issue) **175**: 365-457.

[37] de Leo F, Urzi C and de Hoog GS (2003). *A new meristematic fungus, Pseudotaeniolina globosa.* Antonie Van Leeuwenhoek **83**(4): 351-60.

[38] dela Cruz TE, Schulz BE, Kubicek CP and Druzhinina IS (2006). *Carbon source utilization by the marine Dendryphiella species D. arenaria and D. salina.* FEMS Microbiology Ecology **58**(3): 343-53.

[39] Deng S, van den Ende AH, Ram AF, Arentshorst M, Graser Y, Hu H and de Hoog GS (2008). *Evolution of CDC42, a putative virulence factor triggering meristematic growth in black yeasts.* Studies in Mycology **61**: 121-9.

[40] Diakumaku E, Gorbushina AA, Krumbein WE, Panina L and Soukharjevski S (1995). *Black fungi in marble and limestones - An aesthetical, chemical and physical problem for the conservation of monuments.* Science of the Total Environment **167**: 295-304.

[41] Druzhinina IS, Schmoll M, Seiboth B and Kubicek CP (2006). *Global carbon utilization profiles of wild-type, mutant, and transformant strains of Hypocrea jecorina.* Appl Environ Microbiol **72**(3): 2126-2133.

[42] Edens WA, Goins TQ, Dooley D and Henson JM (1999). *Purification and characterization of a secreted laccase of Gaeumannomyces graminis var. tritici.* Applied and Environmental Microbiology **65**(7): 3071-3074.

[43] Egidi E, de Hoog SG, Isola D, Onofri S, Quaedvlieg W, de Vries M, Verkley GJM, Stielow JB, Zucconi L and Selbmann L (2014). *Phylogeny and taxonomy of meristematic rock-*

inhabiting black fungi in the dothidemycetes based on multi-locus phylogenies. Fungal Diversity (Epub ahead of print, DOI 10.1007/s13225-013-0277-y).

[44] Feng B, Wang X, Hauser M, Kaufmann S, Jentsch S, Haase G, Becker JM and Szaniszlo PJ (2001). *Molecular cloning and characterization of WdPKS1, a gene involved in dihydroxynaphthalene melanin biosynthesis and virulence in Wangiella (Exophiala) dermatitidis.* Infection and Immunity **69**(3): 1781-94.

[45] Flipphi M, van de Vondervoort PJ, Ruijter GJ, Visser J, Arst HN, Jr. and Felenbok B (2003). *Onset of carbon catabolite repression in Aspergillus nidulans. Parallel involvement of hexokinase and glucokinase in sugar signaling.* Journal of Biological Chemistry **278**(14): 11849-57.

[46] Friedl MA, Kubicek CP and Druzhinina IS (2008). *Carbon source dependence and photostimulation of conidiation in Hypocrea atrovifidis.* Appl Environ Microbiol **74**(1): 245-250.

[47] Friedmann EI (1982). *Endolithic microorganisms in the antarctic cold desert.* Science **215**(4536): 1045-53.

[48] Gerrits PO (1985). *Verfahren zur Färbung von Gewebe, das in 2-Hydroxyethyl-Methacrylat eingebettet wird.* Heraeus Kulzer GmbH, Werheim, Deutschland.

[49] Gerrits PO and Smid L (1983). *A new, less toxic polymerization system for the embedding of soft-tissues in glycol methacrylate and subsequent preparing of serial sections.* Journal of Microscopy **132**(Oct): 81-85.

[50] Gimeno CJ, Ljungdahl PO, Styles CA and Fink GR (1992). *Unipolar cell divisions in the yeast S. cerevisiae lead to filamentous growth: regulation by starvation and RAS.* Cell **68**(6): 1077-90.

[51] Gorbushina AA (2003). *Microcolonial fungi: Survival potential of terrestrial vegetative structures.* Astrobiology **3**(3): 543-54.

[52] Gorbushina AA (2007). *Life on the rocks.* Environmental Microbiology **9**(7): 1613-31.

[53] Gorbushina AA, Beck A and Schulte A (2005). *Microcolonial rock inhabiting fungi and lichen photobionts: Evidence for mutualistic interactions.* Mycological Research **109**(11): 1288-96.

[54] Gorbushina AA and Broughton WJ (2009). *Microbiology of the atmosphere-rock interface: How biological interactions and physical stresses modulate a sophisticated microbial ecosystem.* Annual Review of Microbiology **63**: 431-50.

[55] Gorbushina AA, Kort R, Schulte A, Lazarus D, Schnetger B, Brumsack HJ, Broughton WJ and Favet J (2007). *Life in Darwin's dust: Intercontinental transport and survival of microbes in the nineteenth century.* Environmental Microbiology **9**(12): 2911-2922.

[56] Gorbushina AA, Kotlova ER and Sherstneva OA (2008). *Cellular responses of microcolonial rock fungi to long-term desiccation and subsequent rehydration.* Studies in Mycology **61**: 91-7.

[57] Gorbushina AA, Krumbein WE, Hamman CH, Panina L, Soukharjevski S and Wollenzien U (1993). *Role of black fungi in color-change and biodeterioration of antique marbles.* Geomicrobiology Journal **11**(3-4): 205-221.

[58] Gorbushina AA, Krumbein WE and Volkmann M (2002). *Rock surfaces as life indicators: New ways to demonstrate life and traces of former life.* Astrobiology **2**(2): 203-213.

[59] Gorbushina AA, Whitehead K, Dornieden T, Niesse A, Schulte A and Hedges JI (2003). *Black fungal colonies as units of survival: Hyphal mycosporines synthesized by rock-dwelling microcolonial fungi.* Canadian Journal of Botany **81**(2): 131-138.

[60] Gostincar C, Grube M, de Hoog S, Zalar P and Gunde-Cimerman N (2010). *Extremotolerance in fungi: Evolution on the edge.* FEMS Microbiology Ecology **71**(1): 2-11.

[61] Gostincar C, Gunde-Cimerman N and Turk M (2012). *Genetic resources of extremotolerant fungi: A method for identification of genes conferring stress tolerance.* Bioresource Technology **111**: 360-367.

[62] Gostincar C, Muggia L and Grube M (2012). *Polyextremotolerant black fungi: Oligotrophism, adaptive potential, and a link to lichen symbioses.* Frontiers in Microbiology **3**: 390.

[63] Gueidan C, Ruibal C, De Hoog GS and Schneider H (2011). *Rock-inhabiting fungi originated during periods of dry climate in the late Devonian and middle Triassic.* Fungal Biology **115**(10): 987-996.

[64] Gueidan C, Villasenor CR, de Hoog GS, Gorbushina AA, Untereiner WA and Lutzoni F (2008). *A rock-inhabiting ancestor for mutualistic and pathogen-rich fungal lineages.* Studies in Mycology **61**: 111-9.

[65] Gunde-Cimerman N, Ramos J and Plemenitas A (2009). *Halotolerant and halophilic fungi.* Mycological Research **113**(Pt 11): 1231-41.

[66] Harutyunyan S, Muggia L and Grube M (2008). *Black fungi in lichens from seasonally arid habitats.* Studies in Mycology **61**: 83-90.

[67] Henssen A (1987). *Lichenotelia, a genus of microfungi on rocks*. In *Progress and problems in lichenology in the Eighties*, Peveling E (Ed.). Lichenologia No. 25. J. Cramer (Berlin-Stuttgart, Germany): 257-293.

[68] Herschleb J, Ananiev G and Schwartz DC (2007). *Pulsed-field gel electrophoresis.* Nature Protocols **2**(3): 677-684.

[69] Holker U, Bend J, Pracht R, Tetsch L, Muller T, Hofer M and de Hoog GS (2004). *Hortaea acidophila, a new acid-tolerant black yeast from lignite.* Antonie Van Leeuwenhoek **86**(4): 287-94.

[70] Hondmann DH and Visser J (1994). *Carbon metabolism.* Progress in Industrial Microbiology **29**: 61-139.

[71] Isola D, Marzban G, Selbmann L, Onofri S, Laimer M and Sterflinger K (2011). *Sample preparation and 2-DE procedure for protein expression profiling of black microcolonial fungi.* Fungal Biol **115**(10): 971-7.

[72] Isola D, Selbmann L, de Hoog GS, Fenice M, Onofri S, Prenafeta-Boldu FX and Zucconi L (2013). *Isolation and screening of black fungi as degraders of volatile aromatic hydrocarbons.* Mycopathologia **175**(5-6): 369-379.

[73] Kogej T, Gostincar C, Volkmann M, Gorbushina AA and Gunde-Cimerman N (2006). *Mycosporines in extremophilic fungi - Novel complementary osmolytes?* Environmental Chemistry **3**(2): 105-110.

[74] Kogej T, Stein M, Volkmann M, Gorbushina AA, Galinski EA and Gunde-Cimerman N (2007). *Osmotic adaptation of the halophilic fungus Hortaea werneckii: Role of osmolytes and melanization.* Microbiology **153**(12): 4261-73.

[75] Kogej T, Wheeler MH, Lanisnik Rizner T and Gunde-Cimerman N (2004). *Evidence for 1,8-dihydroxynaphthalene melanin in three halophilic black yeasts grown under saline and non-saline conditions.* FEMS Microbiology Letters **232**(2): 203-9.

[76] Krumbein WE and Jens K (1981). *Biogenic rock varnishes of the Negev Desert (Israel): An ecological study of iron and manganese transformation by cyanobacteria and fungi.* Oecologia **50**(1): 25-38.

[77] Langfelder K, Streibel M, Jahn B, Haase G and Brakhage AA (2003). *Biosynthesis of fungal melanins and their importance for human pathogenic fungi.* Fungal Genetics and Biology **38**(2): 143-58.

[78] Larena I, Salazar O, Gonzalez V, Julian MC and Rubio V (1999). *Design of a primer for ribosomal DNA internal transcribed spacer with enhanced specificity for ascomycetes.* Journal of Biotechnology **75**(2-3): 187-194.

[79] MacLean D, Jones JD and Studholme DJ (2009). *Application of 'next-generation' sequencing technologies to microbial genetics.* Nature Reviews Microbiology **7**(4): 287-96.

[80] Madigan MT and Matinko JM (2006). *Brock - Biology of microorgamisms.* 11th Edition. Pearson Prentice Hall (New Jersey, US).

[81] Matos T, de Hoog GS, de Boer AG, de Crom I and Haase G (2002). *High prevalence of the neurotrope Exophiala dermatitidis and related oligotrophic black yeasts in sauna facilities.* Mycoses **45**(9-10): 373-7.

[82] Matos T, Haase G, Gerrits van den Ende AH and de Hoog GS (2003). *Molecular diversity of oligotrophic and neurotropic members of the black yeast genus Exophiala, with accent on E. dermatitidis.* Antonie Van Leeuwenhoek **83**(4): 293-303.

[83] Matsumoto T, Padhye AA and Ajello L (1987). *Medical significance of the so-called black yeasts.* European Journal of Epidemiology **3**(2): 87-95.

[84] Matsumoto T, Padhye AA, Ajello L and McGinnis MR (1986). *Sarcinomyces phaeomuriformis: A new dematiaceous hyphomycete.* Journal of Medical and Veterinary Mycology **24**(5): 395-400.

[85] Meeks JC (1998). *Symbiosis between nitrogen-fixing cyanobacteria and plants - The establishment of symbiosis causes dramatic morphological and physiological changes in the cyanobacterium.* BioScience **48**(4): 266-276.

[86] Meeks JC, Campbell EL, Summers ML and Wong FC (2002). *Cellular differentiation in the cyanobacterium Nostoc punctiforme.* Archives of Microbiology **178**(6): 395-403.

[87] Meeks JC and Castenho.Rw (1971). *Growth and photosynthesis in an extreme thermophile, Synechococcus lividus (Cyanophyta).* Archives of Microbiology **78**(1): 25-&.

[88] Milstein OA, Vered Y, Sharma A, Gressel J and Flowers HM (1983). *Fungal biodegradation and biotransformation of soluble lignocarbohydrate complexes from straw.* Applied and Environonmental Microbiology **46**(1): 55-61.

[89] Muggia L, Gueidan C, Knudsen K, Perlmutter G and Grube M (2013). *The lichen connections of black fungi.* Mycopathologia **175**(5-6): 523-535.

[90] Mulisch M and Welsch U (2010). *Romeis - Mikroskopische Technik.* XII. Auflage. Springer Verlag (Berlin, Deutschland).

[91] Nai C, Wong HY, Pannenbecker A, Broughton WJ, Benoit I, de Vries RP, Gueidan C and Gorbushina AA (2013). *Nutritional physiology of a rock-inhabiting, model microcolonial fungus from an ancestral lineage of the Chaetothyriales (Ascomycetes).* Fungal Genetics and Biology **56**: 54-66.

[92] Noack-Schönmann S, Spagin O, Grunder KP, Breithaupt M, Gunter A, Muschik B and Gorbushina AA (2014). *Sub-aerial biofilms as blockers of solar radiation: Spectral properties as tools to characterise material-relevant microbial growth.* International Biodeterioration & Biodegradation **86**: 286-293.

[93] Omsland A, Cockrell DC, Howe D, Fischer ER, Virtaneva K, Sturdevant DE, Porcella SF and Heinzen RA (2009). *Host cell-free growth of the Q fever bacterium Coxiella burnetii.* Proceedings of the National Academy of Sciences **106**(11): 4430-4.

[94] Onofri S, Barreca D, Selbmann L, Isola D, Rabbow E, Horneck G, de Vera JP, Hatton J and Zucconi L (2008). *Resistance of Antarctic black fungi and cryptoendolithic communities to simulated space and Martian conditions.* Studies in Mycology **61**: 99-109.

[95] Onofri S, Selbmann L, de Hoog GS, Grube M, Barreca D, Ruisi S and Zucconi L (2007). *Evolution and adaptation of fungi at boundaries of life.* Advances in Space Research **40**(11): 1657-1664.

[96] Palmer FE, Emery DR, Stemmler J and Staley JT (1987). *Survival and growth of microcolonial rock fungi as affected by temperature and humidity.* New Phytologist **107**(1): 155-162.

[97] Palmer FE, Staley JT and Ryan B (1990). *Ecophysiology of microcolonial fungi and lichens on rocks in Northeastern Oregon.* New Phytologist **116**(4): 613-620.

[98] Patel D, Ford TC and Rickwood D (1998). *Fractionation of cells by sedimentation methods*. In *Cell separation - A practical approach*, Fisher D, Francis GE and Rickwood D eds. Oxford University Press (Oxford, UK).

[99] Plemenitas A, Vaupotic T, Lenassi M, Kogej T and Gunde-Cimerman N (2008). *Adaptation of extremely halotolerant black yeast Hortaea werneckii to increased osmolarity: A molecular perspective at a glance.* Studies in Mycology **61**: 67-75.

[100] Prenafeta-Boldú FX, Ballerstedt H, Gerritse J and Grotenhuis JTC (2004). *Bioremediation of BTEX hydrocarbons: Effect of soil inoculation with the toluene-growing fungus Cladophialophora sp strain T1.* Biodegradation **15**(1): 59-65.

[101] Prenafeta-Boldú FX, Guivernau M, Gallastegui G, Vinas M, de Hoog GS and Elias A (2012). *Fungal/bacterial interactions during the biodegradation of TEX hydrocarbons (toluene, ethylbenzene and p-xylene) in gas biofilters operated under xerophilic conditions.* FEMS Microbiology Ecology **80**(3): 722-734.

[102] Prenafeta-Boldú FX, Illa J, van Groenestijn JW and Flotats X (2008). *Influence of synthetic packing materials on the gas dispersion and biodegradation kinetics in fungal air biofilters.* Applied Microbiology and Biotechnology **79**(2): 319-327.

[103] Prenafeta-Boldú FX, Kuhn A, Luykx DMAM, Anke H, van Groenestijn JW and de Bont JAM (2001). *Isolation and characterisation of fungi growing on volatile aromatic hydrocarbons as their sole carbon and energy source.* Mycological Research **105**: 477-484.

[104] Prenafeta-Boldú FX, Summerbell R and Sybren de Hoog G (2006). *Fungi growing on aromatic hydrocarbons: biotechnology's unexpected encounter with biohazard?* FEMS Microbiology Review **30**(1): 109-30.

[105] Prenafeta-Boldú FX, Vervoort J, Grotenhuis JTC and van Groenestijn JW (2002). *Substrate interactions during the biodegradation of benzene, toluene, ethylbenzene, and xylene (BTEX) hydrocarbons by the fungus Cladophialophora sp strain T1.* Applied Environmental Microbiology **68**(6): 2660-2665.

[106] Reeslev M and Kjoller A (1995). *Comparison of biomass dry weights and radial growth-rates of fungal colonies on media solidified with different gelling compounds.* Applied and Environmental Microbiology **61**(12): 4236-4239.

[107] Rehfuss M and Urban J (2005). *Rhodococcus phenolicus sp nov., a novel bioprocessor isolated actinomycete with the ability to degrade chlorobenzene, dichlorobenzene and phenol as sole carbon sources.* Systemic and Applied Microbiology **28**(8): 695-701.

[108] Rice AV and Currah RS (2005). *Profiles from Biolog FF plates and morphological characteristics support the recognition of Oidiodendron fimicola sp nov.* Studies in Mycology (53): 75-82.

[109] Robertson KL, Mostaghim A, Cuomo CA, Soto CM, Lebedev N, Bailey RF and Wang Z (2012). *Adaptation of the black yeast Wangiella dermatitidis to ionizing radiation: Molecular and cellular mechanisms.* PLoS One **7**(11).

[110] Ruibal C, Gueidan C, Selbmann L, Gorbushina AA, Crous PW, Groenewald JZ, Muggia L, Grube M, Isola D, Schoch CL, Staley JT, Lutzoni F and de Hoog GS (2009). *Phylogeny of rock-inhabiting fungi related to Dothideomycetes.* Studies in Mycology **64**: 123-133S7.

[111] Ruibal C, Platas G and Bills GF (2008). *High diversity and morphological convergence among melanised fungi from rock formations in the Central Mountain System of Spain.* Persoonia **21**: 93-110.

[112] Sambrook J and Russell DW (2001). *Molecular cloning - A laboratory manual*. Vol. 1-3, 3rd Edition. Cold Spring Harbor Laboratory Press (Cold Spring Harbor, New York).

[113] Sanchez C (2009). *Lignocellulosic residues: Biodegradation and bioconversion by fungi.* Biotechnology Advances **27**(2): 185-94.

[114] Satow MM, Attili-Angelis D, de Hoog GS, Angelis DF and Vicente VA (2008). *Selective factors involved in oil flotation isolation of black yeasts from the environment.* Studies in Mycology **61**: 157-63.

[115] Schnitzler N, Peltroche-Llacsahuanga H, Bestier N, Zundorf J, Lutticken R and Haase G (1999). *Effect of melanin and carotenoids of Exophiala (Wangiella) dermatitidis on phagocytosis, oxidative burst, and killing by human neutrophils.* Infection and Immunity **67**(1): 94-101.

[116] Schoch CL, Crous PW, Groenewald JZ, Boehm EWA, Burgess TI, de Gruyter J, de Hoog GS, Dixon LJ, Grube M, Gueidan C, Harada Y, Hatakeyama S, Hirayama K, Hosoya T, Huhndorf SM, Hyde KD, Jones EBG, Kohlmeyer J, Kruys A, Li YM, Lucking R, Lumbsch HT, Marvanova L, Mbatchou JS, Mcvay AH, Miller AN, Mugambi GK, Muggia L, Nelsen MP, Nelson P, Owensby CA, Phillips AJL, Phongpaichit S, Pointing SB, Pujade-Renaud V, Raja HA, Plata ER, Robbertse B, Ruibal C, Sakayaroj J, Sano T, Selbmann L, Shearer CA, Shirouzu T, Slippers B, Suetrong S, Tanaka K, Volkmann-Kohlmeyer B, Wingfield MJ, Wood AR, Woudenberg JHC, Yonezawa H, Zhang Y and Spatafora JW (2009). *A class-wide phylogenetic assessment of Dothideomycetes.* Studies in Mycology **64**: 1-15.

[117] Schwartz DC and Cantor CR (1984). *Separation of yeast chromosome-sized DNAs by pulsed field gradient gel electrophoresis.* Cell **37**(1): 67-75.

[118] Selbmann L, de Hoog GS, Mazzaglia A, Friedmann EI and Onofri S (2005). *Fungi at the edge of life: Cryptoendolithic black fungi from Antarctic desert.* Studies in Mycology **51**: 1-32.

[119] Selbmann L, de Hoog GS, Zucconi L, Isola D, Ruisi S, van den Ende AH, Ruibal C, De Leo F, Urzi C and Onofri S (2008). *Drought meets acid: Three new genera in a dothidealean clade of extremotolerant fungi.* Studies in Mycology **61**: 1-20.

[120] Selbmann L, de Hoog SG, Sterflinger K, Isola D, van der Ende BG, Gueidan C, Ruibal C and Onofri S (2010). *Millions of years without sex and still happy*. In *Emerging pontetial of black yeasts*. Conference of the Working Group Black Yeasts. Ljubljana, Slovenia.

[121] Sert HB, Sumbul H and Sterflinger K (2007). *Sarcinomyces sideticae, a new black yeast from historical marble monuments in Side (Antalya, Turkey).* Botanical Journal of the Linnean Society **154**(3): 373-380.

[122] Seyedmousavi S, Badali H, Chlebicki A, Zhao JJ, Prenafeta-Boldu FX and De Hoog GS (2011). *Exophiala sideris, a novel black yeast isolated from environments polluted with toxic alkyl benzenes and arsenic.* Fungal Biology **115**(10): 1030-1037.

[123] Staley JT, Palmer F and Adams JB (1982). *Microcolonial fungi: Common inhabitants on desert rocks?* Science **215**(4536): 1093-5.

[124] Sterflinger K (1998). *Temperature and NaCl-tolerance of rock-inhabiting meristematic fungi.* Antonie Van Leeuwenhoek **74**(4): 271-281.

[125] Sterflinger K (2000). *Fungi as geologic agents.* Geomicrobiology Journal **17**(2): 97-124.

[126] Sterflinger K (2006). *Black yeasts and meristematic fungi: Ecology, diversity and identification*. In *Biodiversity and ecophysiology of yeasts*, Rosa CA and Peter G eds. Springer (Berlin, Germany): 501-514.

[127] Sterflinger K (2010). *Fungi: Their role in deterioration of cultural heritage.* Fungal Biology Review **24**: 47-55.

[128] Sterflinger K, de Baere R, de Hoog GS, de Wachter R, Krumbein WE and Haase G (1997). *Coniosporium perforans and C. apollinis, two new rock-inhabiting fungi isolated from marble in the Sanctuary of Delos (Cyclades, Greece).* Antonie Van Leeuwenhoek **72**(4): 349-63.

[129] Sterflinger K, de Hoog GS and Haase G (1999). *Phylogeny and ecology of meristematic ascomycetes.* Studies in Mycology (43): 5-22.

[130] Sterflinger K and Krumbein WE (1995). *Multiple stress factors affecting growth of rock-inhabiting black fungi.* Botanica Acta **108**(6): 490-496.

[131] Sterflinger K and Krumbein WE (1997). *Dematiaceous fungi as a major agent for biopitting on Mediterranean marbles and limestones.* Geomicrobiology Journal **14**(3): 219-230.

[132] Sterflinger K and Prillinger H (2001). *Molecular taxonomy and biodiversity of rock fungal communities in an urban environment (Vienna, Austria).* Antonie Van Leeuwenhoek **80**(3-4): 275-86.

[133] Sudhadham M, Prakitsin S, Sivichai S, Chaiyarat R, Dorrestein GM, Menken SB and de Hoog GS (2008). *The neurotropic black yeast Exophiala dermatitidis has a possible origin in the tropical rain forest.* Studies in Mycology **61**: 145-55.

[134] Tanzer MM, Arst HN, Skalchunes AR, Coffin M, Darveaux BA, Heiniger RW and Shuster JR (2003). *Global nutritional profiling for mutant and chemical mode-of-action analysis in filamentous fungi.* Functional and Integrative Genomics **3**(4): 160-70.

[135] Tesei D, Marzban G, Zakharova K, Isola D, Selbmann L and Sterflinger K (2012). *Alteration of protein patterns in black rock inhabiting fungi as a response to different temperatures.* Fungal Biology **116**(8): 932-40.

[136] Tetsch L (2005). *Laccasen und Laccasegene des acidophilen Ascomyceten Hortaea acidophila*. Ph.D. Thesis. Rheinischen Friedrich-Wilhelms-Universität Bonn, Deutschland.

[137] Tetsch L, Bend J and Holker U (2006). *Molecular and enzymatic characterisation of extra- and intracellular laccases from the acidophilic ascomycete Hortaea acidophila.* Antonie Van Leeuwenhoek **90**(2): 183-94.

[138] Thurston CF (1994). *The Structure and function of fungal laccases.* Microbiology **140**: 19-26.

[139] Tsuneda A, Hambleton S and Currah RS (2011). *The anamorph genus Knufia and its phylogenetically allied species in Coniosporium, Sarcinomyces, and Phaeococcomyces.* Botany **89**(12): 523-536.

[140] Untereiner WA, van den Ende AHGG and de Hoog GS (1999). *Nutritional physiology of species of Capronia.* Studies in Mycology (43): 98-106.

[141] Valaskova V and Baldrian P (2006). *Estimation of bound and free fractions of lignocellulose-degrading enzymes of wood-rotting fungi Pleurotus ostreatus, Trametes versicolor and Piptoporus betulinus.* Research in Microbiology **157**(2): 119-24.

[142] van der Walt JP and Yarrow D (1984). *Methods for the isolation, maintenance, classification and identification of yeasts*. In *The yeasts: A taxonomic study*, Kreger-Van Rij NJW (Ed.). Elsevier Science Publishers (Amsterdam, The Netherlands): 45-104.

[143] Vaupotic T, Gunde-Cimerman N and Plemenitas A (2007). *Novel 3'-phosphoadenosine-5'-phosphatases from extremely halotolerant Hortaea werneckii reveal insight into molecular determinants of salt tolerance of black yeasts.* Fungal Genetics and Biology **44**(11): 1109-1122.

[144] Vaupotic T, Veranic P, Jenoe P and Plemenitas A (2008). *Mitochondrial mediation of environmental osmolytes discrimination during osmoadaptation in the extremely halotolerant black yeast Hortaea werneckii.* Fungal Genetics and Biology **45**(6): 994-1007.

[145] Vicente VA, Attili-Angelis D, Pie MR, Queiroz-Telles F, Cruz LM, Najafzadeh MJ, de Hoog GS, Zhao J and Pizzirani-Kleiner A (2008). *Environmental isolation of black yeast-like fungi involved in human infection.* Stud Mycol **61**: 137-44.

[146] Vinck A, Terlou M, Pestman WR, Martens EP, Ram AF, van den Hondel CA and Wosten HA (2005). *Hyphal differentiation in the exploring mycelium of Aspergillus niger.* Molecular Microbiology **58**(3): 693-9.

[147] Voglmayr H, Mayer V, Maschwitz U, Moog J, Djieto-Lordon C and Blatrix R (2011). *The diversity of ant-associated black yeasts: Insights into a newly discovered world of symbiotic interactions.* Fungal Biology **115**(10): 1077-1091.

[148] Volkmann M (2004). *Analyse und Charakterisierung von Mycosporinen aus gesteinsbesiedelnden mikrokolonialen Pilzen*. Ph.D. Thesis. Carl von Ossietzky Universität Oldenburg, Deutschland.

[149] Volkmann M and Gorbushina AA (2006). *A broadly applicable method for extraction and characterization of mycosporines and mycosporine-like amino acids of terrestrial, marine and freshwater origin.* FEMS Microbiology Letters **255**(2): 286-95.

[150] Volkmann M, Whitehead K, Rutters H, Rullkotter J and Gorbushina AA (2003). *Mycosporine-glutamicol-glucoside: A natural UV-absorbing secondary metabolite of rock-inhabiting microcolonial fungi.* Rapid Communicatoins in Mass Spectrometry **17**(9): 897-902.

[151] VV.AA. (2011). *Hidden danger, bright promise*. Conference of the Working Group Black Yeast. Curitiba, Brazil.

[152] VV.AA. (2013). *The black fungi around us - Harm and benefit*. Conference of the Working Group Black Yeast. Guangzhou, China.

[153] Warscheid T and Braams J (2000). *Biodeterioration of stone: A review.* International Biodeterioration & Biodegradation **46**(4): 343-368.

[154] White TJ, Bruns T, Lee SC and Taylor J (1990). *Amplification and direct sequencing of fungal ribosomal RNA genes for phylogenetics*. In *PCR protocols: A guide to methods and applications*, Innis MA, et al. eds. Academic Press Inc. (California, US): 315-322.

[155] Witteveen CFB, Busink R, Vandevondervoort P, Dijkema C, Swart K and Visser J (1989). *L-Arabinose and D-xylose catabolism in Aspergillus niger.* Journal of General Microbiology **135**: 2163-2171.

[156] Wollenzien U, de Hoog GS, Krumbein W and Uijthof JM (1997). *Sarcinomyces petricola, a new microcolonial fungus from marble in the Mediterranean basin.* Antonie Van Leeuwenhoek **71**(3): 281-8.

[157] Wong FCY and Meeks JC (2002). *Establishment of a functional symbiosis between the cyanobacterium Nostoc punctiforme and the bryophyte Anthoceros punctatus requires genes involved in nitrogen control and initiation of heterocyst differentiation.* Microbiology **148**: 315-323.

[158] Zakharova K and Sterflinger K (2010). *Taxonomy and ecology of rock inhabiting fungi: State of the art and perspectives*. In *Emerging potential of black yeasts*. Conference of the CAREX (Summer School on Life in Extreme Environments). Pieve Tesino, Italy.

[159] Zakharova K, Tesei D, Marzban G, Dijksterhuis J, Wyatt T and Sterflinger K (2013). *Microcolonial fungi on rocks: A life in constant drought?* Mycopathologia **175**(5-6): 537-547.

[160] Zalar P, Novak M, De Hoog GS and Gunde-Cimerman N (2011). *Dishwashers - A man-made ecological niche accommodating human opportunistic fungal pathogens.* Fungal Biology **115**(10): 997-1007.

[161] Zeng JS, Sutton DA, Fothergill AW, Rinaldi MG, Harrak MJ and de Hoog GS (2007). *Spectrum of clinically relevant Exophiala species in the United States.* Journal of Clinical Microbiology **45**(11): 3713-20.

[162] Zhang JM, Wang L, Xi LY, Huang HQ, Hu YX, Li XQ, Huang X, Lu S and Sun JF (2013). *Melanin in a meristematic mutant of Fonsecaea monophora inhibits the production of nitric oxide and Th1 cytokines of murine macrophages.* Mycopathologia **175**(5-6): 515-522.

[163] Zhao J, Zeng J, de Hoog GS, Attili-Angelis D and Prenafeta-Boldu FX (2010). *Isolation and identification of black yeasts by enrichment on atmospheres of monoaromatic hydrocarbons.* Microbial Ecology **60**(1): 149-56.

APPENDIX

A.1 Detailed table of contents

A.2 List of figures

A.3 List of tables

A.4 Abbreviations and units

Abs	Absorbance or optical density [dimensionless]
ABTS	2,2'-azino-bis(3-ethylbenzothiazoline-6-sulphonic acid)
ASM	A95-Specific Medium
ATCC	American Type Culture Collection
atm	standard atmosphere
bar	unit of pressure [1 bar = 0.1 MPa]
BLAST	Basic Local Alignment Search Tool
BLASTn	BLAST with nucleotide-to-nucleotide search algorithm
BLASTp	BLAST with protein-to-protein search algorithm
bp	base pair
c	concentration [g/L or mol/L]
C	carbon
ca.	circa
CBS-KNAW	Fungal Biodersity Centre
cDNA	complementary DNA
CF	cell fragments
CFU	colony-forming unit
Chl *a*	Chlorophyll *a*
CO_2	carbon dioxide
d	day
ddH_2O	double-distilled water
DEPC	diethylpyrocarbonate
1,8-DHN	1,8-dihydroxynaphtalene
DNA	deoxyribonucleic acid
dNTP	deoxynucleoside triphosphate
dsDNA	double-stranded DNA
DSMZ	German Collection of Microorganisms and Cell Cultures
EDTA	ethylenediaminetetraacetic acid
e.g.	for example
FF-IF	inoculating fluid for filamentous fungi
Fig.	Figure
g	grams
g	gravity [1 $g \approx 9.81$ m/s^2]

g = t/n	generation time [h]
GC-FID	gas chromatography with flame ionization detector
GC-TCD	gas chromatography with thermal conductivity detector
gDNA	genomic DNA
h	hour
H_C	Henry's Law constant [atm × L/mol]
HEMA	2-hydroxyethyl methacrylate
HPLC	high-performance liquid chromatography
Hz	hertz [s^{-1}]
i.e.	*id est* (that is)
k	kilo- [× 10^3]
kb	kilobase
L	litre
m	meters or milli- [× 10^{-3}]
µ	micro- [× 10^{-6}]
M	mega- [× 10^6] or molarity [mol/L]
MEA	malt-extract agar
MEB	malt-extract broth
Mb	megabase
MCF	microcolonial fungi
min	minute
mol	mole [1 mol ≈ 6.022 × 10^{23} molecules]
mRNA	messenger RNA
n	nano- [× 10^{-9}]
n	number of generations [dimensionless]
N	nitrogen
nt	nucleotide
p	pico- [× 10^{-12}]
p-value	significance value
$p = H_C \times c$	partial pressure of solute in the gas phase [atm]
Pa	Pascal
PAS	periodic acid-Schiff
PCR	polymerase chain reaction
PFGE	pulsed-field gel electrophoresis
pH	*potentia hydrogenii* (power of hydrogen)
PM	Phenotype MicroArray
PP	protoplasts
psi	pressure per square inch [1 psi ≈ 6.89 kPa]
qPCR	quantitative PCR
Ref.	Reference
RIF	rock-inhabiting fungi
RIN	RNA integrity number
RNA	ribonucleic acid
ROFE	rotating-field gel electrophoresis
rpm	revolutions per minute
rRNA	ribosomal RNA
s	second
SAB	subaerial biofilm
SDS-PAGE	sodium dodecyl sulfate polyacrylamide gel electrophoresis

t	time [h, min or s]
T	temperature [°C]
T_{opt}	growth-temperature optimum [°C]
Tab.	Table
U	enzyme unit
UV	ultraviolet
VBNC	viable but non-culturable
VOC	volatile organic compound
vs.	versus
w	week
W	watt [J/s]
wt	wild type
°C	degree Celsius
% v/v	percent weight/volume
% w/v	percent volume/volume

A.5 Supplementary data

Below are reported supplementary figures and tables. Data are shown in the same order as mentioned in the text.

```
A95_ITS-1           ------------------------------GAGCCCGACCTCCCAACCCTTTGTCTAATT 30
A95pm1_ITS-1        ------------------------------GGAGCCCGACCTCCCAACCCTTTGTCTAATT 31
CBS600.93_ITS-1     ATCATTACCGAGTTAGGGTTTCCCCTCCAGGAGCCCGACCTCCCAACCCTTTGTCTAATT 60
                                                 ******************************

A95_ITS-1           TACCTTGTCGTTGCTTCGGCGGACCGGTTGACCAACTGGTCTTGACCGCCGGGGGGGCTT 90
A95pm1_ITS-1        TACCTTGTCGTTGCTTCGGCGGACCGGTTGACCAACTGGTCTTGACCGCCGGGGGGGCTT 91
CBS600.93_ITS-1     TACCTTGTCGTTGCTTCGGCGGACCGGTTGACCAACTGGTCTTGACCGCCGGGGGGGCTT 120
                    ************************************************************

A95_ITS-1           CCCCCCCCTGGAGAGCGTCCGCCGACGGCCCAACCACAAAACTCTTGTACCAAACCATGT 150
A95pm1_ITS-1        CCCCCCCCTGGAGAGCGTCCGCCGACGGCCCAACCACAAAACTCTTGTACCAAACCATGT 151
CBS600.93_ITS-1     CCCCCCCCTGGAGAGCGTCCGCCGACGGCCCAACCACAAAACTCTTGTACCAAACCATGT 180
                    ************************************************************

A95_ITS-1           CGTCTGAATGTACTTGATTAAGAATCAAAAAACAAAACTTTCAACAACGGATCTCTTGGT 210
A95pm1_ITS-1        CGTCTGAATGTACTTGATTAAGAATCAAAAAACAAAACTTTCAACAACGGATCTCTTGGT 211
CBS600.93_ITS-1     CGTCTGAATGTACTTGATTAAGAATCAAAAAACAAAACTTTCAACAACGGATCTCTTGGT 240
                    ************************************************************

A95_ITS-1           TCTGGCATCGATGAAGAACGCAGCGAAATGCGATAAGTAATGCGAATTGCAGAATTTCCG 270
A95pm1_ITS-1        TCTGGCATCGATGAAGAACGCAGCGAAATGCGATAAGTAATGCGAATTGCAGAATTTCCG 271
CBS600.93_ITS-1     TCTGGCATCGATGAAGAACGCAGCGAAATGCGATAAGTAATGCGAATTGCAGAATTTCCG 300
                    ************************************************************

A95_ITS-1           TGAGTCATCGAATCTTTGAACGCACATTGCGCCCACTGGTATTCCGGTGGGCATGCCTGT 330
A95pm1_ITS-1        TGAGTCATCGAATCTTTGAACGCACATTGCGCCCACTGGTATTCCGGTGGGCATGCCTGT 331
CBS600.93_ITS-1     TGAGTCATCGAATCTTTGAACGCACATTGCGCCCACTGGTATTCCGGTGGGCATGCCTGT 360
                    ************************************************************

A95_ITS-1           TCGAGCGTCATTATCCTCCCTCAAACCCCGGGTTTGGTGTTGGACCCAAGTTGTGCATCT 390
A95pm1_ITS-1        TCGAGCGTCATTATCCTCCCTCAAACCCCGGGTTTGGTGTTGGACCCAAGTTGTGCATCT 391
CBS600.93_ITS-1     TCGAGCGTCATTATCCTCCCTCAAACCCCGGGTTTGGTGTTGGACCCAAGTTGTGCATCT 420
                    ************************************************************

A95_ITS-1           GAACAACTGGTCTCAAAGACAATGACGGCGTCCGTGGGACCCTCGGTGCAACGAGCTTTC 450
A95pm1_ITS-1        GAACAACTGGTCTCAAAGACAATGACGGCGTCCGTGGGACCCTCGGTGCAACGAGCTTTC 451
CBS600.93_ITS-1     GAACAACTGGTCTCAAAGACAATGACGGCGTCCGTGGGACCCTCGGTGCAACGAGCTTTC 480
                    ************************************************************

A95_ITS-1           AGGAGCACGCGTCGAGTTTAAAGGACCTTCCGGGCCGGTCTCCTTTACATCTTTATTTAC 510
A95pm1_ITS-1        AGGAGCACGCGTCGAGTTTAAAGGACCTTCCGGGCCGGTCTCCTTTACATCTTTATTTAC 511
CBS600.93_ITS-1     AGGAGCACGCGTCGAGTTTAAAGGACCTTCCGGGCCGGTCTCCTTTACATCTTTATTTAC 540
                    ************************************************************

A95_ITS-1           AAGGTTGACCTCGGATCAGGTAGGAATACCCGCTGAACTTAAGCATATCAATAAGCGGAG 570
A95pm1_ITS-1        AAGGTTGACCTCGGATCAGGTAGGAATACCCGCTGAACTTAAGCATATCAATAAGCGGAG 571
CBS600.93_ITS-1     AAGGTTGACC---------------------------------------------------- 550
                    **********
```

Supplementary Figure 1. Multiple sequence alignment of ITS regions – ITS-1

Multiple sequence alignment of ITS regions from *Knufia petricola* A95 and pink mutant A95pm1 with those from strain CBS 600.93 (available on www.ncbi.nlm.nih.gov, [156]). Genomic sequence was amplified with primer pair ITS-1, ITS-4 and amplicon was sequenced with primer ITS-1 (*Section 3.I.3*); alignment was performed with ClustalW2 tool. Bold: primer ITS-Int binding site; Italic: primer ITS-4 binding site. Gap (red) was closed by sequencing amplicon with primer ITS-Int (*Suppl. Fig. 2*). Asterisks indicate sequence identity. Same results were obtained for all other pink mutants of *K. petricola* A95 (A95pm2-5 and A95pm3A-C; not shown).

```
A95_ITS-Int_rc          TCCGTAGGTGAACCTGCGGAAGGATCATTACCGAGTTAGGGTTTCCCCTCCAGGAGCCCG 60
A95pm1_ITS-Int_rc       TCCGTAGGTGAACCTGCGGAAGGATCATTACCGAGTTAGGGTTTCCCCTCCAGGAGCCCG 60
CBS600.93_ITS-1         ----------------------ATCATTACCGAGTTAGGGTTTCCCCTCCAGGAGCCCG 37
                                               ************************************

A95_ITS-Int_rc          ACCTCCCAACCCTTTGTCTAATTTACCTTGTCGTTGCTTCGGCGGACCGGTTGACCAACT 120
A95pm1_ITS-Int_rc       ACCTCCCAACCCTTTGTCTAATTTACCTTGTCGTTGCTTCGGCGGACCGGTTGACCAACT 120
CBS600.93_ITS-1         ACCTCCCAACCCTTTGTCTAATTTACCTTGTCGTTGCTTCGGCGGACCGGTTGACCAACT 97
                        ************************************************************

A95_ITS-Int_rc          GGTCTTGACCGCCGGGGGGGCTTCCCCCCCCTGGAGAGCGTCCGCCGACGGCCC------ 174
A95pm1_ITS-Int_rc       GGTCTTGACCGCCGGGGGGGCTTCCCCCCCCTGGAGAGCGTCCGCCG------------- 167
CBS600.93_ITS-1         GGTCTTGACCGCCGGGGGGGCTTCCCCCCCCTGGAGAGCGTCCGCCGACGGCCCAACCAC 157
                        *********************************************

A95_ITS-Int_rc          ---------------------------------------------------
A95pm1_ITS-Int_rc       ---------------------------------------------------
CBS600.93_ITS-1         AAAACTCTTGTACCAAACCATGTCGTCTGAATGTACTTGATTAAGAATCAAAA 210
```

Supplementary Figure 2. Multiple sequence alignment of ITS regions – Gap closure with ITS-Int

Multiple sequence alignment of ITS regions from *Knufia petricola* A95 and pink mutant A95pm1 with those of strain CBS 600.93 (available on www.ncbi.nlm.nih.gov, [156]). Genomic sequence was amplified with primer pair ITS-1, ITS-4 and amplicon was sequenced with primer ITS-Int to close gap in *Suppl. Fig. 1* (red); alignment with reverse-complement sequences (A95_ITS-Int_rc and A95pm1_ITS-Int_rc) was performed with ClustalW2 tool. Italic: primer ITS-1 binding site; Bold: primer ITS-Int binding site. Asterisks indicate sequence identity. Same results were obtained for all other pink mutants of *K. petricola* A95 (A95pm2-5 and A95pm3A-C; not shown).

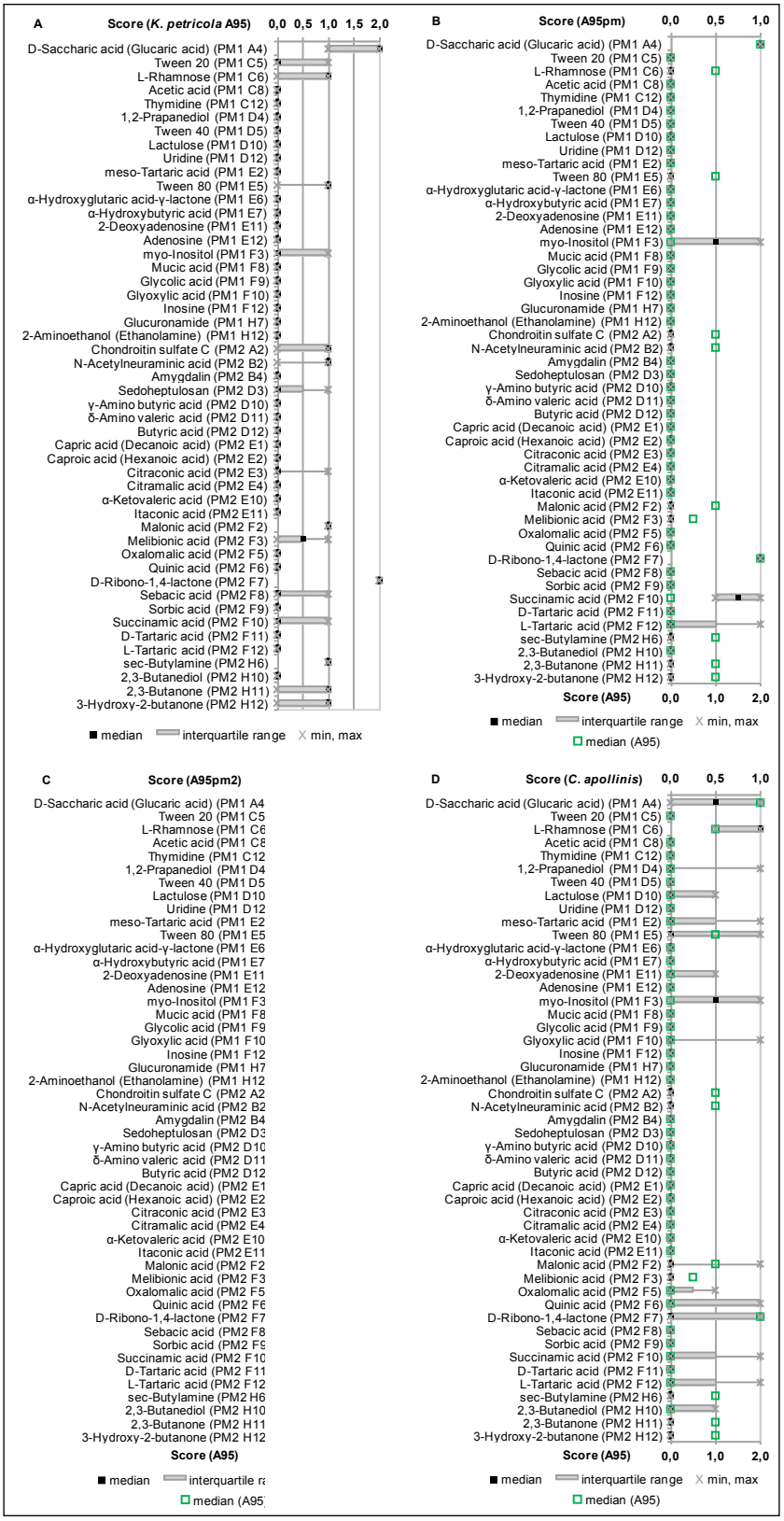

Supplementary Figure 3. Utilization of additional carbon sources by black-fungal strains (Biolog's plates PM1-2)

(A-D) Utilisation of carbon sources not reported previously (i.e. not grouped into major fungal metabolic pathways) by **(A)** *K. petricola* A95; **(B)** pink mutant A95pm1; **(C)** pink mutant A95pm2; and **(D)** *C. apollinis*. Results are shown as in the corresponding figure captions (*Figs. 12, 17-18, 22* in *Section 3.II.3*).

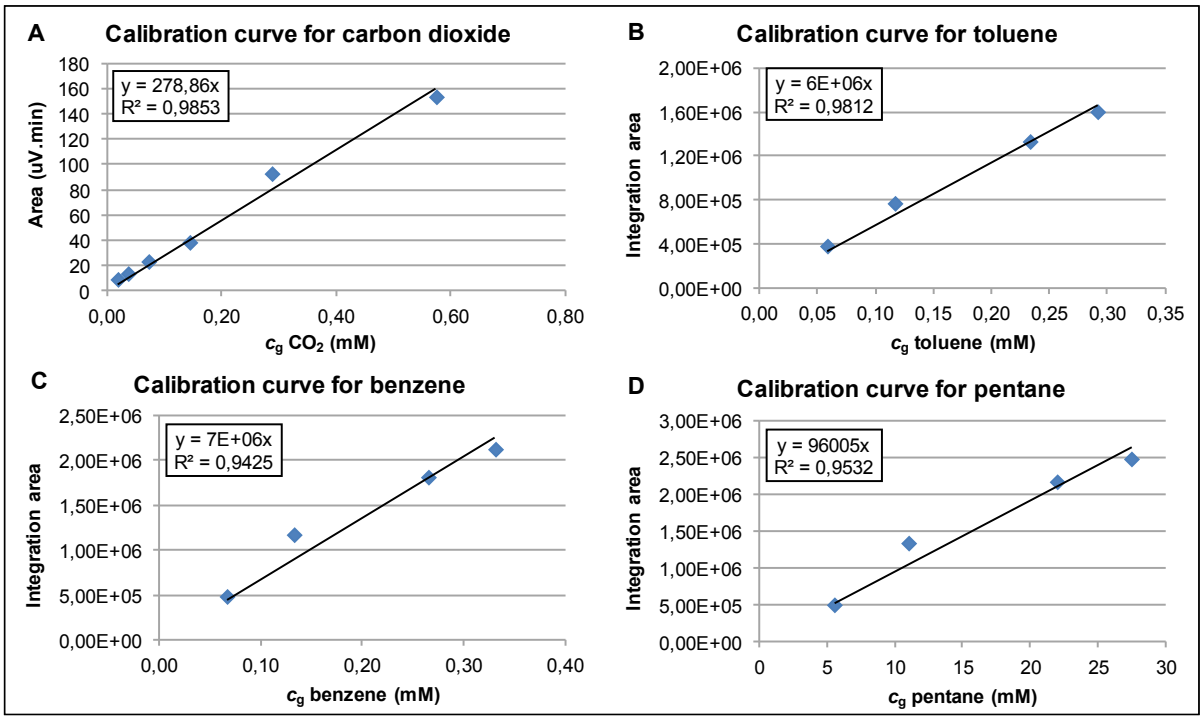

Supplementary Figure 4. Calibration curves for hydrocarbon-utilisation assay

(A-D) Gas-chromatographic calibration curves for **(A)** carbon dioxide (CO_2), **(B)** toluene, **(C)** benzene and **(D)** pentane. Curves were generated by gas chromatography (GC-TCD for CO_2, GC-FID for volatile organic compounds). Linear regressions were calculated by forcing intercept to zero (MS Excel). Data were used to extrapolate results presented in *Section 3.II.4*.

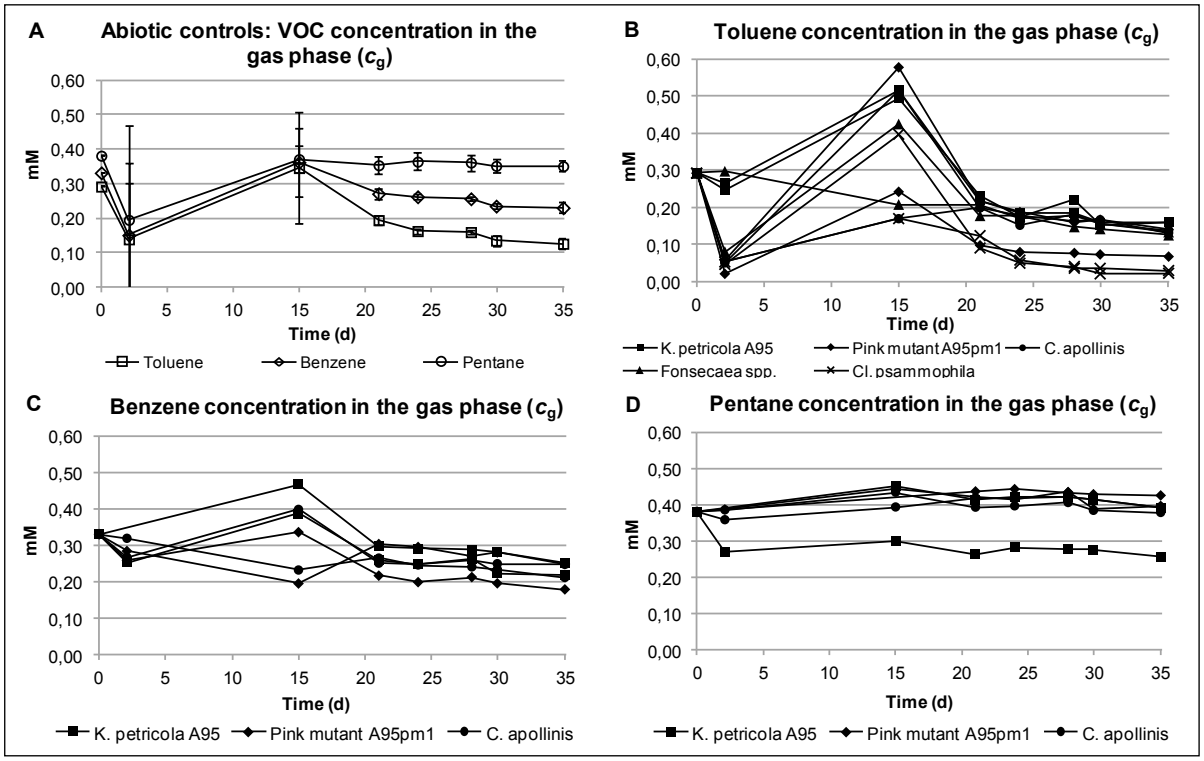

Supplementary Figure 5. Concentration of VOCs in hydrocarbon-utilisation assay

(A-D) Gas-phase concentration of volatile organic compounds (VOCs) over growth (35 d) in **(A)** abiotic control flasks (without fungi) and flasks with **(B)** toluene, **(C)** benzene and **(D)** pentane either with (solid lines) or without glucose (dashed lines). In **(A-C)**, strong fluctuations in first measurements (until 15 d) were due to experimental problems and should not be considered.

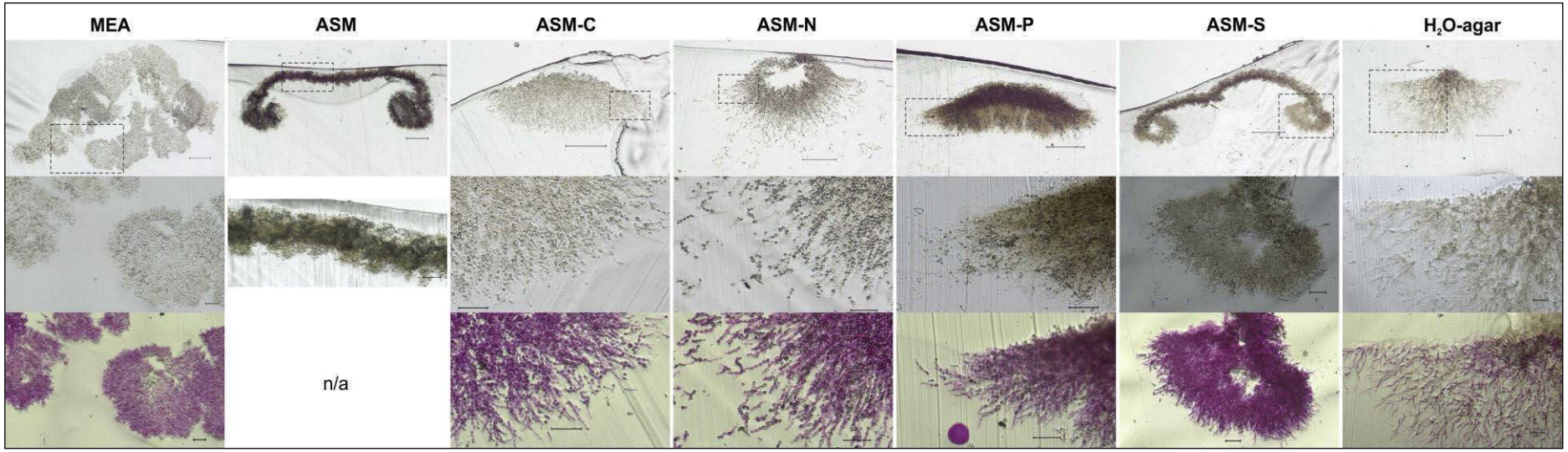

Supplementary Figure 6. Histological sections of* Knufia petricola *A95 colonies on nutrient-deprived media after 2 weeks

See next page for figure legend

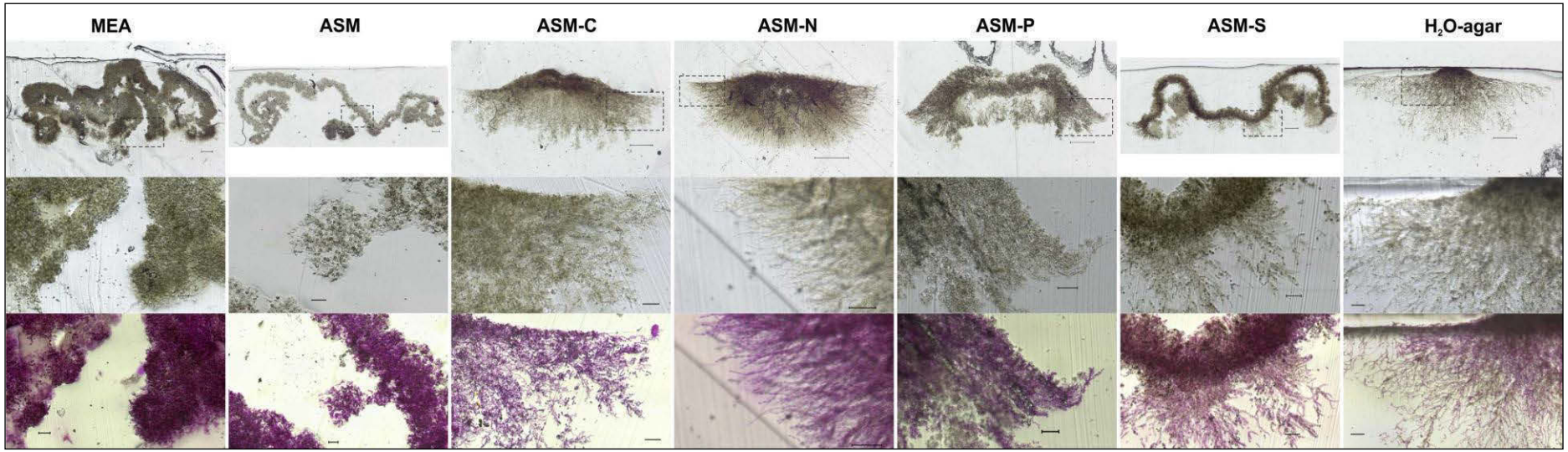

Supplementary Figure 7. Histological sections of* Knufia petricola *A95 colonies on nutrient-deprived media after 4 weeks

See next page for figure legend

Supplementary Figures 6-7 (previous page). Histological sections of* Knufia petricola *A95 colonies on nutrient-deprived media after 2 w or 4 w of incubation

(Upper panels) Histological sections of whole colonies after 2 w or 4 w of incubation (magnification 200X). **(Middle and lower panels)** Particulars of colonies without or with PAS staining (magnification 500-1'000X). ASM: A95-Specific Medium; ASM-C, -N, -P, -S: ASM deprived of carbon, nitrogen, phosphorus or sulphur source. For sake of illustration, pictures are not in scale but provided with scale bar (400 µm upper panels, 40 µm middle and lower panels). Dotted squares in upper panels: particular of colonies shown in middle and lower panels. n/a: picture missing.

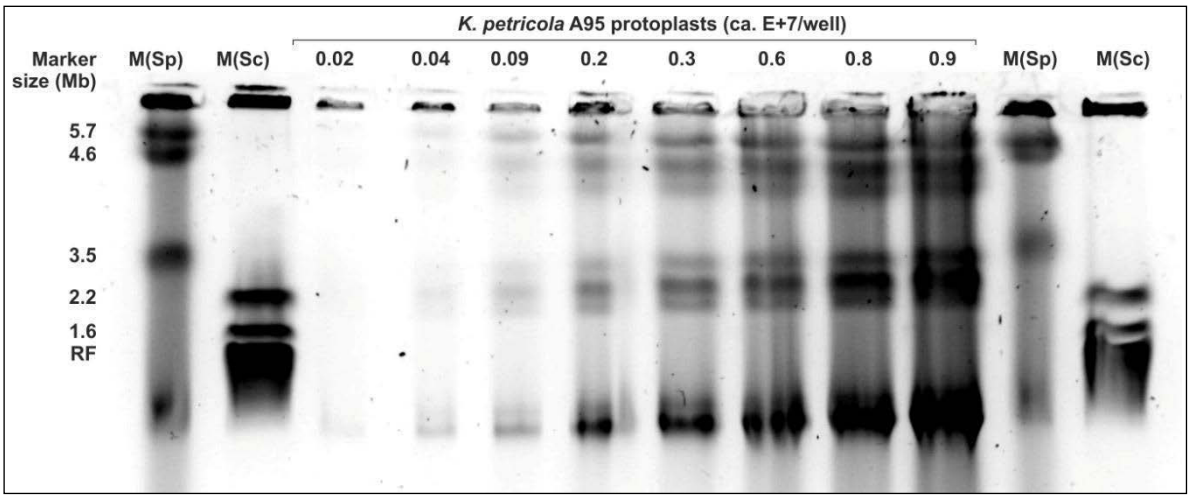

Supplementary Figure 8. Rotating Field Gel Electrophoresis with* Knufia petricola *A95 protoplasts to determine suitable loading concentrations (negative image)

This figure is the same as in *Fig. 44* (*Section 3.IV.2*) but with reversed image and brightness -40, contrast +20, intensity +50 (generated with Corel PHOTO-PAINT of CorelDRAW Graphic Suite X5 from Corel Corp., Canada).

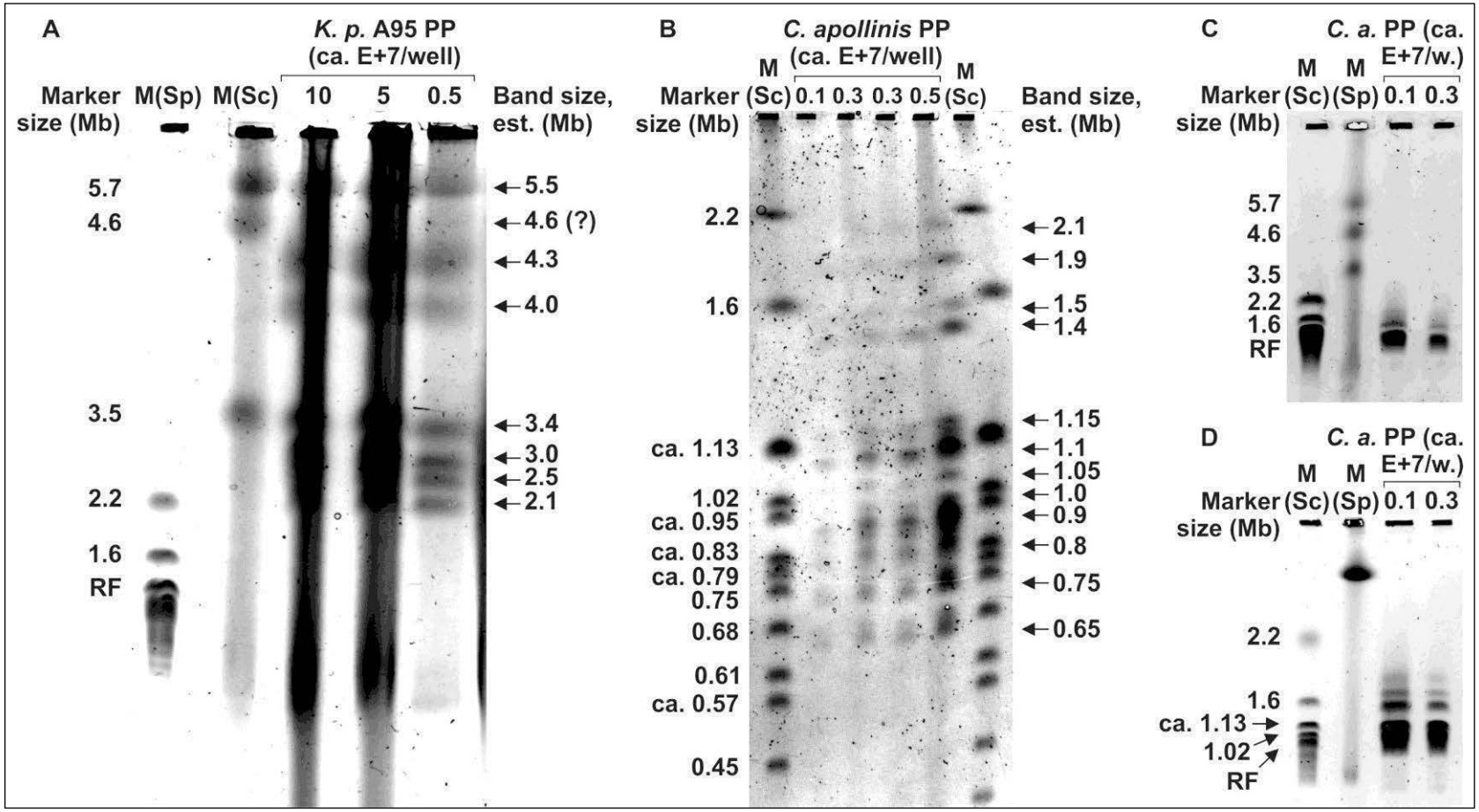

Supplementary Figure 9. Karyotyping of* Knufia petricola *A95 and* Coniosporium apollinis *by Rotating Field Gel Electrophoresis (negative images)

This figure is the same as in *Fig. 45* (*Section 3.IV.2*) but with reversed images and **(A)** brightness -20, contrast +20, intensity +30; **(B)** brightness -40, contrast +20, intensity +50; **(C)** brightness -60, contrast +40, intensity +50; **(D)** brightness -20, contrast +50, intensity +50 (generated with Corel PHOTO-PAINT of CorelDRAW Graphic Suite X5 from Corel Corp., Canada).

Supplementary Table 1. Rationale behind mineral composition of A95-Specific Medium[a]

Trace element	YNB[b]	B&D[c]	ASM	Observations
Mg	+	+	+	Essential for growth [9]
K	+	+	+	Essential for growth [9]
Fe	+	-	+	Iron chelators (dip, fusaric acid) inhibitory[d]
Mn	+	+	+	$MnCl_2$ not inhibitory[d]
Zn	+	+	+	
Mo	+	+	+	
Cl	+	-	+	Chloride anions not inhibitory[d]
H_3BO_3	+	+	-	Inhibitory[d]
Cu	+	+	-	$CuCl_2$ inhibitory [d]
Co	-	+	-	$CoCl_2$ inhibitory[d]
Ca	+	-	-	EGTA (Ca^{2+} chelator) not inhibitory [d]
I	+	-	-	

+ present, - not present

[a] Both YNB and B&D nutrient solution are able to support *K. petricola* A95 growth in ASM without minerals (not shown). Some minerals were omitted from the final formulation to deprive the medium from those with a negative effect on A95 growth and to generate a medium as simple as possible

[b] Yeast nitrogen base

[c] B&D nutrient solution from MP Biomedicals LLC, Illkirch-Graffenstaden (France)

[d] For *K. petricola* A95 growth; determined by phenotype microarrays (*Figs. 10, 20*)

(Adopted from Nai *et al.*, 2013 [91].)

Supplementary Table 2. Dead fungal biomass enhances growth of* Knufia petricola *A95 in nutrient-deprived media (I) – numerical values in liquid media

	Viable count (× 10^5 CFU/mL)[a]					
	ASM	**ASM-C**	**ASM-N**	**ASM-P**	**ASM-S**	**H_2O**
Control	26.20±7.32	3.01±0.38	3.16±1.19	6.43±0.93	1.19±0.40	2.19±0.26
+ EtO[b]	42.40±14.7	11.40±2.09	11.80±3.73	16.50±4.98	13.20±3.97	16.40±3.71
Fold	1.62	3.77	3.74	2.57	11.03	7.46
p-value	0.163	**0.002**	**0.019**	**0.026**	**0.006**	**0.003**
Control	27.70±13.6	2.37±1.15	1.88±0.83	6.25±1.97	1.13±0.45	1.63±0.45
+ Autocl.[c]	38.70±7.94	7.05±3.72	7.25±2.11	29.50±1.96	6.80±1.43	5.43±2.84
Fold	1.40	2.97	3.87	4.71	6.03	3.33
p-value	0.292	0.106	**0.015**	**0.000**	**0.003**	0.084
Control	19.70±4.68	4.03±0.63	2.74±0.76	6.43±1.12	1.20±0.43	2.27±0.36
+ Autocl. CF[d]	17.80±3.06	5.00±1.14	4.80±0.98	14.40±2.47	1.99±0.46	3.08±0.58
Fold	0.91	1.24	1.75	2.23	1.66	1.36
p-value	0.597	0.266	**0.046**	**0.007**	0.093	0.108
Control	22.60±9.41	1.26±0.29	1.30±0.76	4.40±0.78	0.85±0.35	1.29±0.37
+ Autocl. PP[e]	33.00±4.82	0.73±0.02	2.37±1.16	11.40±4.78	1.83±0.35	2.28±0.32
Fold	1.46	0.58	1.82	2.59	2.15	1.77
p-value	0.145	0.092	0.196	**0.028**	**0.015**	**0.033**
Control	26.20±8.50	2.97±0.43	1.74±0.81	5.73±2.14	0.75±0.26	1.83±0.90
+ Intracell.[f]	36.50±9.54	7.35±2.88	3.31±1.93	5.67±1.98	1.95±0.57	3.93±0.26
Fold	1.39	2.48	1.91	0.99	2.59	2.16
p-value	0.235	0.060	0.264	0.970	**0.030**	**0.018**
Control	24.90±10.3	2.33±0.49	n/a	n/a	n/a	1.61±0.34
+ EtO CF[g]	34.20±0.72	2.62±0.37	n/a	n/a	n/a	2.53±0.59
Fold	1.37	1.13	n/a	n/a	n/a	1.57
p-value	0.270	0.456	n/a	n/a	n/a	0.080
Control	24.90±10.3	2.33±0.49	n/a	n/a	n/a	1.61±0.34
+ EtO PP[h]	35.70±8.78	3.58±1.22	n/a	n/a	n/a	3.54±0.77
Fold	1.44	1.54	n/a	n/a	n/a	2.20
p-value	0.238	0.176	n/a	n/a	n/a	**0.016**

[a] After cultivation for 1 w in nutrient-deprived media and plating on MEA for viable counting. Average ± error from at least three repetitions; Fold: fold-increase with 10 % v/v biomass relative to control with saline solution; *p*: significance value in unpaired two-sample, two-tailed Student's *t*-test (bold < 0.05).
[b] Ethylene-oxide-sterilised biomass
[c] Autoclaved biomass
[d] Autoclaved cell fragments
[e] Autoclaved protoplasts
[f] Intracellular fraction
[g] Ethylene-oxide-sterilised cell fragments
[h] Ethylene-oxide-sterilised protoplasts

Supplementary Table 3. Dead fungal biomass enhances growth of* Knufia petricola *A95 in nutrient-deprived media (II) – numerical values on solid media

	Average colony surface area (mm^2)[a]					
	ASM	**ASM-C**	**ASM-N**	**ASM-P**	**ASM-S**	**H_2O-agar**
Control	8.18±1.24	0.81±0.19	0.18±0.03	0.78±0.16	2.94±0.34	0.15±0.04
+ EtO[b]	9.06±1.29	1.48±0.30	1.22±0.32	6.03±2.04	3.96±0.38	1.66±0.73
Fold	1.11	1.83	6.81	7.73	1.35	10.85
p-value	0.257	**0.001**	**0.000**	**0.000**	**0.002**	**0.006**
Control	8.37±1.02	1.29±0.29	0.24±0.08	1.19±0.49	5.29±0.97	0.28±0.12
+ Autocl.[c]	9.23±1.02	2.07±0.54	0.70±0.09	5.79±2.91	5.21±1.97	1.84±0.32
Fold	1.10	1.61	2.96	4.87	0.99	6.66
p-value	0.172	**0.018**	**0.000**	**0.003**	0.932	**0.000**
Control	8.01±1.96	1.14±0.32	0.36±0.21	0.82±0.21	4.76±2.34	0.24±0.09
+ Autocl. CF[d]	10.07±2.79	1.66±0.73	0.57±0.29	1.74±0.89	5.46±3.06	1.29±0.31
Fold	1.26	1.46	1.56	2.12	1.15	5.49
p-value	0.203	0.154	0.221	**0.036**	0.667	**0.000**
Control	8.41±2.24	1.14±0.28	0.57±0.52	0.99±0.48	5.28±2.07	0.76±0.65
+ Autocl. PP[e]	8.38±1.47	1.65±0.38	0.61±0.34	2.24±0.99	3.63±0.53	0.46±0.08
Fold	1.00	1.44	1.07	2.25	0.69	0.61
p-value	0.975	0.113	0.884	**0.042**	0.122	0.400
Control	9.24±3.93	0.98±0.03	0.50±0.40	1.24±0.76	4.82±2.08	0.28±0.09
+ Intracell.[f]	10.21±4.99	2.38±0.67	0.35±0.05	1.57±1.17	4.59±1.81	0.85±0.69
Fold	1.10	2.42	0.70	1.26	0.95	3.09
p-value	0.727	**0.039**	0.485	0.605	0.870	0.144
Control	7.26±1.00	0.57±0.21	n/a	n/a	n/a	0.17±0.05
+ EtO CF[g]	7.40±2.29	1.30±0.26	n/a	n/a	n/a	0.38±0.05
Fold	1.02	2.26	n/a	n/a	n/a	2.23
p-value	0.894	**0.000**	n/a	n/a	n/a	**0.000**
Control	7.26±1.00	0.57±0.21	n/a	n/a	n/a	0.17±0.05
+ EtO PP[h]	7.17±1.04	1.45±0.27	n/a	n/a	n/a	0.31±0.08
Fold	0.99	2.52	n/a	n/a	n/a	1.80
p-value	0.883	**0.000**	n/a	n/a	n/a	**0.006**

[a] After 3 w of incubation on nutrient-deprive media. Average ± error from at least three repetitions (average of two duplicates); Fold: fold-increase with 10 % v/v biomass relative to control with saline solution; *p*: significance value in unpaired two-sample, two-tailed Student's *t*-test (bold < 0.05).
[b] Ethylene-oxide-sterilised biomass
[c] Autoclaved biomass
[d] Autoclaved cell fragments
[e] Autoclaved protoplasts
[f] Intracellular fraction
[g] Ethylene-oxide-sterilised cell fragments
[h] Ethylene-oxide-sterilised protoplasts

A.6 Third-party contributions

Several persons contributed directly to the experiments. Leoni Lang, Annette Pannenbecker (both at the Freie Universität Berlin, Germany), Michael Riddermann (University of Applied Sciences Aachen, Germany), Marco Tosi (University of Camerino, Italy) and Helen Y. Wong (University of British Columbia, Canada) performed several valuable repetition experiments in the framework of their Bachelor Thesis or Internship as DAAD RISE Interns in the group "Model Biofilm in the Material Sciences" at the BAM; in particular growth curves, co-analysis of phenotype microarray plates, determination of fungal colony sizes in growth-temperature optimum profiles and growth in oligotrophic media, laccase screenings and viability changes upon ultraviolet irradiation. Cécile Gueidan (The Natural History Museum of London, UK) performed phylogenetic analysis to rename *Sarcinomyces petricola* to *Knufia petricola* as well as morphological observations of the strain as reported in Nai *et al.*, 2013 (*Figs. 5-6*). Francesc X. Prenafeta-Boldú (IRTA, Spain) assisted in the analysis of the data of hydrocarbon-utilisation assay and validated results with 5 µL toluene. Ronald de Vries and Isabelle Benoit (CBS-KNAW Fungal Biodiversity Centre, The Netherlands) grouped carbon compounds in phenotype microarrays in major fungal metabolic pathways. Nicole Knabe (BAM Berlin, Germany) designed primers for amplification of putative laccase genes. Jörg Toepel (BAM Berlin, Germany) first observed and isolated the pink mutant A95pm2. Kerstin Flieger (Leipzig University, Germany) performed carotenoid extractions and HPLC analysis. Axel Neffe (Helmholtz Zentrum Geesthacht, Germany) sterilised lyophilized biomass with ethylene oxide. All of them are kindly acknowledged for their precious contributions.

A.7 Publications and conference proceedings

Parts of this work were published in a scientific manuscript and presented at several national and international conferences. Another publication regarding genome analysis of black fungi is currently in preparation and will integrate some results presented here. Other publications loosely related with this work or with the time spent at the BAM and the Freie Universität Berlin are also reported.

Peer-reviewed publications

Nai C, Wong HY, Pannenbecker A, Broughton WJ, Benoit I, de Vries RP, Gueidan C and Gorbushina AA (2013), *Nutritional physiology of a rock-inhabiting, model microcolonial fungus from an ancestral lineage of the chaetothyriales (ascomycetes),* Fungal Genetics and Biology **56**: 54-66.

Conference proceedings

Nai C and Gorbushina AA, *Physiological analysis and karyotyping of the two rock-inhabiting black yeasts Knufia petricola A95 and Coniosporium apollinis*. Black Yeasts Conference "The

black fungi around us – harm and benefit", Guangzhou, China, December 2013 (talk, presenting author Corrado Nai)

Noack-Schönmann S, **Nai C**, Seiffert F, Milke M and Gorbushina AA, *Microcolonial fungi: Suspended life at the air-rock interface*. Conference "How dead is dead III: Life cycles", Berlin, Germany, June 2013 (poster presentation)

Nai C and Gorbushina AA, *Characterization of a rock-inhabiting microcolonial (black) fungus with the Biolog™: Restrictions, solutions, results*. Biolog/SRI International Conference, Menlo Park, California, United States, March 2013 (talk, presenting author Corrado Nai)

Nai C, Broughton WJ and Gorbushina AA, *Physiological characterisation of a phylogenetic ancestor of pathogenic ascomycetes: Adaptation of the Biolog™ system for slow-growing melanised fungi*. International Society for Human and Animal Mycology (ISHAM) Conference, Berlin, Germany, June 2012 (poster presentation)

Nai C, Wong HY, Broughton WJ and Gorbushina AA, *Physiological characterization and synthetic medium development for a model rock-inhabiting black fungus*. Association for General and Applied Microbiology (VAAM) Conference, Tübingen, Germany, March 2012 (poster presentation)

Gorbushina AA, Noack-Schönmann S, Bus T, **Nai C**, Schneider L, Banasiak R, *DNA extraction methods, as well as genome analysis of several black fungi*. Black Yeasts Conference "Hidden danger, bright promise", Curitiba, Brazil, December 2011 (talk, presenting author Anna Gorbushina)

Nai C, Pannenbecker A, Wong HY, Broughton WJ and Gorbushina AA, *Nutritional physiology and growth phenotypes of a rock-inhabiting fungus from an ancestral lineage of Chaetothyriales*. Black Yeasts Conference "Hidden danger, bright promise", Curitiba, Brazil, December 2011 (poster presentation)

Nai C, Pannenbecker A, Noack S, Broughton WJ and Gorbushina AA, *Growth Physiology of Sarcinomyces petricola A95, a model black fungus to study primary successions in terrestrial ecosystems and subaerial biofilms*. VAAM Conference, Karlsruhe, Germany, April 2011 (poster presentation)